

Copyright is owned by the Author of the thesis. Permission is given for a copy to be downloaded by an individual for the purpose of research and private study only. The thesis may not be reproduced elsewhere without the permission of the Author.

**Polymer coated controlled release  
agrichemicals as mitigation tools in pastoral  
farming**

A thesis presented in partial fulfilment of the requirements for  
the degree of  
Doctor of Philosophy in Soil Science  
at Massey University, Palmerston North  
New Zealand.

Peter Andrew Bishop

2010

## Abstract

---

Controlled release coating technology and nitrification inhibitors offer potential mitigation options, for the reduction of pastoral nitrate leaching. Previous published research on this topic was reviewed indicating two potential areas of new research and development around two main hypotheses:

- That polymer coated urea can allow high urea N applications in winter reducing application costs, nitrate leaching, herbage N content and urine N return to pasture.
- That polymer coated nitrification inhibitor dicyandiamide (DCD) can increase the longevity of DCD in soil and effectively inhibit nitrification of dairy urine affected soils.

To facilitate this research a range of coated urea and nitrification inhibitor dicyandiamide (DCD) products were produced using low cost, reactive layer, polyurethane (RLP) and were assessed in laboratory and field studies.

The mechanism of urea release from modified RLP coated urea was investigated, leading to the development of a comprehensive model of release, based on the porous water repellent nature of the RLP coating. The “hydraulic convection” model was validated using water extraction and under field conditions for modified RLP coated urea.

In, field trials (June-Nov 2007) using Italian ryegrass, a single application of 150 kgN ha<sup>-1</sup> of palmitic acid modified RLP coated urea (5UCU) reduced winter nitrate leaching by 7 kgN ha<sup>-1</sup> compared to uncoated urea and reduced peak herbage N levels over this period (150 days). Using an empirical N partitioning model for grazing cows, the reduction in herbage N was predicted to reduce urine N return by 5 to 10 kgN ha<sup>-1</sup> over the 150 day trial.

The effectiveness of laboratory prepared controlled release nitrification inhibitor dicyandiamide (PDCD) was tested as a surface application in repacked core studies on two soils contrasting in organic matter content and anion sorption capacity, Manawatu fine sandy silt and Dannevirke silt loam. The data from this trial was used to develop a model to explain DCD movement and degradation soils, which predicted that PDCD can potentially increase DCD longevity by 120 days at 20 °C over uncoated DCD.

## **Acknowledgements**

---

I would like to acknowledge the assistance of my supervisors, Dr. M. Hedley, Dr. J. Jones and Dr. P. Loganathan for their guidance and support. The technical staff; Mr. I. Furkert, Mr. B. Toes from the Institute of Natural Resources, Mr. W. Johnson and Mrs. M. Tamehana from the Institute of Food, Nutrition and Human Health, for their assistance with laboratory work. I would also like to acknowledge the assistance of Mrs. H. Liu and Mrs. J. Bishop in the field work and sample preparation. This work was made possible by an INR scholarship.

## Table of Contents

---

Polymer coated controlled release agrichemicals as mitigation tools in pastoral farming .....	i
Abstract .....	ii
Acknowledgements .....	iv
Table of Contents .....	v
Table of Figures .....	xii
Table of Tables .....	xxi
Nomenclature .....	xxiv
Chapter 1 Review: Mitigation of pastoral nitrate leaching by nitrification inhibitors and polymer coated fertilisers - applications, release characteristics and production .....	1
1.1 Introduction .....	1
1.2 Controlled release coated fertilisers: their production and applications .....	3
1.2.1 Sulphur Coated Fertiliser .....	3
1.2.2 Polymer Coated Sulphur Coated Urea (PCSCU).....	6
1.2.3 Alkyd Resin ( Osmocote® ).....	7
1.2.4 Reactive isocyanate coatings .....	10
1.2.5 Poly-Olefins coatings- Solvent based .....	14
1.2.6 Poly-Olefins coatings -Thermoplastic.....	16
1.2.7 Inorganic coatings .....	17
1.3 Release Mechanisms of Controlled Release Fertilisers .....	18
1.3.1 Rupture Model .....	20
1.3.2 Permeability Models .....	22
1.3.3 Osmotic pumping model.....	24
1.3.4 Orifice diffusion model.....	26
1.3.5 Combined models.....	27

1.3.6	Modelling parameters.....	29
	Film Elasticity and Volume Change .....	29
	Variable Permeability.....	30
	Temperature effect .....	30
1.3.7	Modelling developments.....	32
1.4	Nitrification inhibitors.....	33
1.4.1	Types and Mode of Action.....	33
1.4.2	Agronomic impact of nitrification inhibitors .....	38
1.5	Conclusion: .....	40

## Chapter 2 Modelling of nutrient release rate of modified Castor/MDI coated

	urea.....	42
2.1	Introduction.....	42
2.2	Hydraulic convection of solute from a coated granule .....	43
2.2.1	Lag time .....	44
2.2.2	Equilibrium release period .....	47
2.2.3	Constant equilibrium rate period.....	48
2.2.4	Falling rate period .....	49
2.2.5	Terminal period.....	51
2.2.6	Summary of spherical model .....	52
2.2.7	Non-spherical coated granules .....	52
2.3	Working model for reactive layer poly-urethane coated urea.....	53
2.3.1	Water extraction model .....	54
2.3.2	Field condition model .....	55
2.4	Objectives.....	56
2.5	Methods and Materials:.....	57
2.5.1	Preparation of film and coated urea .....	57

2.5.2	Physical testing of polymer films for Young's modulus and tensile strength .....	58
2.5.3	Water vapour permeability $W'$ of laboratory prepared polymer films.....	58
2.5.4	Release rate from coated urea in water .....	59
2.5.5	Digital analysis of particle size and volume change distributions .....	59
2.5.6	Film thickness distribution.....	60
2.5.7	Permeability of film with coating thickness.....	60
2.5.8	Hydraulic permeability $H'$ .....	60
2.6	Results and discussion: .....	62
2.6.1	Physical testing of polymer films for Young's modulus and tensile strength .....	62
2.6.2	Water vapour permeability $W'$ of laboratory prepared films.....	63
2.6.3	Permeability of film with coating thickness (coated granular urea).....	64
2.6.4	Critical Pressure and hydraulic conductivity .....	66
2.6.5	Estimation of equilibrium pressure $P_{eq}$ .....	67
2.6.6	Volume change following extraction .....	67
2.6.7	Digital Analysis.....	68
2.6.8	Coating thickness distribution.....	69
2.6.9	Release rate in water .....	70
2.7	Modelling of release rates based on physical film and granular parameters .....	71
2.7.1	Effect of temperature on models .....	75
2.7.2	Field trial release rate data .....	75
2.7.3	Summary and Conclusions.....	75
Chapter 3 Evaluation of polymer coated urea in grazed pasture systems.....		78
3.1	Introduction .....	78
3.2	Materials and methods .....	79
3.2.1	Site.....	79

3.2.2	Design and treatments .....	79
3.2.3	Plant analysis.....	81
	Drymatter .....	81
	Herbage N .....	81
3.2.4	Soil Analysis .....	81
	Soil bulk density and estimated field capacity.....	81
	Total soil carbon and nitrogen.....	81
3.2.5	Statistics .....	81
3.3	Results and Discussion.....	82
3.3.1	Dry matter .....	82
3.3.2	Herbage N recovery .....	83
3.3.3	Drainage .....	85
3.3.4	Climatic conditions .....	86
3.3.5	Nitrogen use efficiency .....	86
3.3.6	Nitrogen recycling via grazing.....	88
3.4	Conclusion.....	89
Chapter 4 Distribution and fate of fertilizer N in the soil profile.....		91
4.1	Introduction.....	91
4.2	Materials and Methods.....	91
4.2.1	Experimental site.....	91
4.2.2	Soil analysis .....	91
	Mineral N .....	92
4.2.3	Residual fertiliser N – amount and release characteristics.....	93
4.3	Results and Discussion.....	93
4.3.1	N Balance .....	100
4.3.2	Residual N in soil from UCU.....	101

4.3.3	Agronomic availability of residual N.....	102
4.4	Conclusion.....	103
Chapter 5	A model of nitrification inhibitor (DCD) movement in soil columns from conventional granular DCD and a new polymer coated granule: development and validation. ....	105
5.1	Introduction.....	105
5.2	Theory and experimental design .....	107
5.2.1	Diffusion of solute in soil.....	107
5.2.2	Boundary conditions for uncoated and coated granules .....	108
5.2.3	Summary of diffusion modelling factors .....	109
5.3	Equipment and methods.....	110
5.3.1	Soil microtone .....	110
5.3.2	Soil bulk density and volumetric field capacity.....	111
5.3.3	Total soil carbon and nitrogen.....	111
5.3.4	DCD analysis in soil and fertiliser .....	111
5.3.5	Mineral N .....	112
5.3.6	Preparation of Coated granular DCD.....	112
5.3.7	Soils.....	113
5.4	Methodology .....	113
5.4.1	Main experiment .....	113
	Diffusion column study.....	113
	DCD and urine redistribution and N transformations .....	114
5.4.2	Supporting experiments.....	114
	DCD degradation rate .....	114
	DCD adsorption isotherm .....	115
	Release rate of DCD.....	116

5.5 Results - Supporting experiments .....	116
5.5.1 DCD degradation rate .....	116
5.5.2 DCD absorption isotherms .....	118
5.5.3 Release rate of coated DCD .....	120
5.6 Diffusion Column study- observations and model development .....	121
5.6.1 Total DCD in soil over time .....	121
5.6.2 DCD concentrations at each soil depth over time .....	124
5.7 Model application to predict DCD profiles .....	126
5.7.1 Uncoated DCD .....	126
5.7.2 Coated PDCDs .....	130
5.8 Application of model to determine longevity of PDCD release over DCD .....	134
5.9 Conclusion: .....	136
Chapter 6 Nitrification inhibitory effect of polymer coated DCD in two contrasting New Zealand soils .....	138
6.1 Introduction .....	138
6.2 Methodology .....	139
6.2.1 Measurement of soil mineral N .....	139
6.2.2 Estimation of nitrification rate with depth .....	139
6.2.3 Measurement of soil DCD concentration .....	139
6.2.4 Measurement of inhibitory effect of DCD on nitrification .....	140
6.2.5 Mass flow of solute .....	140
6.2.6 Urine $\text{NH}_4^+$ -N isotherm .....	141
6.2.7 Modelling .....	141
6.3 Results .....	142
6.3.1 Urine $\text{NH}_4^+$ -N isotherm .....	142
6.3.2 Nitrification rate with depth .....	143
6.3.3 Soil core incubation with urine application .....	146

6.3.4	Nitrification with depth .....	149
6.3.5	Inhibitor constant for Manawatu and Dannevirke soils .....	152
6.3.6	Soil pH profiles and electrical conductivity .....	154
6.4	Modelling urine movement and conversion .....	156
6.5	Conclusion .....	158
Chapter 7	Conclusions and recommendations for future work .....	160
7.1	Conclusions .....	160
7.1.1	Mechanism of release from UCU .....	160
7.1.2	Field trials of modified RLP coated urea 5UCU and 7UCU .....	161
7.1.3	Evaluation of PDCD in repacked soil core studies .....	161
7.2	Further work .....	162
Appendix 1	Model of release of urea from reactive layer polyurethane coated urea .....	164
A1.1	Field conditions .....	168
Appendix 2	Model of diffusion, sorption and degradation of DCD in soil .....	172
Appendix 3	Model of diffusion, sorption and Nitrification of dairy urine in soil .....	177
References	.....	182

## Table of Figures

---

Figure 1.1	Schematic of TVA pilot plant for sulphur coated urea, using twin fluid sulphur spray. Redrawn from Rindt et al.,(1968).....	4
Figure 1.2	Comparative dry matter yields of Bumarda grass in glasshouse pot trials grown with the addition of 160 kgNha <sup>-1</sup> of 9%(■) and 15% (▲) sulphur coated urea, urea(◆) and a blend of 40% urea and 60% SUC(x). Data from (Rindt et al. 1968) .....	6
Figure 1.3	Cumulative release of urea from Soya-cyclopentadiene resin coated urea, with coating expressed as % initial fertilizer weight, data from (Hansen, 1965) .....	8
Figure 1.4	Effect of leaching volume on electrical conductivity of a 1:1.5 extract of potting media exposed to high temperatures in summer 31.8±2.6 °C. Data from Huett (1997). .....	10
Figure 1.5	Schematic of continuous reactive urethane coating process derived from Detrick and Carney (1994).....	12
Figure 1.6	Schematic of Spouted bed coater for the application of poly-olefin coatings. Derived from Fujita et al. (1977). .....	15
Figure 1.7	Release characteristics of 3 % low density polyethylene coatings with the addition of 0 to 15% surfactant (octaoxyethylene nonylphenyl ether) in the coating. Data from Fujita et al. (1977). .....	16
Figure 1.8	Summary of factors contributing to release of nutrients from a coated controlled release fertiliser .....	20
Figure 1.9	Biological oxidation of ammonia to nitrite by membrane bound ammonium monooxygenase (AMO) and hydroxylamine oxidoreductase (HAO) .....	34

Figure 1.10	Structure of the nitrification inhibitors cyanamide and dicyandiamide.....	36
Figure 1.11	Effectiveness of heterocyclic nitrogen compounds, as nitrification inhibitors with % inhibition in soil with (high and low) organic matter contents. (McCarty and Bremner 1989).....	37
Figure 1.12	Structures of highly effective heterocyclic nitrogen containing nitrification inhibitors (commercial name)(McCarty 1999). ....	37
Figure 2.1	Transformation of digital image to spherical equivalent model granule for estimation of potential volume change $\gamma$ .....	53
Figure 2.2	Membrane diffusion and permeability apparatus. ....	61
Figure 2.3	Pressure calibration curve for dead weight syringe system .....	62
Figure 2.4	Release rate profiles for RLP coated urea with film thickness, $\Delta$ 0.00104, $\diamond$ 0.00156, $\square$ 0.00206, $\times$ 0.0026, $\circ$ 0.0036 and $\bullet$ 0.0052 cm.....	65
Figure 2.5	Relationship between water vapour permeability ( $W'$ ) and mean coating thickness of RLP coated urea (control, MDI) Dashed line represents model $W' = 2.68 \times 10^{-8} + 4.05 \times 10^{-6} e^{-2800l_0}$ .....	65
Figure 2.6	Flow rate of urea solution (50% w/w) through laboratory prepared coating films as the result of applied pressure, control ( $\circ$ ) and 20% Palmitic acid (+) amended polymer films. Solid lines represent linear regressions for control membrane and dashed lines 20% Palmitic acid .....	66
Figure 2.7	Granule image morphology of urea prior to coating. ....	68
Figure 2.8	Proportional urea release with time in water at 20 °C, for urea coated with $\blacklozenge$ RLP and RLP modified with $\blacksquare$ Canola oil, $\blacktriangle$ Palmitic acid and $\bullet$ Soya oil at levels of 10% (hollow), 15% (gray) and 20% (solid). ....	70

Figure 2.9	Proportional urea release with time in water at 10 °C , for urea coated with ♦ RLP and RLP modified with ,■ Canola oil,▲ Palmitic acid and ● Soya oil at levels of 10% (hollow), 15% (gray) and 20% (solid). .....	71
Figure 2.10	Correlation plot of modelled and measured urea release for 5(●), 7(+ ) and 10% (X) coating levels of the control polymer MDI: Castor oil: TEA in water at 20°C with lag period calculated.....	72
Figure 2.11	Correlation plot of modelled and measured urea release for 5(●), 7(+ ) and 10% (X) coating levels of the control polymer (MDI: castor oil: TEA) in water at 20°C with no lag period calculated .....	73
Figure 2.12	Plot of the measured proportion of urea released at 20°C in water extraction of 5% coating level of 20% Palmitic acid amended coated urea(▲), compared to modelled results using hydraulic convection model, with (solid) and without lag period (dashed) line.....	74
Figure 2.13	Plot of the measured proportion of urea released at 10°C in water extraction of 5% coating level of 20% Palmitic acid amended coated urea(▲), compared to modelled results using hydraulic convection model, with (solid) and without lag period (dashed) line.....	74
Figure 2.14	Proportional herbage N recovery for surface applications 5UCU(▲) and 7UCU (●) at 150 kg N ha <sup>-1</sup> on Italian ryegrass crop (Bishop et al. 2008) with release of urea modelled using Hydraulic convection model (black dashed line) using mean daily temperature(black line) and soil volumetric water content (gray line).....	76
Figure 3.1	Randomized block layout for RLP coated urea field trial at Massey University Palmerston North. Gray blocks treatments applied at 50 kgN ha <sup>-1</sup> while black blocks recovered treatments at 150 kgN ha <sup>-1</sup> .....	80

Figure 3.2	Estimated nitrate-N leaching from 150 kg N ha <sup>-1</sup> treatments during drainage events. Significance of difference between treatments expressed as LSD (P=0.05) for each leaching event.....	85
Figure 3.3	Monthly dry matter production to herbage N recovery over the trial period for all treatments. Showing N use efficiency increasing from winter to summer .....	87
Figure 3.4	Monthly herbage N contents of pasture at harvest for 150 N treatments. Vertical bars indicate LSD (P=0.05). .....	87
Figure 4.1	Soil pits used for bulk density and field water capacity measured in the trial plots on Tokomaru silt loam, Massey University, Palmerston North, New Zealand.....	94
Figure 4.2	Initial mineral N profile of soil cores in 5 cm sections (19/06/2007). Error bars represent standard error of mean for n = 7. ....	95
Figure 4.3	Mineral N soil profiles on 28 <sup>th</sup> June 2007, 10 days following treatment applications. ....	97
Figure 4.4	Measured soil exchangeable NH <sub>4</sub> <sup>+</sup> -N (kgN ha <sup>-1</sup> ) to a depth of 25 cm, for the 150 kgN ha <sup>-1</sup> treatments (◇ U, ■ DCUDU, ▲ 5UCU, × 7UCU, ○ control (nil-N)). The vertical error bars represent the least significant difference between treatments on each date. ....	98
Figure 4.5	Measured soil exchangeable NH <sub>4</sub> <sup>+</sup> -N (kgN ha <sup>-1</sup> ) to a depth of 25 cm, for the 50 kgN ha <sup>-1</sup> treatments (◇ U, ■ DCUDU, ▲ 5UCU, × 7UCU, ○ control (nil-N)). The vertical error bars represent the least significant difference between treatments on each date. ....	98
Figure 4.6	Measured soil exchangeable NO <sub>3</sub> <sup>-</sup> -N (kgN ha <sup>-1</sup> ) to a depth of 25 cm, for the 150 kgN ha <sup>-1</sup> treatments (◇ U, ■ DCUDU, ▲ 5UCU, × 7UCU, ○ control (nil-N)). The vertical error bars represent the least significant difference between treatments on each date. ....	99

Figure 4.7	Measured soil exchangeable $\text{NO}_3^-$ -N ( $\text{kgN ha}^{-1}$ ) to a depth of 25 cm, for the 50 $\text{kgN ha}^{-1}$ treatments ( $\diamond$ U, $\blacksquare$ DCDU, $\blacktriangle$ 5UCU, $\times$ 7UCU, $\circ$ control (nil-N)). The vertical error bars represent the least significant difference between treatments on each date. ....	99
Figure 5.1	The PVC pipe packed with soil used to study the diffusion of DCD and urine-N into soil and subsequent N transformations. ....	110
Figure 5.2	Degradation rates of DCD in Manawatu ( $\circ$ ) and Dannevirke ( $\square$ ) soils incubated at 20°C and 75% FC.....	117
Figure 5.3	Change in extractable $\text{NO}_3^-$ -N in Manawatu ( $\circ$ ) and Dannevirke ( $\square$ ) soils incubated at 20°C and 75% FC following treatment DCD and urea solution (30 mg DCD $\text{kg}^{-1}$ soil and urea as 27 mgN $\text{kg}^{-1}$ soil). ....	118
Figure 5.4	Freundlich absorption isotherm plots for DCD in Manawatu ( $\Delta$ ), Dannevirke ( $\diamond$ ) top soil (3-10 cm) and the DCD soil carbon isotherm for both soils(solid fill) on the secondary axis. ....	119
Figure 5.5	DCD release rate from polymer coated products in water, $\blacklozenge$ PDCD3, $\blacksquare$ PDCD4. ....	120
Figure 5.6	Measured degradation of DCD ( $\text{mg (soil column)}^{-1}$ ) in cores of Manawatu ( $\Delta$ ) and Dannevirke ( $\circ$ ) soils following the application of uncoated DCD (9.5 mg) at day 1 and fresh cow urine (44ml) added at day 28, incubated at 20°C and 75% of field capacity for a total of 99 days. Initial decay function to day 21 (solid lines) and post urination decay function from day 41 (dashed lines)(Error bars +/- $P < 0.05$ ). ....	122
Figure 5.7	Measured and modelled results for DCD ( $\text{mg (soil column)}^{-1}$ ) accumulation in Manawatu ( $\blacktriangle$ ) and Dannevirke ( $\bullet$ ) soil columns treated with 9.5 mg of DCD in the form of PDCD4. The black lines represents the release rate of DCD by water, gray lines the estimated rate in soil based on the $\theta = 0.39$ and	

	dashed lines simultaneous release and degradation of DCD using the two rate functions (Error bars LSD ( P<0.05)).	123
Figure 5.8	Concentration of DCD at different soil depths in the Dannevirke and Manawatu soil at increasing time following the application of uncoated DCD (DCD) and RLP Coated DCD (PDCD) to the core surface ( ♦ day 7, ■ day 15, ▲ day 21, × day 34, * day 41, ●day 55 and + day 99).	125
Figure 5.9	Correlation of modelled and measured amounts of DCD at different depths in the Dannevirke soil ( ♦ day 7, ■ day 15, ▲ day 21, × day * day 41, ●day 55 and + day 99; Model parameters are given Table 5.6).	127
Figure 5.10	Concentration of DCD in the Dannevirke soil core profile with modelled DCD profile( dashed lines) at each sampling period (♦ day 7, ■ day 15, ▲ day 21, × day 34, * day 41, ●day 55 and + day 99; Model parameters are given Table 5.6).	128
Figure 5.11	Correlation of modelled and measured amounts of DCD at different depths in the Manawatu soil (♦ day 7, ■ day 15, ▲ day 21, × day 34, * day 41, ●day 55 and + day 99; Model parameters are given Table 5.6).	129
Figure 5.12	Concentrations of DCD in Manawatu soil core profiles with modelled DCD profile( dashed lines) at each sampling period (♦ day 7, ■ day 15, ▲ day 21, × day 34, * day 41, ●day 55 and + day 99; Model parameters Table 5.6).	129
Figure 5.13	Correlation of modelled and measured amounts of DCD at different depths in the Dannevirke soil treated with PDCD (♦ day 7, ■ day 15, ▲ day 21, × day 34, * day 41, ●day 55 and + day 99; Model parameters are given in Table 5.5 & 5.6).	130

Figure 5.14	Correlation of modelled and measured amounts of DCD at different depths in the Manawatu soil treated with PDCD (◆ day 7, ■ day 15, ▲ day 21, × day 34, * day 41, ● day 55 and + day 99; Model parameters are given in Table 5.5 & 5.6).....	131
Figure 5.15	Correlation of modelled and measured amounts of DCD at different depths in the Manawatu soil treated with PDCD. (◆ day 7, ■ day 15, ▲ day 21, × day 34, * day 41, ● day 55 and + day 99; Model parameters are given in Table 5.6 & 5.7).....	133
Figure 5.16	Correlation of modelled and measured amounts of DCD at different depths in the Dannevirke soil treated with PDCD. (◆ day 7, ■ day 15, ▲ day 21, × day 34, * day 41, ● day 55 and + day 99; Model parameters are given in Table 5.6 & 5.7).....	133
Figure 5.17	Modelled soil DCD concentrations in soil columns 150mm deep for DCD and PDCD applied to Manawatu silt loam over 300 days (◆ day 15, ■ day 30, ▲ day 60, × day 120, * day 180, ● day 240 and + day 300; Model parameters are given in Table 5.7 & 5.8).....	135
Figure 5.18	Modelled soil DCD concentrations in soil columns 150mm deep for combination of PDCD:DCD (80:20) applied to Manawatu silt loam at 25 kgDCD ha <sup>-1</sup> over 300 day (◆ day 15, ■ day 30, ▲ day 60, × day 120, * day 180, ● day 240 and + day 300; Model parameters are given in Table 5.7 & 5.8). .....	136
Figure 6.1	NH <sub>4</sub> <sup>+</sup> -N Freundlich isotherm plots for urine treated Manawatu Silt loam (+) and Dannevirke loam (×).....	143
Figure 6.2	The change in soil extractable NH <sub>4</sub> <sup>+</sup> -N concentrations in Dannevirke soil layers over time following dairy urine application (□ 0-0.2 cm, ◇ 0.2-0.6 cm, Δ 0.6-1.4 cm, × 1.4-2.5 cm, + 2.5-3.5 cm and ○ 3.5-4.5 cm depths; Lines of best (fit slope Table 6.2); vertical error bars LSD (P=0.05)). .....	144

Figure 6.3	The change in soil extractable $\text{NH}_4^+$ -N concentrations in Manawatu soil layers over time following dairy urine application ( $\square$ 0-0.2 cm, $\diamond$ 0.2-0.6 cm, $\Delta$ 0.6-1.4 cm, $\times$ 1.4-2.5 cm, $+$ 2.5-3.5 cm and $\circ$ 3.5-4.5 cm depths; lines of best fit (slopes Table 6.2); vertical error bars LSD (P=0.05)).	145
Figure 6.4	Change in extractable $\text{NH}_4^+$ -N (mean core concentrations) over time (relative to control) following urine application. Error bars 95% confidence interval ( $\circ$ Dannevirke, $\Delta$ Manawatu, no fill is DCD, Black is PDCD and grey is no DCD).	147
Figure 6.5	Change in extractable $\text{NO}_3^-$ -N (mean core concentration) over time (relative to control) following urine application. Error bars 95% confidence interval ( $\circ$ Dannevirke $\Delta$ Manawatu, no fill is DCD, Black is PDCD and grey is no DCD).	148
Figure 6.6	The change with time of extractable $\text{NH}_4^+$ -N concentrations in Dannevirke soil treated with DCD and dairy urine ( $\square$ 0-0.2 cm, $\diamond$ 0.2-0.6 cm, $\Delta$ 0.6-1.4 cm, $\times$ 1.4-2.5 cm, $+$ 2.5-3.5 cm and $\circ$ 3.5-4.5 cm depths; vertical error bars LSD (P=0.05)).	149
Figure 6.7	The change with time of extractable $\text{NH}_4^+$ -N concentrations in Dannevirke soil treated with PDCD and dairy urine ( $\square$ 0-0.2 cm, $\diamond$ 0.2-0.6 cm, $\Delta$ 0.6-1.4 cm, $\times$ 1.4-2.5 cm, $+$ 2.5-3.5 cm and $\circ$ 3.5-4.5 cm depths; Vertical error bars LSD (P=0.05)).	150
Figure 6.8	The change with time in extractable $\text{NH}_4^+$ -N concentrations in Manawatu soil treated with DCD ( $\square$ 0-0.2 cm, $\diamond$ 0.2-0.6 cm, $\Delta$ 0.6-1.4 cm, $\times$ 1.4-2.5 cm, $+$ 2.5-3.5 cm and $\circ$ 3.5-4.5 cm depths; vertical error bars LSD (P=0.05)).	151
Figure 6.9	The change with time of extractable $\text{NH}_4^+$ -N concentrations in Manawatu soil treated with PDCD and dairy urine ( $\square$ 0-0.2 cm, $\diamond$ 0.2-0.6 cm, $\Delta$ 0.6-1.4 cm, $\times$ 1.4-2.5 cm, $+$ 2.5-3.5 cm and $\circ$ 3.5-4.5 cm depths; vertical error bars LSD (P=0.05)).	152

Figure 6.10	Inhibitor effect plot of DCD concentration in soil vs. relative nitrification velocity in Manawatu soils ( $\Delta$ silt loam and $\circ$ fine sandy loam data J. Asing ) and initial DCD degradation incubation trials ( $\bullet$ Manawatu and $\blacksquare$ Dannevirke soils) .....	153
Figure 6.11	Soil core pH profile Manawatu soil 7 days following urine addition, $\blacktriangle$ PDCD, $\blacktriangle$ DCD and $\Delta$ control with no urine. ....	155
Figure 6.12	Soil core pH profile of Dannevirke soil 7days following urine addition, $\bullet$ PDCD, $\bullet$ DCD and $\circ$ is the control with no urine. ....	155
Figure 6.13	Correlation plots of modelled and measured amounts of soil $\text{NH}_4^+$ -N in soil sections for Manawatu soil cores treated with dairy urine over 68 day ( $\bullet$ soil + DCD, $\bullet$ soil + PDCD, $\circ$ soil alone, $\times$ excluded data; Modelling parameters Tables 6.1, 6.2 and 6.4 and $K=0.035$ ).....	157
Figure 6.14	Correlation plots of modelled and measured amounts of soil $\text{NH}_4^+$ -N in soil sections for Dannevirke soil cores treated with dairy urine over 65 days ( $\bullet$ soil + DCD, $\bullet$ soil + PDCD and $\circ$ soil alone; Modelling parameters Tables 6.1, 6.2 and 6.4 and $K=0$ ). ....	158
Figure A1	Layout of input parameters and output fields for the Hydraulic convection model in Excel 2007.....	164
Figure A1.1	Layout of input parameters and output fields for Hydraulic convection model with daily field data in Excel 2007.....	168
Figure A2.	Worksheet layout for DCD release, diffusion, adsorption and degradation in soil at 20°C.....	172
Figure A3	Worksheet layout for modelled urine N nitrification and movement in soil cores at 20°C. ....	177

## Table of Tables

---

Table 1.1	Operating conditions for the Pursell Process .....	13
Table 1.2	Expected yields increases for Maize grown in the US Corn belt based on data from (Blaylock et al. 2005) .....	13
Table 2.1	Physical properties of laboratory polymer films.....	63
Table 2.2	Water vapour permeability of laboratory prepared polymer films .....	64
Table 2.3	Critical pressure ( $P_{critical}$ ) and hydraulic permeability ( $H'$ ) of the control and 20% Palmitic acid amended films. ....	67
Table 2.4	Measured mean volume change of coated granules following 100 days of extraction in water .....	68
Table 2.5	Modelled volume change of granule population based on measures spheroid shape parameters $r_{max}$ $e$ and Feret radii for the transition from equivalent spherical volume (ESV) to oblate spheroid. ....	69
Table 2.6	Polymer film thickness means and standard deviation's for the control coated and palmitic acid amended coatings .....	69
Table 2.7	Polymer film thickness and distribution within products to be modelled.....	72
Table 3.1	Soil properties at the trial site .....	79
Table 3.2	(a) Cumulative additional dry matter (DM) (cumulative treatment DM minus cumulative Nil-N control DM ) in kg DM/ha for 50 and 150 kg N/ha treatments and (b) Cumulative control yields on different harvest dates. ....	83

Table 3.3	(a) Additional herbage N recovered from treatments (treatment minus nil-N control (b)) (kg N/ha) on different harvest dates after N applications at 50 and 150 kg/ha. ....	84
Table 3.4	Summary of climatic data over harvest periods from NIWA <sup>a</sup> and Site <sup>b</sup> .....	86
Table 3.5	Urine-N return to pasture following grazing based on .....	87
Table 4.1	Soil profile properties after cultivation just prior to treatment application.....	93
Table 4.2	Measured soil moisture deficit in soil profile relative to field capacity at 0.05 bar suction with standard error of means.....	96
Table 4.3	Soil nitrogen balance from the pre-trial condition to following the third harvest at 94 days, for 150 kgN ha <sup>-1</sup> treatment applications .....	97
Table 4.4	Soil nitrogen balance from the pre-trial condition to following the third harvest at 94 days, for 50 kgN ha <sup>-1</sup> treatment applications .....	98
Table 4.5	Residual N unreleased from coated urea after 158 days in winter field trial.....	98
Table 4.6	Effect of soil core moisture content on the release of residual N from polymer coated urea granules. ....	99
Table 4.7	Herbage nitrogen and dry matter recovered from the residual polymer coated fertiliser core study under dry and wet conditions.....	103
Table 5.1	DCD content of polymer coated DCD granules and estimated coat thickness .....	112
Table 5.2	Physical and chemical properties of soils .....	113
Table 5.3	First order decay rate $k$ (d <sup>-1</sup> ) constants and half life of DCD in soils incubated at 20°C and 75% FC.....	117

Table 5.4	Freundlich coefficients derived from the isotherm plot for Manawatu and Dannevirke top soil 3-10 cm and soil carbon ( $C_{ad} = a C_1^b$ ) .....	119
Table 5.5	Cumulative release rate function of polymer coated DCD in water and 20°C for coating levels of 3 and 4. ....	121
Table 5.6	Model parameters for DCD diffusion and degradation in Manawatu and Dannevirke soils .....	126
Table 5.7	Modelled release rate of DCD from polymer coated DCD in soil at 75% FC and 20°C .....	132
Table 6.1	Freundlich isotherm coefficients for $NH_4^+$ -N adsorption in urine treated Manawatu and Dannevirke soils .....	143
Table 6.2	Nitrification velocity $U$ ( $mol\ g^{-1}\ day^{-1}$ ) in Manawatu and Dannevirke soil cores as a function of soil depth in cm. ....	146
Table 6.3	% Inhibition of nitrification in total soil cores over 68 days of incubation .....	148
Table 6.4	Inhibitor response constant (K) for Manawatu, Dannevirke and Iowa soils, Harps, Webster and Storden (McCarty and Bremner 1989) .....	153

## Nomenclature

---

Symbol	units	description
$a$	mg kg <sup>-1</sup> dry soil	Freundlich coefficient
$A_p$	cm <sup>2</sup>	area of pores
$A_t$	cm <sup>2</sup>	total film/granule surface area
$a_w$	-----	activity of water
$A_{wp}$	cm <sup>2</sup>	area of water filled pores
$B$	-----	activity coefficient
$C_{(ext)}$	g cm <sup>-3</sup>	external solute concentration
$C_{(int)}$	g cm <sup>-3</sup>	internal solute concentration
$C_s$	g cm <sup>-3</sup>	solute concentration
$C_{s(t)}$	g cm <sup>-3</sup>	concentration of solute at time t
$C_{sat}$	g cm <sup>-3</sup>	concentration saturated solute
$C_u$	g cm <sup>-3</sup>	concentration urea solution
$D$	cm <sup>2</sup> d <sup>-1</sup>	diffusion coefficient
$d_{eqv}$	cm	diameter of equivalent spherical volume
$dP/dt$	Pa d <sup>-1</sup>	change in pressure with respects to time
$\Delta P_{wv}$	Pa	deference in water vapour pressure
$D_s$	cm <sup>2</sup> d <sup>-1</sup>	diffusion coefficient of solute in water
$D'_s$	cm <sup>2</sup> d <sup>-1</sup>	diffusion coefficient of solute in film
$dV_{water}/dt$	cm <sup>3</sup> d <sup>-1</sup>	change in volume with respects to time
$D_{wv}$	cm <sup>2</sup> d <sup>-1</sup>	diffusion coefficient of water vapour in air
$E_a$	kJ mol <sup>-1</sup>	activation energy of water membrane transport
$f$	-----	tortuosity coefficient
$F$	cm <sup>3</sup> d <sup>-1</sup>	volumetric water flux
$F'$	-----	dimensionless volumetric water flux
$F_{(t)}$	cm <sup>3</sup> d <sup>-1</sup>	volumetric water flux at time t
$F_{sat}$	cm <sup>3</sup> d <sup>-1</sup>	volumetric water flux saturated solution
$H'$	cm <sup>2</sup> d <sup>-1</sup> Pa <sup>-1</sup>	specific hydraulic resistance
$K$	μmol g <sup>-1</sup>	inhibitor response constant
$k$	d <sup>-1</sup>	first order decay constant
$k'$	cm <sup>3</sup> d <sup>-1</sup>	volumetric release rate of solution
$l_{(t)}$	cm	film thickness at time t
$l_e$	cm	film thickness at equilibrium
$l_o$	cm	initial film thickness
$L_p$	cm <sup>2</sup>	mechanical permeability coefficient
$m$	g	mass released
$M_o$	g	initial mass
$M_{wt(s)}$	g mol <sup>-1</sup>	molar wt of solute

$N$	$\text{mol}^{-1}$	Avogadro's number
$P_{\text{coating}}$	Pa	coating stress
$P_{\text{critical}}$	Pa	critical pressure required for flow
$P_{\text{eq}}$	Pa	Internal equilibrium pressure
$P_h$	$\text{cm}^2\text{d}^{-1}\text{Pa}^{-1}$	film water vapour permeability
$P_{\text{internal}}$	Pa	internal granule pressure
$P_{\text{wv}}^0$	Pa	vapour pressure of water above pure water
$P_{\text{rupture}}$	Pa	rupture pressure
$P_s$	$\text{cm}^2\text{d}^{-1}$	film solute permeability
$P_{s(T)}$	$\text{cm}^2\text{d}^{-1}$	film solute permeability as a function of temperature
$P_{\text{wv}(ext)}$	Pa	external water vapour pressure
$P_{\text{wv}(int)}$	Pa	internal water vapour pressure
$P_{\text{wv}(soln)}$	Pa	water vapour pressure of solution
$Q(t)$	-----	cumulative fractional release of solute at time t
$Q_c$	-----	cumulative fractional release of solute at end of constant rate period
$R$	$\text{J mol}^{-1} \text{K}^{-1}$	gas constant
$R_f$	cm	Feret radius
$r_{\text{max}}$	cm	maximum radius of spheroid
$r_{\text{min}}$	cm	minimum radius of spheroid
$r_o$	cm	radius time zero
$S_y$	Pa	tensile yield strength
$t'$	d	time required prior to solute release occurs at constant rate
$t^*$	d	time at which constant rate ends and falling rate starts
$t_o$	d	time zero
$U$	$\text{mol cm}^{-1}\text{d}^{-1}$	nitrification velocity
$U_m$	$\text{cm s}^{-1}$	mean fluid velocity
$U_{\text{max}}$	$\text{mol cm}^{-1}\text{d}^{-1}$	maximum nitrification velocity
$V$	$\text{cm}^3$	volume
$V_{\text{critical}}$	$\text{cm}^3$	Volume of granule at critical pressure
$V_{\text{eq}}$	$\text{cm}^3$	volume of granule at equilibrium pressure
$V_{\text{soln}}$	$\text{cm}^3$	volume of solution
$V_w$	$\text{cm}^3$	volume of water
$w$	$\text{g d}^{-1}$	weight change per day
$W'$	$\text{cm}^2\text{d}^{-1}\text{Pa}^{-1}$	specific water vapour permeability
$W'_{\text{min}}$	$\text{cm}^2\text{d}^{-1}\text{Pa}^{-1}$	minimum specific water vapour permeability
$Y$	Pa	Youngs Modulus

### Greek Symbols

Symbol	units	description
$\Delta C$	$\text{g cm}^{-3}$	concentration difference across film
$\Delta \pi$	Pa	osmotic pressure difference across film
$\Delta P$	Pa	hydrostatic pressure difference across film
$\Delta P_{\text{wv}}$	Pa	water vapour pressure difference across film
$\Delta E_{\text{vis}}$	$\text{kJ mol}^{-1}$	activation energy of viscous flow
$\Delta V$	$\text{cm}^3$	volume change
$\Delta V_{\text{critical}}$	$\text{cm}^3$	critical volume change
$\Delta V_{\text{g}}$	$\text{cm}^3$	granule volume change
$\Delta l$	-----	coating strain
$\Delta \pi$	Pa	osmotic pressure
$\Delta \pi_{\text{sat}}$	Pa	osmotic pressure of saturated solution
$\varepsilon_f$	-----	voidage film
$\varepsilon_{f\text{max}}$	-----	voidage
$\varepsilon_g$	-----	voidage granule
$\varepsilon_w$	-----	
$\gamma$	-----	proportional granule volume change
$\eta$	Pa s	viscosity
$\emptyset$	cm	diameter of permeability of membrane cell
$\theta$	$\text{cm}^3 \text{ cm}^{-3}$	volumetric water content
$\rho_s$	$\text{g cm}^{-3}$	density of solid
$\beta_e$	-----	water activity coefficient
$\delta$	$\text{Pa}^{-1}\text{d}^{-1}$	hydraulic resistance coefficient to flow
$\mu$	Pa s	viscosity
$\varphi$	P	viscosity constant
$\eta$	P	viscosity
$\theta$	$\text{cm}^3 \text{ cm}^{-3}$	volumetric water content

# **Chapter 1            Review: Mitigation of pastoral nitrate leaching by nitrification inhibitors and polymer coated fertilisers - applications, release characteristics and production**

---

## **1.1 Introduction**

The increasing human population and limited land resource is placing stress on the agricultural sector to increase food production from the current area of farmed land. This is illustrated by the intensification of New Zealand pastoral dairy farming with increased milk yield from 5,000 to 7,000 l/ha (MacLeod and Moller 2006) and national nitrogen (N) fertilizer consumption from 20,000 to 244,000 tonnes of N per year from 1989 to 2007 (MAF 2007). The intensification of dairy farming in New Zealand has also seen the conversion of low intensity sheep and cattle farming and forestry to dairy (MacLeod and Moller 2006). This increase in production intensity and N input to the dairy systems raises the risk of environmental damage via nitrate leaching and greenhouse gas emissions from cow urine patches (Ball et al. 1979; Ledgard et al. 1999; Di and Cameron 2002; Silva et al. 2005; Wachendorf et al. 2005).

In New Zealand pastoral dairy farming systems, cows spend most of their day on pasture with only 5 to 6 hr per day spent off the pasture moving to and from milking. This results in over 75% of the urine and dung being returned directly to the pasture. The return of urine poses a significant environmental risk as the concentration of N (mainly as urea) can produce soil surface concentrations equivalent to 500-1000 kgN ha<sup>-1</sup>. The urine N is rapidly converted to nitrate by soil microorganisms, while the nitrogen returned as dung is converted more slowly posing a lower risk (Haynes and Williams 1993).

The high concentration of N in urine patches is the direct result of the oversupply of N as crude protein in the cow's diet. The oversupply from N rich pasture cannot be utilized for the production of milk, maintenance or increasing live weight and is excreted in the form of urea in the urine. The conversion efficiency of N for lactating cows is dominated by the mass balance between the N used for milk production and

feed crude protein (N) intake (Castillo et al. 2001), with the highest efficiency obtained when the feed protein concentration is below 13% (2% N) and total feed ration restricted to 400g N cow<sup>-1</sup> day<sup>-1</sup>. This level of herbage N poses a significant limitation for ryegrass pasture which has an optimal herbage N of between 3 and 5% to maximise dry matter production in summer and winter conditions respectively.

In New Zealand pastures the crude protein content of grass is influenced mainly by an interaction between growth limiting factors such as soil moisture, temperature, fertility, sunshine hours and the supply of N. In the winter with low temperatures and low sunshine hours, or the summer with limiting soil moisture, the application of N to stimulate growth results in luxurious uptake of N by the grass. To minimize the impact of excessive plant N, split dressings of 25 to 50 kg N/ha of N fertiliser applied between grazings over the growing season. This is a labour, energy and cost intensive practice. The application of the nitrification inhibitor dicyandiamide (DCD) post grazing has been proposed as a mitigation strategy to reduce nitrate leaching and nitrous oxide emissions from grazed pasture (Di and Cameron 2002b, 2004b, 2005, 2008; Saggar et al. 2004; Chen et al. 2008; Smith et al. 2008; Di et al. 2009; Sprosen et al. 2009). The application of nitrification inhibitors however, retains soil N and is likely to increase the pasture utilization of urine-N, producing excessive herbage N levels in subsequent grazing cycles, by which time the inhibitor may be inactive or need re-application. DCD is susceptible to both leaching (Corre and Zwart 1995) and decomposition by micro-organisms to ammonia (Kelliher et al. 2008), losses which are strongly influenced by rainfall and temperature respectively

Controlled release coating technology may produce additional benefits when used with N fertiliser and inhibitor products, by allowing more controlled management of herbage N with a synchronous supply of N, and by increasing the longevity of nitrification inhibitors. For this strategy to be effective a low cost controlled release system is required, which can be easily produced and with predictable solute release characteristics. To this end a review of controlled release coated fertiliser production technology, release mechanisms, and of nitrification inhibitors was undertaken to provide information on appropriate coatings and technologies. The review concludes

that polymer coating of both urea and the nitrification inhibitor DCD are worthy for further experimental assessment in both the laboratory (Chapter 2, 5 and 6) and in field trials (Chapter 3 and 4) under New Zealand pastoral systems.

## **1.2 Controlled release coated fertilisers: their production and applications**

Previous reviews of controlled and slow release fertilisers by Shaviv (2001) and Trenkel (1997) have concentrated on the application of these fertilisers to cropping and horticultural systems which produce high value products that offset the higher fertiliser costs. The current market price of coated controlled release fertiliser does not reflect the production costs, but rather the historical market position which has been stabilized by excessive retail margins, with suppliers wholesaling coated fertiliser at NZ\$1,500-2,000 per tonne which retails for NZ\$5,000 to 10,000 per tonne in (2009). This review examines current process technology and reveals a number of production methods which are available for use as coatings, including: sulphur, alkyd resins, reactive layer polyurethanes, poly-olefin, and a number of inorganic compounds.

### ***1.2.1 Sulphur Coated Fertiliser***

Sulphur coating of fertiliser was developed in the 1960s by the Tennessee Valley Authority, in this process ( Figure 1.1) the fertiliser, urea, is preheated to 80 °C and spray coated with molten sulphur heated to 148 °C in a rotary coating drum. The sulphur solidifies forming the initial coating. The coating, however, is prone to numerous flaws (fine cracks) produced by mechanical faults and transformation of the allotropic forms of sulphur during cooling and storage (McClellan and Scheib 1975). These faults are overcome by a secondary coating of 2% wax sealant and coal tar biocide applied to the hot product prior to cooling. On cooling the product may become tacky due to residual oil present in the wax, so a conditioner (2% diatomaceous earth) may be applied to prevent caking (Rindt et al. 1968).

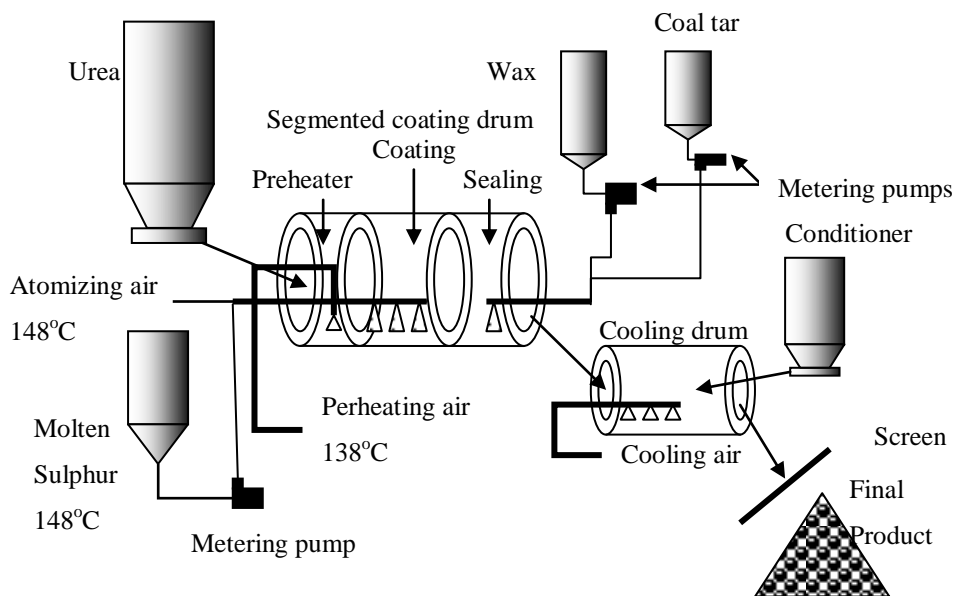


**Figure 1.1 Schematic of TVA pilot plant for sulphur coated urea, using twin fluid sulphur spray. Redrawn from Rindt et al.,(1968).**

The agronomic effectiveness of sulphur coated fertilisers is dependent on their release characteristics, the plant uptake rate and cropping duration. Urea release from sulphur coated urea (SCU) is the result of biological oxidation of the sulphur and sealant, which unblocks sealed pores and reduces the thickness of the coating structure until the coating ruptures resulting in “catastrophic release” or diffusion release via pores. The rate of release is dependent on the granule coating thickness and distribution, which may vary from insufficient to excessive. Typically for a 20% S coated urea, one third of the urea releases immediately, a third over the crop growth period (90 to 150 days) and the remainder over a longer term (Shaviv 2001). The ideal coated product (9% S) produced by TVA using their pilot plant showed advantages over uncoated urea in terms of the dry matter yield of Bermuda grass in a 17 week green-house trial (Rindt et al. 1968). The result showed that a coated product with a release rate of 1% per day produced only 50% of the dry matter relative to uncoated urea in the first 3 weeks. However in the subsequent cuts over the following 14 weeks the cumulative dry matter yield increased to 120% of the uncoated urea yield (Figure 1.2).

A similar yield pattern was observed in field trials of winter forage oat grown on an alkali (pH 8.4) sandy clay loam at the Indian Agricultural Research Institute, New Delhi, India (Joshi and Prasad 1977) during a mild winter (minimum monthly temperature 6.3-8.1°C). In these field trials treatments of 100 and 200 kgN ha<sup>-1</sup> of uncoated urea and SCU with 16% S coating (supplied by TVA) were applied. The uncoated urea was applied in a split application, with 2/3 being drilled in at sowing followed by 1/3 after the first harvest, while all the SCU was drilled at sowing. During the mild winter there was no significant difference in dry matter yield at the first harvest 74 days after sowing, while at the second harvest, 80 days later, the SCU treatment produced a dry matter yield 146% of the urea treatment. However, during the second cooler winter (minimum monthly temperature 4.9-5.9°C) the SCU treatment produced a significantly lower yield in the second harvest with a dry matter yield 56% of the urea treatment, which was attributed to the lower soil temperature.

SCU in New Zealand (NZ) has been evaluated in high country pasture (NZ) to improve the survival and vigour of ryegrass and clover following direct drilling of seed and SCU in weed infested soil (Pollock 1989; Pollock et al. 1994). In Australia, SCU was used as an annual N application (250 kgN ha<sup>-1</sup>) to annual ryegrass (Au) crops (Maschmedt and Cocks 1976). These trials showed that drilling SCU (25-75 kgN ha<sup>-1</sup>) with ryegrass seed increased seedling vigour, while a single application of SCU to annual ryegrass increased herbage N recovery from 44% for urea to 78%. In contrast to these long term results, quick maturing vegetable crops such as potatoes, cantaloupes and tomatoes have shown significantly reduced yield with the application of SCU with 13.5% S coating in comparison to ammonium sulphate and urea (Lorenz et al. 1972). The low yield and N uptake that occurred in these cases was due to a large proportion of granules remaining intact for longer than the crop growing period (Raban 1994).

The studies reported by Rindt et al, (1968) and Joshi and Prasad (1977) showed, while SCU can be effectively produced with low sulphur coating (9% S), the fragile nature of the coating required commercial products to use higher coating levels (16% S) to allow bulk handling and storage. This increase in coating thickness results in a high proportion of urea being released late, which may in cropping situations be longer than

the cropping period, resulting in low yields and wastage of product. Sulphur coated urea with ‘long-tail’ release characteristics has limited application for short term crops. The maximum benefit of SCU is obtained when it is applied in semi-permanent turf and long-term potting mixtures for ornamental plants allowing the full recovery of the applied N (Furuta et al. 1967; Maschmedt and Cocks 1976; Sharma et al. 1982; Sartain and Ingram 1984).

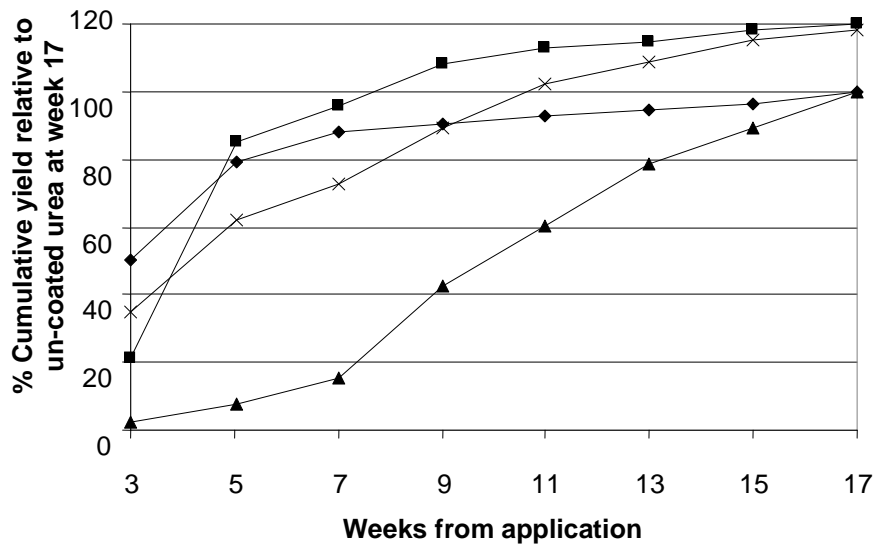


**Figure 1.2** Comparative dry matter yields of Bumarda grass in glasshouse pot trials grown with the addition of  $160 \text{ kgNha}^{-1}$  of 9% (■) and 15% (▲) sulphur coated urea, urea (◆) and a blend of 40% urea and 60% SUC (x). Data from (Rindt et al. 1968)

### 1.2.2 Polymer Coated Sulphur Coated Urea (PCSCU)

A significant improvement to SCU can be made by the addition of a further coating of polymer and/or wax. The combination of polyethylene and paraffin wax in a ratio of 30:70 (Fox 1968) was recommended in TVA bulletin Y-181 (1983) as the industry standard (Goertz et al. 1993). The wax and polymer coating, however, did not reduce the proportion of nutrients released in the tailing period (Raban 1994).

O. M. Scott & Sons Co. in the early 1990's introduced a synthetic wax (Gulftene C30)/ polyethylene- vinyl acetate (ELVAX 420) coating for urea, allowing the sulphur coating to be reduced to 13%, increasing the N content and preventing the "tailing" effect due to excessive coating thickness (Goertz et al. 1993). In this class of product the release rate characteristics were transformed from the 'catastrophic failure' type to a zero order diffusion controlled process dependent on temperature and water vapour pressure. Goertz et al. (1993) used such a product in greenhouse pot trials and demonstrated slower and more even growth and improved colour of Coventry Kentucky Blue-grass over 120 days compared to traditional sulphur coated urea.

In turf response trials PCSCU has reduced nitrate leaching (from 16.8% to 1.7% of applied nitrogen) in comparison to ammonium nitrate [AN] (Guillard and Kopp 2004). This was determined over three years of plot trials using a mixed lawn of Kentucky bluegrass, perennial ryegrass and creeping red fescue grown on Paxton fine sandy loam in southern New England, with a total application of 147 kg-N ha<sup>-1</sup> applied in 3 split dressings in October, May and July, with major leaching events in autumn.

In addition to polyethylene, vinyl acetate and wax coatings, reactive polyurethane coatings (Moore 1987, 1989) have been applied to SCU to increase durability.

The studies described above show that PCSCU can effectively reduce the quantity of sulphur required for coating urea and can improve durability, which in some instances also reduces the "tailing period" and improves N uptake and yields, whilst still significantly reducing nitrate leaching.

### ***1.2.3 Alkyd Resin ( Osmocote® )***

The first commercial product in the USA was developed by Archer Daniels Midland of Minneapolis in the early 1960's (Hansen 1965) resulting in the product marketed as "Osmocote ®" initially by Sierra Chemicals and more recently O. M. Scott and Sons. In the initial patent disclosure, Hansen described a multilayer coating of the co-polymer of cyclopentadiene and soya/linseed oils in a ratio of 18:82 dissolved in 50% solvent (mineral spirits or Kerosene). This was applied to preheated fertiliser at 80 to 100°C in a

drum coater. The drying/curing of the resin was also accelerated by the addition of metal drying agents such as lead oxide or cobalt soap. The copolymer solution was applied at a rate of 3% of the initial fertiliser weight and allowed to dry for 20 min until tack free. Subsequent coatings were applied at 0.5 to 1 % until the required coating level was achieved. The effectiveness of this system was illustrated by coating a number of fertilisers at varying levels and subjecting these to dissolution trials in water at a ratio of 20g in 100 ml at 20°C (Figure 1.3).

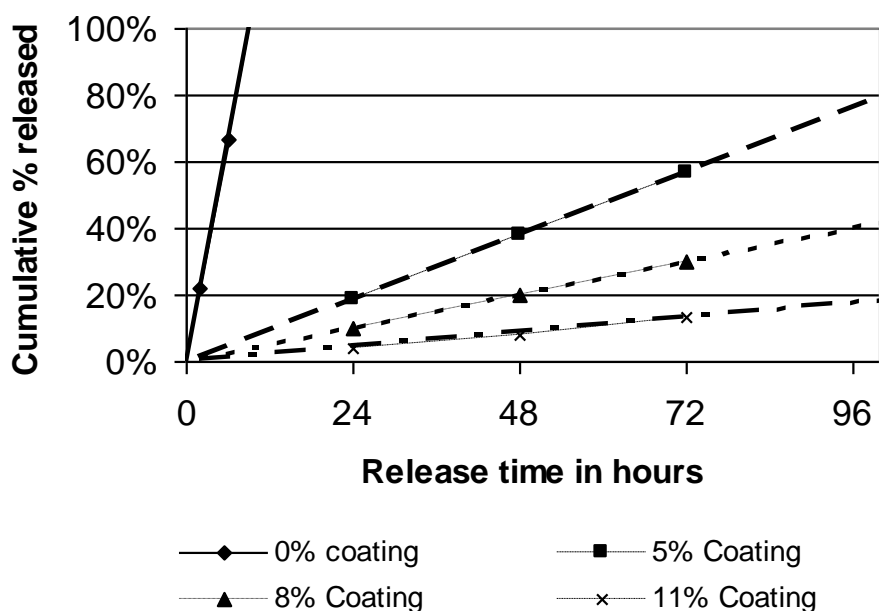


**Figure 1.3** Cumulative release of urea from Soya-cyclopentadiene resin coated urea, with coating expressed as % initial fertilizer weight, data from (Hansen 1965)

Further development of the “Osmocote ®” type product has seen a range of products with release rates from 30 to 270 day developed which are exclusively marketed into the high value nursery and turf markets. Osmocote ® supports a wholesale price of NZ \$26/kg N compared to pastoral farming with a price NZ \$1.34/kg N (2008).

The application of alkyd resin coated fertilisers in the nursery production of trees and shrubs is common practice reducing labour and reducing nutrient runoff. The evaluation of Osmocote ® 38N in potting media compared with the weekly addition of AN solution as N sources, in the growing of Japanese Holly, *Ilex crenata Thunb. Hetzi*. (Sharma et

al. 1982), has shown that over a six month trial period Osmocote<sup>®</sup> 38N produced less leaf nitrogen and dry matter compared to weekly liquid AN feeding at the equivalent amount of N. Osmocote<sup>®</sup> 38N however, reduced N leaching relative to the liquid AN feeding. This revealed a significant conflict between production and environmental concerns in nursery product systems.

In addition to lower productivity, the high initial application rates of controlled release fertilisers in potting media has a potential disadvantage if high temperatures are experienced, as salts may be rapidly released producing osmotic stress on the plant (Huett 1997). In glasshouse trials Huett (1997) found that Osmocote 3-4 month (19N:2.6P:10K) and 90 day Nutricote (16N: 4.4P: 8.3K), which released 80% of their nutrient in 3-4 months and 90 days at 25°C, respectively, posed a significant risk to plant health when mean daily maximum temperatures reached of  $31.8 \pm 2.6$  °C for application rates of  $0.8 \text{ kg N m}^{-3}$  (4.2 and  $5 \text{ kg m}^{-3}$ , respectively). Huett (1997) showed that to maintain the electrical conductivity (EC) of the medium below 1.0 dS/m (1:1.5 extract) in excess of 33.5% of the media volume must be leached every two days, Figure 1.4.

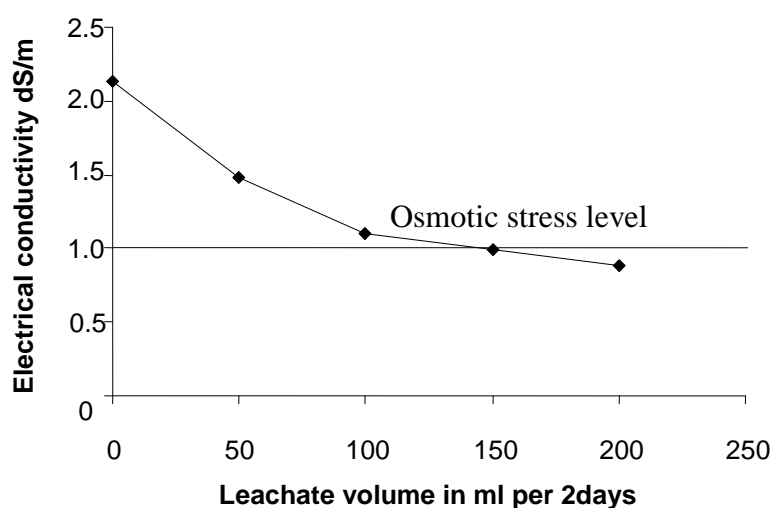


**Figure 1.4** Effect of leaching volume on electrical conductivity of a 1:1.5 extract of potting media exposed to high temperatures in summer  $31.8 \pm 2.6$  °C. Data from Huett (1997).

The results of Huett (1997) are also similar to that of Sartain and Ingram (1984), who found under limited drainage 9 month release Osmocote 18N-2.6P-10K applied at  $0.46 \text{ kg N m}^{-3}$  ( $2.5 \text{ kg m}^{-3}$ ) produced media EC 2 to 3 times higher than compared to SCU and liquid feeding AN at the completion of a 6 month trial.

The application alkyl resin coatings to fertilisers is typically achieved by dissolving the resin in an organic solvent (Hansen 1965), which is likely to result in environmental issues at increased production levels. In potting trials the effectiveness of the coating system was found to be similar to SCU and other low solubility N products.

#### **1.2.4** *Reactive isocyanate coatings*

The development of reactive isocyanate coated fertilisers from the initial catalyzed urethane varnish system (Hansen 1966) to the modern reactive layer coatings RLC<sup>®</sup> system has revitalized coated fertiliser production, allowing rapid coating with low cost equipment and chemicals (Moore 1987;1989; 1990; Detrick and Carney 1994).

In the initial patent by Hansen (1966), the fertiliser was coated with 3% synthetic drying oil (Admerol 351) followed by multiple coatings of catalyzed urethane varnish (50% by weight solution of the reactive isocyanate resin (Arothane 156) dissolved in the volatile organic solvents xylene and Cellosolve acetate (2-ethoxyacetate)) at 104-118 °C to produce a durable slow release fertiliser with a total of 12% resin coating by weight. This system, as in the alkyd resin system, required large quantities of solvent to reduce the viscosity of the polymer, allowing it to coat the granules without agglomeration. The solvents used by Hansen (1966) pose a risk to the aquatic environment (LC<sub>50</sub> of 10 mg l<sup>-1</sup> and 40 mg l<sup>-1</sup>, HSNO data base) and workplace due to toxicity and explosion issues.

These problems were overcome by the RLC® system (Moore 1987;1989;1990) in which no solvent is required, as the reactants have low viscosities and high reaction rates. Moore recognized that nucleophilic groups present in fertilisers such as –NH<sub>2</sub> and –OH ( greater than 15% by weight) could be utilized in a reaction with excess poly-functional isocyanate, poly bisphenyl methyl diisocyanate (MDI ) with 15% unreacted isocyanate (NCO) content by weight, to form a strong adhesive film on the surface of fertiliser granules. The excess isocyanate (1% of initial fertiliser weight) then allows the application of an anhydrous organic polyol (1.4% of initial fertiliser weight) such as PET (polyethyleneterephthalate) dissolved in triethylene glycol with 10% TEA (Triethanolamide) added as a catalyst. The coating process described by Moore (1987, 1989, 1990) were conducted at 110 °C in a drum coater with a curing time of 2 min between applications of MDI and PET solution. Sequential coatings produced products with high abrasion resistance and slow release characteristics exemplified by 3 sequential coating of urea giving an accumulated urea release of 7.4% over 24 hr in water at 37 °C.

Products of polyurethane coatings have been further advanced by Pursell Technologies with the successful production of Polyon® based on the 1994 patent of Detrick and Carney which disclosed a process similar to Moore 1990. Detrick and Carney (1994) pre-wetted the urea with scrubber water, glycerine and TEA, which increases the adhesion of the primary coating and accelerates curing. The sequential coatings were

achieved in this process by injecting reactants into the moving bed of granules at varying positions in the rotary drum, 10 m long and 2 m in diameter. This process is illustrated Figure 1. 5.

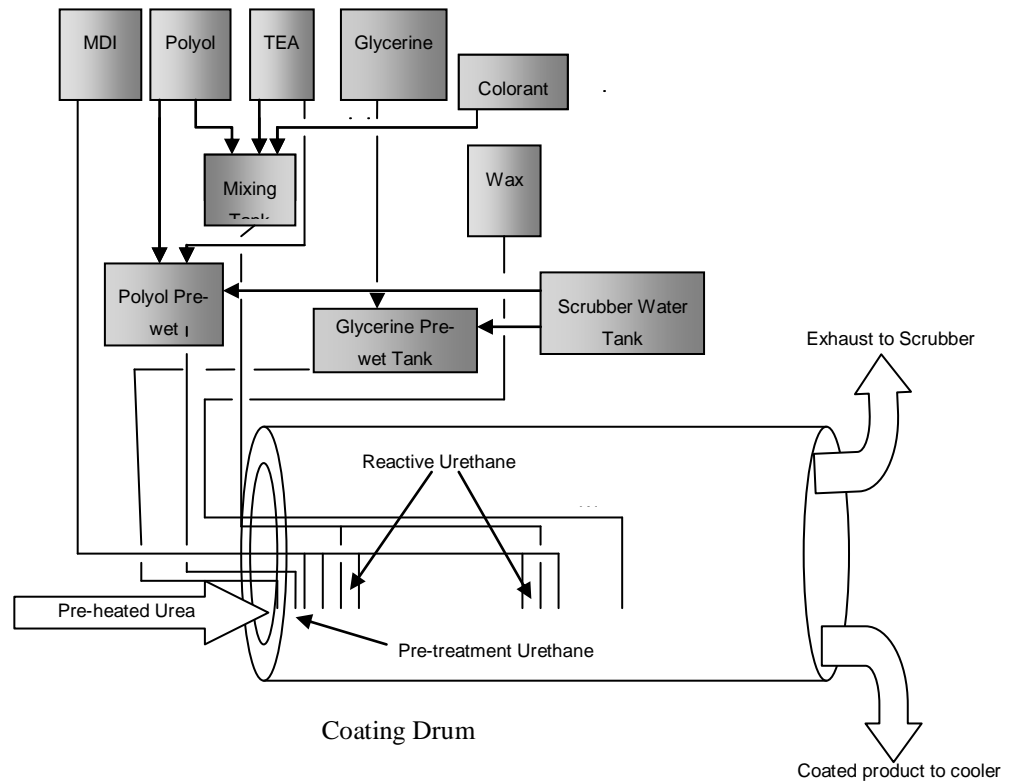


**Figure 1.5 Schematic of continuous reactive urethane coating process derived from Detrick and Carney (1994)**

The positioning of the injectors along the path of the granule flow through the flighted drum allows continuous coating of urea at 2267 kg/hr (Table 1.1).

Agrium has further lowered the cost of production by the use of castor oil (Wynnyk et al. 2004) as a substitute for expensive polyol and has made slow release coated fertilisers viable in the production of maize, rice and wheat. The method described in the patent is similar to that of Hudson and Woodward (1993) with the exception that the wax is added as part of the MDI/Polyol mixture not as a separate coating (Hudson and Woodward 1993).

**Table 1.1 Operating conditions for the Pursell Process  
(Detrick and Carney 1994)**

<b>Product</b>	<b>Flow Rate kg/hr</b>	<b>Addition Point</b>	<b>Reactants</b>
Urea	2267		
First Layer			
Pretreat- water/polyol/ catalyst	11.3	0.304 m	70% water,20% glycerine, 10% TEA
Second Pretreat			
Polyol/catalyst/water	5.6	0.609 m	81% Polyol, 9% TEA, 10% water
MDI	7.5	0.910 m	MDI( diphenylmethane diisocynate)
Second Layer			
MDI	3.7	1.000 m	
Polyol	5.7	1.100 m	
MDI	3.7	1.478 m	
Third Layer			
MDI	3.7	2.230 m	
Polyol	5.7	2.387 m	
MDI	3.7	2.640 m	
Fourth Layer			
Wax	4.2	3.000 m	

Agrium has carried out over 135 field trials of their polyurethane coated urea product marketed as ESN® in Canada and the US corn belt (Blaylock et al. 2005). They report an average yield increase in maize of 0.55 t/ha with 21% of trials obtaining an increase greater than of 0.75 t/ha compared to equivalent N applications in the form of UAN (urea ammonium nitrate liquid injection) pre-planting over the 2000-2003 seasons (Table 1.2).

**Table 1.2 Expected yields increases for Maize grown in the US Corn belt  
based on data from (Blaylock et al. 2005)**

<b>Corn yield difference T /ha</b>	<i>-0.5</i>	<i>-0.25</i>	<i>0</i>	<i>0.25</i>	<i>0.5</i>			
	<i>to</i>	<i>to</i>	<i>to</i>	<i>to</i>	<i>to</i>			
	<i>&lt; -0.5</i>	<i>-0.25</i>	<i>0</i>	<i>0</i>	<i>0.25</i>	<i>0.5</i>	<i>&gt; 0.75</i>	
% of total comparisons	4.3%	2.9%	8.0%	16.0%	15.3%	15.3%	16.7%	21.0%

Environmentally ESN® has been shown to reduce the loss of N to the environment as nitrous oxide reducing N<sub>2</sub>O losses from 0.73% of applied urea-N to 0.37% and reduced nitrate leaching losses by 42% for fall applications on winter wheat (Agrium 2007b)

ESN® has also been shown to produce similar yields in potatoes with one application (200 kgN ha<sup>-1</sup>) at planting compared with six applications of urea throughout the growing season (Agrium 2007a).

### ***1.2.5 Poly-Olefins coatings- Solvent based***

Polyolefin coatings have been primarily developed in Japan for the rice growing industry by Chisso-Asahi Fertilizer Co, which have marketed their products as Nutricote® and Meister®. This class of coating is applied as a hot resin solution in solvent (Fujita et al. 1977; 1983) using a spouted bed or drum coater. Fujita et al. (1977) applied a coating solution of 3% low density polyethylene or polypropylene (MW ≈ 20,000) by weight dissolved in tetrachloroethylene to fertiliser granules in a spouted bed coater. The temperature within the spouted bed was maintained 10-30 °C higher than the gelation point of the polymer/solvent system. This allows drying of the polymer solution on the granule surface without formation of a gel, which may foam resulting in a porous film. The selection of polymer and solvent is made so that the boiling point of the solvent is at least 20°C higher than the gelation point to allow preparation of a solution at atmospheric pressure. Fujita et al. (1977) demonstrated these coating conditions at a pilot plant scale, coating granular complex fertilizer (Sun Nitro No.1.N: P<sub>2</sub>O<sub>5</sub>:K<sub>2</sub>O 15:15:12 ) with a 3% solution of polyethylene resin ( Asahi Dow Co. M-7620) in tetrachloroethylene (b.p. 121 °C), applied at a rate of 3.5kg/min of resin solution over 15 min to a 50 kg charge of fertiliser. The spouted bed coater was maintained at 60°C (T<sub>2</sub>,T<sub>3</sub>)( gelation point 54°C) by inlet air temperature, T<sub>1</sub>, of 120°C and flow of 15 m<sup>3</sup>/min( Figure 1.6) .

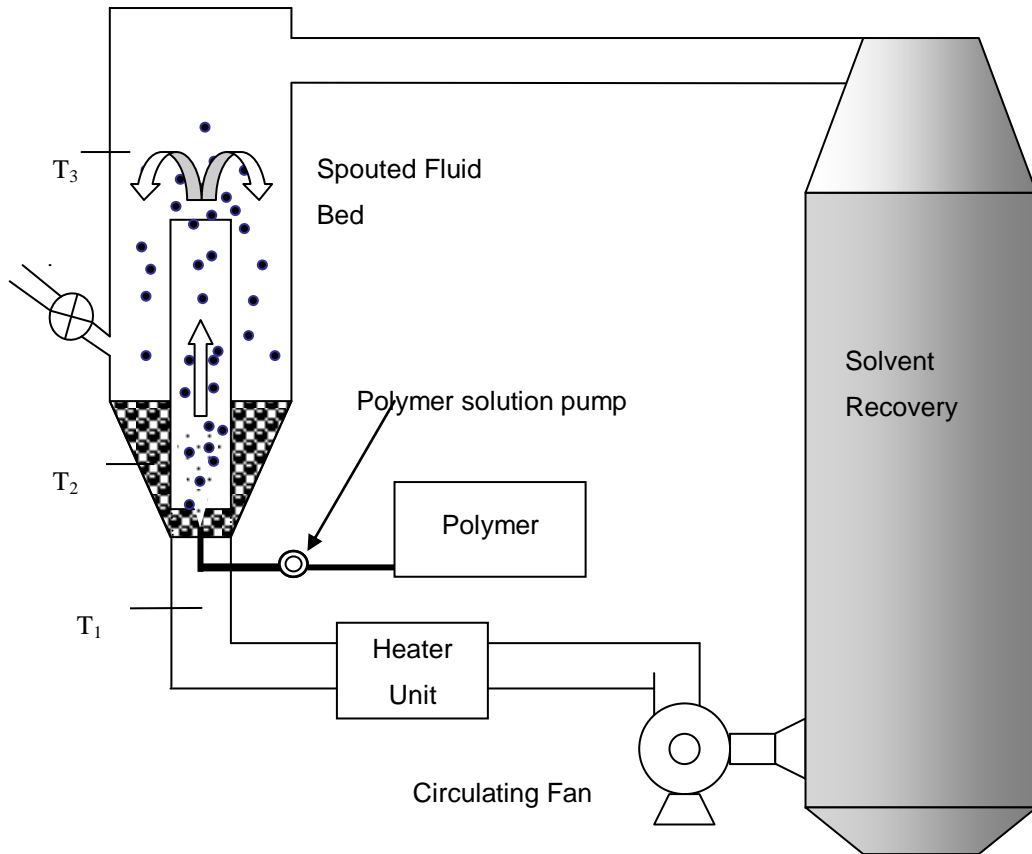


**Figure 1.6 Schematic of Spouted bed coater for the application of poly-olefin coatings. Derived from Fujita et al. (1977).**

The dissolution rate of this product at 25°C in water was found to be 0.5% in 24 hr and less than 20% in 200 days. The addition of nonionic surfactant (octaoxyethylene nonylphenyl ether) from 0.25 % to 15 % allows the adjustment of the release rate of 80% of urea from greater than 200 days to 50 days (Figure 1.7). In addition to the nonionic surfactant octaoxyethylene nonylphenyl ether the addition of polyethylene oxide (Kosuge et al. 1992) also produced similar results.

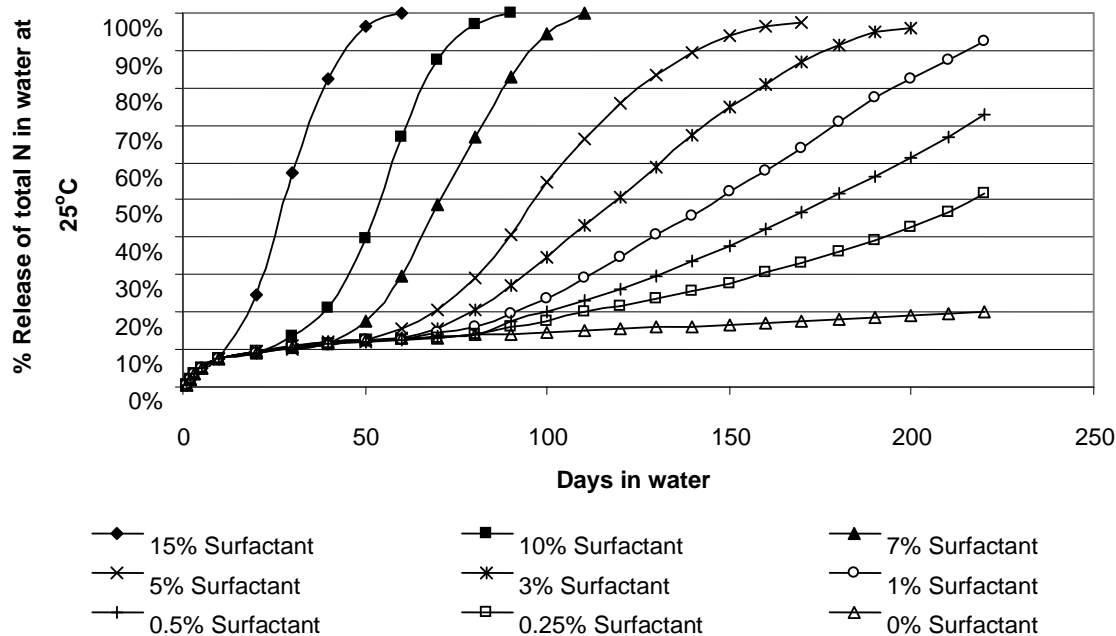


**Figure 1.7 Release characteristics of 3 % low density polyethylene coatings with the addition of 0 to 15% surfactant (octaoxyethylene nonylphenyl ether) in the coating. Data from Fujita et al. (1977).**

### 1.2.6 Poly-Olefins coatings -Thermoplastic

In addition to solvent based coatings a number of thermoplastic melt coatings have been developed using the co-polymer of ethylene- vinyl acetate and wax (Fox 1968) are generally classed as wax coated fertiliser as the polymer weight is lower than the poly-olefin coatings and the wax acts as the solvent.

In three consecutive seasons ( April – Sept 1997, 1998, 1999) of irrigated summer potato production on a loamy sand at Becker, Minnesota, poly-olefin coated urea reduced nitrate leaching by 34 to 49 % compared to three applications of urea over the growing season (Zvomuya et al. 2003). In addition to the reduction in nitrate leaching it has been found that poly-olefin coated urea reduces N<sub>2</sub>O emissions by 35% in barley crops (Pauly et al. 2002) and 80% in carrot production (Shoji and Kanno 1994).

The coating of urea with a film such as low density polyethylene (LDPE) (Salman 1989) has proved a useful method of stabilising mixtures of urea and superphosphate. Salman (1989) found that a 2.8% coating of LDPE prepared in a fluid bed coater with a urea release time of 80% in water at 22°C of 3 days produced compatible (dry and free flowing) mixtures with superphosphate after 10 days storage at 30 °C. However after 30 days the mixture had become damp but remained free flowing. The increase in coating weight to 5.7% reduced the release rate to 10% in 7 days and improved the compatible storage time to 30 days with the mixture becoming damp but free flowing by 60 days.

The application of poly olefin coatings to fertilisers using a spouted bed coater results in high quality products which can be tailored to give different release rates by the addition of surfactants to the polymer/solvent coating agent. The system requires considerable energy to heat and move the air which dries the resins while transporting the coated particle. In addition to the high energy requirement, the recovery of solvent poses a significant safety risk.

### ***1.2.7 Inorganic coatings***

Partially soluble phosphates such as magnesium ammonium phosphate have successfully been used in combination with reactive binders to produce a long lasting coated urea. This appears to have been developed by the Zhengzhou Centre of Popularization & Research in China and commercialized by Lg Fertiliser Corporation. It is marketed as Luxecote for the American golf course and horticultural markets. This type of product is produced (Diping et al. 1998) by the application of formaldehyde solution (37%), urea, magnesium oxide and mono-ammonium phosphate at a ratio of 1.3:3.6: 5: 17 and 7 %, respectively to the initial weight of urea, pre-heated to 60°C. A second coating of ammonium magnesium phosphate is applied using a binder solution of sulphuric and phosphoric acids with the continuous addition of mono-ammonium phosphate and potassium chloride powders at ratios of 7:3:5:21, achieving an additional 26 % of coating by weight. This is finally sealed by a coating of 5% calcium carbonate/stearate to form a hydrophobic layer. The chemical reactions in this coating process produce a range of low solubility salts which appear to slow the release of urea and produce a sustained N release rate from low solubility ammonium compounds.

In New Zealand, two coated ureas have been developed to allow the mixing of urea with single superphosphate to achieve high nutrient analysis blends and chemical and physical stability. One product utilizing an inorganic calcium sulphate concretion and sealant layer is produced by FERTCO and the second, a more recent product Pasturzeal G2<sup>®</sup> by Ballance Agri- Nutrients, also utilizes an inorganic coating system which is undisclosed. These products allow the stable mixing of urea and single superphosphate, but provide no slowing of N release rates.

### **1.3 Release Mechanisms of Controlled Release Fertilisers**

Controlled release fertilisers have shown advantages over traditional, soluble fertilisers in terms of increased yields (Shoji and Kanno 1994; Blaylock et al. 2005), nutrient uptake efficiency (Hutchinson et al. 2003) and the prevention of losses via denitrification, leaching or volatilisation (Pauly et al. 2002; Zvomuya et al. 2003). This is accomplished by coating the core fertilizer particle with a water repellent film such as wax and polymer, or sparingly soluble compounds like sulphur or phosphates, which restrict the contact between the soil and the fertiliser. These coatings can increase yields by sustaining nutrient release over the growing period of the crop, preventing the initial luxurious uptake of nutrients followed by deficiency in the later growth phase (Rindt et al. 1968; Allen and Mays 1971a,b; Shoji and Kanno 1994; Guillard and Kopp 2004; Blaylock et al. 2005). These advantages require a sound understanding of the mechanisms of nutrient release and the production factors effecting product release.

Within the spectrum of coating granules, the internal soluble material may be released by a number of mechanisms depending on the structure of the coating layer. This layer may be *permeable*, *semi-permeable* or *impermeable*. *Permeable* coatings are typical of gels, for example, hydroxymethylcellulose or acrylic. These form a liquid phase across which species may diffuse. An osmotic gradient drives water ingress, and a concentration gradient drives solute diffusion outwards. *Semi-permeable* membrane is typical of alkyd resins. These membranes are elastic and stretch as water ingress occurs along the osmotic gradient. As they stretch, micro-pores open allowing transfer along these channels. When the ingress of water along the osmotic gradient has resulted in a

hydrostatic pressure difference across the membrane, convective flow of the solute solution will occur. If no hydrostatic gradient has formed however, then diffusion will dominate mass transfer. In both the permeable and semi-permeable membrane cases, the ingress of water that causes the membrane to stretch may also result in membrane rupture and catastrophic release of the granule contents. *Impermeable* membranes are typical of sulphur coatings. No transfer occurs across the membrane, but the membrane may be perforated by macro-pores. Two-way diffusion occurs, of water into the granule and solute out of the granule.

Within a population of granules coated by one type of membrane, a combination of release mechanisms may occur, depending on the granule size, the coating thickness and the pore size distribution (if pores are present). As these factors vary within a population of coated granules, the release of nutrients is a population effect and criteria are required to proportion the mechanisms of release throughout the population. Thus, there is potential to manipulate coating properties based on these criteria to give the desired release characteristics.

If the coating hydrates, forming a gel or liquid phase, the release of nutrient may also include molecular diffusion through the coating. Molecular diffusion is not developed further in this thesis as most fertiliser coatings are hydrophobic which limits nutrient release to pore related processes defined by the semi-permeable and impermeable release processes.

Currently the release characteristics of coated controlled-release fertilisers have been described based on four mechanisms which variously apply to the three membrane types described above. These are; the “rupture”(Allen and Mays 1971; Raban 1994; Shaviv et al. 2003a ), the “permeability” (Shaviv et al. 2003a,b; Du et al. 2006), the “osmotic pumping” (Theeuwes 1975; Ko et al. 1996), and the “orifice diffusion” model (Jarrell and Boersma 1980). These mechanisms consider a number of properties of the polymer film, internal granule and external media (Figure 1.8). Each is developed into models and described in detail in the following sections.

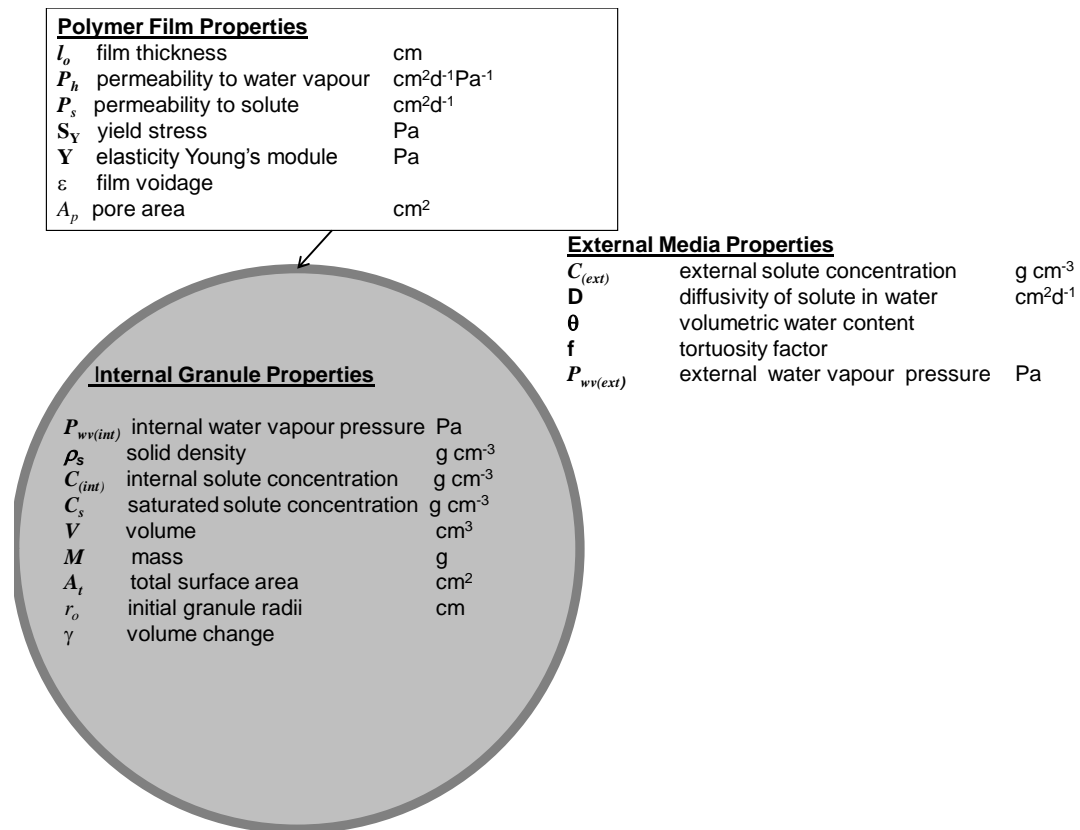


**Figure 1.8 Summary of factors contributing to release of nutrients from a coated controlled release fertiliser**

### 1.3.1 Rupture Model

In the rupture mechanism the release of the nutrient from the coated fertiliser is via:

- the failure of the coating system by either dissolution of the coating assisted by soil environmental factors such as bacterial action, or pH as in the case of sulphur coated urea (Allen et al. 1971).
- and/or mechanical rupture of a polymer coating resulting from an increase in volume and internal pressure from over hydration of coated granules, resulting in “catastrophic release”(Goertz 1993a).

The mechanical rupture release mechanism was described and modelled by Shaviv et al. (2003a,b) S who analysed the internal forces within a single granule and defined the time to rupture in days,  $t_r$ . This is based on an ingress rate of water into the granule

which causes swelling. Initially, the inside of the granule consists only of urea. Water vapour entering the granule will be absorbed by the urea and will follow an adsorption isotherm. However, only a tiny amount of water is required to drive the internal water activity to 1.0, thereafter the water vapour pressure will be that in equilibrium with the saturation solution of urea. Only this latter value is assumed in this work. The water vapour pressure on the external surface of the granule is saturated at the ambient temperature, which may vary. The driving force is therefore the difference between these values,  $\Delta P_w$ . The coating layer has a measured rupture stress, defined here as the yield stress of the coating,  $Y$  (Pa). The ingress of water vapour adds to the volume of the granule. The volume change causes the coating to stretch, where the elasticity of the coating is defined by the Young's modulus. The increase in pressure that this causes is insignificant compared to the osmotic pressure required to equalise the driving water vapour pressure gradient. The time to rupture can then be expressed as function of the granule radius,  $r_o$  (cm), the coating thickness,  $l_o$  (cm), the yield stress of the coating,  $S_Y$  (Pa), the water permeability of the coating,  $P_h$  ( $\text{cm}^2\text{d}^{-1}\text{Pa}^{-1}$ ), the water vapour pressure gradient across the coating,  $\Delta P_{wv}$  (Pa,  $P_{wv(\text{ext})} - P_{wv(\text{int})}$ ), and the Young's modulus of elasticity of the coating,  $Y$  (Pa) (Equation 1.1).

$$t_r \cong \frac{r_o l_o S_Y}{Y P_h \Delta P_{wv}} \quad \text{Eq. 1.1}$$

The variables  $r_o$  and  $l_o$  vary across a population of coated granules. The application of equation 1.1 summed over the population can produce the population release characteristic. However,  $l_o$  is not the average coating thickness, but some statistical lower bound of coating thickness because rupture will occur at the weakest or thinnest section of the coating membrane.

Furthermore, if failure is assisted by dissolution, then  $l_o$  may change with time and needs to be expressed as  $l_t$ . Dissolution can be modelled simply by molecular diffusion using the concentration gradient between the saturation concentration of the coating solute at the surface and an assumed bulk media concentration. The resistance relates to the soil diffusivity which is a function of moisture, temperature and soil structure. The

development of the concentration gradient depends on environmental factors in the soil, such as microbial activity. For example, *thiobacillus* bacteria oxidises sulphur (in sulphur coated urea) to sulphate, which provides a surface to bulk concentration gradient and the oxidation of hydrocarbon sealant by soil microbes allowing pores to become unblocked (Jarrell and Boersma 1979). Therefore, the surface concentration depends on many soil factors and needs to be determined for each soil.

### **1.3.2 Permeability Models**

The above rupture mechanism assumes that rupture occurs a short time after the granule is immersed in the soil environment. If rupture does not occur then, over longer timeframes, diffusion of the material from the granule can occur into the soil. The treatment of diffusion release has been described using three models;

1. a combined water vapour and solute permeability termed the permeable membrane model (Shaviv et al. 2003a),
2. the osmotic pumping model, in which the release is governed by the ingress of water pressurising the granule coating until some of the internal solution is expressed through the pores (Theeuwes 1975; Ko et al. 1996),
3. and the orifice diffusion model in which water and solute diffuse freely via pores in an impermeable coating (Jarrell and Boersma 1979).

In a permeable membrane model the movement of both water and nutrient is allowed, Shaviv et al. (2003a) proposed a three stage model;

1. an initial stage of zero release called the lag period from  $t=0$  to  $t=t'$ ,
2. constant release rate stage between  $t'$  and  $t^*$ ,
3. a gradual decay of the rate stage beginning at  $t= t^*$ .

In the lag period, water vapour penetrates the coating and begins to dissolve the inner fertilizer particle filling the voids within the coated granule without loss of nutrient solution through the coating, as discussed in the rupture model. When the voids are full, the granule then swells if the coating is elastic. In the constant rate stage, a critical volume and thus pressure is reached which is less than the rupture point (discussed

above) and the nutrient solution permeates through the coating into the surrounding media. Permeation can be at a molecular (within the coating) or porous (via wetted channels). This section discusses only molecular permeability. Later, the porous model is discussed, when there are pores in an otherwise impermeable membrane. In the gradual decay stage, the solid core of the particle is totally dissolved and only a solution of solute remains. With continued permeation, the concentration of the internal solution begins to fall reducing the differential concentration and pressure across the coating membrane, which results in a reduced rate of fertiliser release. The three stages are represented mathematically by Shaviv et al. (2003a) as:

$$Q(r,l,t) = \begin{cases} 0 & t_o < t' \quad \text{where } t' = \frac{\varepsilon_g r_o l_o}{3W' \Delta P_{wv}} & \text{Eq.1.2(a)} \\ \frac{3P_s C_{sat}}{r_o \rho_s l_o} (t_o - t'), t' \leq t_o < t^* & \text{where } t^* = t' + \left(1 - \frac{C_{sat}}{\rho_s}\right) \left(\frac{r_o l_o \rho_s}{3P_s C_{sat}}\right) & \text{Eq.1.2(b)} \\ 1 - \frac{C_{sat}}{\rho_s} \exp\left[-\frac{3P_s}{r_o l_o} (t_o - t^*)\right] & \text{where } t_o \leq t^* & \text{Eq.1.2(c)} \end{cases}$$

where  $Q$  is the dimensionless relative release of nutrients  $\left(\frac{M_o - M_t}{M_o}\right)$  as a function of;  $\varepsilon_g$  ~ the total fraction of voids within the granule,  $\Delta P_{wv}$  ~ the differential vapour pressure between the ambient and the saturated solution (Pa),  $W'$  ( $\text{cm}^2 \text{ day}^{-1} \text{ Pa}^{-1}$ ) and  $P_s$  ( $\text{cm}^2 \text{ day}^{-1}$ ) ~ the water and solute permeability coefficients of the coating,  $\rho_s$  ~ density of solid ( $\text{g cm}^{-3}$ ), and  $C_{sat}$  ~ concentration of saturated solution ( $\text{g cm}^{-3}$ ).

The term  $\varepsilon_g$  requires discussion. In this model, the void fraction is calculated by determining the density of the granule and comparing it to the substance density of the material. If the granule density is lower, then the difference is attributed to void volume. This expression is analogous, but different, to the ratio  $S_y/Y$  in the rupture model, where  $S_y/Y$  represents the maximum proportional volume change due to elastic stretching of the granule during swelling. The rupture model does not account of any void volume, and the permeability model does not account for any elasticity. While the concepts are different, the result will be similar. The differences will be greatest at the

two extremes of high voidage or high elasticity; when voidage is high at  $t = 0$ , the rupture model will grossly under predict the rupture time, and when the coating is highly elastic, the permeability model then  $\varepsilon_g$  will underestimate the volume change.

Also requiring discussion are the permeabilities, which results from the conditions under which mass transport occurs in the membrane. During the lag time (Equation 1.2a) transport across the membrane is assumed to be in the vapour phase, while the in constant and falling release rates (Equations 1.2 b and c) it is assumed to be liquid phase. This mass transport phase difference means the constant rate period to be simply solved, but the falling rate period requires a numerical solution. This is explored in Chapter 2.

### 1.3.3 Osmotic pumping model

In the osmotic pumping model the release assumes a semi-permeable coating (Theeuwes 1975; Ko et al. 1996) and is described by five stages of solute release:

1. the solute causes water to move osmotically in through the coating;
2. due to the semi-permeable property of the coating hydrostatic pressure is developed inside the coated shell;
3. the pressure stretches the coating until holes or cracks appear;
4. the nutrient is released by osmotic pumping and diffusion from the holes at a constant rate; and
5. once all the solute within the coating has dissolved the release rate falls as the concentration and so the osmotic pressure difference fall.

Theeuwes (1975) and Ko et al. (1996) mathematically define the constant release rate,

$\left(\frac{dm}{dt}\right)_{const}$ , (Equation 1.3) and the falling rate periods,  $\left(\frac{dm}{dt}\right)_{falling}$ , (Equation 1.6).

$$\left(\frac{dm}{dt}\right)_{const} = \frac{A_t}{l_o} L_p \delta (\Delta\pi - \Delta P) C_{sat} \quad Eq. 1.3$$

where  $A_t$  is the total membrane area,  $l_o$  is the film thickness (cm),  $L_p$  is the hydraulic permeability ( $\text{cm}^2$ ),  $\delta$  is the a hydraulic resistance coefficient to flow ( $\text{Pa}^{-1}\text{d}^{-1}$ , the inverse of viscosity),  $\Delta\pi$  is the osmotic pressure difference (Pa) and  $\Delta P$  is the hydrostatic pressure difference (Pa). As the osmotic pressure is assumed to be far greater than the hydrostatic pressure resisting the flow, the equation simplifies to;

$$\left(\frac{dm}{dt}\right)_{const} = \frac{A_t}{l_o} L_p \delta \Delta\pi C_{sat} \quad \text{Eq. 1.4}$$

The actual osmotic pressure however is limited by the tensile strength of the coating preventing rupture and the balance between water ingress and the viscous resistance of the internal solution egress through the large pores of the coating.

At time  $t^*$ , defined in equation 1.2b, all the solid inside the granule has dissolved. After this time the internal solution concentration ( $C_{(int)}$ ) falls and the release rate slows. Theeuwes (1975) ignored the initial lag period and calculated the time at which all internal solid dissolved from the constant rate,  $(dm/dt)_{const}$ , per equation 1.5.

$$t^* = M_o \left(1 - \frac{C_{sat}}{\rho_s}\right) \frac{1}{(dm/dt)_{const}} \quad \text{Eq. 1.5}$$

Theeuwes (1975) then calculated the falling rate based on the conservation of volume of the system and defining a new constant the volumetric flux at time  $t$  as,  $F_{(t)} = \frac{A_t}{l_o} L_p \delta \Delta\pi$  ( $\text{cm}^3\text{d}^{-1}$ ) and expressed the falling rate period in terms of the dimensionless flux at time  $t > t^*$ ,  $F'_{(t)} = \frac{F_{(t)}}{F_{(t^*)}}$ , with is the flux at time  $t$  ( $F_{(t)}$ ), when  $t > t^*$  divided by the constant rate flux at time  $t^*$  ( $F_{(t^*)}$ ). Theeuwes (1975) assumes that the hydraulic conductivity of the membrane ( $L_p \delta$ ) remains constant during this period; however this is a simplification, as the internal concentration falls the viscosity of the internal fluid will reduce resulting in an increase in  $\delta$  and thus hydraulic conductivity. In addition to this simplification it is assumed that the flux  $F_{(t)}$  is proportional change in osmotic pressure defined by the ratio of internal solute concentration at time  $t$  ( $C_{(t)}$ ) over the

saturated solution concentration ( $C_{sat}$ ),  $F'(t) = \frac{F(t)}{F(t^*)} = \frac{\Delta\pi(t)}{\Delta\pi_{sat}} = \frac{C(t)}{C_{sat}}$ . However this is only true for dilute and ideal solution at equilibrium. Theeuwes (1975) then use this approximation to solve the falling rate.

$$\left(\frac{dm}{dt}\right)_{falling} = \frac{\left(\frac{dm}{dt}\right)_{const}}{\left[1 + \frac{1}{C_s V} \left(\frac{dm}{dt}\right)_{const} (t - t^*)\right]^2} \quad \text{for } t > t^* \quad \text{Eq. 1.6}$$

Theeuwes (1975), in the evaluation of the model, measured a value of  $L_p \delta \Delta\pi$ , termed solute permeability,  $P_s$ , and marked the permeability component of Equation 1.4 equivalent to the solution of Shaviv et al.(2003a), who derived their model using a diffusivity approach.

#### 1.3.4 Orifice diffusion model

If the coating is impermeable to both water and the solute, such as an elemental sulphur coat, mass transport can only occur by simple orifice diffusion. Jarrell and Boersma (1980) considered the constant rate period (Equation 1.7) to be a function of the solute diffusion coefficient,  $D_s$  ( $\text{cm}^2\text{d}^{-1}$ ) through a pore area,  $A_p$  ( $\text{cm}^2$ ) across the coating thickness,  $l_o$  (cm). Assuming the concentration of nutrient to be zero at the coating surface, the driving force concentration gradient, becomes the saturated solution concentration,  $C_{sat}$ .

$$\left(\frac{dm}{dt}\right)_{const} = \frac{D_s A_p C_{sat}}{l_o} \quad \text{for } t < t^* \quad \text{Eq. 1.7}$$

Following the constant rate period which lasts until the solute within the coated granule has dissolved (Equation 1.8). The rate of release the falls as the concentration of the internal solution falls (Equation 1.9),

$$t^* = \frac{l_o}{D_s A_p} \left( \frac{M_o - C_{sat} V_c}{C_{sat}} \right) \quad \text{Eq. 1.8}$$

$$Q_{(t)} = 1 - (1 - Q_{(t^*)}) e^{\left( \frac{D_s A_p}{V l_o} (t - t^*) \right)} \quad \text{for } t > t^* \quad \text{Eq. 1.9}$$

where  $V_c$  (cm<sup>3</sup>) is the volume of the granule at the end of the constant rate period,  $M_o$  is the initial granule mass (g) and  $Q_{(t^*)}$  is the dimensionless relative mass released at time  $t^*$ .

### 1.3.5 Combined models

In the combined model Ko *et al.* (1996) consider the net release from a coated granule to be combined result of osmotic pumping, orifice diffusion and molecular diffusion through the coating.

$$\left( \frac{dm}{dt} \right)_{const} = \frac{A_t}{l_o} L_p \delta \Delta \pi C_{sat} + \frac{A_t}{l_o} \varepsilon_{mac} D_s \Delta C + \frac{A_t}{l_o} D'_s \Delta C \quad \text{Eq 1.10}$$

where  $\varepsilon_{mac}$  is the relative macro-pore area of the coating,  $D_s$  is the diffusion coefficient for the solute in water (cm<sup>2</sup> d<sup>-1</sup>) and  $D'_s$  is the diffusion coefficient of solute in the coating media.

Assuming  $C_{sat}$  and  $\Delta C$  are equivalent, Ko *et al.* (1996) produced a bulked solute permeability coefficient ( $L_p \delta \Delta \pi + \varepsilon_{mac} D_s + D'_s$ ) equivalent to the permeability coefficient used by Shaviv *et al.* (2003)  $P_s$ .

$$\left( \frac{dm}{dt} \right)_{const} = \frac{A_t}{l_o} (L_p \delta \Delta \pi + \varepsilon_{mac} D_s + (1 - \varepsilon_{mac}) D'_s) C_{sat} \quad \text{Eq1.11}$$

For this to represent a fundamental model, the osmotic pumping component requires a solution as  $\Delta \pi$  is not independently known, due to the osmotic pressure development

within the coated granule being a dynamic equilibrium between water ingress, volume change, coating elasticity and hydraulic conductivity (Section 2.2). Ko et al. (1996) use the ideal solution approximation to define the osmotic pressure during the falling rate period as,  $\Delta\pi = \frac{\Delta\pi_{sat} C_s}{C_{sat}}$ , the osmotic pressure at the saturated solution concentration ( $\Delta\pi_{sat}$ ) multiplied by the ratio of internal solute concentration ( $C_s$ ) over the saturated solution concentration ( $C_{sat}$ ) and ignored the diffusion of solute through the coating material. As the change in mass of solute with time  $\frac{dm}{dt}$  is equal to the granule volume (assumed to be  $V_o$  and constant) multiplied by the rate of concentration change with time within the granule  $\frac{dm}{dt} = -V \frac{dC}{dt}$ . By substitution into Equation 1.11 the rate equation 1.12 is then obtained.

$$\frac{-dC_s}{dt} = \frac{A_t L_p \delta \Delta \pi_{sat}}{V_o l_o C_{sat}} C_{s(t)}^2 + \frac{A_t \varepsilon_{mac} D_s}{V_o l_o} C_{s(t)} \quad Eq. 1.12$$

The integration of equation 1.12 with respects to time  $t$  allows the concentration at time ( $C_{s(t)}$ ) during the falling rate to be calculated.

$$C_{s(t)} = \frac{\varepsilon_{mac} D_s C_{sat}}{(L_p \delta \Delta \pi_{sat} + \varepsilon_{mac} D_s) e^{\left(\frac{A_t \varepsilon_{mac} D_s}{V_o} (t-t^*)\right)} - L_p \delta \Delta \pi_{sat}} \quad Eq. 1.13$$

The rate function for the falling rate period is then calculated by substitution into equation 1.12 multiplied by the volume of the granule to give the mass rate.

$$\begin{aligned} & \left(\frac{dm}{dt}\right)_{falling} \\ &= \frac{A_t (\varepsilon_{mac} D_s)^2 C_{sat} (L_p \delta \Delta \pi_{sat} + \varepsilon_{mac} D_s) e^{\left(\frac{A_t \varepsilon_{mac} D_s}{V_o} (t-t^*)\right)}}{l_o \left[ (L_p \delta \Delta \pi_{sat} + \varepsilon_{mac} D_s) e^{\left(\frac{A_t \varepsilon_{mac} D_s}{V_o} (t-t^*)\right)} - L_p \delta \Delta \pi_{sat} \right]^2} \quad Eq. 1.14 \end{aligned}$$

To avoid integration of the equation over time to determine, Ko et al. (1996) calculate the proportional amount released at time ( $t$ ) by subtracting the mass of solute remaining

( $m_t = C_{s(t)}V$ ) from the initial mass( $M$ ).

$$\begin{aligned}
 Q_{(t)} &= 1 - \frac{C_{s(t)}V}{M_o} \\
 &= 1 - \frac{V\varepsilon_{mac}D_sC_{sat}}{M_o(L_p\delta\Delta\pi_{sat} + \varepsilon_{mac}D_s) e^{\left(\frac{At\varepsilon_{mac}D_s}{V_o}(t-t^*)\right)} - L_p\delta\Delta\pi_{sat}} \quad Eq. 1.15
 \end{aligned}$$

### 1.3.6 Modelling parameters

The modelling parameters used in the previous descriptions of nutrient release from coated fertilisers require further discussions as they are not all independent variables, or considered in the same way by different authors.

#### *Film Elasticity and Volume Change*

In the case of elastic coatings, the volume of the granule can increase prior to permeation occurring (hole formation), or rupture. This is described by Shaviv et al. (2003a) in the rupture model (Equation 1.1) by the stretching of the coating to its ultimate strain ( $S_y/Y$ ). This is later substituted by  $\varepsilon_g$  the volume increase (Shaviv et al. 2003a), which accounts for the porosity of the coated granule (Equation 1.2a). Both these factors result in the expression of a lag time, which allows the granule to fill prior to release or rupture. In the osmotic pumping model, Theeuwes (1975) and Ko et al. (1996) considered a lag phase that corresponds to the time taken for the internal pressure in the coated granule to stretch the coating resulting in hole development. This was not presented as a mathematical expression. For the orifice diffusion model of Jarrell & Boersma (1980), no lag time occurs as the rate of dissolution of the solid and diffusion are only limited by the pore or hole area resulting in a rapid onset of release. In addition to the stretching of the polymer coating and the filling of internal voids in the coated granule, the non-spherical nature of commercial fertilisers must also be considered, as the volume change associated with the transformation of the coating from irregular shaped or spheroid geometries to more spherical geometries is likely to result in additional granular volume changes.

### *Variable Permeability*

The change in permeability with coating thickness was reported by Raban (1994) as being inversely proportional to the thickness. This was used in a modification of Equation 1.2 by the substitution of  $P_s$  by  $\tilde{P}_s/l_o$ . This results in a range of release rates when applied to a population of coated granules with differing individual coating thickness, which results from the coating process. Ko et al. (1996) incorporated orifice diffusion into their model and showed that the observed permeability of the coatings is governed by a critical coated thickness required to reduce the hole or pore size below the maximum size for osmotic pumping. The modelling of the release rate of a coated fertiliser requires the relationship between the permeability factors for solute ( $P_s$ ) and water vapour ( $P_h$ ) to be accurately defined as functions of coating thickness ( $l_o$ )

### *Temperature effect*

Temperature affects both the solubility and the diffusion rate of the solute. Solubility of urea with temperature is empirically modelled (cited in Jarrell & Boersma, 1980).

$$C_u = 6.96 \times 10^{-3} T(^{\circ}C) + 0.45 \text{ (g cm}^{-3}\text{)} \quad \text{Eq.1.16}$$

Diffusion in controlled nutrient release models responds to temperature based on the Arrhenius equation. Two approaches are considered, that of Jarrell & Boersma (1980) for solute diffusion through an orifice, and Shaviv et al. (2003a) for lumped parameter permeability. Jarrell & Boersma (1980) define the temperature dependence of diffusion as a function of fluid viscosity (Equation 1.17) and the activation energy of fluid flow,  $\Delta E_{vis}$  (Equation 1.18),

$$D_s = \frac{RT}{N\hbar\eta} \quad \text{Eq.1.17}$$

where  $D_s$  is the diffusivity [ $\text{cm}^2 \text{s}^{-1}$ ],  $R$  is the gas constant [ $\text{J mol}^{-1} \text{K}^{-1}$ ],  $T$  is temperature [K],  $N$  is Avogadro's number and  $\hbar$  is the frictional constant and  $\eta$  is the viscosity in poise ( $\text{P (g cm}^{-1}\text{s}^{-1}\text{)}$ ). The viscosity is a function of temperature represented by the Arrhenius type equation

$$\eta = \varphi e^{\frac{\Delta E_{vis}}{RT}} \quad Eq.1.18$$

Jarrell & Boersma (1980) combined and simplified equations 1.17 and 1.18 after they obtained values for the pre-exponential factor, ( $\varphi = 7.02 \times 10^{-6}$  P(poise)) and activation energy of viscous flow ( $\Delta E_{vis} = 1.85 \times 10^{11}$  erg mole<sup>-1</sup> or 1.85 kJ mol<sup>-1</sup>) using experimental data (Gosting and Akeley 1952). Using these values they solved Equation 1.18 for  $\ell$  and simplified to describing the temperature dependence of urea diffusion in water (Equation 1.20).

$$D = \frac{RTe^{\frac{-\Delta E_{vis}}{T}}}{N\ell\varphi} \quad Eq.1.19$$

$$D_u = 5.55 \times 10^{-5} T e^{\frac{-2135}{T}} \text{ (cm}^2\text{s}^{-1}\text{)} \quad Eq.1.20$$

In contrast, the permeability models of Shaviv et al. (2003a) define the temperature (T, K) effect on solute permeability ( $P_{s(T)}$ ) in terms of the activation energy of transport ( $E_a$ ) of solute and water across the membrane.

$$P_{s(T)} = P_o e^{\frac{-E_a}{RT}} \quad Eq.1.21$$

$E_a$  values were determined by Raban (1994) for polyethylene and alkyd resin coating as 51 and 32 kJ mol<sup>-1</sup>, respectively. These values are comparable to the enthalpy of vaporization of water (40kJ mol<sup>-1</sup>). Because the polyethylene  $E_a$  is higher this implies that it is hydrophobic which increase the surface energy and contact angle between the coating and water, while the alkyd resin is hydrophilic reducing the surface energy and contact angle.

Based on these two temperature dependencies it is expected that the release rate of urea modelled by “orifice diffusion” would grow by a factor of 1.5 between 10 and 20°C, where as for the membrane diffusion models the growth would be 1.8 to 2.0 depending whether it is calculated for polyethylene or alkyd resin respectively.

However the controlled release via orifice diffusion and osmotic pumping may result in more flexible product design, as it allows for both fast and slow release by manipulation of pore size and area, rather than manipulating water and solute diffusion through the membrane polymer, as required in the rupture or permeability models. This may allow further improvements to release rates giving lower temperature dependence, allowing controlled release systems to produce efficient crop response in cool winter conditions.

### ***1.3.7 Modelling developments***

The above review of the release rate models for coated controlled release fertilisers shows that the models are relatively simple and can be solved mathematically up to the start of the falling rate phase. For materials such as urea with low density and high solubility the falling rate period is important, as at 20°C 59% of the urea is released during this period. The falling rate period can be mathematically modelled in the case of solute diffusion through water filled pores, 'orifice diffusion' and permeable membranes in which the solute is soluble in the coating phase. These release mechanisms are however relatively fast limiting the duration of nutrient supply and thus the potential for labour and energy savings by reducing applications.

The osmotic pumping model using a micro-porous impermeable coating is the most promising strategy to extend the release time, as the mass transfer of water vapour across the coating will limit the release. This model will have to be further developed from the work of Theeuwes (1975) and Ko et al. (1996), utilizing a numerical solution for the falling rate period, validated from water extraction and field application experiments.

Chapter 2 develops the model from fundamental concepts and validates it with data from a range of laboratory studies using prepared reactive layer polyurethane coated commercial urea with variable granule shape and resulting volume change potentials.

## **1.4 Nitrification inhibitors**

Agronomists attempting to improve soil and fertiliser N use in crops and pasture, and to reduce N loss via nitrate leaching and denitrification, have researched and developed commercial nitrification inhibitors. The theory is that by reducing nitrification a greater proportion of the mineralised N remains as  $\text{NH}_4^+$  on the soil cation exchange sites, making it less susceptible to leaching than nitrate.

Nitrification inhibitors have been shown to increase yields in horticultural and grain crops by 2 to 4.5% (Pasda et al. 2001) by reducing the nitrate leaching and denitrification (Weiske et al. 2001) during the winter period where plant uptake was low. In the New Zealand dairy industry the nitrification inhibitor dicyandiamide (DCD) is widely accepted as a mitigation tool to reduce nitrate leaching and nitrous oxide emissions from grazed pasture (Di and Cameron 2002a, b, 2004b, 2008; Saggar et al. 2004; Smith et al. 2005, 2008; Monaghan et al. 2009). The following review looks at the type and mode of action of these products and their limitations in current practice.

### ***1.4.1 Types and Mode of Action***

In soil the oxidation of ammonia to nitrites and nitrates is carried out by the action of the autotrophic soil bacteria in the genera *Nitrosomonas*, *Nitrobacteraceae* and heterotrophic bacteria *Arcea*. The oxidation to nitrite is accomplished in two stages with the initial oxidation of the ammonia to hydroxylamine by the membrane associated enzyme ammonium monooxygenase (AMO) followed by the oxidation to nitrite by the enzyme hydroxylamine oxidoreductase (HAO), Figure 1.9.

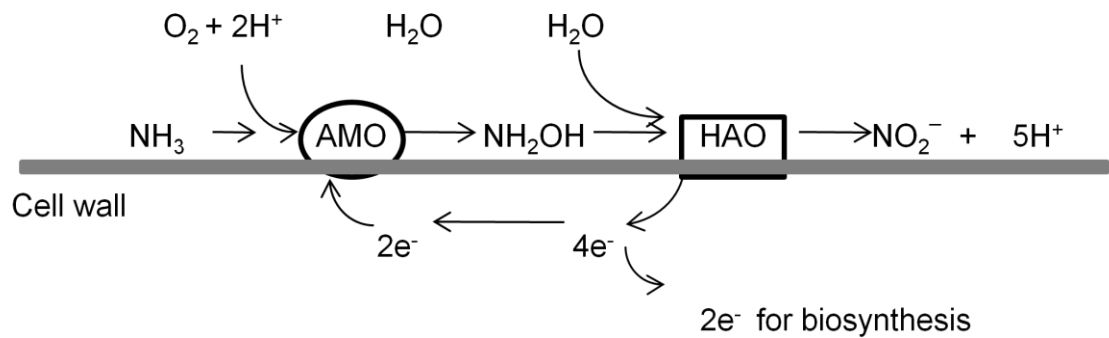


**Figure 1.9 Biological oxidation of ammonia to nitrite by membrane bound ammonium monooxygenase (AMO) and hydroxylamine oxidoreductase (HAO)**

The initial oxidation of ammonia to hydroxylamine is energetically unfavourable for the cell resulting in the consumption of electrons and hydrogen ions. This is however compensated for by the final oxidation by HAO producing the energy for cell function and biosynthesis.

The activity of these enzymes can be inhibited by the action of specific molecules, mainly alkynes, alkenes, phenols, sulphides and heterocyclic amides. These bind to the enzyme active sites, slowing turnover or permanently altering the configuration of the active sites of the enzyme.

Irreversible inhibition occurs when the oxidation of the substrate produces a highly reactive product such as unsaturated epoxies produced by the oxidation of acetylene, 2-ethynylpyridine, phenylacetylene, or 1,1,1-trichloroethylene (Hyman et al. 1988; McCarty and Bremner 1989). These products react rapidly and covalently bond to the enzymes' active site resulting in permanent deactivation of the enzyme. These inhibitors have little biocidal effect with the production of AMO continuing until the inhibitor is consumed. The recovery of the bacteria following the removal of the inhibitor acetylene is evident within 2 hr and total recovery of nitrification activity is within 8hr, following the bacteria re-synthesis of AMO (Bollmann and Conrad 1997; Stein et al. 2000). This demonstrates the limited residual effect of this type of inhibitor. Naturally occurring isoprene derivatives and essential oil have also been shown to inhibit nitrification (Patra et al. 2006) in particular the essential oil of peppermint (*Mentha spicata*, MS).

Dementholized oil and terpenes have shown comparable inhibitory activity to dicyandiamide (DCD).

The second class of inhibitors targets the active metal site copper by forming strong complexes with the copper and blocking the site. These inhibitors include phenolic, sulphides, thiols and amides. Phenolic inhibitors are found to occur naturally in soil organic matter in the form of lignins and tannins.

The phenolic type inhibitors are capable of bonding with copper reducing its availability and limiting the development of AMO by micro-organisms. Compounds such as galocatechin extracted from the roots of *Leuceana leucocephala* have been shown to produce a fifth of the inhibitor effect of nitrapyrin (Erickson et al. 2000). However studies of extracts from spruce needles, pine needles (Kanerva et al. 2006; 2008) and *Astragalus mongholicus* root extract (Mao et al. 2006) suggest that the high carbohydrate content of the extracts result in immobilization of the N by an increase in soil biomass.

The mechanism of plant root release of the biological nitrification inhibitor's (BNI's) is stimulated by the presence of ammonium ions in the plant growth medium, resulting in a  $H^+$  flux across the hair roots. This increases the root permeability allowing for example the release of compounds from a tropical grass *Brachiaria humidicola* (Subbarao et al. 2007) and *Sorghum bicolor* (Zakir et al. 2008). These compounds have been identified as the unique cyclic diterpene which has been named “brachialactone” (Subbarao et al. 2009) and the fatty acids linoleic and linolenic (Subbarao et al. 2008) in *Brachiaria humidicola*, and methyl 3-(4-hydroxyphenyl) propionate in sorghum. These three compounds have shown high inhibitory effects of *Nitrosomonas europaea* in-vitro with an effective dose for 80% inhibition ( $ED_{80}$ ) of  $3.5 \mu g ml^{-1}$  for brachialactone,  $16 \mu g ml^{-1}$  for linoleic and linolenic acids and  $1.6 \mu g ml^{-1}$   $ED_{70}$  for methyl 3-(4-hydroxyphenyl) propionate. In soil however linoleic and linolenic acids required levels  $> 600 \mu g g^{-1}$  to effect inhibition of nitrification. This inhibition was however very persistent, the effect lasting for more than 120 days at  $20^{\circ}C$  (Subbarao et al. 2008).

The sulphur containing compounds carbon disulfide (CS<sub>2</sub>), thiourea, allylthiourea, guanylthiourea, 2-mercaptobenzothiazole, 3-mercapto-1,2,4-triazole, thioacetamide, sodium diethyldithiocarbamate, sodiumthiocarbamate, thiosemicarbazide, diphenylthiocarbazon, dithiocarbamate, *s*-ethylidipropylthiocarbamate, ethylene-*bis*-dithiocarbamate, and *N*-methylthiocarbamate (Hauck 1980), containing C=S bonds, with the exception of allylsulphides, produce a competitive inhibition slowing the turnover rate of AMO and producing sulphoxides (Juliette et al. 1993a,b).

The cyanamide and dicyandiamide (Figure 1.10) produce effective inhibition of nitrification and are capable of forming complexes with copper (Williams et al. 2005).

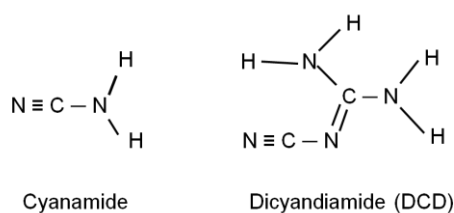


**Figure 1.10 Structure of the nitrification inhibitors cyanamide and dicyandiamide.**

The heterocyclic N compounds with N atoms in adjacent ring positions, pyrazole, 1,2,4-triazole, pyridazine, benzotriazole, indazole (Figure 1.11.) and substituted compounds (Figure 1.12) nitrapyrin, etridiazole, 2-chloropyridine, 2,6-dichloropyridine, 6-chloro-2-picoline, and 3,4-dichloro-1,3,4-thiadiazole 3,4 – dimethylpyrazole phosphate have proven to be effective and economic products for the control of nitrification in agricultural systems. The mode of inhibition is however unclear but structural similarities and pKa's are significantly related to the electron withdrawing group on the carbon adjacent to the N in the ring, lowering the pKa of the N and enhancing complication of the inhibitor within the active site of AMO (McCarty 1999).

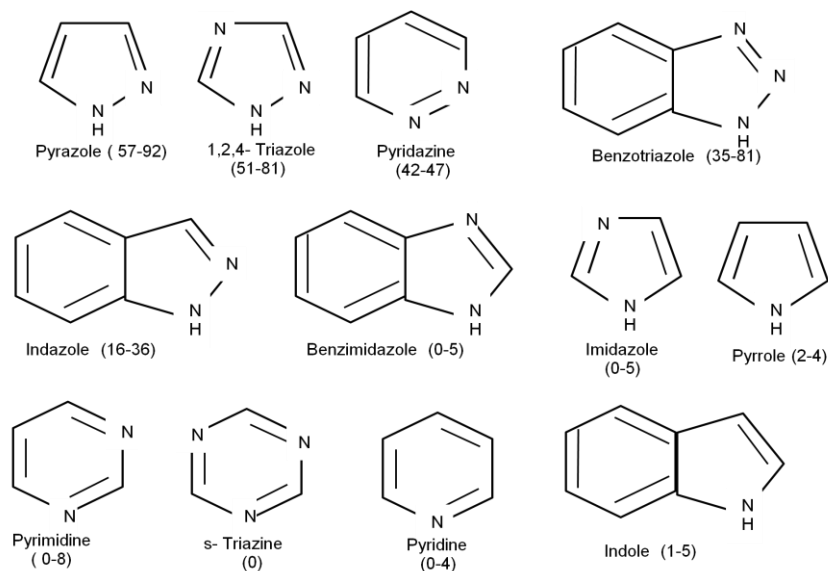


**Figure 1.11 Effectiveness of heterocyclic nitrogen compounds, as nitrification inhibitors with % inhibition in soil with (high and low) organic matter contents. (McCarty and Bremner 1989)**

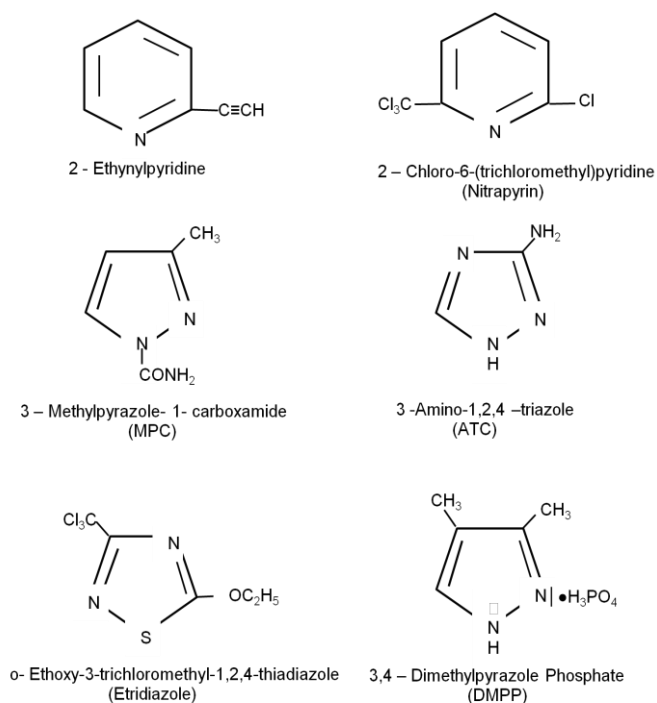


**Figure 1.12 Structures of highly effective heterocyclic nitrogen containing nitrification inhibitors (commercial name)(McCarty 1999).**

#### ***1.4.2 Agronomic impact of nitrification inhibitors***

Commercially there are three nitrification inhibitor compounds in use : DCD (dicyandiamide) marketed as eco-N<sup>®</sup> and DCn<sup>®</sup> , nitrapyrin ( 2-chloro-6-(trichloromethyl)-pyridene) marketed as N-Serve<sup>®</sup> by DowElanco, and 3,4-dimethylpyrazole phosphate (DMPP) ENTEC<sup>®</sup> sold by BASF. DCD is a readily soluble powder, which is usually applied at a rate of between 10 to 12 kgDCD ha<sup>-1</sup> as a slurry (Di and Cameron 2004a). DCD can also be coated on urea, applied as a granulated solid (Smith et al. 2005), or as stabilized fertiliser such as Basammon Stabil<sup>®</sup> containing 1.6% DCD. The high solubility of DCD allows it to migrate through the soil profile in conjunction with applied ammonium fertilisers. This association prevents the rapid conversion of ammonium to nitrite and the subsequent production of both N<sub>2</sub>O and nitrate. Irigoyena et al. (2003) showed ENTEC<sup>®</sup> and Basammon Stabil<sup>®</sup> were both effective in slowing the nitrification of ammonia at temperatures less than 20 °C, increasing the half lives of ammonium from 11 days to >105 days at 10°C and 6 days to 18 ± 2 days at 20 °C .

The effectiveness and longevity of DCD is strongly dependent on soil temperature and application rate as shown by Di and Cameron (2004a), who observed the half life of DCD to be 111 to 116 and 18 to 25 days at temperatures of 8 °C and 20 °C with application rates of 7.5 and 15 kgDCD ha<sup>-1</sup> respectively, on urine patches. The DCD resulted in lower nitrate levels and the prolonged availability of nitrogen for pasture growth. It also increased dry matter yields for pasture by 15 to 33 %, and reduced nitrate leaching from cow urine patches by up to 75% (Di and Cameron 2004b). DCD is however mobile in the soil and has been found to leach into ground water where it may persist for a period greater than one year ( Corre and Zwart 1995).

Nitrapyrin has been used widely in the USA grain belt as a nitrification inhibitor, applied in liquid fertilizer preparations such as anhydrous ammonia and UAN solutions. These products are directly drilled below the soil surface to reduce losses of both ammonia and nitrapyrin via volatilization. Nitrapyrin is very effective, requiring an application rate of only 0.56 kg ha<sup>-1</sup>. However it is strongly adsorbed by soil organic matter limiting its movement from the point of application (Hendrickson and Keeney

1979; Sahrawat et al. 1987). The degradation of nitrapyrin in soil is strongly affected by soil temperature with a half life of 43 to 77 days at 10°C but only 9 to 16 days at 20°C (Herlihy and Quirke 1975). In New Zealand pastoral systems nitrapyrin has been shown to be ineffective in terms of increasing yield but can slow nitrification from N fertiliser applications (Turner and Macgregor 1978).

DMPP is similar to nitrapyrin with application rates of 0.5-1.5 kg ha<sup>-1</sup>. DMPP applied as ENTEC® (0.2% DMPP on AN) from BASF (Azam et al. 2001) has low soil mobility in soil with less than 3% of applied DMPP being found greater than 25mm from the granule and 90% still being within 5mm of the granule 10 days after application. This slow movement of inhibitor can result in ammonium diffusing beyond the inhibitor affected soil, and rapidly nitrifying there.

The above review of nitrification inhibitors suggests that the most attractive option to reduce losses of mineral N in the New Zealand pastoral systems via nitrate leaching and de-nitrification is the development of BNI producing forage crops or semi-permanent pasture species. BNI pasture removes the requirement for synthetic nitrification inhibitor application and has the potential to give all season effect, while synthetic nitrification inhibitors (DCD, DMPP and Nitrapyrin) are limited to cold seasons application due to their rapid degradation at elevated soil temperatures. This is however a long term strategy requiring an extensive plant breeding and screening programs. In the interim an effective synthetic nitrification inhibitor is required. The three major commercially available synthetic nitrification inhibitors have a number of disadvantages in the dairy pastoral system, in which nitrate leaching and N<sub>2</sub>O are produced primarily from dairy cow urine patches. The mobility of the inhibitor must be sufficient to fully treat the soil to a depth reached by urine.

This requirement makes both nitrapyrin and DMPP unsuitable due to their low mobility leaving the highly mobile DCD (Corre and Zwart 1995) as the most suitable for application to soils affected by dairy cow urine. DCD has limited application in the New

Zealand pastoral dairy system as it rapidly decomposes within the soil at moderate temperatures ( Kelliher et al. 2008), making it most effective during autumn and winter. However as this is also one of the likely times for leaching of DCD, which can result in ground water contamination from DCD (Corre and Zwart 1995). The coating of DCD with a polymer coating to produce a controlled release product may overcome some of these limitations by producing a continuous supply of inhibitor to counter its degradation and leaching.

Modifying DCD in this way requires the development of a coating system. As the DCD is an amide, the application of the reactive poly-urethane coating system developed for urea may also be applicable due to the abundance of  $\text{NH}_2$ - functional groups on DCD, allowing the reactive binding of the diisocyanated (MDI) to the granule surface.

## **1.5 Conclusion:**

The application of coated controlled release products of urea and DCD in the pastoral system may allow the reduction in application costs and increases in yields, while reducing the environmental impacts of nitrate leaching and  $\text{N}_2\text{O}$  emissions.

To achieve a commercially viable controlled release urea the lowest cost system is required, which from the review of technology is the reactive layer poly-urethane process based on MDI: castor oil: TEA. This coating is both suitable for application to urea and granular DCD due to the availability of  $\text{NH}_2$ - functional groups on the surface allowing the coating to reactively bond. This process requires no solvent and can be carried out in a simple drum, applying the coating using either a batch or continuous process.

The research plan for the work described in this thesis was to develop a range of coatings for commercially available urea (PetroChem urea), altering the castor oil composition by blending 5,10 and 15% by weight of canola oil (mono-unsaturated),

soya oil(poly-unsaturated) and palmitic acid (saturated fatty acid) into the castor oil. This change in oil composition was expected to mildly alter the physical properties of the polymer by reducing cross linking and in the case of the fatty acid foaming the polymer. The effect of these amendments on the physical properties of the polymer film was then tested and used in the assessment of a comprehensive model developed based on the hydraulic convective of urea through the coating on polymer coated urea (PCU) (described in Chapter 2). The tests were done in water in the laboratory and in agronomic field experiments (Chapter 3& 4). A study investigating the relationship between the coating level and the release rate in water, is described in Chapter 2 using polymer application rates of 2, 3, 4, 5, 7 and 10% (w/w) of the control coating (MDI: Castor oil: TEA) to urea. This was used to estimate the effective permeability of the coating as a function of coating thickness which was incorporated into the release model for coated urea.

Chapter 6 describes the development of a controlled release nitrification inhibitor, PDCD. It was carried out by the granulation of DCD powder and the coating of the DCD granules with control coating (MDI: Castor oil: TEA) at two levels and their release rate determined in water. The most appropriate of these products was then used as a surface application in a repacked core study to determine the migration and inhibition of nitrification in urine effected Manawatu and Dannevirke soils. In the study the diffusion of DCD and urine N in the form of ammonium is modelled to determine the potential efficacy of PDCD in mitigating nitrate leaching.

## Chapter 2

### Modelling of nutrient release rate of modified Castor/MDI coated urea

---

#### 2.1 Introduction

The modelling of the release rate of polymer coated urea has been reviewed in Chapter 1. This uncovered different theoretical treatments of the polymer coated system with proposed models using a mixture of pore diffusion and osmotic pumping.

In this Chapter a new model is proposed, which describes the release of urea from a reactive layer poly-urethane (RLP) coated urea. This model describes the release in terms of water vapour permeability via micro-pores, which supports hydraulic convection of the nutrient (urea) solution across the coating via macro pores. The model describes five fundamental release periods:

1. *Lag time*, in which the coated granule swells prior to the release of any urea solution. This period is described by the time required for liquid ingress into the coated granule to, fill voids, invert dents and hollows on the granule surface and finally stretch the coating layer. These processes are controlled by the ingress rate of water and the development of enough internal pressure to overcome the initial capillary resistance ( $P_{critical}$ ).
2. *Re-equilibrium release*, once the capillary resistance to flow is overcome the internal solution begins to flow out of the granules via macro pores as a function of internal granule pressure, viscosity, pore diameter and effective pore length. The pressure is increased by the inflow of water via water vapour transport through micro pores in the coating. At this point the inflow and out flow of the coated granule system moves towards an equilibrium volume ( $V_{eq}$ ) and pressure ( $P_{eq}$ ) which may result in the granule continuing to expand ( $P_{eq} > P_{critical}$ ) or contract ( $P_{eq} < P_{critical}$ ) until equilibrium is achieved. The equilibrium pressure ( $P_{eq}$ ) may exceed the coating tensile strength ( $S_Y$ ) resulting in rupture

or hole development and catastrophic release. Whereas if the equilibrium pressure is below the rupture pressure ( $P_{rupture}$ ) a constant release rate is eventually reached.

3. *Constant equilibrium rate*, once the equilibrium volume ( $V_{eq}$ ) and pressure ( $P_{eq}$ ) is reached in which the ingress rate of water and the hydraulic convection of urea solution out of the granule are equal, a period of constant release rate is achieved, until the solid urea core is fully dissolved. At this point the urea concentration inside the coated granule begins to fall leading to the falling rate period.
4. *Falling rate*, as the internal urea concentration falls the internal water vapour pressure increases lowering the rate of water transport across the coating. The internal solution also becomes less viscous increasing the hydraulic flow rate, which is offset by a lowering equilibrium pressure and granule volume. These factors lead to a fall in hydraulic convection of solution across the coating. This continues until the terminal period, when the external forces acting on the coated granule become dominant producing the internal solution pressure, which opposes this force.
5. *Terminal period*, in this final stage of release the coated granules internal pressure falls to a point at which the external forces on the coated granule are the dominant components supporting the hydraulic convection of solution across the coating. In water this will play little effect as the forces act uniformly, however in soil and within root balls, which may form around coated granules significant non-uniform forces may act crushing the granule to release the remaining solution.

## **2.2 Hydraulic convection of solute from a coated granule**

The following model assumes the coated granules are spherical to simplify the modelling process and to allow the mathematical descriptions to be developed. Later in the working models the change in granule shape is modelled along with the affect of soil contact (Section 2.2.1).

In the initial spherical model which follows, it is assumed that;

1. Volume is conserved, that is no swelling or shrinkage of the system occurs.
2. Mixing is perfect, that is, there is no excess volume on mixing the components.
3. Solute dissolution from the core into the solution zone is fast compared to the transport of solute across the coating. This means there is no concentration gradient across the solution zone, which exists between the solid core and coating.
4. The external concentration of solute outside the coated granule is constant.
5. The density of solid and water are constant.
6. The coating polymer has uniform thickness and uniform consistency.
7. The total pressure in the membrane pores through which vapour transports is assumed to be equal the external pressure of the water phase. Any internal pressure built up inside the granule is internal to the membrane. Mechanical stresses (hoop stresses) in the membrane structure are not assumed to affect the pore space pressures

### **2.2.1 Lag time**

In this model the coating is considered to be an impermeable hydrophobic layer with both micro and macro pores. The hydrophobicity of the coating resists the flow of liquid allowing only gas phase transport of water across the pores until sufficient internal pressure ( $\Delta P$ ) is achieved to overcome the capillary resistance ( $\Delta P_{critical}$ ). At this point hydraulic convection of the solute commences, mostly via the larger macro-pores.

The internal pressure is the result of an increase in internal granule volume, which stretches (strains) the coating producing a reactive stress ( $S_{coating}$ ) in the coating and internal pressure on the solution. The volume increase is due to the imbalance in the ingress of water ( $dV_{water}/dt$ ) and the egress of solution ( $dV_{soln}/dt$ ) through the coating represented by Equations 2.1 and 2.2.

$$\frac{dV_{water}}{dt} = \frac{W' A_t \Delta P_{wv}}{l_o} \quad Eq. 2.1$$

$$\frac{dV_{soln}}{dt} = \frac{H' A_t \Delta P}{l_o} \quad Eq. 2.2$$

Where  $W'$  is the specific coefficient of water vapour transport ( $\text{cm}^2 \text{d}^{-1} \text{Pa}^{-1}$ ),  $\Delta P_{wv}$  is the differential water vapour pressure (Pa) across the coating,  $H'$  is the specific coefficient for hydraulic convection ( $\text{cm}^2 \text{d}^{-1} \text{Pa}^{-1}$ ), and  $\Delta P$  is the hydraulic pressure (Pa) difference across the coating.

The internal pressure is assumed to be  $\Delta P$ , as the external pressure is small. To determine the duration of the lag period, the time required for the water entering the coated granule to increase the granule volume to a critical volume ( $\Delta V_{critical}$ ) and producing the internal pressure  $\Delta P_{critical}$ . This problem is solved using the relationship between the internal pressure and the hoop stress (Equation 2.5). The hoop stress is calculated using the tangential strain in the coating, due to volume change and the elasticity of the coating, expressed by Young's modulus ( $Y$ ).

Change in granule volume ( $\Delta V = V_n - V_o$ ) between the initial volume ( $V_o$ ) and the final volume ( $V_n$ ) is related to the tangential strain in the circumference ( $\Delta\omega/\omega_o$ ) by the geometric relationship via the sphere radius ( $r$ ) as follows.

$$V = \frac{4}{3} \pi r^3 \text{ therefore } r = \left( \frac{3V}{4\pi} \right)^{\frac{1}{3}}$$

Substituting  $V$  for  $r$  in the yields.

$$\omega = 2\pi r = 2\pi \left( \frac{3V}{4\pi} \right)^{1/3}$$

Thus the tangential strain can be expressed in terms of volume change,

$$\frac{\Delta\omega}{\omega_o} = \left( \frac{V_n^{1/3} - V_o^{1/3}}{V_o^{1/3}} \right) = \left( \frac{\Delta V}{V_o} + 1 \right)^{1/3} - 1 \quad Eq. 2.3$$

and the coating hoop stress via Young's modulus of elasticity ( $Y$ ).

$$S_{coating} = Y \left( \frac{\Delta\omega}{\omega_o} \right) \quad Eq. 2.4$$

The coating stress is related to the internal pressure ( $\Delta P$ ) in a sphere with a thin coating (Spence 1994).

$$S_{coating} = \frac{\Delta P r_o}{2l_o} \quad Eq. 2.5$$

Combining equations 2.3, 2.4 and 2.5 and rearranging, the granule volume as function of internal pressure is obtained and thus the critical volume obtained by substituting  $\Delta P_{critical}$  for  $\Delta P$ .

$$\Delta V = V_o \left( \left( 1 + \frac{r_o \Delta P}{2l_o Y} \right)^3 - 1 \right) \quad Eq. 2.6$$

The time ( $t'$ ) required for the critical volume ( $\Delta V_{critical}$ ) and pressure to be reached is given by the critical volume divided by the water ingress rate, which is constant during period, while the internal solution is saturated.

$$t' = \frac{\Delta V_{critical}}{\frac{dV_w}{dt}}$$

Assuming perfect mixing, with no excess volume change associated with the dissolution of urea ( $dV_{water} = dV_{urea} = dV_{soln}$ ) allows  $t'$  to be described by dividing equation 2.6 by 2.1.

$$t' = \frac{r_o l_o}{3W' \Delta P_{wv}} \left( \left( \frac{r_o \Delta P_{critical}}{2l_o Y} + 1 \right)^3 - 1 \right) \quad Eq. 2.7$$

Where  $\frac{V_o}{A_t} = \frac{\frac{4}{3}\pi r_o^3}{4\pi r_o^2} = \frac{r_o}{3}$

From the measurement of coating properties the lag time can be calculated from the capillary resistance  $\Delta P_{critical}$ .

### 2.2.2 Equilibrium release period

As the capillary resistance no longer impedes the flow of internal solution through the coating hydraulic viscous flow begins, through the largest pores. The volume and pressure within the coated granule is now determined by the balancing of water ingress and solution egress defined by equations 2.1 and 2.2. This results in an equilibrium internal pressure ( $\Delta P_{eq}$ ) and volume ( $V_{eq}$ ). The equality of equations 2.1 and 2.2 then allow  $\Delta P_{eq}$  to be defined as a function of the specific water vapour permeability ( $W'$ ) and hydraulic ( $H'$ ) coefficients, assuming the water vapour pressure difference ( $\Delta P_{wv}$ ) is unaffected by the internal solution pressure ( $\Delta P$ ) and  $W'$  is not affected by the area of pores filled by the hydraulic convection.

$$\frac{H' A_t \Delta P_{eq}}{l_o} = \frac{W' A_t \Delta P_{wv}}{l_o}$$

$$\Delta P_{eq} = \frac{W' \Delta P_{wv}}{H'} \quad \text{Eq. 2.8}$$

Substitution  $\Delta P_{eq}$  into equation 2.6 gives

$$\Delta V_{eq} = V_o \left( \left( 1 + \frac{r_o \Delta P_{eq}}{2l_o Y} \right)^3 - 1 \right) \quad \text{Eq. 2.9}$$

If  $\Delta P_{eq} < \Delta P_{critical}$  the excess pressure is relieved by the reduction in volume, resulting in a rapid flow of urea solution through the macro- pores until the equilibrium volume is achieved. The average rate of hydraulic flow is proportional to the mean pressure between  $\Delta P_{critical}$  and  $\Delta P_{eq}$ .

$$\frac{dV_{soln}}{dt} = \frac{H' A_t (\Delta P_{critical} + \Delta P_{eq})}{2l_o} \quad \text{Eq. 2.10}$$

The equilibrium time required is defined by the change in volume divided by the rate.

$$t_{eq} = \frac{2l(\Delta V_{critical} - \Delta V_{eq})}{H'A(\Delta P_{critical} + \Delta P_{eq})} \quad Eq. 2.11$$

If  $\Delta P_{eq} > \Delta P_{critical}$  the coated granule will release and swell simultaneously once  $\Delta P_{critical}$  is reached, as this is a slow process the simple linear approximation can no longer be used as in equation 2.10 and 2.11. Instead the numerical solution of the rate equations is required to determine the release rate of solution from the granule, where  $dV_{granule}/dt$  is the rate of granule volume change.

$$\frac{dV_{soln}}{dt} = \frac{dV_{water}}{dt} - \frac{dV_{granule}}{dt} \quad Eq. 2.12$$

If  $\Delta P_{eq}$  is high, it may exceed the structural strength of the coating resulting in rupture. The rupture point pressure ( $\Delta P_{rupture}$ ) is calculated using equation 2.5, substituting the ultimate yield stress,  $S_Y$ , for  $P_{coating}$  and  $\Delta P_{rupture}$  for  $\Delta P_{internal}$ .

### 2.2.3 Constant equilibrium rate period

Following the lag time a new equilibrium volume ( $V_{eq}$ ) and pressure is reached, in which the hydraulic convection is equal to the water vapour diffusion through the micro-pores, expressed below.

$$\frac{dV_{soln}}{dt} = \frac{dV_{water}}{dt} = \frac{W'A_t\Delta P_{wv}}{l_o} = k' \quad Eq. 2.13$$

And the proportional mass released of the initial mass  $\frac{\int \frac{dm}{dt}}{M_o} = (Q)$ , assuming no release prior to the constant equilibrium period.

$$\text{where } \frac{dm}{dt} = k'C_s \text{ and } \int \frac{dm}{dt} = k'C_s(t - t') \text{ so}$$

$$Q = \frac{k'C_s}{V_o\rho_s}(t - t') = \frac{3W'\Delta P_{wv}C_s}{l_or\rho_s}(t - t') \quad Eq. 2.14$$

This constant rate continues until the solid core fully dissolves at time ( $t^*$ ). As the initial volume of solid is conserved, we can write that the initial solid volume is equal to the volume expelled during the constant rate plus the volume remaining in the swelled granule and the volume expelled during equilibration of pressure.

$$V_{solid(0)} = k'(t^* - t') + \frac{C_{sat}}{\rho_s}(V_{solid(0)} + \Delta V_{eq}) + \frac{C_{sat}}{\rho_s}(\Delta V_{critical} - \Delta V_{eq}) \quad Eq. 2.15$$

This is then rearranged to give

$$t^* = \frac{V_{solid(0)}}{k'} \left(1 - \frac{C_{sat}}{\rho_s}\right) - \frac{\Delta V_{critical} C_{sat}}{k' \rho_s} + t' \quad Eq. 2.16$$

#### 2.2.4 Falling rate period

Following the constant rate period the falling rate occurs as  $C_s$  is no longer equal to  $C_{sat}$  resulting in an increase in internal water vapour pressure and a drop in viscosity. The internal water vapour pressure can be defined by the activity of water ( $a_w$ ), which is the ratio of the partial vapour pressure of the solution ( $P_{wv(soln)}$ ) over the partial vapour pressure of pure water ( $P_{wv}^o$ ), which is a function of solute concentration (Chen 1989).

$$a_w = \frac{P_{wv(soln)}}{P_{wv}^o} = \frac{1}{1 + 18 \left( \beta_e - B \left( \frac{1000C_s}{M_{wt(s)}} \right)^n \right) \frac{C_s}{M_{wt(s)}}} \quad Eq. 2.17$$

Chen (1989) gives the coefficients for urea at 25°C as  $\beta_e = 1$ ,  $B = -0.0608$  and  $n = 0.283$ . It is assumed the urea concentration of the liquid surrounding the coated granule is low, so  $P_{wv(external)} \approx P_{wv}^o$  and  $\Delta P_{wv}$  is defined in terms of the vapour pressure of pure water and the activity constant.

$$\Delta P_{wv} = P_{wv}^o(1 - a_w) \quad Eq. 2.18$$

The combination of equations 2.18 and 2.1 then allows the numerical calculation of the falling rate change in  $C_s$  with time as  $\frac{dC_s}{dt} = -\frac{1}{V_{eq}} \frac{dm}{dt}$ .

$$-\frac{dC_s}{dt} = \frac{W' A_t P_{wv}^o (1 - a_w)}{V_{eq} l_o} C_s \quad \text{Eq. 2.19}$$

Assuming spherical geometry the surface area and volume terms can be simplified and substituting equation 2.17 into 2.19 an expression for  $\frac{dC_s}{dt}$  during the falling rate period can be calculated.

$$\frac{dC_s}{dt} = \frac{3W' P_{wv}^o \left( 1 - \left( \frac{1}{1 + 18 \left( \beta_e - B \left( \frac{1000C_s}{M_{wt(s)}} \right)^n \right) \frac{C_s}{M_{wt(s)}}} \right) \right)}{r l_o} C_s \quad \text{Eq. 2.20}$$

where  $r$  is the granule radius.

The integration of equation 2.20 is non-trivial, requiring a numerical approach to calculate the change in concentration on a daily time interval from  $t'$ . To determine the mass released  $\frac{dC}{dt}$  is multiplied by the granule's volume, which also may be reducing with time as the solution viscosity falls with concentration.

The falling internal concentration of the internal solution results in a falling solution viscosity which alters the internal granule pressure and volume. As the flow through the wetted pores is laminar the Hagan Poiseulle equation can be applied.

$$\frac{\Delta P}{l_e} = \frac{32 U_m \mu}{d_{eqv}^2} \quad \text{Eq. 2.21}$$

where  $l_e$  is the effective path length,  $d_{eqv}$  is the equivalent pore diameter,  $U_m$  is the mean velocity of fluid in the pore and  $\mu$  is the viscosity. The volumetric flow is given by the pore area of wetted macro-pore ( $A_{wp}$ ) multiplied by the velocity  $A_{wp} U_m$  for each pore and  $\varepsilon_w A_t U_m$  for the granule where  $\varepsilon_w$  is the ratio of wetted pores area  $A_{wp}/A_t$ , applying this to the hydraulic convection equation we see that the grouped parameter  $H'$  can be separated into its components.

$$H' = \frac{\varepsilon_w d_{eqv}^2}{32l_e} \frac{1}{\mu} = \frac{L_p}{\mu} \quad Eq. 2.22$$

Grouping the constant term into a new hydraulic coefficient  $L_p$  results in Darcie's law of fluid flow in porous media.

$$\frac{dV_{soln}}{dt} = \frac{L_p A_t \Delta P}{l_o \mu} \quad Eq. 2.23$$

Substituting for  $H'$  in equation 2.2 the instantaneous hydrolic pressure across the coating ( $\Delta P$ ) and volume change ( $\Delta V$ ) can be calculated as a function of solute concentration ( $C_s$ ) within the coated granule as both the viscosity ( $\mu$ ) and difference in the partial pressure of water vapour ( $\Delta P_{wv}$ ) are functions of  $C_s$ , equations 2.26 and 2.18.

$$\Delta P = \frac{\mu W' \Delta P_{wv}}{L_p} \quad Eq. 2.24$$

$$\Delta V = V_o \left( \left( 1 + \frac{r_o}{2l_o Y} \frac{\mu W' \Delta P_{wv}}{L_p} \right)^3 - 1 \right) \quad Eq. 2.25$$

For urea the change in viscosity can be calculated by the empirical formula from data (Kawahara and Tanford 1966) which relates the viscosity of the urea solution to that of water at 25°C.

$$\mu_{uw} = \mu_{water} \times (2.095C_s^2 + 0.190C_s + 1) \quad Eq. 2.26$$

Thus the new pressure and volume of the granule may be calculated for each time step in the release rate simulation.

### 2.2.5 Terminal period

As the falling rate period continues the internal pressure falls and the external pressure on the granule applied by soil pressure or plant roots becomes significant. This is however difficult to quantify and requires further research.

### **2.2.6 Summary of spherical model**

In the spherical coated granule model the initial lag time is defined by the coating permeability to water vapour, elasticity and the capillary resistance to macro-pore flow. This results in swelling of the coated granule until sufficient volume and pressure is achieved to overcome the initial resistance to flow. Once wetted flow is achieved the coated granule contracts to a new equilibrium volume releasing a flush of solution. With the new equilibrium volume achieved, the granule continues to release at a constant rate until the solid core is fully dissolved. The internal concentration of the solute solution then continues to fall as no more solid is available within the core to maintain the solute concentration is in addition results in a fall in water vapour transport and a deduction in volume as the viscosity falls. This complex process requires numerical solution using a finite difference approach.

### **2.2.7 Non-spherical coated granules**

Commercially produced urea granules are not simple spheres, but a mixture of varying distortions resulting from the granulation and storage processes. The effect of these distortions may result in significant changes to the granule volume as granules swell to optimize their volume to surface area prior to elastic stretching of the coating. In this initial stage of coating deformations, hollows are inverted as the internal solution pressure increases. The pressure requirement for this process is difficult to estimate accurately due to the individual areas of the deformations, but is expected to be related to the coating elasticity. For simplicity the volume change is expected to occur prior to equilibrium pressure. Thus if  $P_{critical} < P_{eq}$  only a portion of volume change will occur prior to release.

Following this initial swelling the model of release follows that of the spherical approximation with the additional volume term ( $\gamma V_o$ ) added, where  $\gamma$  is the proportional volume change. As  $\gamma$  is a population property it can be estimated from granule core geometry of the granulated urea and can be assigned to individual granules within a population based on the statistical distribution which can be measured. The measurement requires an estimation of granule volume and potential volume based on

surface area. This estimate was carried out by digital image analysis of a population of urea granules using the transformation from the initial volume estimated using the equivalent spherical volume (ESV) based on the Feret radius ( $R$ ) calculated from pixel area and the oblate spheroid (M&M shaped) volume calculated from the maximum ( $r_{max}$ ) and minimum ( $r_{min}$ ) radii, Figure 2.1.

$$\gamma = \frac{4\pi}{3} (R^3 - r_{max}^2 r_{min}) \quad Eq. 2.27$$

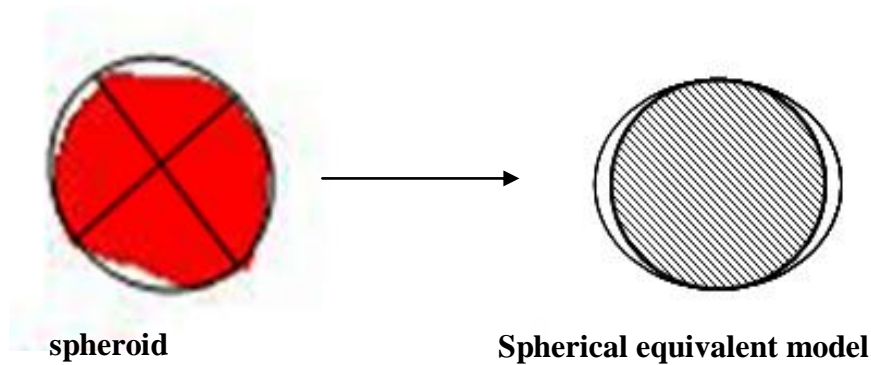


**Figure 2.1 Transformation of digital image to spherical equivalent model granule for estimation of potential volume change  $\gamma$ .**

### **2.3 Working model for reactive layer poly-urethane coated urea**

In the previous section(2.2) the fundamentals of the hydraulic convection model are described however this may be somewhat complex for modelling application the model is simplified by grouping all the granule volume change effects and assuming the equilibrium release phase is short with little volume being expelled.

### 2.3.1 Water extraction model

For prediction of the urea release rate from RLP coated urea, the physical parameters ( $l_o$ ,  $R$ ,  $Y$  and  $S$ ) and permeability properties ( $W'$ ,  $H'$  and  $L_p$ ) of the polymer and urea are first assessed to define the critical, equilibrium and rupture pressures ( $P_{critical}$ ,  $P_{eq}$ ,  $P_{rupture}$ ). The value of  $P_{eq}$  relative to  $P_{critical}$  indicates whether complete swelling of the granule occurs with ( $P_{eq} > P_{critical}$ ) or without ( $P_{eq} < P_{critical}$ ) release, while  $P_{eq} > P_{rupture}$  indicates rupture is likely.

As  $S_Y$  and  $Y$  are expected to be large the working model ignores the effects of volume change due to coating elasticity and uses an estimated volume change due to coating deformation ( $\gamma$ ) to calculate the lag time. The lag time is the result of the water permeation rate and the estimated volume change ( $\gamma$ ) as follows

$$t' = \frac{\gamma V_o l_o}{W' A \Delta P_{wv}} \approx \text{spherical approximation} \frac{\gamma R l_o}{3W' \Delta P_{wv}} \quad \text{Eq. 2.28}$$

As  $Y$  is large the equilibrium period is not significant and following the lag period the constant rate period begins. The constant rate is given by equation 2.14 in which the Feret radius  $R$  is substituted for  $r$ .

$$Q = \frac{\int_{t'}^t m dt}{M_o} = C_s \frac{dV_{soln}}{dt} \frac{1}{V_o \rho_s} (t - t') = \frac{3W' \Delta P_{wv} C_s}{l_o R \rho_s} (t - t') \quad \text{Eq. 2.29}$$

This rate continues until the solid core is dissolved. At time  $t^*$  given by

$$t^* = \frac{R l_o \rho_s}{3W' \Delta P_{wv} C_{sat}} \left( 1 - \frac{C_{sat}(1 + \gamma)}{\rho_s} \right) + t' \quad \text{Eq. 2.30}$$

which is a rearrangement of equation 2.16 in which  $\Delta V_{critical} = V_o - \gamma$ .

Following  $t^*$  the rate of release is calculated using equation 2.20, which is numerically integrated from  $t^*$  to  $t$  giving the change in concentration within the granule with time.

$$\frac{dC_s}{dt} = \frac{3W' P_{wv}^o \left( 1 - \left( \frac{1}{1 + 18 \left( \beta_e - B \left( \frac{1000C_s}{M_{wt(s)}} \right)^n \right) \frac{C_s}{M_{wt(s)}}} \right) \right)}{rl_o} C_s \quad Eq. 2.20$$

As initial mass of solute ( $M_o$ ) is conserved, being either released or remaining within the granule. The cumulative portion of urea released can then be calculated by subtracting the mass of solute remaining from the initial mass, then dividing the result by the initial mass.

$$Q = \frac{M_o}{M_o} - \frac{(1 + \gamma)V_o}{M_o} \left[ C_{sat} - \int_{t^*}^t C dt \right] = 1 - \frac{(1 + \gamma)}{\rho_s} C_{s(t)} \quad Eq. 2.31$$

### 2.3.2 Field condition model

The modelled release of urea from a population of coated urea granules under field conditions (assuming the soil concentration of urea is insignificant relative to the internal urea solution of the coated granule as in the water release model) required the daily soil temperature and soil moisture to be taken into account. As the soil temperature affects  $C_{sat}$  (Conc) and  $P_{wv}^o$  (Pwvo), the lag time and constant rate time can no longer be calculated by equations 2.35 and 2.33 and must be calculated from the summation of the volumetric water inflow. Under soil conditions the wetted surface area of the coated granule is reduced, which in the model was expressed by applying the soil volumetric water content ( $\theta$ ) to correct  $W'$  for the reduced area. Soil volumetric water content ( $\theta$ ) was calculated daily basis on the soil moisture deficit data, assuming a depth of 15cm.

In the model (Appendix 1.1) the end of the constant rate period is determined when the inflow of water has been sufficient to dissolve the solid core. This is expressed in computer language as  $(mass(j) * (1 - ((v + 1) * Conc / densityS)))$  were  $mass(j)$  is the

initial mass of granule ( $j$ ),  $v$  is the volume change ( $\gamma$ ),  $Conc$  is the concentration of the saturated urea solution ( $C_{sat}$ ) and  $densityS$  is the density of the solid urea ( $\rho_s$ ), calculated from the daily mean temperature. If the amount released (amount ( $j,t$ )) at time  $t$  is less than the critical level the daily proportional mass rate of release is given by  $RateM(j, t) = ((3 * w * SW(t) * DeltaP * Conc) / (radii * fi * densityS))$  where  $w$  is  $W'$ ,  $SW(t)$  is the daily volumetric soil moisture,  $DeltaP$  is  $\Delta P_{wv}$ ,  $radii$  is  $r_o$  and  $fi$  is  $l_o$ . During the constant rate period  $DeltaP$  and  $Conc$  are constant, however when the critical amount released is exceeded both  $DeltaP$  and  $Conc$  are recalculated on a daily bases  $\frac{dC}{dt}$  equation 2.25 ( $dC = 3 * w * SW(t) * Pwvo * (1 - a) * Cs(t - 1) / (radii * fi)$ ) where  $Conc$  is renamed as an array  $Cs(t)$  and the time step daily proportional mass release is calculated  $RateM(j, t) = ((3 * w * SW(t) * (v + 1) * DeltaP * Cs(t - 1)) / (radii * fi * densityS))$  for each granule. The total cumulative amount released (amount( $j,t$ ) =  $RateM(j,t)*mass(j)$ ) is then calculated. Finally the cumulative proportion of urea released from the total granule population is calculated.

## 2.4 Objectives

The mathematical formula describing characteristic periods of urea release have been discussed in the preceding sections. They are now validated using a range of laboratory prepared RLP coated urea. Based on sequential coatings of poly-methyl-bis-phenyl-di-isocyanate (MDI, Endurethane R100-A) and polyol's comprising of combinations of Castor oil: vegetable oil: triethanol amine (TEA). The varying combinations of polyol produced a number of different physical and chemical properties of the coating, which in combination with the commercial granule urea allowed validation of the models following the determination of  $W'$  as a function of  $l_o$ ,  $H'$  and  $P_{critical}$ .

The effect of coating thickness on water vapour permeability was determined experimentally using a series of coating thicknesses from 2 to 10 coating sequences. The water permeability was estimated from the urea release rate in water and modelled as an exponential decay towards a minimum permeability.

$$W' = W'_{min} + ae^{-kl_o} \quad Eq. 2.32$$

The critical pressure ( $P_{critical}$ ) and the hydraulic permeability ( $H'$ ) were also determined for a select number of the coatings, which showed significant changes in release character to the control coating. This was achieved by the measurement of urea solution flow under varying pressure through polymer films produced during the urea coating and using a pressurised permeability cell. The coating films were also tested for water vapour permeability in a vapour diffusion cell.

The model was validated using water extraction data and field herbage N recovery data from winter pasture growth trials.

## **2.5 Methods and Materials:**

### ***2.5.1 Preparation of film and coated urea***

The preparation of the RLP films and coated urea were carried out in a one litre 100 mm round screw cap glass jar which was charged with 300 g of granular urea and preheated to 80°C in an oven. Following preheating sequential additions of 1.5 g of poly-diisocyanate (Endurathane R100-A) and 1.5 g of polyol (composed of 10% w/w triethanol amine (TEA) in castor oil) were made. The sequence of application was repeated at five minute intervals, with the jar and contents being orbitally shaken, to allow good mixing of the two reactive components over the surfaces. The coating jar was then returned to the oven at 80°C and rotated at 30 sec intervals while the resin cured for 4 min. This coating process was repeated 5 times to produce a 5% coated product.

A number of amendments were made to the polyol mixture to increase the permeability by:

- the addition of canola and soya bean oils to increase the levels of unsaturated triglycerides and promote steric voids in the coating film
- the addition of palmitic acid to act as a foaming agent and reduce hydrophobicity and increase pore size.

These amendments were introduced to the castor oil /TEA mixture at 10, 15 and 20% by weight.

On completion of the coating operation, the coated urea and jar were allowed to cool, the urea transferred to a sealed plastic bag and the jar left to stand for 24 hr prior to the recovery of the film. The film was separated from the internal glass wall by carefully lifting the top edge of the film at the opening of the jar and slowly applying water between the film and glass allowing the hydraulic pressure at the film: glass interface to separate the 30-45 micron film from the glass surface. The film was then cut into sheets and air dried prior to physical testing.

### ***2.5.2 Physical testing of polymer films for Young's modulus and tensile strength***

The films were cut into 5 x 50 mm strips and conditioned at 80% RH for 24 hr prior to testing on a texture analyser (TA-XTplus, Stable Microsystems, Surrey, UK) for tensile strength and elasticity as expressed by Young's modulus. The measurements were carried out at a draw rate of 5 mm/min. Up to 5 repeats were performed where possible.

### ***2.5.3 Water vapour permeability $W'$ of laboratory prepared polymer films***

The measurement of water vapour permeability was carried out at 10, 20 and 26°C using a gravimetric method based on BS3177. In this method the thickness of the film is measured using a micrometer and the film glued to the open end of a 50 ml polyethylene cell (45mm diameter). Following curing of the glue, a constant humidity solution of 25 ml of 50% urea solution in water was injected into the cell through a 1 mm diameter hole in the upper portion of the side wall and sealed with Bostic sealant. The cells were placed in a constant humidity (0% RH silica gel or 100% RH water) and temperature chamber for 24 hr to equilibrate. Following equilibration the weight of the cell was measured to 0.001g accuracy, and placed back in the chamber. Weighing was then repeated every 24 hr. From these results the water permeability was calculated.

$$W' = (-w*V_w*l/(\pi/4\phi^2)\Delta P_{wv}) \text{ cm}^2 \text{ d}^{-1} \text{ Pa}^{-1} \quad \text{Eq. 2.33}$$

Where  $w$  is the weight change per day in g,  $V_w$  is the specific volume of water ( $1 \text{ cm}^3/\text{g}$ ),  $l_o$  is the polymer film thickness cm and  $\varnothing$  is the diameter of the film disc cm.

#### ***2.5.4 Release rate from coated urea in water***

The release of urea from the coated products was determined over a 110 day period at 10 and 20°C with a product to water ratio of 20 g to 250 ml in a sealed plastic bottle, which was shaken daily. The quantity of urea released was measured on a 0.5 ml sample of the extraction solution using a handheld refractometer and reported in % Brix. The % urea released was then calculated based on the % Brix ratio between sample and control (urea). The % Brix was found to be linear to the urea concentration with a constant of proportionality of 0.951 with  $R^2 = 0.999$ .

The change in granule volume ( $\gamma$ ) was determined at the end of the extraction period by recovering the granules from the extraction solution and measuring the granule weight and density to determine the volume of granules. This was expressed as a % increase in volume of the original granule before extraction.

#### ***2.5.5 Digital analysis of particle size and volume change distributions***

The particle size distribution was measured in triplicate on 5 g samples, approximately 250 granules. The granules were carefully placed, so that they were separated, on an A4 matt black background within a calibration array of 9 x 10.2 mm diameter white plastic beads. A photo of the granules was then taken using a 4.1Mega pixel camera mounted at 45° to the surface to avoid light reflection. The image was analysed using Sigmascan Pro 5<sup>®</sup> software to measure the Feret particle diameter and maximum/minimum length of the individual particles. From these data the surface areas of the particles were estimated using an oblate approximation. The potential volume change  $\gamma$  is then estimated as the difference between the initial volume, calculated from the Feret radii and equivalent spherical volume and the final volume of the oblate spheroid. This analysis recognizes that only two of the three significant dimensions are recorded (length, width, height). However, the 45° of inclination of the camera effectively takes

an average of the two minimum dimensions. Thus, the volume calculations are relatively accurate, and this was confirmed in later comparisons with the volume change measured by weight and density. This procedure was carried out for coated urea granules and granules which were in equilibrium with water.

#### ***2.5.6 Film thickness distribution***

The distribution of film thickness was measured on 50 randomly selected granules that had been separated from a large sample using a riffle box. The granules were individually measured using a micrometer across the maximum and minimum diameters and weighed and then cut and placed in numbered cells in spotting tiles. Water was then added to dissolve the urea and the residual coating shells were washed, dried and weighed. From this weight and the granule dimensions the % coating and the film thickness were determined.

#### ***2.5.7 Permeability of film with coating thickness***

To investigate the effect of film thickness on water vapour and nutrient solution permeability a series of coating experiments were carried out applying 2, 3, 4, 5, 7 and 10 % coating levels of the control reactive poly-urethane resin to urea, producing mean film thickness of 0.00104, 0.00156, 0.00208, 0.0026, 0.0036 and 0.0052 cm, estimated from granule mass, surface area and coating weight.

The urea release rate from these products was then tested in water at 20°C (as described earlier) and the constant release rates and permeability of urea and thus water (Equation 2.30) determined from the release curve between 30-50%.

#### ***2.5.8 Hydraulic permeability $H'$***

The measurement of hydraulic permeability was carried out using a pressurised permeability apparatus which allows the determination of the hydraulic flow at varying pressures provided by a syringe and dead weights, Figure 2.2.

In this apparatus the diffusion/permeability cell is filled with 50% urea solution on the high pressure side via the pressure syringe with the air from the cell exhausted via the

high pressure exhaust line prior to it being clamped. On the low pressure side the cell is filled with water using the priming syringe and air from the cell exhausted via the low pressure exhaust line. With the cell primed, the high pressure syringe with platform is placed in the vertical position, the low pressure exhaust line is then primed and placed in the weighed receiver. At this point load is applied to the high pressure syringe using spotting plates (approximately 170g each). Two minutes is allowed for the system to come to equilibrium, the receiver is then weighed and replaced under the low pressure exhaust line. The quantity of liquid passing through the membrane is then determined by weighing the receiver 10 to 15 minutes later. The load was then further increased and flow's recorded until mechanical failure of the membrane or cell occurred. The pressure was then calculated based on the weight of spotting plates and corrected using a pressure vs. load calibration curve obtained earlier using a compression tube gauge, Figure 2.3.

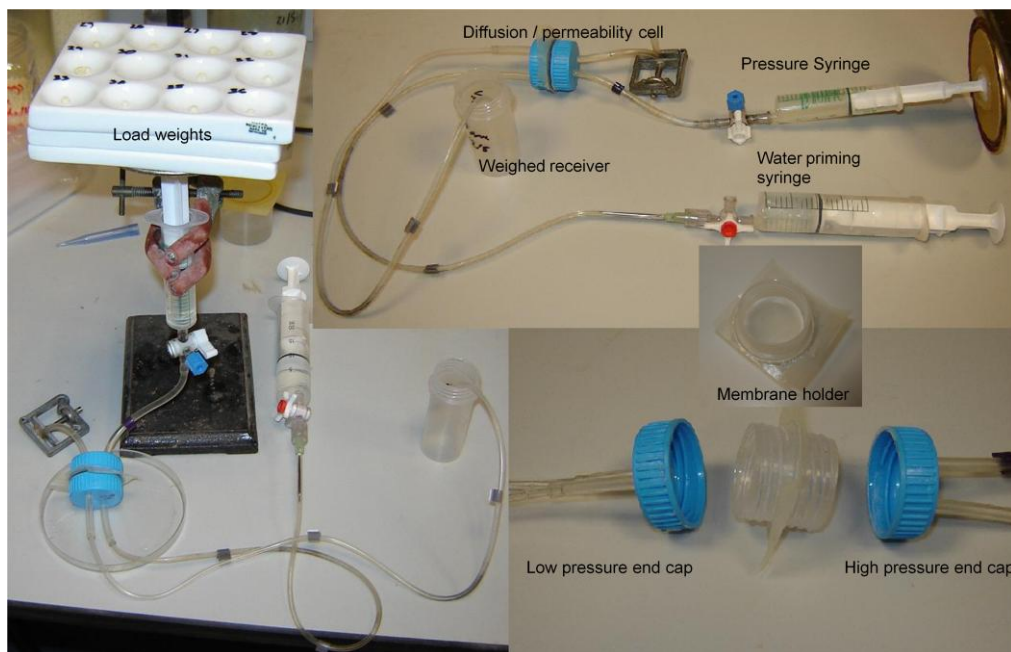


**Figure 2.2 Membrane diffusion and permeability apparatus.**

The calibration curve Figure 2.3, shows a zero offset of 14.1 kPa with a linear correlation to 120 kPa.

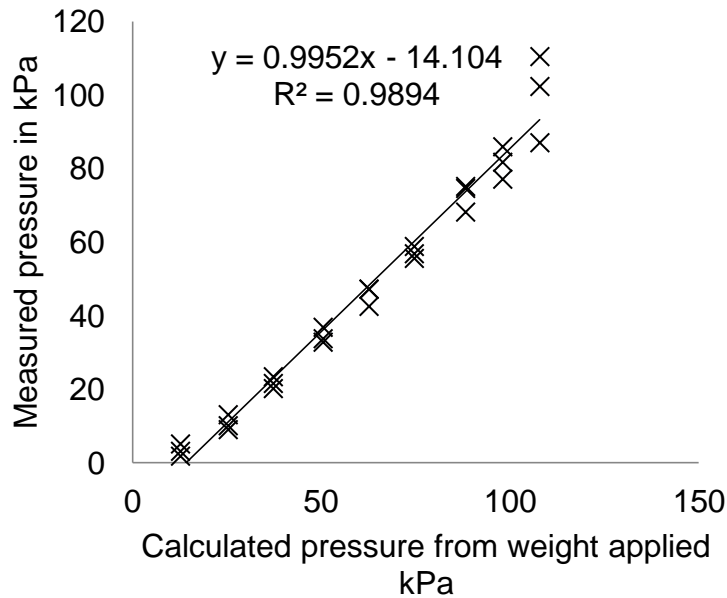


**Figure 2.3 Pressure calibration curve for dead weight syringe system**

The hydraulic permeability  $H'$  and critical pressure  $P_{critical}$  were then calculated from the plot of flow ( $\text{cm}^3 \text{d}^{-1}$ ) against the corrected pressure (Pa), as  $H'$  is the slope and  $P_{critical}$  is the x-intercept.

## 2.6 Results and discussion:

### 2.6.1 Physical testing of polymer films for Young's modulus and tensile strength

Analysis of the physical polymer film has shown that the addition of the amendments generally reduced the ultimate tensile strength and Young's modulus compared to the control in the following order Control > Palmitic acid > (Soya and Canola oil). No significant difference in ultimate elongation was observed (Table 2.1). Based on these measurements the rupture pressures were estimated using equation 2.5 for the coatings of between 253 and 515 kPa, based on a urea granule diameter of 0.4cm with a coating film thickness of 0.0025 cm.

**Table 2.1 Physical properties of laboratory polymer films**

<b>Polyol amendments</b>	<b>Tensile Strength MPa</b>	<b>Young's modulus MPa</b>	<b>Elongation %</b>	<b>Estimated Rupture Pressure*, kPa</b>
Control	20.6 ± 1.6	828 ±49	2.5 ±0.06	515
10% Palmitic	11.4 ± 0.7	569 ±17	2.0 ±0.07	285
15% Palmitic	15.3 ± 1.7	686 ±20	2.2 ±0.3	383
20% Palmitic	20.1 ± 0.4	707 ±16	2.9 ±0.07	503
10% Canola	10.1 ± 0.5	636 ±40	1.6 ±0.08	253
15% Canola	13.0 ± 0.7	499 ±32	2.6 ±0.05	325
20% Canola	15.5 ± 0.3	580 ±20	2.7 ±0.07	388
10% Soya	11.9 ± 0.7	568 ±15	2.1 ±0.02	298
15% Soya	13.3 ± 0.4	489 ±9	2.7 ±0.04	333
20% Soya	14.5 ± 0.6	548 ±19	2.6 ±0.08	363
LSD(P=0.05)	2.5(n=5)	76(n=5)	0.3(n=5)	

\* based on  $R = 0.2$  cm and  $l_o = 0.0025$  cm

### 2.6.2 Water vapour permeability $W'$ of laboratory prepared films

The addition of palmitic acid to the coating formulation resulted in no significant ( $P > 0.05$ ) change in water vapour permeability (Table 2.2) from the control, while the addition of canola and soya oils resulted in generally higher water vapour permeability. The water vapour permeability of all the polymer coatings showed no significant ( $P > 0.05$ ) change with temperature. However at 100% RH chambers the results were highly variable due to surface condensation of water at the low temperatures which resulted in inaccurate weights being measured due to condensation formation on the apparatus.

From these results it is expected that the canola and soya amended coatings should release nutrients at a higher rate from a coated fertilizer than the control and palmitic acid amendments.

The permeability results are also within the range of  $2.5 \times 10^{-9}$  to  $5.0 \times 10^{-9}$  (Shaviv et al. 2003a,b).

**Table 2.2 Water vapour permeability of laboratory prepared polymer films**

Polyol amendments	<i>Water Vapour Permeability as liquid</i> <i>x 10<sup>-9</sup> cm<sup>2</sup> day<sup>-1</sup> Pa<sup>-1</sup></i>				
	At 10°C 0% RH	20°C 0%RH	26°C 0%RH	20°C 100% RH	26°C 100% RH
Control	3.0±0.2	2.9±0.3	2.9±0.1	4.0±0.3	4.3±0.2
10% Palmitic	3.0±0.3	2.2±0.2	3.1	6.07±0.3	3.8±0.3
15% Palmitic	3.5±0.1	3.3±0.4	3.4±0.0.1	6.3±0.6	5.4±0.2
20% Palmitic	2.9±0.1	3.0±0.3	3.0±0.1	4.5±0.3	4.1±0.2
10% Canola	3.1±0.1	2.8±0.2	3.8±0.1	6.0±0.1	5.6±0.3
15% Canola	4.9±0.1	4.7±0.5	4.5±0.1	7.7±0.4	7.1±0.5
20% Canola	4.3±0.1	4.2±0.5	4.4±0.3	8.0±1.9	6.1±0.5
10% Soya	4.9±0.1	3.0±0.7	3.7±0.6	6.9±0.6	6.5±0.2
15% Soya	3.4±0.2	3.9±0.4	3.9±0.2	5.7±0.9	7.3±0.9
20% Soya	4.7±0.1	3.7±0.2	4.3±0.1	6.9±0.6	6.5±0.2
LSD	0.4(n=9)	1.5 (n=4)	0.6(n=4)	2.9(n=4)	1.9(n=5)

### 2.6.3 Permeability of film with coating thickness (coated granular urea)

The water vapour permeability,  $W'$ , of the coated urea as function of film thickness was determined for urea coated with the control coating (MDI:Castor Oil:TEA) receiving 2,3,5,7 and 10 coatings, which resulted in mean coating thicknesses of 0.00104, 0.00156, 0.00208, 0.0026, 0.0036 and 0.0052 cm.  $W'$  was determined from the release curve at values representing the constant release rate, Equation 2.19 (Figure 2.4) and the dependence of  $W'$  on  $l_o$  modelled using equation 2.37 (Figure 2.5).

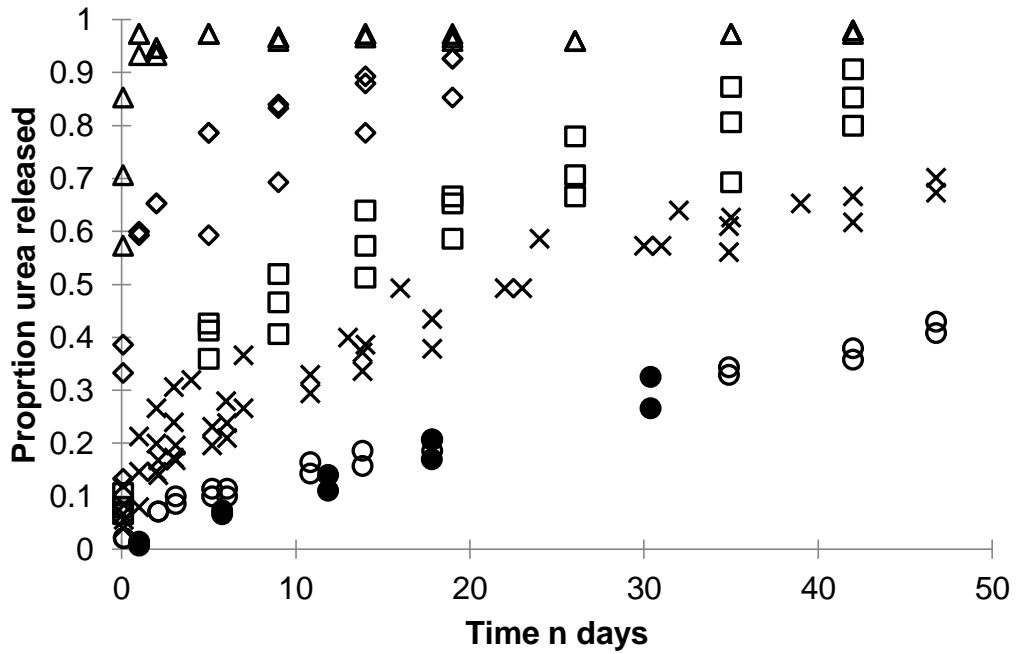


**Figure 2.4** Release rate profiles for RLP coated urea with film thickness,  $\Delta$  0.00104,  $\diamond$  0.00156,  $\square$  0.00206,  $\times$  0.0026,  $\circ$  0.0036 and  $\bullet$  0.0052 cm.

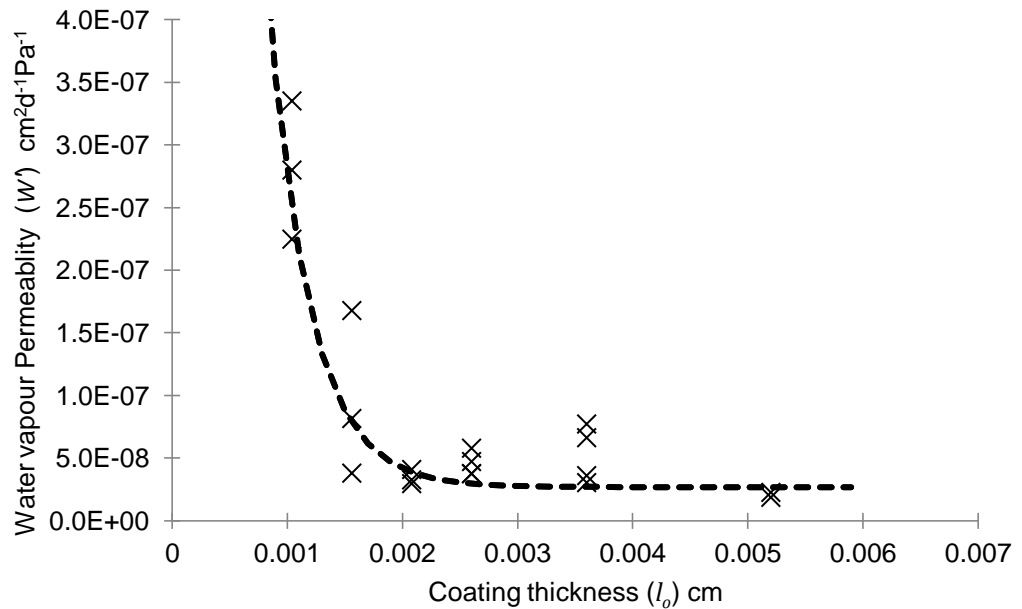


**Figure 2.5** Relationship between water vapour permeability ( $W'$ ) and mean coating thickness of RLP coated urea (control, MDI). Dashed line represents model  $W' = 2.68 \times 10^{-8} + 4.05 \times 10^{-6} e^{-2800l_0}$

The results show that the permeability falls rapidly until the coating thickness of 0.0026 cm was reached, at which point it becomes constant with increasing thickness at  $W'_{min}$ .

For the control coating the  $W'_{min}$ ,  $a$  and  $k$  were obtained (Figure 2.5) as  $2.68 \times 10^{-8} \text{ cm}^2 \text{ d}^{-1} \text{ Pa}^{-1}$ ,  $4.05 \times 10^{-6} \text{ cm}^2 \text{ d}^{-1} \text{ Pa}^{-1}$  and  $2800 \text{ cm}^{-1}$  respectively. The value of  $W'$  estimated from the release rate of granules in water is higher than the laboratory prepared films (Table 2.2) by a factor of 10, indicating that the coating process and granule urea surface asperity may have contributed to an increase in  $W'$ , compared to films that were recovered from the glass wall of the coating drum.

#### 2.6.4 Critical Pressure and hydraulic conductivity

The plot of flow rate against membrane pressure difference on four replicates of the control coating and 20% palmitic acid amended coatings show a high degree of variability (Figure 2.6). The results of this assessment showed a difference in critical pressure ( $P < 0.11$ ) but no difference in hydraulic conductivity.

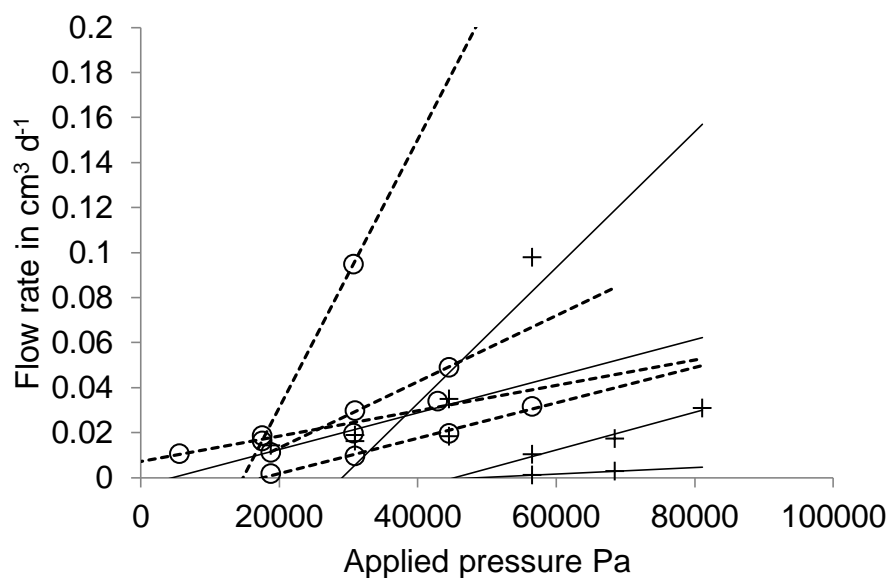


**Figure 2.6** Flow rate of urea solution (50% w/w) through laboratory prepared coating films as the result of applied pressure, control (○) and 20% Palmitic acid (+) amended polymer films. Solid lines represent linear regressions for control membrane and dashed lines 20% Palmitic acid

**Table 2.3 Critical pressure ( $P_{critical}$ ) and hydraulic permeability ( $H'$ ) of the control and 20% Palmitic acid amended films.**

	Critical pressure( $P_{critical}$ ) kPa		Hydraulic permeability ( $H'$ ) $cm^2 d^{-1} Pa^{-1}$	
	Control	20% Palmitic acid amended	Control	20% Palmitic acid amended
Rep 1	33.3	26.5	2.2E-06	1.3E-06
Rep 2	66.9	10.9	1.4E-07	1.4E-06
Rep 3	57.7	22.9	8.8E-08	4.6E-05
Rep 4	8.7*	-8.3*	8.1E-07	5.6E-07
Mean	41.7	13.0	8.3E-07	1.2E-05

\* Not included in mean or statistical analysis due to abnormally low result, likely due to large pore size being present.

### 2.6.5 Estimation of equilibrium pressure $P_{eq}$

With both  $W'$  and  $H'$  estimated, the equilibrium pressure within the coated granule can be calculated (Equation 2.8) for both the control and 20% palmitic acid amended coatings. The results show that for  $W'$  estimated using the water vapour diffusion cells ( $3 \times 10^{-9} cm^2 d^{-1} Pa^{-1}$ )  $P_{eq}$  is 1.5 and 0.1 Pa for the control and 20% palmitic acid amended coating, respectively. These values appear low and indicate a more direct measurement of  $P_{eq}$  is required. The low result also indicates that the release of urea following the initial lag time is likely to progress directly to the constant rate release period following a short re-equilibration period ( $P_{critical} \gg \gg P_{eq}$ ).

### 2.6.6 Volume change following extraction

The change in coated granule weight and density following extraction in water for 100 days, showed an average volume change ( $\gamma$ ) of 16.0% with a mean standard deviation of 2.5 % (Table 2.3). This is greater than the 2-3 % increase due to measured film elasticity (Table 2.1), indicating the volume change has resulted from a change of granule shape (Figure 2.1).

**Table 2.4 Measured mean volume change of coated granules following 100 days of extraction in water**

<i>Product</i>	<i>Mean</i> $\gamma$	<i>SD</i>
MDI	14.6%	2.3%
10% canola	17.2%	0.7%
15% canola	15.1%	0.6%
20% canola	14.2%	1.5%
10% soya	17.0%	2.3%
15% soya	18.9%	1.0%
20% soya	16.0%	0.9%
10% palmitic	13.1%	4.1%
15% palmitic	15.9%	3.9%
20% palmitic	17.8%	0.1%
Average	16.0%	

### 2.6.7 Digital Analysis

The digital image analysis of the coated urea showed spheroid geometry (Figure 2.7). Measurement of the maximum ( $r_{max}$ ) and minimum ( $r_{min}$ ) radii using the sigmascan program revealed a eccentricity ( $e = r_{min}/r_{max}$ ) distribution mean 0.83  $\sigma$  0.11 with a maximum radii distribution of 0.243  $\sigma$  0.124 cm and a Feret radii distribution with mean 0.26  $\sigma$  0.034 cm.

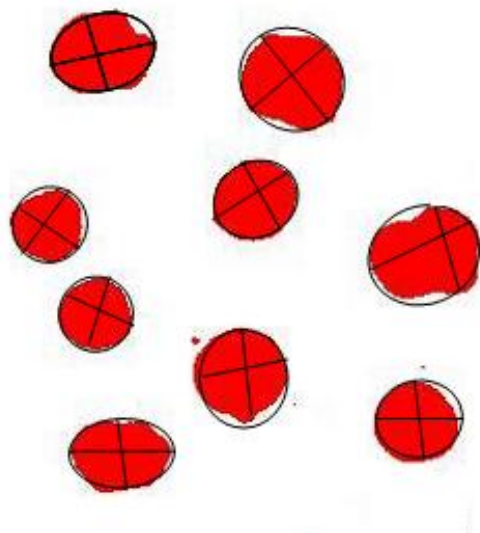


**Figure 2.7 Granule image morphology of urea prior to coating.**

The range in spheroid shape partly explains the greater than predicted volume change when the granules were equilibrated in water (Table 2.4). From the digital analysis of the granule shape the volume changes can be calculated for the volume equivalent sphere to the oblate spheroid geometric change (Table 2.5).

**Table 2.5 Modelled volume change of granule population based on measures spheroid shape parameters  $r_{max}$ ,  $e$  and Feret radii for the transition from equivalent spherical volume (ESV) to oblate spheroid.**

Shape transformation	$\gamma$ mean	$\sigma_\gamma$ standard deviation
ESV to Oblate	16.7%	21.2%

This result gives a similar mean volume change to that observed for the water equilibrated coated granules (Table 2.4) and allows the individual population distribution ( $\sigma_\gamma$ ) to be estimated.

### 2.6.8 Coating thickness distribution

In the control coating (MDI) product the distribution of coating thickness was observed to be uniform and normal with a mean of  $l_o$  0.0026  $\sigma_l$  0.00038 cm with a correlation coefficient of 0.983 between the observed and normal distribution. This distribution was then assumed to represent the coating distributions of the canola oil, soya oil and palmitic acid amended products. However, following the water extraction trials in which the palmitic acid amended products showed a dramatic increase in initial release of urea (Figures 2.8 and 2.9), further analysis of the coating thickness distribution was carried out on the palmitic acid amended products. The results confirmed the assumption was correct and the increased release was not due to a change in coating distribution (Table 2.6).

**Table 2.6 Polymer film thickness means and standard deviation's for the control coated and palmitic acid amended coatings**

Products	Mean film thickness	Standard deviation of
	cm	film thickness
		cm
Control	0.0026	0.0004
10% Palmitic	0.0030	0.0005
15% Palmitic	0.0030	0.0006
20% Palmitic	0.0027	0.0005
LSD	<b>0.0002</b>	

### 2.6.9 Release rate in water

The observed release of urea in water from the RLP coated urea's at 10 and 20°C, (Figures 2.8 and 2.9) show three distinctive release characteristics ; a instant release of nutrient from imperfectly coated granules (0-2hr), a constant rate 1- 10 days, and a falling rate for 10 days+.

The amendment of the castor oil with palmitic acid at levels greater than 10% show a significant increase in the constant release rate with 50 to 60 % of the urea being released in the initial 10 to 15 days without rupture, as the granules were recovered (Table 2.4). The high constant release rate of urea from the palmitic acid amended products was also less affected by temperature (Figures 2.8 and 2.9).

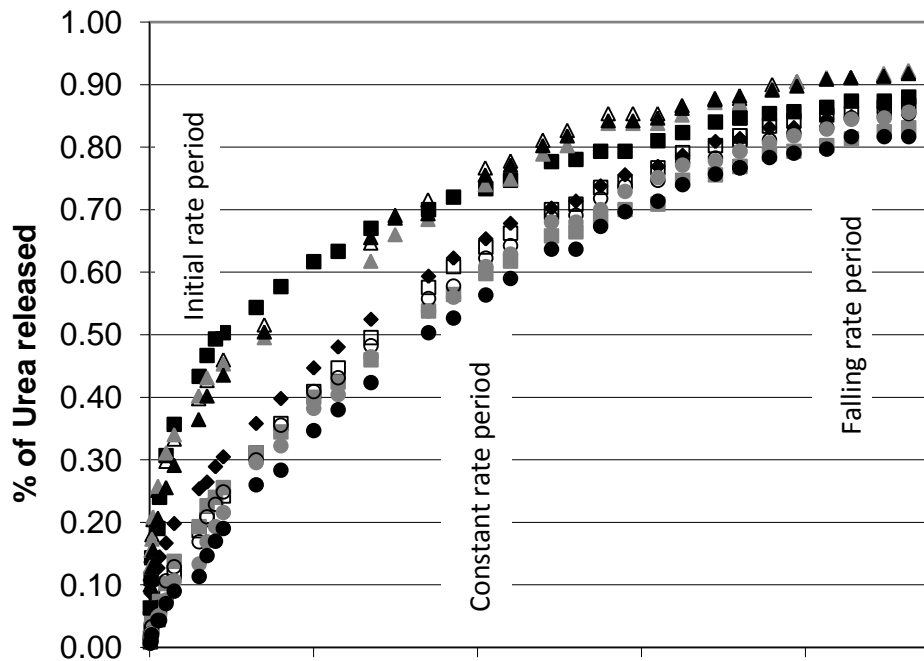


**Figure 2.8** Proportional urea release with time in water at 20 °C, for urea coated with ♦ RLP and RLP modified with ■ Canola oil, ▲ Palmitic acid and ● Soya oil at levels of 10% (hollow), 15% (gray) and 20% ( solid).

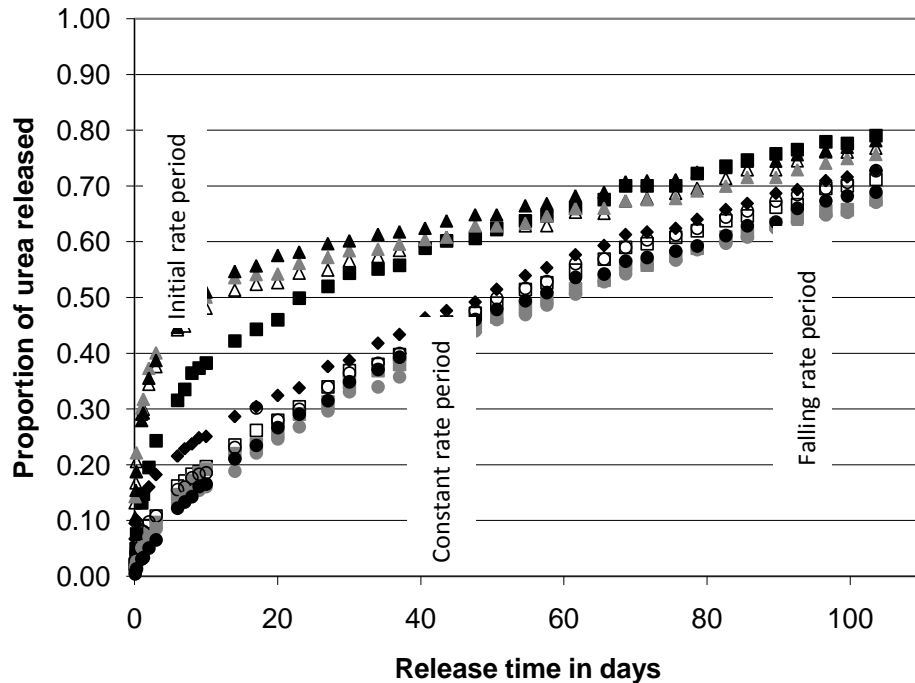


**Figure 2.9** Proportional urea release with time in water at 10 °C , for urea coated with ♦ RLP and RLP modified with, ■ Canola oil, ▲ Palmitic acid and • Soya oil at levels of 10% (hollow), 15% (gray) and 20% (solid).

## 2.7 Modelling of release rates based on physical film and granular parameters

The validation of the proposed models was carried out using a randomly generated population of 500 coated granules based on the mean and standard deviation's of granule Feret radius  $R$ , film thickness  $l_o$ , volume change  $\gamma$  and water vapour permeability  $W'$  calculated using equation 2.37.

The model equations were written into visual basic programs for release in water (Appendix 1.) and in field conditions (Appendix 1.1). The water extraction model was tested against the observed water extraction rates of urea from, the control (MDI) at 5, 7 and 10% coating levels and the 20% palmitic acid amended treatment at a 5% coating level. In field conditions (Chapter 3 &4) coating levels of 5(5UCU) and 7% (7UCU) 20 % palmitic acid amended coatings were trialled and the cumulative additional herbage N recovered compared to the model predictions of urea N release.

**Table 2.7 Polymer film thickness and distribution within products to be modelled.**

Modelling parameters	5% MDI	7% MDI	10% MDI	5UCU	7UCU
Mean film thickness					
$l_o$ cm	0.0026	0.0036	0.0052	0.0027	0.0036
$\sigma_l$ cm	0.00035	0.0007	0.001	0.0005	0.0007
Volume change $\gamma$	-----0.16-----				
$\sigma_\gamma$	-----0.21-----				
Feret radius $R$ cm	-----0.26-----				
$\sigma_R$ cm	-----0.036-----				
$W'_{min}$ $\text{cm}^2\text{d}^{-1}\text{Pa}^{-1}$	-----2.68x10 <sup>-8</sup> -----			-----4x 10 <sup>-8</sup> -----	
$a$ $\text{cm}^2\text{d}^{-1}\text{Pa}^{-1}$	4.05x10 <sup>-6</sup>				
$k$	2800				
$P^o_{wv}$ Pa	133.32 *EXP(20.386- (5132/(273+ T(°C ))))				
$C_{sat}$ $\text{g cm}^{-3}$	6.96 x 10 <sup>-3</sup> T(°C )+0.45				
$\rho_s$ $\text{g cm}^{-3}$	1.26				

From the previous sections the urea release modelling parameters were obtained (Table 2.7) and used to simulate the release of urea from coated urea in water and field conditions.

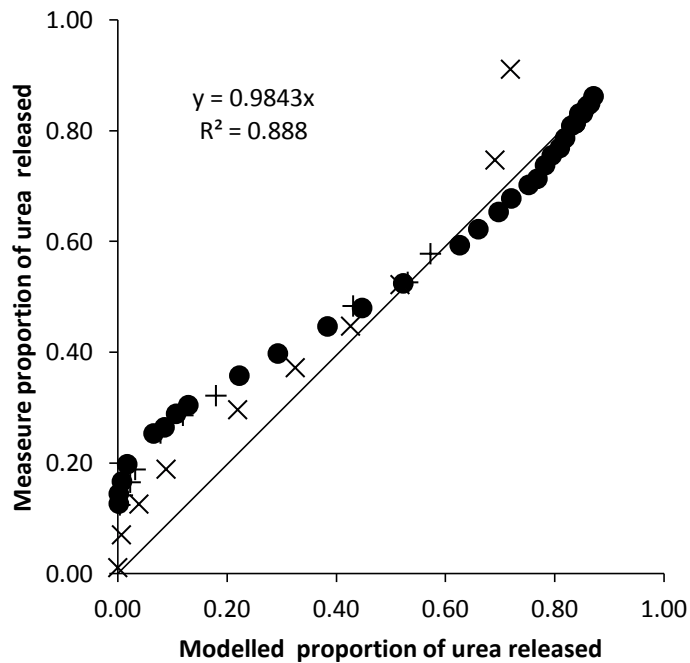


**Figure 2.10 Correlation plot of modelled and measured urea release for 5(●), 7(+), and 10% (X) coating levels of the control polymer MDI: Castor oil: TEA in water at 20°C with lag period calculated**

The model produced a good correlation with the measured water release rate data for the urea coated with the control MDI: Castor oil: TEA at 5, 7 and 10% coating levels (Figure 2.10 and 2.11). However the application of the lag period (Figure 2.10) results in the model significantly underestimating the initial release stage for all products.

The removal of the lag period from the model improved the correlation with the measured data (Figure 2.11). The application of lag time assumes uniform internal liquid pressure within the granule, which would occur when uniform permeability of water and solute occurs over the coating surface. However the results indicate that this may not be correct and the initial dissolution of urea may occur in isolated areas allowing the critical internal pressure to be rapidly achieved without full volume change. This would allow both release and volume change to occur at the same time.

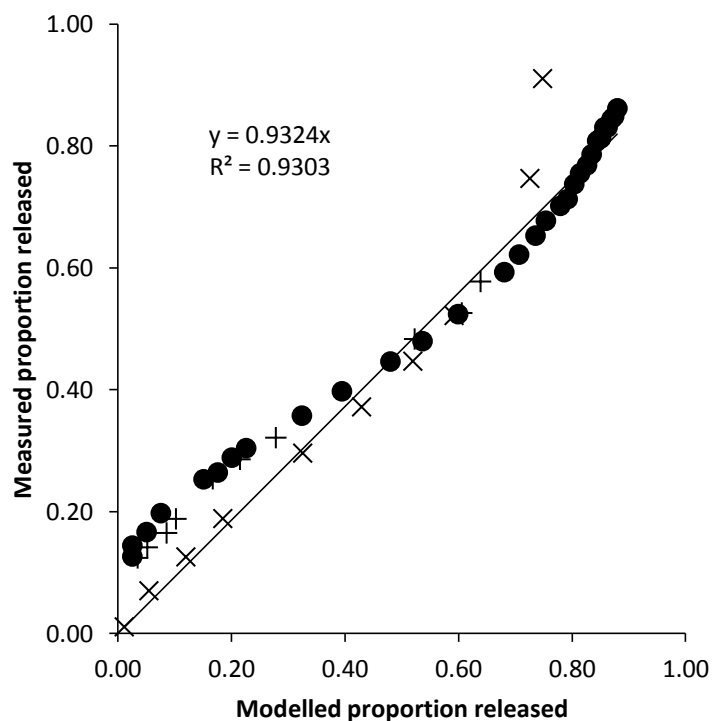


**Figure 2.11 Correlation plot of modelled and measured urea release for 5(●), 7(+)  
and 10% (X) coating levels of the control polymer (MDI: castor oil:  
TEA) in water at 20°C with no lag period calculated**

The application of the hydraulic convection model to the release of urea from the urea coated with 5% of the Palmitic acid amended polyol's, showed an increase in permeability with  $W'_{min}$  estimated as  $4 \times 10^{-8} \text{ cm}^2 \text{ d}^{-1} \text{ Pa}^{-1}$  based on optimising the fit to the release rate data (Figure 2.12).

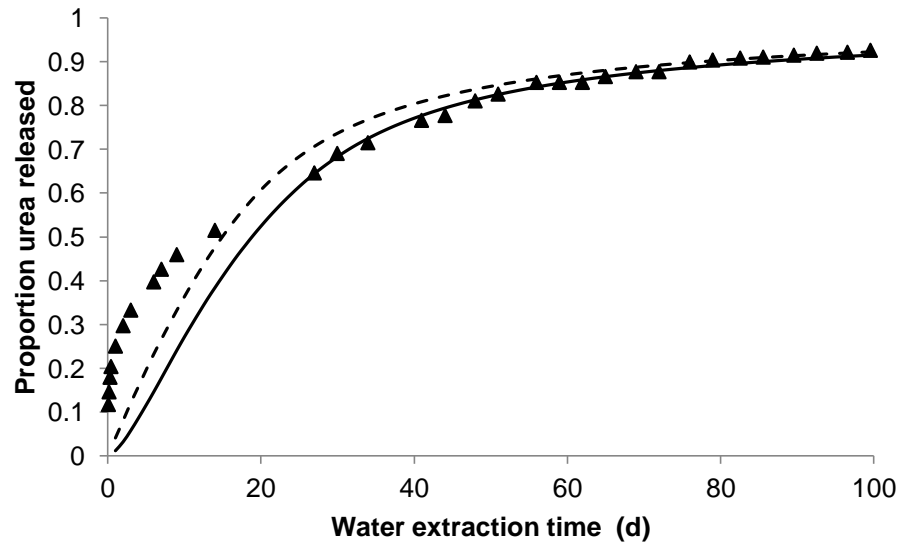


**Figure 2.12** Plot of the measured proportion of urea released at 20°C in water extraction of 5% coating level of 20% Palmitic acid amended coated urea(▲), compared to modelled results using hydraulic convection model, with (solid) and without lag period (dashed) line.

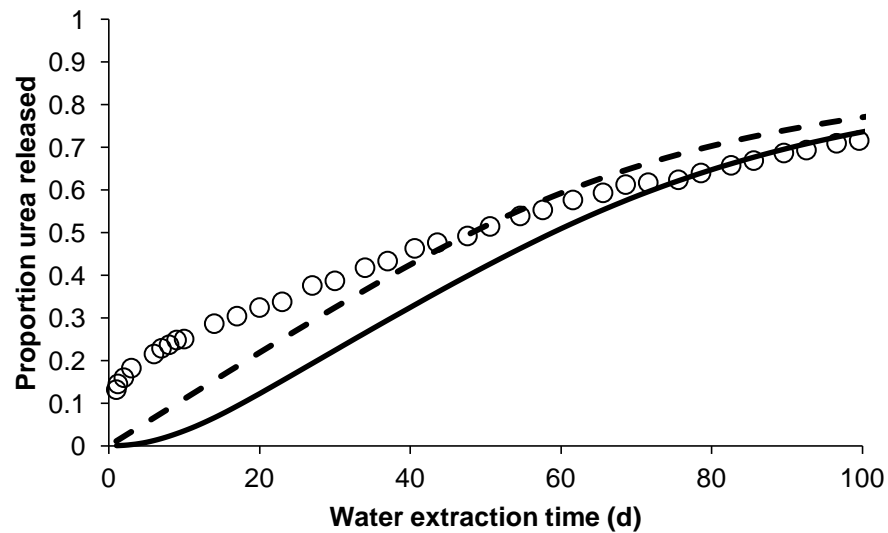


**Figure 2.13** Plot of the measured proportion of urea released at 10°C in water extraction of 5% coating level of 20% Palmitic acid amended coated urea(○), compared to modelled results using hydraulic convection model, with (solid) and without lag period (dashed) line.

### **2.7.1 Effect of temperature on models**

The comparison of the modelled and measured results, for the release of urea from the 5% control polymer (MDI: castor oil: TEA ) coated urea (Figure 2.13), at 10°C in water, showed the model underestimates the release of urea in the initial 30 days. This is consistent with the 20°C assessments of the model against the measured release of urea in water. The model will require further work to improve this initial release estimation, which is controlled within the current model by the estimated water vapour permeability of the film as a function of coating thickness (Equation 2.37) and the coating thickness distribution. Improvements to these estimates may result in a better correlation between the observed and predicted results in the initial month of release.

### **2.7.2 Field trial release rate data**

The application of the 5% (5UCU) and 7% (7UCU) palmitic acid amended RLP coated urea in field trials (Bishop et al. 2008) allows the comparison of additional nitrogen recovery and the modelled release rate. The model was applied with daily correction for soil temperature and soil moisture (kindly provided by J. Hanly per. com.) The observed release rate should exceed the predicted due to increasing temperature, however the recovery of nitrogen in the herbage significantly reduced as the soil moisture fell below 50% of field capacity ( $\theta = 0.25$ ), Figure 2.14.

### **2.7.3 Summary and conclusion**

The objectives of this Chapter (section 2.4) was to develop and evaluate a fundamental model to explain the release of urea from RLP coated urea using a range of modified RLP coating formulations in water extraction trials and palmitic acid modified RLP coated urea in a subsequent field trial.

The new hydraulic convection model developed differs from the more traditional permeability/diffusion models and osmotic pumping models as it includes geometric volume change, based on the digital analysis of coated granules, and a falling release rate equation based on the change in differential water vapour pressure ( $\Delta P_{wv}$ ) not the solute concentration gradient across the coating. These new features increase the potential lag period and produce a slower falling rate period compared to the

exponential decay (Jarrel and Boersma, 1980; Shaviv *et al.* 2003a) or the quadratic decay (Theewes, 1975) models.

The application of the hydraulic convection model described the release rate of urea from reactive layer polyurethane coated urea in both water and soil systems. In the water extraction system the laboratory prepared coated urea produced higher release rates of urea than predicted by the model, which cannot yet be explained. For surface applied coated urea in field trials the initial rapid release was not evident, as the first measurement of herbage N recovery was at 28 days by which point the model produced a good fit with measured results.

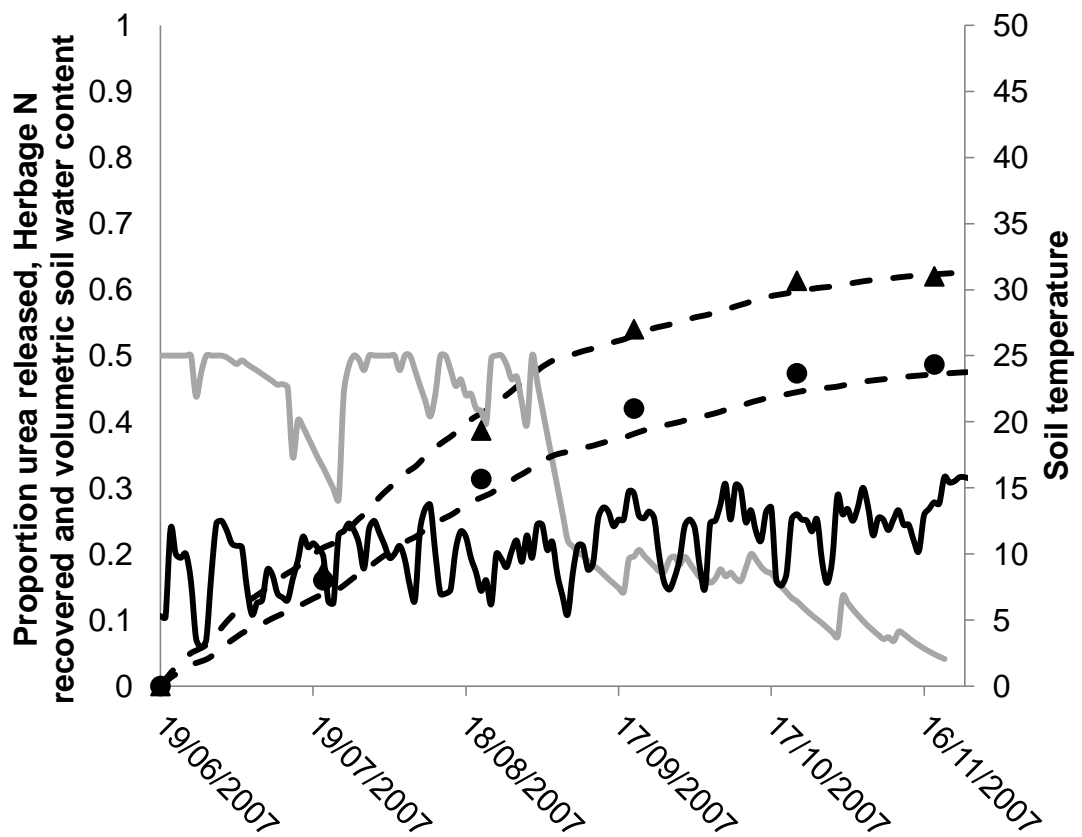


**Figure 2.14** Proportional herbage N recovery for surface applications 5UCU(▲) and 7UCU (●) at 150 kg N ha<sup>-1</sup> on Italian ryegrass crop (Bishop *et al.* 2008) with release of urea modelled using Hydraulic convection model (black dashed line) using mean daily temperature (black line) and soil volumetric water content (gray line).

The model suggests that release occurs without a lag period as a better fit between the model and data is obtained with  $t' = 0$ . However volume change has been measured in the coated urea granules after 100 days in water of 16 % (Table 2.4), which implies release and swelling of the granule have occurred simultaneously.

The modification of the RLP by addition of polyunsaturated vegetable oil (Soya) at levels up to 20% in the castor oil produced no significant change in N release from the coated urea. However the addition of palmitic acid (saturated fatty acid) at levels greater than 5% and canola oil (mono-unsaturated oil) at 20% of the castor oil produced significant increase in initial release rates. This is likely due to reduced reactivity with the diisocyanate (MDI), which in the case of palmitic acid reduced the critical pressure at which hydraulic flow commenced (section 2.6.4), thus lowering the initial lag time.

The modelled urea release successfully explains the release of urea in the winter field trials on Italian ryegrass (Chapter 3) and the prevention of mineral N accumulation in the soil profile (Chapter 4), as the predicted release of urea and the recovery of N in herbage is in good agreement. The field model suggests that in addition to soil temperature, soil moisture is a critical requirement for urea release from RLP coated urea. This is an important feature in rain fed pastoral systems that are prone to wet and dry cycles which limit plant growth. The synchronisation of N release and the soil moisture dependent growth may show additional benefits in the reduction of nitrate toxicity in pasture following dry periods. The N release from the RLP coated urea is further explored in Chapter 4 (sections 4.3.2 and 4.3.3) in terms of residual N remaining in RLP coated urea granule and N availability under two soil moisture regimes.

The model will require further development to account for an initial release involving both volume change and N release processes. The direct measurement of internal granule pressure (using micro-sensors) and release rate may give additional information of this initial release period and whether the re-equalisation period, which is ignored in the working model, is required.

## **Chapter 3**

### **Evaluation of polymer coated urea in grazed pasture systems**

---

The review of literature (Chapter 1) indicates that polymer coated urea offers the potential to reduce direct leaching losses of N and to increase uptake efficiency of N in pasture systems. The increase in plant N use efficiency is also expected to reduce N returns via urine to pasture by lowering the peak herbage N content. Chapters 3 and 4 describe field research that was undertaken to test this potential. Chapter 3 reports the pasture growth responses to N uptake and the relative loss of N from the pasture via leaching. This work has been published.

*Bishop et al. (2008). New Zealand made controlled release coated urea increases winter growth rates of Italian ryegrass with lower N leaching than uncoated urea. Proceedings of the New Zealand Grasslands Association 70: 141-145.*

In addition to the published work the fate of applied N in the soil profile is examined in Chapter 4 and more detailed implications of controlled-release urea on N recycling by grazing cows are explored.

#### **3.1 Introduction**

Increases in dairy stocking rates often result in a winter feed deficit which require either supplementary feed to be brought in, stock to be grazed off-farm, or “N boosted” winter pasture growth, all of which incur additional costs. The application of N in winter is an effective means of increasing N-limited pasture growth, although this often results in direct losses of N via leaching with winter drainage causing potential risk to ground water quality. More significantly, elevated herbage N contents shortly after N fertiliser application may result in highly concentrated urine N (Castillo et al. 2000) being returned to the pasture in patches and leached (Ball et al. 1979; Magesan et al. 1996; Ledgard et al. 1999; Di and Cameron 2002). To combat these effects, N fertilisers are usually applied in split applications at rates of 25–50 kg N ha<sup>-1</sup> month<sup>-1</sup> to limit direct leaching losses. Nitrification inhibitors such as DCD can be applied in autumn to slow nitrification and leaching of returned urine N from grazing (Di and Cameron 2004b).

Split applications of urea may increase production cost in terms of a potential NZ\$100 t<sup>-1</sup> urea for each additional application (pers. com. Manawatu Mini-spreaders, 2008). DCD application increases costs by NZ\$95 and 190 ha<sup>-1</sup> (EcoN, Ravensdown 2011 price list, for single and double applications, respectively) and results in higher N recovery from pasture (Di and Cameron 2004a) and thus contributes to higher urine N returns. An alternative to split applications is a single large application of coated controlled release urea, which may reduce direct leaching losses and lower peak herbage N levels and thus urine N returns to pasture.

To assess the effectiveness of different forms of winter N applications, laboratory manufactured RLP coated urea at 5 and 7% coating levels (5 UCU and 7UCU), 10% DCD coated urea (DCDU), urea (U) and split applications of urea (SU) were trialled on a short rotation Italian ryegrass at application rates of 50 and 150 kg N/ha.

### 3.2 Materials and methods

#### 3.2.1 Site

The trial was located on Tokomaru silt loam (Pallic Soil) at the Mognie sheep farm block of Massey University, Palmerston North, New Zealand, the soil properties at this site are shown in Table 3.1. The trial paddock had been cultivated and resown with Italian ryegrass (Feast II<sup>®</sup>) in March 2007. The climatic conditions over the trial period (Table 3.4) provided sufficient rainfall and soil temperatures to maintain growth.

**Table 3.1 Soil properties at the trial site**

Soil depth (cm)	Total C (LOI) (%)	Total N (%)	Olsen P (mg/kg)	pH (1:2.5 w/w soil:water)	Bulk density kg/m <sup>3</sup>
0-10	3.7-4.4	0.27-0.35	54-75	5.6	1190-1250

#### 3.2.2 Design and treatments

All five N treatments (U, 5UCU, 7UCU, SU, DCDU) were tested at the application rate of 150 kg N/ha (150 N) and four (U, 5UCU, 7UCU, DCDU) at 50 kg N/ha (50 N) plus a nil-N control treatment. The treatments were replicated three times and arranged in 50 N and 150 N complete randomised block designs, Figure 3.1.



**Figure 3.1 Randomized block layout for RLP coated urea field trial at Massey University Palmerston North. Gray blocks treatments applied at  $50 \text{ kgN ha}^{-1}$  while black blocks recovered treatments at  $150 \text{ kgN ha}^{-1}$ .**

The trial area was fenced around with electric wire to keep livestock away, mown to a height of 6 cm and 33 plots of 1 m x 2 m were pegged out. Each plot was cored 0 -25cm and sectioned into 5cm intervals, the core sections were weighed and air dried at  $65^{\circ}\text{C}$  and reweighed to determine moisture content. The dried samples were then sieved  $< 2 \text{ mm}$  and prepared for standard soil analysis (Table 3.1 result of the combined 0-5 and 5-10cm sections, methods given by Blakemore et al.(1987). The treatments were broadcast by hand on the 20 June 2007 with the SU treatment applied again at 50 N immediately following each of the next two harvests. The plots were mown on a monthly basis to measure dry matter (DM) and herbage N content, starting on 22 July. The amount of nitrate leached was calculated based on the nitrate concentration measured in soil solution collected following significant rainfall ( $>10\text{mm/day}$ ) from ceramic suction cup lysimeters positioned at the base of the cultivation zone (25 cm), in each of the duplicate plot of the 150 kg N/ha treatments,. The total estimated drainage was calculated based on climatic data from NIWA/AgResearch.

### **3.2.3 Plant analysis**

#### *Drymatter*

The dry matter yield from each plot was determined by mowing the plots to a height of 5 cm and weighing the total clip. A sub-sample of between 200 to 300 g of green herbage was then taken from each plot and the dry matter content determined by drying at 65°C until constant weight was achieved. This was then used to calculate the total dry matter yield for each plot.

#### *Herbage N*

The herbage N was determined following the grinding of the dry matter sample using a ultra-centrifugal grinder. The ground herbage was then digested using a micro-Kjeldahl digestion followed by ammonium-N analysis using an auto-analyser (Blakemore et al., 1987).

### **3.2.4 Soil Analysis**

#### *Soil bulk density and estimated field capacity*

The bulk density and field capacities were measured using repacked cores measuring 1 cm high and 5cm in diameter, which were saturated with water by submersion for 24 hr and then placed on a suction plate and allowed to equilibrate for 48 hrs with a suction pressure of 5 kPa. Following this the cores were weighed and dried at 105°C for 24 hrs to determine the bulk density and field capacity.

#### *Total soil carbon and nitrogen*

Total soil carbon and nitrogen were analysed simultaneously using a LECO FP2000 combustion analyser on samples of air dry soil sieved to < 2mm.

### **3.2.5 Statistics**

The treatment results were analysed using SAS software to determine least significant difference (LSD) between treatments with a confidence level of 95% for individual 50 N and 150 N treatments, using a general linear model.

### 3.3 Results and Discussion

The trial progressed well until just prior to the October harvest (labour weekend 20 to 22 October 2007) when lambs broke through the surrounding electric fence and grazed the plots. The lost data were able to be modelled using factor analysis of the previous and the subsequent harvest using Minitab statistical software, which revealed a strong correlation ( $R^2=0.92$ ) between DM produced, N uptake and solar radiation, equation 3.1. The plot N uptake trends were also analysed allowing the October N uptake to be estimated. Equation 3.1 models the DM response based on the natural log of the solar radiation in  $\text{MJ m}^{-2}\text{d}^{-1}$  and N uptake in  $\text{kg N ha}^{-1}\text{d}^{-1}$ .

$$DM(\text{kg ha}^{-1}\text{d}^{-1}) = -7.18 + 19.9 \ln(\text{solar radiation}) + 30.3 \ln(\text{N uptake rate}) \quad \text{Eq. 3.1}$$

Due to the uncertainty in these estimated values the cumulative yield results are taken at the third harvest (September), while the October and November harvest are analysed individually.

#### 3.3.1 Dry matter

The cumulative additional dry matter production Table 3.2a (equals cumulative DM yield (data not shown) minus cumulative nil-N control DM yield (Table 3.2b)) over the first 3 months (column 21/09/2007 in Table 3.2a) for the 50 N treatments ranged from 857 to 1121 kg of additional DM/ha with no significant differences between treatments. Following the third month, a small increase in growth rate was obtained in October (modelled) followed by no significant increase in production due to the 50N treatments.

At the higher rate of 150 N, the DM production increased significantly ( $P<0.05$ ) over the initial 3 months compared to the control, producing between 1666 and 2288 kg DM  $\text{ha}^{-1}$  additional growth over the period (column 21/09/2007, Table 3.2a) with no significant difference between N treatments. The trends followed similar patterns to the lower N rate treatments. The SU treatment (3 x 50 N) continued to increase production over the 3 months. The estimated peak additional accumulated yield occurred in October (modelled eq. 3.1) and ranged between 2009 to 2995 kg with no significant difference between N treatments. At the last harvest in November, DM yields on the 5UCU, SU, DCU and U treatments were 185, 308, 393 and 471 kg DM/ha lower than

the control ( single harvest LSD P=0.05, 145 kg DM ha<sup>-1</sup>), shown as a drop in additional cumulative DM (Table 3.2a), whereas the 7UCU treatment showed no significant difference from the control.

**Table 3.2 (a) Cumulative additional dry matter (DM) (cumulative treatment DM minus cumulative Nil-N control DM) in kg DM/ha for 50 and 150 kg N/ha treatments and (b) Cumulative control yields on different harvest dates.**

Treatments	22/07/2007	22/08/2007	21/09/2007	23/10/2007*	19/11/2007
<b>(a) Additional DM</b>					
150 U	522	1515	2288	2757	2286
150 DCU	290	1199	1955	2009	1700
150 5UCU	477	1244	2009	2477	2291
150 7UCU	504	1079	1666	2065	2093
150 SU	309	1157	2240	2995	2723
50 U	344	747	953	1057	962
50 DCU	295	764	1121	1319	1188
50 5UCU	232	598	1073	1397	1572
50 7UCU	141	492	857	1060	1075
LSD 150	283	570	767	1125	1411
LSD 50	138	326	525	859	984
<b>(b) DM for Nil N only</b>					
Control	853	1556	2491	3380	4540
s.d.	98	349	583	886	1180

\* Estimated harvest

The negative growth response was suspected to be as a result of suppressed N mineralisation/fixation in these treatments of 4 to 5 kg N/ha over this month (calculated from the plant and soil N differences between the control and treatments) and the stalling of N release from the 7UCU due to low surface soil moisture.

The controlled release coated urea products have shown similar DM production over the trial period with 150 7UCU producing a significantly lower negative growth effect in the November period compared to 150 5UCU, SU, 150U and 150 DCU.

### 3.3.2 *Herbage N recovery*

The additional herbage N recovered (difference between treatment and nil-N) (Table 3.3a) above that in the control (Table 3.3b) over the trial period peaked in August (the

second harvest) for the 150 N treatments, U, DCDU and 5UCU, reflecting 79, 68 and 61% of the total N recovered, respectively. The utilisation of N to produce DM was, however, low over these months, due to short days and low solar radiation (Table 3.4), resulting in low N to DM conversion efficiency (c.f. Table 3.2). N recovery peaked in the SU treatment in September (the third harvest) following the final application of urea, while the 7UCU produced an initial peak with a gradual reduction in the recovery rate over the trial.

In terms of cumulative percent N recovery (= cumulative N recovered x 100/N supplied), there was no significant difference between treatments at the 50 N rate, with N recoveries by November ranging between 42 to 66%. At 150 N, the 5UCU, DCDU, U and SU treatments had cumulative percent N recoveries between 61 to 77% with the 7UCU being significantly lower (49%,  $P < 0.03$ ) based on the quantity of N applied. The apparently low percent N recovery in the 7UCU treatment was due to 27% of the applied N remaining unreleased from the coated granules at the completion of the trial.

**Table 3.3 (a) Additional herbage N recovered from treatments (treatment minus nil-N control (b)) (kg N ha<sup>-1</sup>) on different harvest dates after N applications at 50 and 150 kg N ha<sup>-1</sup>.**

Treatments	22/07/2007	22/08/2007	21/09/2007	23/10/2007*	19/11/2007
<b>(a) Additional N</b>					
150 U	35	46	22	7	-7
150 DCDU	20	42	22	11	-4
150 5UCU	26	32	23	11	-1
150 7UCU	24	23	16	8	2
150 SU	17	36	46	20	-3
50 U	16	8	4	2	-4
50 DCDU	14	11	10	1	-5
50 5UCU	8	7	12	5	1
50 7UCU	6	7	9	3	-2
LSD 150	7.0	5.3	3.0	2.3	1.2
LSD 50	7.3	7.3	5.2	4.4	3.3
<b>(b) Herbage N in Nil-N</b>					
Control	33	20	19	19	18
s.d.	6	8	5	5	6

\* Estimated harvest

The application of the DCDU, SU and U treatments at both rates showed lower herbage N recoveries at the November harvest than the control. The low herbage N recovery is

also related to the low DM production over the November relative to the control, 5UCU and 7UCU treatments. The results were amplified in the DM data, due to the rate of N to DM conversion during November of 52.5 kg DM/kg N (Fig. 3.1). The release rate of the 5UCU and 7UCU appears to have stalled over November due to dry surface conditions giving lower than expected N release/uptake and DM yields (soil moisture, data not shown).

### 3.3.3 Drainage

The application of urea using split applications, in the form of controlled release coated urea, or as DCDU, significantly reduced soil solution nitrate levels and estimated cumulative leaching losses at the application rate of 150 N (Figure 3.2). During the initial drainage on 6/07/2007 the soil solution N concentrations were highly variable producing no significant difference between the treatments and control. This initial nitrate-N leaching of  $2.5 \pm 2.2$  kg N/ha resulted from the initial cultivation as indicated by the analysis of pre-treatment core samples collected on 15/6/2007 that showed high levels of soil nitrate at the 15 to 25 cm depths (Figure 4.2). For this reason the initial drainage has been excluded from the data in Figure 3.2.

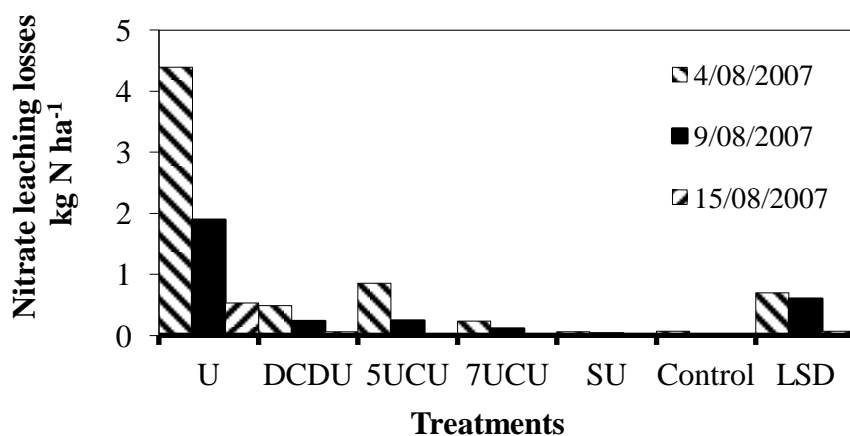


**Figure 3.2** Estimated nitrate-N leaching from 150 kg N ha<sup>-1</sup> treatments during drainage events. Significance of difference between treatments expressed as LSD (P=0.05) for each leaching event.

### 3.3.4 Climatic conditions

The climatic conditions (Table 3.4) over the trial period provided sufficient rainfall and suitable soil temperatures to maintain growth over the 5 month period with the increasing day length and solar radiation increasing the potential effective conversion of N to DM from 22 to 59 kg DM/kg N at a N uptake rate of 1 kg N/ha/day.

**Table 3.4** Summary of climatic data over harvest periods from NIWA<sup>a</sup> and Site<sup>b</sup>

Period	Total solar radiation <sup>a</sup> MJ m <sup>-2</sup>	Mean daily ground Temp <sup>b</sup> °C	Rainfall <sup>a</sup> mm	Drainage <sup>a</sup> mm
20 Jun -22 Jul	176	8.2	84.8	27.1
22 Jul-22 Aug	217	10.0	108.4	61.6
22 Aug- 21 Sept	337	11.0	29.7	14.1
21 Sept-23 Oct	433	12.4	86.8	13.2
23 Oct-19 Nov	572	14.7	64.2	0

### 3.3.5 Nitrogen use efficiency

The N use efficiency (NUE) in terms of additional kg DM produced per kg of N released into the pasture ranged between 12–15 kg DM/kg N for both the 50 and 150 N rates applied as U, SU and DCUDU while 5UCU and 7UCU treatments produced NUE's of 22–24 kg DM/kg N for both rates of N application over the initial 3 months based on the amounts of N released. At the 150 N rate, the 5UCU and 7UCU products released 90 and 72 kgN ha<sup>-1</sup>, respectively, over the initial 3 months (based on release rate studies and soil temperature, Figure 2.14) resulting in more efficient (P<0.0001) use of N to produce DM than the 150 N urea and DCUDU treatments. However, based on the amount of N applied there was no significant difference in NUE over the initial 3 months.

The increased efficiency of the controlled release urea 5UCU and 7UCU can be in part be explained by the increase in potential NUE from 15.7 kg DM/kg N during the July period to 52.5 kg DM/kg N in the November period (Figure 3.3) associated with the increase in solar radiation (Table. 3.4 and Equation 3.1). Thus the portion of N released

later in the trial is able to be converted more efficiently to dry matter, increasing the overall performance of the 5UCU and 7UCU products.

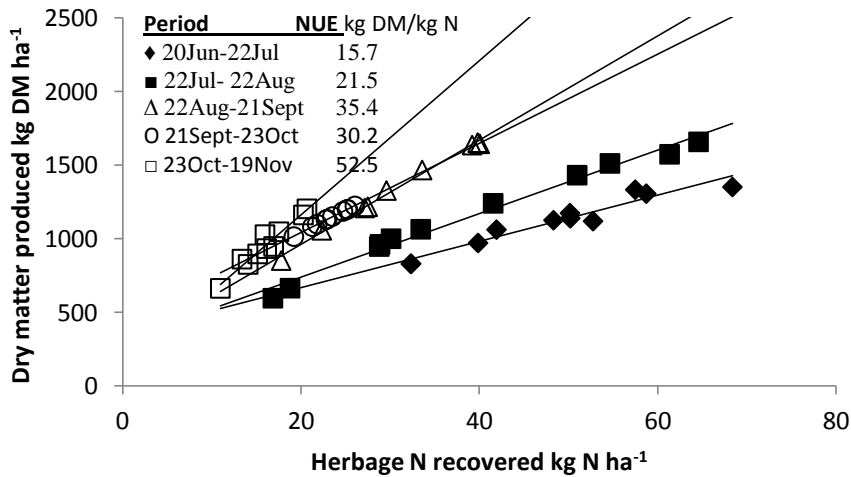


**Figure 3.3 Relationships between monthly dry matter production and fertiliser N recovery in herbage over the trial period for all treatments. Showing N use efficiency (NUE) increasing from winter to summer**

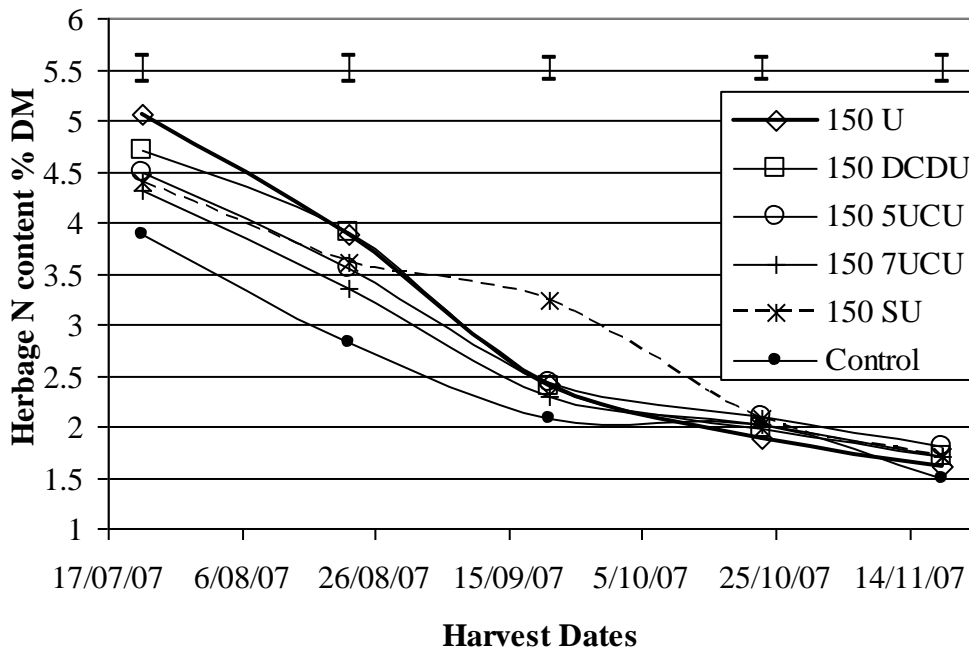


**Figure 3.4 Monthly herbage N content of pasture at harvest for 150 N treatments. Vertical bars indicate LSD (P=0.05).**

Trends in N use efficiency are evident from the herbage N contents (Figure 3.4) which were highest in winter in the “N boosted” pasture produced by the U and DCU at 150 N, while the 7UCU produced lower herbage N over the duration of the trial. The SU treatment initially produced lower herbage N compared with 150 U, but this increased in September due to dry conditions prior to the harvest producing poor N conversion to DM and so a high N content. An increase in herbage N above 2.5% N will result in proportionally more N deposited as urine (Castillo et al. 2001). In winter this raises the risk of increasing N leaching from urine patches.

### 3.3.6 Nitrogen recycling via grazing

The grazing of herbage by cows results in the return of N to the pasture in the forms of dung and urine. The quantity of these returns is modelled using the empirical partitioning formula's (Equation's 3.2, 3.3 and 3.4) of Castillo et al. 2000 based on the review of N balances carried out on 580 dairy cows over 91 different diets. These equations relate the daily N intake (NI) in grams for early lactation to the urinary N, fecal N and milk N.

$$\text{urinary N (g/d)} = 30.4 e^{0.0036 (\text{NI})} \quad R^2 = 0.76 \quad \text{Eq. 3.2}$$

$$\text{fecal N (g/d)} = 52.3 + 0.21 (\text{NI}) \quad R^2 = 0.48 \quad \text{Eq. 3.3}$$

$$\text{milk N (g/d)} = 41 + 0.17 (\text{NI}) \quad R^2 = 0.42 \quad \text{Eq. 3.4}$$

These equations show both the fecal N and milk N relationships are linear with low sensitivity to daily NI while urinary N increases exponentially with NI.

**Table 3.5** Urine-N return ( $\text{kgN ha}^{-1}$ ) to pasture following grazing based on  $15 \text{ kgDM cow}^{-1} \text{ d}^{-1}$ , 18 hours on pasture and 87% intake efficiency

Grazing Dates	150 U	150 DCU	150 5UCU	150 7UCU	150 SU	Control
22/07/2007	19.8	17.6	16.4	15.3	13.7	8.0
22/08/2007	15.0	15.7	11.7	9.1	12.6	3.9
21/09/2007	8.0	7.8	8.2	6.5	13.9	3.6
23/10/2007	5.4	5.2	5.4	5.0	7.4	3.3
19/11/2007	2.3	2.6	3.3	3.9	3.0	3.6
Total	50.6	48.9	45.1	39.9	50.6	22.4

From the dry matter and nitrogen content data (Table 3.2 and 3.3) the number of effective grazing cow days is calculated on a per hectare basis assuming a daily feed allocation of  $15 \text{ kgDM cow}^{-1} \text{ d}^{-1}$  and an intake efficiency of 87% (Dillon 2006). From this the total nitrogen intake per cow and urine N returning to pasture is estimated for each grazing cycle, Table 3.5 (assuming 18hr grazing per day on pasture resulting in 75% of urine being re-deposited to pasture as urine patch's).

The estimated urine-N return shows the application of 5UCU and 7UCU can potentially reduce urine N returns by 5 to  $10 \text{ kgN ha}^{-1}$  respectively over the trial period, a percentage reduction of 10 to 20 % over single and split applications of urea (Table 3.5).

### **3.4 Conclusion**

The objective of this chapter was to evaluate

Compared to uncoated urea the RLP coated urea (5UCU and 7UCU) produced similar dry matter production over the five month trial at both 50 and  $150 \text{ kg N ha}^{-1}$  application rates but with lower N uptake compared to the uncoated urea and DCD coated urea. This resulted in an increased NUE based on the amount of N released, however due to the short term of this trial the RLP coated urea was not fully released thus no difference in NUE was observed based on the total N applied.

The slow supply of N by the 5UCU and 7UCU products showed the potential to reduce peak herbage N concentrations (Figure 3.4) and therefore urine N returns to pasture following grazing by 5 to  $10 \text{ kg N ha}^{-1}$  for 5UCU and 7UCU, respectively, compared to single and split applications of urea at  $150 \text{ kg N ha}^{-1}$  and DCD coated urea at  $150 \text{ kgN ha}^{-1}$  (Table 3.5).

The application of uncoated urea as a single application resulted in a significant increase in estimated nitrate leaching above the nil-N control, split application (3 monthly applications of 1/3 each), the polymer coated and DCD coated urea at  $150 \text{ kg N ha}^{-1}$ .

While these results indicate the potential of RLP coated urea (5UCU and 7UCU) to reduce the impact of large single application of urea on nitrate leaching and dairy cow urine N returns to pasture following grazing from split applications of urea, there is a considerable quantity of unreleased urea remaining unaccounted for in the soil at the end of the trial. Unfortunately the effectiveness of the residual N was unable to be assessed in the subsequent autumn due to re-cultivation of the trial area in late summer 2008. Chapter 4, examines the soil mineral N profile for the treatments and the agronomic effectiveness of the residual polymer coated urea.

## Chapter 4 Distribution and fate of fertilizer N in the soil profile

---

### 4.1 Introduction

Efficient use of fertiliser N has two components:

1. Maximising the pasture growth response to applied N.
2. Minimising the loss of N to the wider environment – atmosphere and water.

Component 1 and nitrate leaching was evaluated in Chapter 3. Component 2, the loss of N from soil to the environment is a function of the concentration of reactive N ( $\text{NO}_3^-$  and  $\text{NH}_4^+$ ) remaining in the soil profile (particularly under urine patches) and the size and frequency of drainage events (Bergstrom and Brink 1986; Francis et al. 1998). In New Zealand dairy pasture dominated by perennial ryegrass (*Lolium perenne*) the risk of nitrate leaching is further increased by the shallow rooting habit of *L. perenne* and poor nitrate interception ability below 15 cm (Popay and Crush 2010).

In addition to the agronomic and environmental results in Chapter 3, studies of mineral-N movement in the soil profile, N mass balance of the soil pasture system and the residual effectiveness of the polymer coated urea were conducted. These studies are reported in this Chapter (4).

### 4.2 Materials and Methods

#### 4.2.1 Experimental site

The site and experimental set up are described in Chapter 3 section 3.2.1

#### 4.2.2 Soil analysis

Soil mineral-N and soil moisture deficit for each plot to a depth of 25cm were determined commencing on the 19<sup>th</sup> June 2007, prior to fertiliser application and following the first 3 harvests. Soil cores (0 - 25 cm) were divided into 5 cm segments weighed and immediately (within 3 hr) dried rapidly at 60°C for 24 hrs to preserve samples prior to analysis (Ma et al. 2005; van Epr et al. 2001) for mineral-N ( $\text{NO}_3^-$  and  $\text{NH}_4^+$ ) extracted in 2M KCl. Total N and C were measured on initial samples only. The soil bulk density was determined at the end of the field experiment by digging four pits

randomly over the trial area. Duplicate cores (5cm x 5cm) were taken every 5 cm to 25 cm depth to determine the bulk density and field moisture capacity. Field moisture capacity was determined using a suction plate apparatus. After equilibration at a suction pressure of 0.05 bar soils were dried (105°C) and weighed to determine water content.

#### *Mineral N*

The concentration of soil mineral N ( $\text{NH}_4^+$  -N and  $\text{NO}_3^-$  -N) were determined by extraction of 2 g of soil with 20 ml of 2M KCl on an end over end shaker for 1 hr in 50 ml screw capped centrifuge tubes. The extractant as recovered after centrifuging at 9000 rpm for 3 min and the supernatant filtered through Wattman No.42 and analysed on a Technicon Autoanalyser, Series 2 for  $\text{NH}_4^+$  -N and  $\text{NO}_3^-$  -N (Blakemore et al. 1987).

A daily, climate record and soil water balance for the trial period was kindly provided from an adjacent site (No. 4 Dairy farm, 0.5 km east. J. Hanly pers. comm.)

A N balance for the pastoral system was calculated based on measured and estimated N losses from the soil in terms of; plant uptake ( $\text{Herbage (N)}_{\text{Total}}$ ), leaching (N), denitrification, volatilisation and immobilisation, while N inputs are fertiliser N, biological fixation and the mineralisation of soil organic N. The contribution to the system from mineralisation of soil organic N, de-nitrification, volatilisation and immobilisation losses were not measured but the net contribution of these factors is expressed by the N requirement to balance the N demand and supply in the relationship expressed below.

$$\begin{aligned} \text{Net Balance(N)} &= \Delta\text{Soil mineral N} + \text{Fertiliser N} + \text{Net Soil Mineralisation N} \\ &\quad - \text{Herbage } N_{\text{Total}} - \text{Leached N} \end{aligned}$$

Net soil mineralisation ( $38.4 \text{ kg N ha}^{-1}$ ) was calculated from the control plot data over the first three months of the trial period.

$$\text{Net Soil Mineralisation N} = \text{Herbage(N)}_{\text{Total}} - \Delta\text{Soil mineral N} - \text{Leached(N)}$$

### 4.2.3 Residual fertiliser N – amount and release characteristics

The quantity of residual polymer coated urea was estimated at the end of the trial following the final harvest (day 158) on the 25<sup>th</sup> of November. Sods (0.23 x 0.33 m) to a depth of 2 cm were removed from each of the plots treated with 150 kgN ha<sup>-1</sup> of either 5UCU or 7UCU products. The sods were then wet sieved to remove soil less than 2 mm and the residue examined for residual coated fertiliser granules. The number and weight of empty coating shells and liquid filled granules was recorded. Ten empty and partially released granules from each sod were randomly selected then analysed for total Kjeldahl N (TKN) and the quantity of N not released was calculated. The release characteristics of the residual N not released was examined using duplicate intact cores 15 cm in diameter by 15 cm tall taken from the trial plots 150 5UCU, 150 7UCU and the control (0N). The cores were stored under cover with one of each set of duplicates being un-watered while the other was placed in a shallow (1 cm) deep dish of water to maintain core moisture. After 40 days the grass was clipped to 5 cm and herbage N and dry matter analyzed. The top 2 cm of soil removed and residual granules recovered using the same method as in the field sods.

## 4.3 Results and Discussion

The soil profile at the time of treatment application showed a soil moisture deficit of 14 mm over the 25 cm profile (Table 4.1).

**Table 4.1 Soil profile properties after cultivation just prior to treatment application ±S.E.M.**

Soil Depth cm	Total Carbon %	Total Nitrogen %	Bulk Density kg/m <sup>3</sup>	Gravimetric water holding capacity (g/g dry soil, 0.05bar)	Initial Soil moisture deficit mm
<b>0-5</b>	3.2 ± 0.2	0.278 ± 0.01	1.19 ± 0.06	0.42 ± 0.02	5.2
<b>5-10</b>	3.2 ± 0.3	0.281 ± 0.02	1.25 ± 0.01	0.42 ± 0.02	2.0
<b>10-15</b>	2.8 ± 0.2	0.255 ± 0.02	1.18 ± 0.06	0.36 ± 0.01	3.3
<b>15-20</b>	2.5 ± 0.2	0.225 ± 0.01	1.28 ± 0.03	0.33 ± 0.02	2.2
<b>20-25</b>	1.8 ± 0.3	0.162 ± 0.02	1.28 ± 0.04	0.29 ± 0.01	1.7

The cultivation of the area resulted in the formation of a relatively uniform profile in terms of total soil nitrogen and carbon (Table 4.1) to a depth of 20 cm, below which unaltered subsoil was encountered, Figure 4.1.

The cultivation zone has increased water holding capacity of the soil and reduced bulk density (Table 4.1) allowing rapid bypass flow from the surface to the base of the cultivation zone (22-25cm) at which point the drainage moves transversely to mole drains spaced every 2.5 m, pulled at a depth of 40-50cm, Figure 4.1.



**Figure 4.1** Soil pits used for bulk density and field water capacity measured in the trial plots on Tokomaru silt loam, Massey University, Palmerston North, New Zealand.

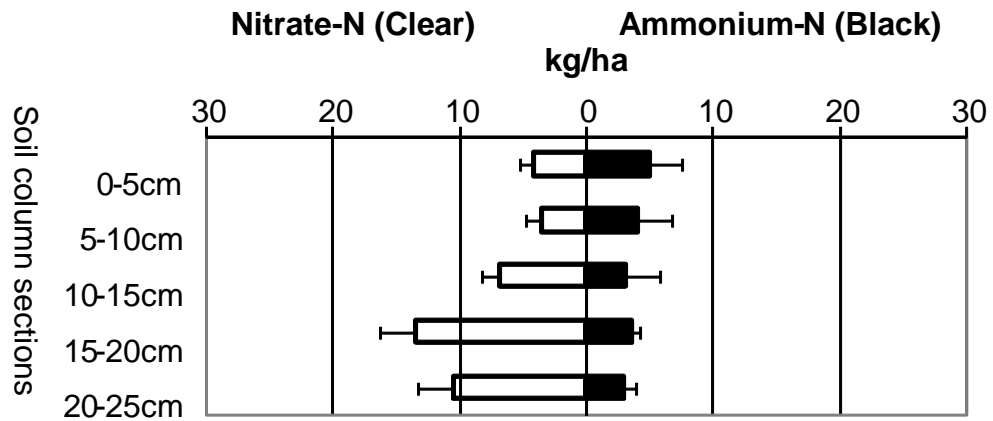


**Figure 4.2 Initial mineral N profile of soil cores in 5 cm sections (19/06/2007). Error bars represent standard error of mean for n = 7.**

The prior basal fertiliser application ( $400\text{ kg ha}^{-1}$  of Cropmaster 15.1% N: 10% P:10% K) at sowing of the Italian ryegrass in April 2007, the cumulative mineralisation following cultivation produced  $70.8\text{ kg N ha}^{-1}$  ( $32.4\text{ kg NH}_4^+\text{-N ha}^{-1}$  and  $38.4\text{ kg NO}_3^-\text{-N ha}^{-1}$ ) total mineral N to 25 cm at the time of treatment application (19/06/2007). Thirty three  $\text{kg N ha}^{-1}$  ( $9\text{ kg NH}_4^+\text{-N ha}^{-1}$  and  $24\text{ kg NH}_4^+\text{-N ha}^{-1}$ ) of this was below a depth of 15cm. This represents 27% of the exchangeable soil  $\text{NH}_4^+\text{-N}$  and 62% of the  $\text{NO}_3^-\text{-N}$  (>15 cm, Figure 4.2) and poses a significant risk of nitrate leaching, as the crop root zone had not developed at a rate capable of capturing the deep mineral N.

Following the application of the treatments light rain fall (20<sup>th</sup> to 26<sup>th</sup> June 2007) occurred 20 mm, which resulted in 6 mm of drainage, based on initial measured soil water deficits (Table 4.2). Unfortunately this drainage event was not sampled as the data from the NIWA(AgResearch) site some 500m away indicated an initial moisture deficit of 45 mm ,while the measured deficit was only 14 mm leading to an early than expected drainage. While the soil solution measurements missed this event, soil cores, sampled on the 28<sup>th</sup> June 2007 (Figure 4.3) showed a significant ( $P = 0.012$ ) loss of nitrate- N ( $8.8\text{ kg NO}_3^-\text{-N ha}^{-1}$  , c.f. nitrate concentrations in Figures 4.2 and 4.3) from below 15 cm and large increases in soil mineral N in the upper 5 cm from the 50 and 150  $\text{kgN ha}^{-1}$  applications of urea and DCDU (Figure 4.3).

Over the following 22 days a further 64 mm of rain fell maintaining the soil in a saturated state above field capacity due to imperfect drainage, this is evident in the soil moisture profiles obtained following the first harvest, 22<sup>nd</sup> July 2007,(Table 4.2).

**Table 4.2 Measured soil moisture deficit in soil profile relative to field capacity at 0.05 bar suction with standard error of means.**

<b>Soil Depth cm</b>	<b>19/06/2007 mm</b>	<b>28/06/2007 mm</b>	<b>22/07/2007 mm</b>	<b>22/08/2007 mm</b>	<b>24/09/2007 mm</b>
<b>0-5</b>	5.2 ± 1.1	-3.7 ± 0.1	-6.9 ± 0.2	0.3 ± 0.1	-8.2 ± 0.1
<b>5-10</b>	2.0 ± 1.7	-6.0 ± 0.3	-8.1 ± 0.3	-2.7 ± 0.2	-10.0 ± 0.2
<b>10-15</b>	3.3 ± 1.2	-2.7 ± 0.2	-4.6 ± 0.2	-0.5 ± 0.1	-6.9 ± 0.4
<b>15-20</b>	2.2 ± 0.4	-2.0 ± 0.2	-3.2 ± 0.2	4.2 ± 0.9	-5.3 ± 0.2
<b>20-25</b>	1.7 ± 0.8	-1.8 ± 0.1	-2.5 ± 0.1	3.2 ± 0.3	-3.9 ± 0.3
<b>Total</b>	14.4 ± 3.7	-16.2 ± 0.7	-25.3 ± 0.5	4.4 ± 0.9	-34.4 ± 0.9

This transition to field saturation was associated with an increase in soil ammonium of 24 kg N ha<sup>-1</sup> over all treatments (Figure 4.4, 4.5), while nitrate increased only in plots treated with 150 kg N ha<sup>-1</sup> of Urea (Figure 4.6).

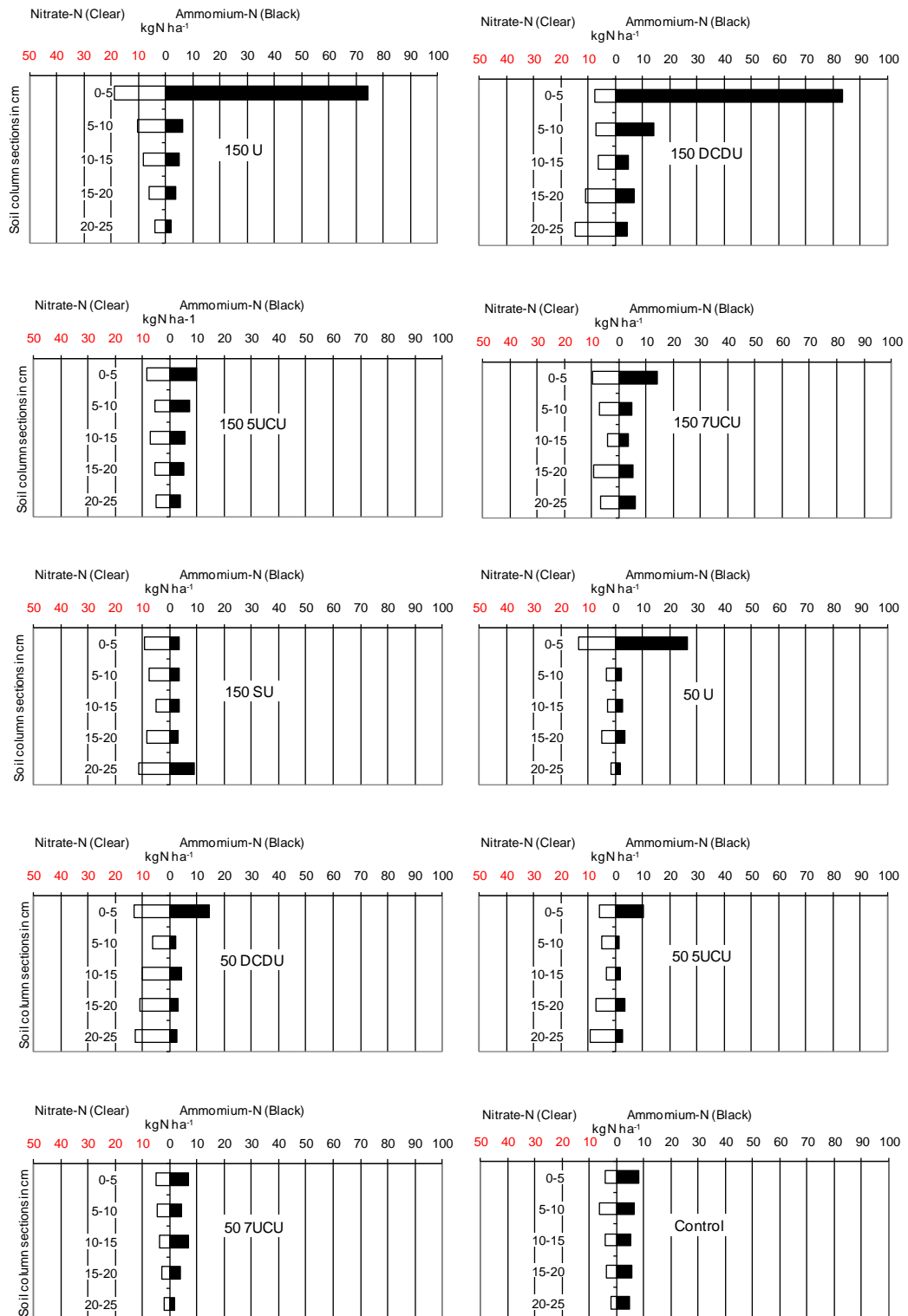


**Figure 4.3 Mineral N soil profiles on 28<sup>th</sup> June 2007, 10 days following treatment applications.**

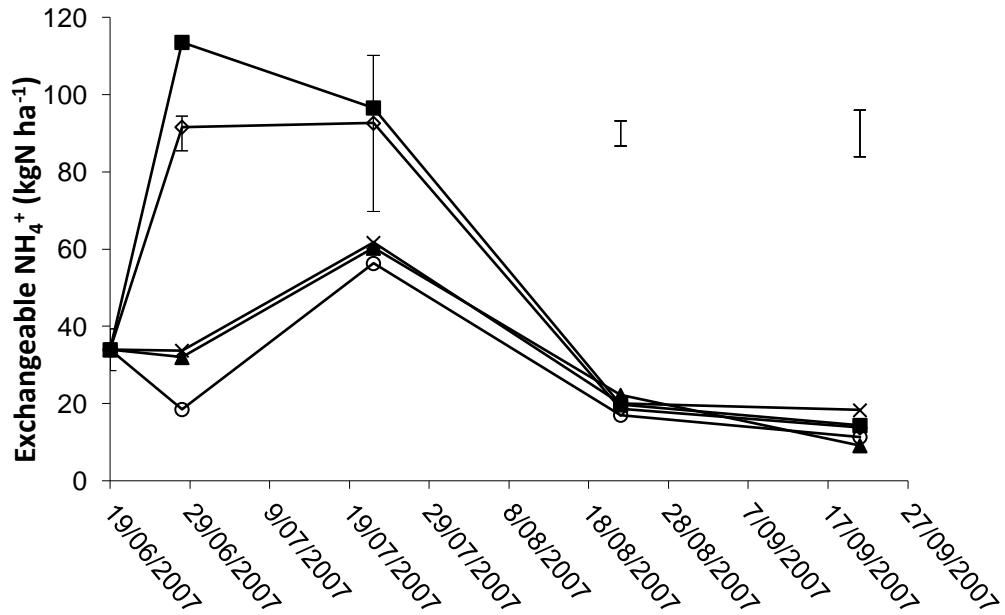


**Figure 4.4** Measured soil exchangeable  $\text{NH}_4^+\text{-N}$  ( $\text{kgN ha}^{-1}$ ) to a depth of 25 cm, for the  $150 \text{ kgN ha}^{-1}$  treatments (◇ U, ■ DCU, ▲ 5UCU, × 7UCU, ○ control (nil-N)). The vertical error bars represent the least significant difference between treatments on each date.

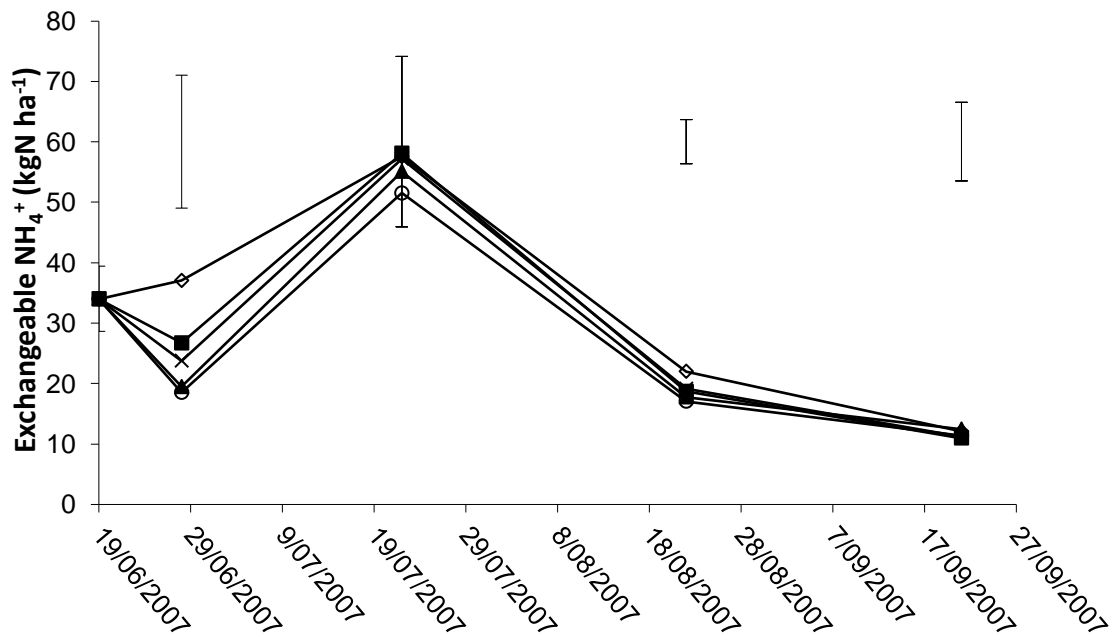


**Figure 4.5** Measured soil exchangeable  $\text{NH}_4^+\text{-N}$  ( $\text{kgN ha}^{-1}$ ) to a depth of 25 cm, for the  $50 \text{ kgN ha}^{-1}$  treatments (◇ U, ■ DCU, ▲ 5UCU, × 7UCU, ○ control (nil-N)). The vertical error bars represent the least significant difference between treatments on each date.

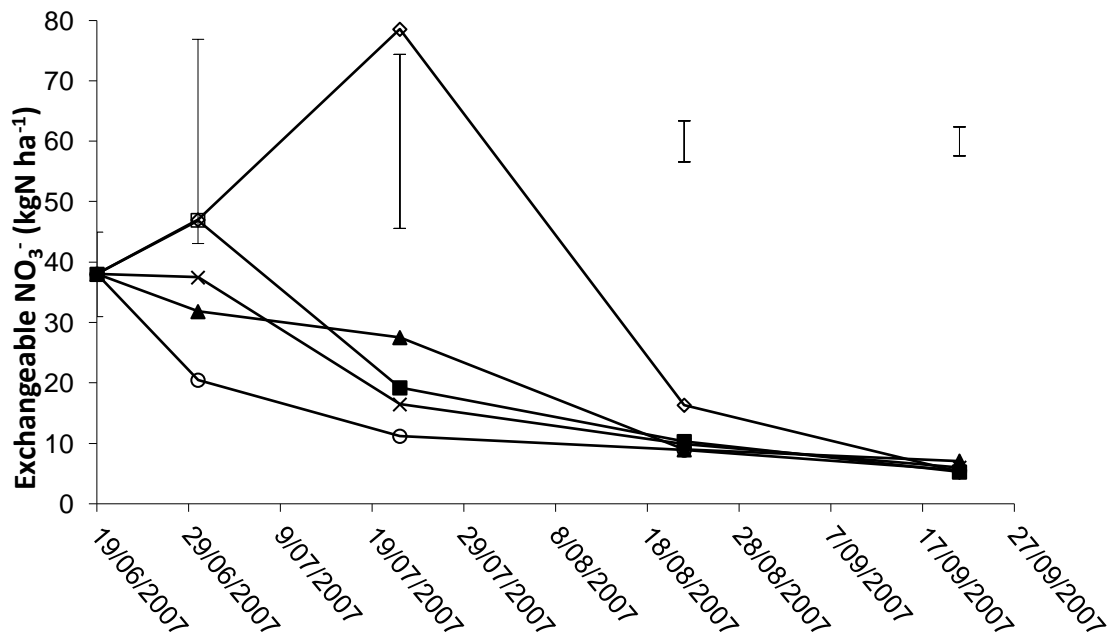


**Figure 4.6** Measured soil exchangeable  $\text{NO}_3^-$ -N ( $\text{kgN ha}^{-1}$ ) to a depth of 25 cm, for the  $150 \text{ kgN ha}^{-1}$  treatments (◇ U, ■ DCU, ▲ 5UCU, × 7UCU, ○ control (nil-N)). The vertical error bars represent the least significant difference between treatments on each date.

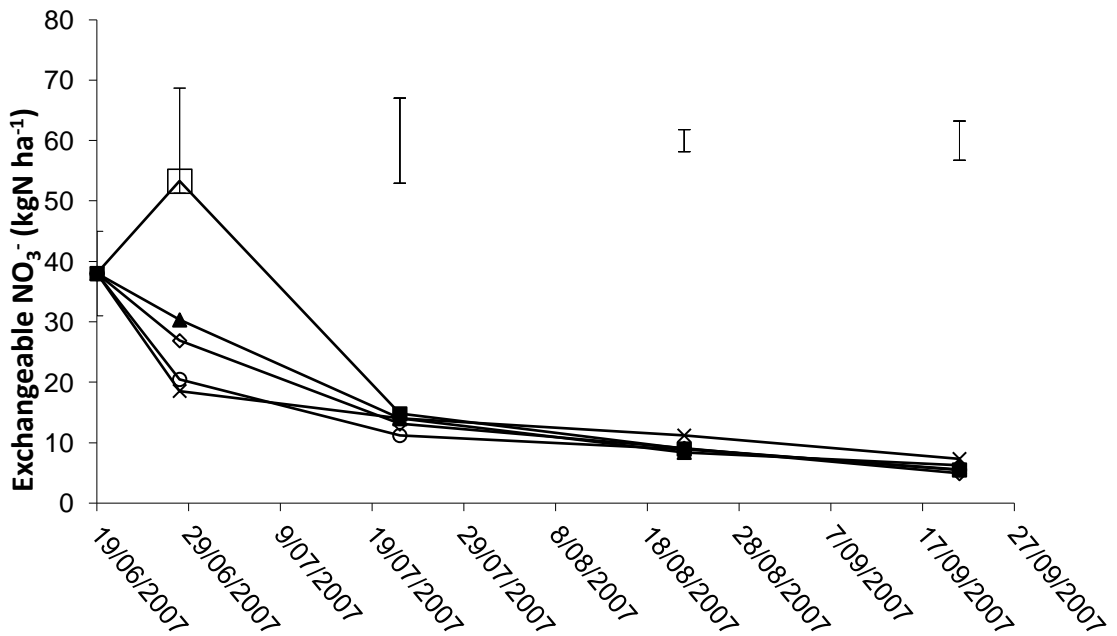


**Figure 4.7** Measured soil exchangeable  $\text{NO}_3^-$ -N ( $\text{kgN ha}^{-1}$ ) to a depth of 25 cm, for the  $50 \text{ kgN ha}^{-1}$  treatments (◇ U, ■ DCU, ▲ 5UCU, × 7UCU, ○ control (nil-N)). The vertical error bars represent the least significant difference between treatments on each date.

\* The marker □ indicates one plot of the DCDU treatment which contained high residual nitrate below 15cm not associated with the treatment but the initial soil nitrate which had not been leached as in all the other plots sampled (see Figure 4.3).

The results, Figures 4.4 and 4.6, illustrate the  $\text{NO}_3^-$  drainage risk posed by high application rates ( $150 \text{ kg N ha}^{-1}$ ) of uncoated urea in the winter with limited pasture growth and the potential for anaerobic mineralization of soil organic-N producing excessive soil mineral-N. In contrast, application of urea at  $50 \text{ kgN ha}^{-1}$  per month and the application of urea in the forms of 5 UCU, 7UCU resulted in no significant increase in soil mineral N.

#### 4.3.1 N Balance

The N balance for the soil system from the initial state, prior to the treatment applications, until the third harvest 94 days later are shown in Tables 4.3 and 4.4 with losses indicated by negative signs. The net mineralisation (Table 4.3) of the soil system is calculated from the control plots by assuming the soil profile mineral N balance plus the N demand on the soil from leaching and plant growth equals net mineralisation, this indicates that the net mineralisation of soil organic matter contributed  $38.4 \text{ kgN ha}^{-1}$ .

**Table 4.3 Soil nitrogen balance from the pre-trial condition to following the third harvest at 94 days, for  $150 \text{ kgN ha}^{-1}$  treatment applications**

	U	DCDU	5UCU	7UCU	SU
	.....kgN ha <sup>-1</sup> .....				
Herbage	-201.0	-186.0	-183.0	-162.0	-210.0
Δ Soil	51.2	51.1	54.3	43.8	45.7
Leaching suction cups	-10.5	-4.0	-4.2	-4.0	-2.2
leaching pre suction cups	-8.8	-8.8	-8.8	-8.8	-8.8
Net Mineralisation	38.4	38.4	38.4	38.4	38.4
Treatment N	150	150	150	150	150
Nitrogen Balance	19.3	40.7	46.7	57.5	13.2

**Table 4.4 Soil nitrogen balance from the pre-trial condition to following the third harvest at 94 days, for 50 kgN ha<sup>-1</sup> treatment applications**

	U	DCDU	5UCU	7UCU	Control
	.....kgN ha <sup>-1</sup> .....				
Herbage	-121.0	-127.0	-123.0	-116.0	-91.0
Δ Soil	51.9	55.0	51.1	50.7	61.7
Leaching suction cups	-2.0	-4.7	-3.3	-0.3	-0.4
leaching pre suction cups	-8.8	-8.8	-8.8	-8.8	-8.8
Net Mineralisation	38.4	38.4	38.4	38.4	38.4
Treatment N	50	50	50	50	0
N Balance	8.5	2.9	4.4	14.1	0.0

Larger nitrogen surpluses are calculated for the DCDU and the polymer coated urea's (5UCU, 7UCU) applied at 150 kgN ha<sup>-1</sup>, which corresponds to increased losses such as volatilisation of ammonia for the DCD treatment (Zaman et al. 2009) and incomplete release from the polymer coated urea (Pauly et al. 2002). Largest leaching losses are reported for the urea treatment.

#### **4.3.2 Residual N in soil from UCU**

Following the completion of the field trial, considerable quantities (19.3-57.5 kgN ha<sup>-1</sup>) of N were unaccounted for in the soil mineral N or the Herbage N recovered from the trial plots (Table 4.3). In the case of the uncoated urea applied at 150 kgN ha<sup>-1</sup>, 8% of the N inputs (238 kgN ha<sup>-1</sup>) are unaccounted for, while for the DCD coated urea and RLP coated urea 17% and 19% to 24% respectively. These unaccounted for losses of N from the system are expected to be due to; the accuracy of the estimated inputs and losses, the combination of volatilisation (Zaman et al. 2009), de-nitrification and immobilisation. However in the cases of the RLP coated urea it is possible that a portion of the N had not fully released from the granule (Pauly et al. 2002). The quantity of residual N unreleased from the coated urea after 158 days is given in Table 4.5, which shows 11.2 and 34.3 kgN ha<sup>-1</sup> was recovered in intact coated granules from the 150 kgN ha<sup>-1</sup> 5UCU and 7UCU treatments, respectively. The variation in weight of granules recovered between replicate samples was high resulting in a large uncertainty in the levels recovered from the sods of the 5UCU treatment.

**Table 4.5 Residual N unreleased from coated urea after 158 days in winter field trial**

	<b>Wt. empty g</b>	<b>Wt. full g</b>	<b>TKN %N</b>	<b>Residual N kgN ha<sup>-1</sup></b>
Empty coating shell's			5.8 ± 0.4	1.0 ± 0.4
5UCU	0.08 ± 0.04	0.55 ± 0.3	14.5 ± 1.2	11.2 ± 5.9
7UCU	0.18 ± 0.04	1.0 ± 0.18	24.7 ± 0.9	34.3 ± 6.3

The results show that the heavier coating level of 7% polymer addition resulted in larger quantities of urea remaining unreleased, which explains the low uptake and high N to dry matter conversion efficiencies. The correction of the N balance, by removing the residual N from the calculation, reduces the N losses from 46.7 and 57.7 to 35.5 and 23.3 kgN ha<sup>-1</sup> for the 150 5UCU and 150 7UCU treatments, respectively.

#### 4.3.3 Agronomic availability of residual N

The residual N analysis as described in section 4.2.3 (Table 4.6) showed that under moist soil conditions (43% FC) both 5UCU and 7UCU continued to release nitrogen, albeit at a low rate with the concentration of N in the granules falling by 6.2% and 14.0%, respectively over the 40 days. Under the dry conditions (16% FC) no release of N was observed for the 5UCU granules, while the 7UCU released 5.8% N. Due to the number of cores used in this trial and the high spatial variability in granule distribution the total release of N from the RLP coated urea could not be determined.

**Table 4.6 Effect of soil core moisture content on the release of residual N from polymer coated urea granules after 40 days.+SEM**

<b>Product</b>	<b>Initial TKN %</b>	<b>Dry condition (16% FC)</b>		<b>Moist condition (43% FC)</b>
		<b>Final TKN %</b>	<b>Final TKN %</b>	<b>Final TKN %</b>
5UCU	14.5 ± 1.2	14.3 ± 0.9		8.3 ± 0.9
7UCU	24.7 ± 0.9	18.9 ± 1.6		10.7 ± 1.7

The grass growth on the cores during the residual N assessment was dramatically affected by soil moisture levels (Table 4.7). The dry matter production at 16% FC

showed no significant difference between the 5UCU, 7UCU and the nil-N control, producing between 169 and 198 kgDM ha<sup>-1</sup>. At 43% FC the dry matter and uptake of N significantly increased over the dry conditions (P<0.025), ranging from 817 to 1310 kgDM ha<sup>-1</sup> and 11.3 to 19.4 kgN ha<sup>-1</sup>, respectively. The release of N from the 5UCU and 7UCU granules at 43% FC produced significantly more dry matter and herbage N than the control under the same conditions (P< 0.08 for 5UCU and P< 0.004 for 7UCU) producing additional 492 and 424 kgDM ha<sup>-1</sup>, 8.1 and 3.8 kgN ha<sup>-1</sup> for the 150 5UCU and 150 7UCU treatments, respectively.

**Table 4.7 Herbage nitrogen (kgN ha<sup>-1</sup>) and dry matter ( kg ha<sup>-1</sup>) recovered from the residual polymer coated fertiliser core study under dry (16% FC) and moist (43% FC) conditions after 40 days.**

Treatment	Herbage Nitrogen		Dry Matter		Nitrogen recovery	
	Dry -----%-----	Moist	Dry -----kg ha <sup>-1</sup> -----	Moist	Dry -----kgN ha <sup>-1</sup> -----	Moist
150 5UCU	2.3 ± 0.2	1.48 ± 0.01	169 ± 28	1310 ± 223	3.9 ± 1.1	19.4 ± 3.3
150 7UCU	2.8 ± 0.2	1.21 ± 0.01	183 ± 14	1242 ± 25	5.1 ± 0.7	15.1 ± 0.2
Control	2.8 ± 0.1	1.38 ± 0.01	198 ± 6	817 ± 31	5.6 ± 0.4	11.3 ± 0.5

The results show that the RLP coated urea under dry conditions limited N release in synchronicity with soil moisture limited plant growth, while under moist conditions the N release continues producing significant increases in dry matter production.

#### 4.4 Conclusion

Under the conditions of the field trial (Table 3.4), RLP coated urea prevented the accumulation of excess mineral N in the soil profile. The two different coating levels 5UCU and 7UCU resulted in no significant increase in soil mineral-N in the first 94 days at application rates of 150 and 50 kgN ha<sup>-1</sup>, while both U and DCUDU treatments resulted in high surface mineral-N levels of 93 and 91 kgN ha<sup>-1</sup>, respectively, in the top 5cm of the soil profile at 10 days following application at 150 kgN ha<sup>-1</sup>. The increase in soil mineral N is associated with increased herbage N (section 3.3.1) and in the case of the urea treatment at 150 kgN ha<sup>-1</sup> an increase in nitrate leaching (section 3.3.3).

Part of the reason for the lack of excess soil N accumulation with the RLP coated urea is that intact granules retain urea; 7UCU treatment being more effective than 5UCU. The retention of urea in the granules contributed to lower N recovery by the pasture. The residual urea in the granules however, continues to be agronomically effective being released under moist conditions.

These RLP coated urea (5UCU and 7 UCU) show considerable potential to be used to provide controlled release N to pasture. These two experimental Chapters 3 and 4 have provided data to test their agronomic performance. From this it is possible to list potential advantages and disadvantages of using PCU and where further research is required.

<b><u>Advantages</u></b>	<b><u>Further research</u></b>
<p>5UCU and 7UCU lower the peak herbage N without reducing production.</p> <p>5UCU and 7UCU allow large single applications of N prior to cultivation with no significant increase in <math>\text{NO}_3^-</math>-N leaching. Preventing pasture damage from multiple ground spreading applications, saving labour and energy.</p>	<p>Grazing trials are required to confirm the potential reduction in urine N return to pasture and subsequent risk of <math>\text{NO}_3^-</math>-N leaching and run off.</p> <p>Both the field trial data and modelling (Chapter 2) and the residual N availability trial (Section 4.3.3) suffer from extreme soil moisture conditions. Therefore the release of urea from RLP coated urea granules requires further research to more clearly assess the rate of release as a function of soil moisture.</p>

## **Chapter 5 A model of nitrification inhibitor (DCD) movement in soil columns from conventional granular DCD and a new polymer coated granule: development and validation.**

---

### **5.1 Introduction**

Nitrous oxide emissions currently contribute to 17% of New Zealand's total GHG emissions and 35% of total agricultural GHG emissions (Saggar et al. 2004). Nitrous oxide emissions generated by denitrification in soil of urine derived N (Sherlock and Goh 1983) can be reduced by the nitrification inhibitor dicyandiamide (DCD) (de Klein and Vanlogtestijn 1994). A recent review (Di and Cameron 2008) of field lysimeter studies indicate that nitrous oxide ( $N_2O$ ) emissions can be reduced by about 70% by treatment of dairy cow urine patches with DCD. This reduction however, may range from 40% to 90% dependent on soil type, location and climatic conditions (Di and Cameron 2008; Hoogendoorn et al. 2008; Smith et al. 2008). The results from controlled experiments indicate that inhibition of nitrification by DCD may be an effective mitigation tool in the reduction of  $N_2O$  emissions from grazed pasture at the farm scale. The application of DCD has also been shown to reduce nitrate leaching from pasture by 5 to 7 kgN/ha/yr (Di and Cameron 2005; Bishop et al. 2008) reducing the environmental risks to ground and surface water.

The effectiveness of a DCD application at reducing  $N_2O$  emissions and nitrate leaching is associated with its half-life in soils, which is controlled mainly by its rate of degradation by soil microorganisms. The rate of DCD degradation is a function of soil moisture and temperature (Di and Cameron 2004,2005; Kelliher et al. 2008). Rapid decomposition rates of DCD at temperatures above 8 °C limit the effectiveness of single DCD applications to autumn and winter months in New Zealand (Di and Cameron 2004a). More frequent application of DCD (as granules or spray) (Di and Cameron 2005; Menneer et al. 2008; Smith et al. 2008) would be required to maintain DCD concentrations in spring and summer when most urine N is deposited on grazed dairy pasture, this is however a costly option.

Coated and controlled release nitrogen fertilisers are commonly used to maintain low mineral nitrogen concentrations in soils (Bishop et al. 2008) under conditions where large leaching losses of nitrate or denitrification losses are expected (Shoji et al. 2001; Chen et al. 2008) . In this Chapter the potential for using polymer coated DCD granules to deliver slowly released DCD into pasture soils, prior to grazing and urine deposition is evaluated. To assess the effectiveness of this type of slow release granular product requires detailed understanding of the soil processes, including adsorption, degradation and diffusion of DCD and urine-derived soil N. Little discussion, or research, has focussed on the relative spatial distribution of DCD and urine in the soil and its effect on DCD efficacy. Intimate association is important for the successful operation of a controlled release form of DCD that may already be present in soil prior to urine deposition. There is also a total absence of published data on the measurement and simulation modelling of DCD movement in soils.

In this Chapter DCD is applied to uniformly repacked cores that can be sampled to measure DCD movement away from the point of application. These measurements are used to test a computer model (developed in Visual Basic) designed to predict the diffusion, adsorption and degradation of DCD in soil.

The combination of modelled and experimental measurements allowed the following hypotheses to be tested:

1. DCD is able to diffuse rapidly in soil to match urine-N movement.
2. The application of polymer coating will lengthen the effectiveness of DCD by maintaining DCD input to counteract DCD degradation.
3. Urine application has no effect on the rate of DCD degradation.

This research work is presented in two parts:

1. Model development and validation of nitrification inhibitor (DCD) movement in soil columns from conventional granular DCD and a new polymer-coated granule is presented in this Chapter (5).
2. The spatial and temporal variation in the inhibition of nitrification of urine-N by coated and uncoated DCD, presented in Chapter 6.

## 5.2 Theory and experimental design

### 5.2.1 Diffusion of solute in soil

The diffusion of a degradable water soluble solute without boundaries in soil is governed by a number of continuity equations (Rachhpal-Singh and Nye 1984; Kirk and Nye 1985). Assuming one dimensional geometry, the change in concentration  $\frac{\partial C_L}{\partial t}$  at any point (layer) in time can be defined by Equation 5.1,

$$\frac{\partial C_L}{\partial t} = D_l \theta f \frac{\partial^2 C_L}{\partial x^2} - \frac{\partial C_s}{\partial t} - \frac{\partial C_d}{\partial t} \quad \text{Eq. 5.1}$$

as a function of rate of diffusion and distance  $D_l \theta f \frac{\partial^2 C_L}{\partial x^2}$ , adsorption rate  $\frac{\partial C_s}{\partial t}$  and degradation rate  $\frac{\partial C_d}{\partial t}$ .

Here D is the diffusion coefficient of the solute in free solution,  $\Theta$  is the volumetric moisture fraction of the soil, f is the diffusion impedance factor of the soil (involving such properties as tortuosity of the pathway, discontinuous pores and changes in pore size introducing capillarity factors),  $C_L$  is the solute concentration in the soil solution and x is the distance being considered. The solution of these equations bounded by upper and lower surface (layer) conditions may be obtained numerically using a finite difference model in which the individual components of diffusion, adsorption and degradation are calculated over small intervals in distance and time.

The following modelling equations in this section are presented in computer language to allow recognition in the appendix modelling programs.

The quantity of solute diffusing from across the small distance (dx) may be expressed in the terms of flux estimated using Fick's law of diffusion ( $D^*(C_{(II)}-C_{(II+1)})/dx$ ), where  $C_{(II)}-C_{(II+1)}$  is the difference in solution concentration between layer II and II+1. This flux ( $\text{moles cm}^{-2}\text{s}^{-1}$ ) is then multiplied by the soil volumetric water content ( $\theta$ ) and soil

impedance factor  $f$  (0.3) and the time interval  $dt$  (s) to determine the quantity (moles) of solute entering the next layer per  $cm^2$ , Equation 5.2.

$$\text{Flux}_{(II)} = D * f * \theta * dt * (C_{(II)} - C_{(II+1)}) / dx \quad \text{Eq.5.2}$$

The total concentration ( $C_s$ ) in the soil layer, which includes adsorbed solute and free solution, is then calculated by the addition of the incoming  $\text{Flux}_{(II-1)}$  and the outgoing  $\text{Flux}_{(II)}$  divided by the volume of soil in the layer to give a change in concentration, which is then added to the previous amount in the layer, Equation 5.3.

$$C_{s(II)} = C_{s(II)} + ((\text{Flux}_{(II-1)} - \text{Flux}_{(II)}) / (dx)) \quad \text{Eq.5.3}$$

The concentration of the new solution is then estimated using the analytical Freundlich isotherm  $C_{s(II)} = a * C_{(II)}^b$  where  $a$  is the distribution coefficient and  $b$  the intensity coefficient. In the soil the isotherm must be recalculated based on the volumetric ratio of water to soil,  $\theta$ . Thus the total soil concentration ( $C_s$ ) in a layer is related to  $C$  the solution concentration by  $C_{s(II)} = a * C_{(II)}^b + \theta * C_{(II)}$ . As  $C_s$  is known the equation must be solved for  $C$ , this is typically achieved numerically using a Newton-Raphson method (Kirk and Nye 1985), as this equation may be written in the form of  $f(x) = 0 = a * C_{(II)}^b + \theta * C_{(II)} - C_s$  thus the estimate may be made using several iterations of the algorithm, Equation 5.4.

$$C_{(x+1)} = C_{(x)} - f(C_{(x)}) / f'(C_{(x)}) \quad \text{Eq.5.4}$$

However, this can result in non- convergence and negative solutions which cause the computer program to become unstable. This instability is usually related to the initial value being over estimated and the  $x$  intercept being negative with no real solution resulting of  $f(x)$  or  $f'(x)$  existing. This can be avoided by using an initial estimation of solute concentration of one millionth of the total soil concentration  $C_{(x)} = C_{s(II)} / 10^6$ , which results in stable approximation of  $C_{(x)}$  to  $10^{-50}$  moles/ $cm^3$ , for DCD. These conditions allow the estimation of  $C$  given  $C_s$  in 8 iterations with less than 1% error. Finally the first order degradation factor ( $-k$ ) is applied to the layer to recalculate the concentration of solute in the layer prior to the next time step, where  $C_{s(II)} = C_{s(II)} * e^{-kdt}$ .

### 5.2.2 *Boundary conditions for uncoated and coated granules*

The finite difference model defines the soil processes between the two boundaries, the surface and the final depth. This allows us to define the boundary flux conditions depending on the treatment applied. In the case of a single application of soluble DCD

the initial surface boundary condition is defined by the assumed instant solubilisation of the DCD in the initial planar surface layer thus  $C_{s(1)} = \text{mol} / (\text{area} * dx)$  at time step 1. For the slow-release, coated DCD the flux across the boundary ( $\text{Flux}_{(0)}$ ) is defined by the release rate function initially estimated by its release rate in water (Wang et al. 1998). In both cases the finite depth of the cores (without any drainage) defines the base boundary condition of zero flux leaving through the base ( $\text{Flux}_{(x)} = 0$ ). In this shallow experimental unit this will result in an increase in DCD concentration at the boundary leading to a reduced concentration gradient and slower diffusion.

### 5.2.3 Summary of diffusion modelling factors

The finite difference model required the following factors to be measured or estimated:

1. The diffusion coefficient ( $D$ ) of DCD in water, this is not known but was expected to be similar but lower than urea ( $1.32 \times 10^{-5} \text{ cm}^2\text{s}^{-1}$ ) based on their similar molecular weight difference of 60 and 84 respectively. This was optimised at  $1 \times 10^{-5} \text{ cm}^2\text{s}^{-1}$  using the uncoated diffusion data sets and then applied to all further modelling.
2. The tortuosity factor was estimated using the following relationships (Barraclough and Tinker 1981) for coarse soil  $f = 0.99\theta - 0.17$  and clay soils  $f = 1.58\theta - 0.17$  where  $\theta$  is the volumetric water content.
3. The Freundlich isotherm coefficients  $a$  and  $b$  were determined experimentally and derived from the relationship between the natural log of DCD solution concentration, and the natural log of the concentration of soil adsorbed DCD.
4. The degradation rate of DCD was estimated for both soils by conducting a preliminary incubation experiment to determine the first estimate, which was then optimized for the DCD treated core data in the modelling.
5. DCD release rate from polymer coated DCD (PDCD) was experimentally determined by measuring release of DCD in water.

## 5.3 Equipment and methods

### 5.3.1 Soil microtone

The basic experimental unit (Figure 5.1), a cylinder of soil repacked to a known bulk density in a 50 mm section of 80 mm diameter PVC pipe, was designed to control soil moisture conditions and allow sampling of soil at small distance intervals away from the point of application of DCD ( $9.5 \pm 0.4\text{mg}$ ,  $21\text{kgDCD ha}^{-1}$ ) and cow urine ( $44\text{ ml}$ ,  $600\text{kgN ha}^{-1}$ ). The high rate of DCD, over twice the normal rate, was required to measure the expected slow release of DCD from PDCD granules. At set times after application of DCD, or urine, the soil cylinders were sectioned horizontally (using a piston microtome, Figure 5.1) to provide soil samples at 0.2, 0.6, 1.2, 2.4, 3.5, 4.5 cm distances from the point of application. These samples were immediately analysed for DCD, moisture and mineral N (section 5.2.3)

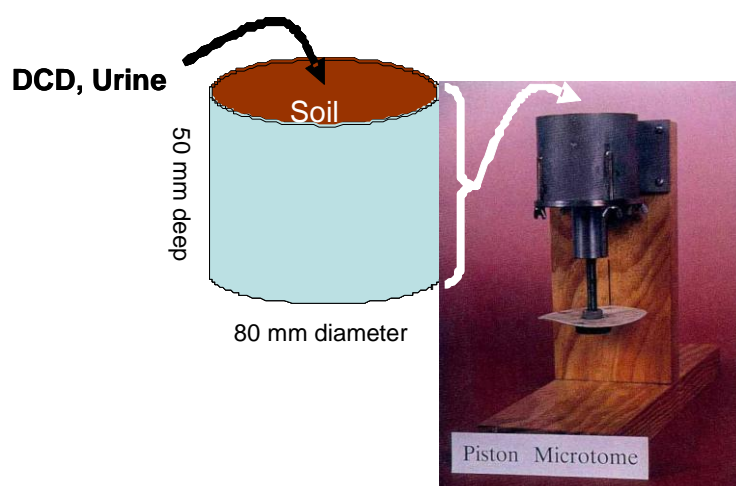


**Figure 5.1** The PVC pipe packed with soil used to study the diffusion of DCD and urine-N into soil and subsequent N transformations.

To simplify the modelling and reduce intra-treatment variation, a large number of small (0.8-1.0 mm diameter) coated and uncoated particles of DCD were prepared and applied in a uniform layer to the surface of the soil cores. This allowed the diffusion model to remain simple considering a unidirectional mode of diffusion away from a planar application surface.

### ***5.3.2 Soil bulk density and volumetric field capacity***

The bulk density and field capacities were measured using repacked cores measuring 1 cm high and 5cm in diameter, which were saturated with water by submersion for 24hr and then placed on a suction plate and allowed to equilibrate for 48hrs with a suction pressure of 5kPa. Following this the cores were weighed and dried at 105°C for 24 hrs to determine the bulk density and field capacity.

### ***5.3.3 Total soil carbon and nitrogen***

Total soil carbon and nitrogen were analysed simultaneously using a LECO FP2000 combustion analyser using samples of air dry soil sieved to < 2mm.

### ***5.3.4 DCD analysis in soil and fertiliser***

DCD in soil was measured following the extraction of 10g of moist soil in 20 ml of deionised water, which was shaken for 1 hr on an end over end shaker. The extraction tubes were then centrifuged (9000 rpm for 3 min.) and the supernatant filtered through No. 42 Whatman filter paper. A 5 ml sample of the extract was then acidified with the addition of 0.2 ml of 0.66 M H<sub>2</sub>SO<sub>4</sub> and allowed to stand for at least 30 minutes prior to centrifuging (4500rpm for 10min) to remove precipitated material. The concentration of DCD in the acidified supernatant was determined using a cation-H guard column (30x4.6mm) with a 0.025M H<sub>2</sub>SO<sub>4</sub> mobile phase at a flow rate of 0.9ml/min and a 210nm UV detector on a Waters 2695 high pressure liquid chromatograph (Schwarzer and Haselwandter 1996).

The DCD content of the coated and uncoated DCD products was determined in duplicate on 35mg samples following crushing in a mortar and pestle, with the sample being rinsed from the mortar and pestle with deionised water and diluted to 250 ml in a volumetric flask. The solution was then filtered through No.42 Whatman paper, acidified and DCD concentration determined as for the soil method.

### 5.3.5 Mineral N

Mineral N in the forms of  $\text{NH}_4^+$  -N and  $\text{NO}_3^-$  -N were extracted from 2 g of soil with 20 ml of 2 M KCl on an end over end shaker for 1hr in centrifuge tubes. After shaking the tubes were centrifuged at 9000 rpm for 3 min and the supernatant filtered through Whatman No.42 and analysed on a Technicon Autoanalyser, Series 2 for  $\text{NH}_4^+$  -N and  $\text{NO}_3^-$  -N (Blakemore et al. 1987).

### 5.3.6 Preparation of Coated granular DCD

Micro-granules were prepared initially by agglomeration of a fine powdered mixture of DCD (90% w/w) and carboxyl methyl cellulose (CMC)( 10% w/w) in a high shear mixer (food processor) with the addition of water as a liquid granulation aid. Following this the micro-granules were dried at 65 °C in an air-flow oven for 3hr, and screened to between 0.85 to 1.0 mm. These porous granules were then sealed with a hot aqueous mixed solution of 28g DCD and 2.8g CMC /100ml using a heated pan coater. Following ten coating and drying operations the final product was removed and screened to between 0.85 to 1.0 mm. This was then coated with 3 (PDCD3) and 4 (PDCD4) layers (5% w/w/layer) of castor oil/ MDI resin at 60°C. The resulting products were analysed for total DCD following crushing (Table 5.1) and water extraction (Figure 5.5 & Table 5.1).

**Table 5.1 DCD content of polymer coated DCD granules and estimated coat thickness**

<b>Product</b>	<b>% DCD</b>	<b>Estimated coat thickness (cm)</b>
<b>PDCD3</b>	76	0.0043
<b>PDCD4</b>	66	0.0066

### 5.3.7 Soils

Two soil materials of varying organic matter content and contrasting mineralogy were chosen for the study, (Table 5.2). Manawatu silt loam (a Weathered Fluvial Recent Soil, (Hewitt 1993)) was collected from dairy grazed pasture on the Massey University No. 1 Dairy farm, Palmerston North, NZ (40°23'05.71"S, 175°36'05.01"E) and Dannevirke Loam (a Typic Orthic Allophanic Soil, Hewitt, 1993) was collected from a grazed pasture at Hukanui, Wairarapa, NZ (40°33'49.23"S, 175°41'03.63"E). The top 3 cm of the turf was removed and the soil samples were taken from the surface 3-10 cm. Soils were air dried and sieved to pass a 4 mm sieve.

**Table 5.2 Physical and chemical properties of soils**

<b>Soil (3-10cm)</b>	<b>Bulk Density (g cm<sup>-3</sup>)</b>	<b>Field Capacity</b>		<b>Total Carbon (% w/w)</b>	<b>Total Nitrogen (% w/w)</b>	<b>C:N Ratio</b>
		<b>(% w/w)</b>	<b>(%v/v)</b>			
<b>Manawatu silt loam</b>	1.17	42.7	36.4	2.62	0.27	9.7
<b>Dannevirke loam</b>	0.90	62.6	69.6	7.75	0.65	11.9

## 5.4 Methodology

### 5.4.1 Main experiment

#### *Diffusion column study*

The application of solid DCD to soil and its migration in the soil is affected by two major processes, mass flow of water associated with rainfall, drainage and plant uptake and diffusion of DCD in soil water. This experiment was designed to measure the rate at which DCD migrates from a surface application of micro-granules of PDCD and DCD (90%), applied in a uniform layer to the surface of a soil column packed into a section of PVC pipe (Figure 5.1). The pipes were packed to the bulk densities shown in Table 5.2 with air dried soils that had been sieved to < 4 mm particle size. To bring soil biochemical processes to equilibrium, the soil was adjusted to a moisture content of 75 % field capacity and pre-incubated in a humidity chamber at a constant 20°C for 30

days, prior to the application of DCD. Each treatment and sampling time was established in triplicate. Replicate soil columns were placed in a piston microtome and sectioned for DCD extraction and analysis (section 5.2.3) at 7, 15, 22, 34, 41, 55 and 99 days following the DCD application.

Twenty eight days after DCD application, 10mm (44 ml) of fresh dairy urine (6000 mg N/l) was applied to the soil column surface to simulate the sequence of DCD application following grazing and the urine deposition from the subsequent grazing and allow time for DCD migration from PDCD. This was equivalent to 600kg N/ha being applied to simulate a typical urination (Ball et al. 1979; Haynes and Williams 1993). To allow this addition of liquid the cores were removed from the humidity chamber in the constant 20°C room for four days prior to the urine addition in order to lower the field capacity to 42%  $\pm$  4% and to 61%  $\pm$  4% for the Manawatu and Dannevirke soils, respectively. The urine addition then raised the soil moisture content to 84% and 97%  $\pm$  6% of field capacity, respectively. The cores were allowed to dry for a further three days to return the cores back to 75% field capacity before returning the cores to the humidity chamber to prevent further water loss.

#### *DCD and urine redistribution and N transformations*

The migration of DCD was determined by sectioning the soil cores at 0.2, 0.6, 1.4, 2.5, 3.5 and 4.5 cm from the soil surface using a piston microtome (Figure 5.1). The sections were weighed and immediately moist samples extracted to determine DCD, ammonium-N and nitrate-N concentrations (Section 4.2.2). This sampling was carried out on triplicate cores from each treatment on days 7, 15, 22, 34, 41, 55 and 99 following the DCD application.

#### **5.4.2 Supporting experiments**

##### *DCD degradation rate*

The degradation rate of DCD was determined using duplicate 500 g samples of air dry soil from sites on the Manawatu silt loam and Dannevirke loam soils taken from a depth

of 3-10cm. These were placed in 2 litre plastic bags and remoistened to field capacity with 213 ml (Manawatu) and 313 ml (Dannevirke) of a combined 60 ppm DCD and 120ppm of urea solution. The moist soils were then incubated at a temperature of 20°C for 76 days. The soil incubations were sampled at 7 to 14 day intervals and extracted with water (1:2 w/v) and analysed for DCD. The soil was also analysed for extractable mineral N ( $\text{NH}_4^+$  -N and  $\text{NO}_3^-$  -N, as per Section 5.3.1) to determine inhibitor effect on nitrification.

#### *DCD adsorption isotherm*

The adsorption isotherm of DCD in the Dannevirke and Manawatu soils was determined in duplicate adsorption experiments in which 20g of air dried soil was shaken for 2hrs with 20ml of DCD solutions with concentrations from 1 to 200 ppm. The soil DCD mixture was then centrifuged at 9000 rpm for 3 min and an aliquot of the supernatant taken filtered and acidified prior to DCD analysis using the HPLC method described in Section 5.3.1.

The amount of DCD adsorbed was calculated from the difference in DCD concentration between the original solution and the samples after equilibration with the soil. These resulting values were fitted to a Freundlich isotherm  $C_{ad} = a C_l^b$ . Where  $C_{ad}$  ( $\text{mg kg}^{-1}$ ) is concentration of DCD adsorbed at equilibrium concentration  $C_l$  ( $\text{mg L}^{-1}$ ) and  $a$  &  $b$  denote the sorption capacity and intensity factor, respectively. Both these coefficients are determined by plotting  $\ln(C_l)$  over  $\ln(C_{ad})$  giving a linear function of slope  $b$  and intercept  $\ln(a)$ .

The results were also expressed per unit mass of soil carbon, as soil organic matter is expected to be the major absorption site for non-ionic compounds, via hydrogen bonding. The normalization of DCD sorption using soil carbon content was carried out by recalculating the amount absorbed based on the weight of carbon in the soil (from Table 5.2).

### *Release rate of DCD*

The release rate of DCD from two polymer coated DCD granules was measured in triplicate by placing an accurately weighed 0.032 g sample of either PDCD4, PDCD3 or the control uncoated DCD90 in 250 ml of deionised water pre-heated to (20°C) and incubated (20°C) with once daily agitation. Samples of 5 ml were taken at 2, 4, 6, 12, 24 hours daily for 14 days, then at 3 day intervals to 60 days and analysed for DCD by the HPLC method. The results were then expressed as the cumulative % of DCD release (Figure 5.5)

## **5.5 Results -Supporting experiments**

### **5.5.1 DCD degradation rate**

The addition of 60 ppm DCD and 120ppm of urea solutions to air-dried soils resulted in initial concentrations of 27 mg DCD kg<sup>-1</sup> dry soil in the Dannevirke soil and 24 mgDCD kg<sup>-1</sup> dry soil in the Manawatu soil (Figure 5.2). This initial variation in DCD concentration could be accounted for by the difference in field capacity (Table 5.2). After initially wetting the soil there was no significant change in DCD levels until day 14 for the Manawatu silt loam and day 17 for the Dannevirke soil, so the first order decay curve was only fitted to the observed soil DCD concentrations from day 25 (Figure 5.2).

These results illustrate that the air dried soils should have been pre-incubated moist for a minimum of 20 day prior to the application of treatments. This would have allowed the microbial population to re-establish and their biochemical processes to reach equilibrium conditions prior to DCD and urea application.

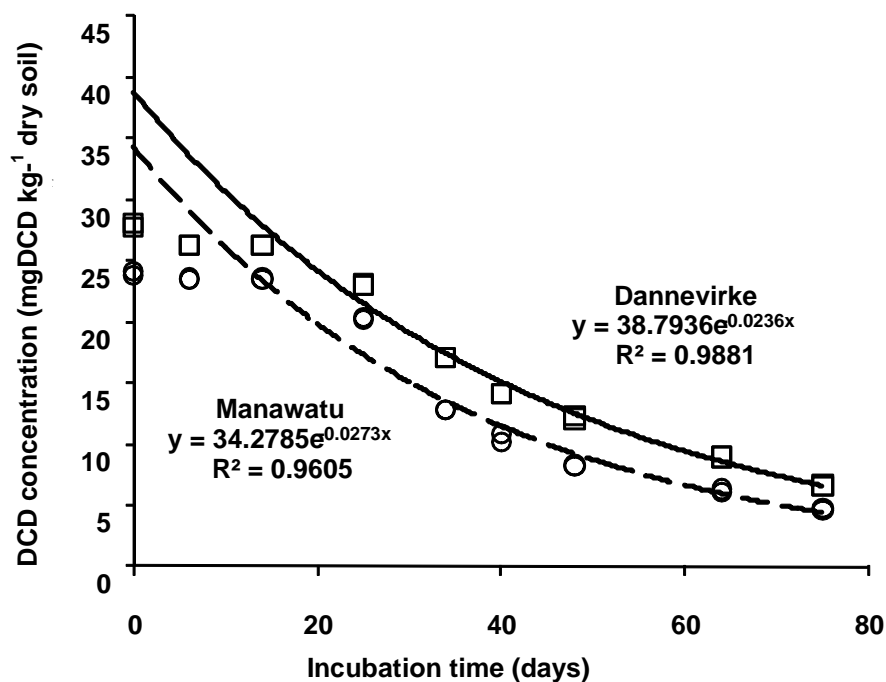


**Figure 5.2** Degradation rates of DCD in Manawatu (○) and Dannevirke (□) soils incubated at 20°C and 75% FC.

After 25 days the rate of DCD degradation in the soil followed a first order decay (Figure 5.2) with the rate constants presented in Table 5.3. The Manawatu soil showed a slightly greater capacity to degrade DCD compared to the Dannevirke with half lives of 25.1 and 29.3 days at 20°C, respectively. These results fall within the reported range of results for DCD degradation in soils (Di and Cameron 2004a; Kelliher et al. 2008)

**Table 5.3** First order decay rate  $k$  ( $\text{d}^{-1}$ ) constants and half life of DCD in soils incubated at 20°C and 75% FC

Soil	Depth (cm)	Decay constant for DCD in soils		Half life (days)
		$k$ (rep 1)	$k$ (rep 2)	
Manawatu	3-10	-0.0274	-0.0273	25.1
Dannevirke	3-10	-0.0237	-0.0235	29.3

Analysis of the soils for mineral N over the 75 day period showed the production of  $\text{NO}_3^-$ -N within the Manawatu and Dannevirke soils continued at a slow rate even in the presence of DCD (Figure 5.3). By day 75, 133 % and 22 % of the sum of the added N as DCD and urea had been converted to  $\text{NO}_3^-$ -N in the Manawatu and Dannevirke soils, respectively. The excess  $\text{NO}_3^-$ -N in the Manawatu soil is attributed to mineralisation of soil organic N, as no N control was used in the preliminary DCD degradation study.

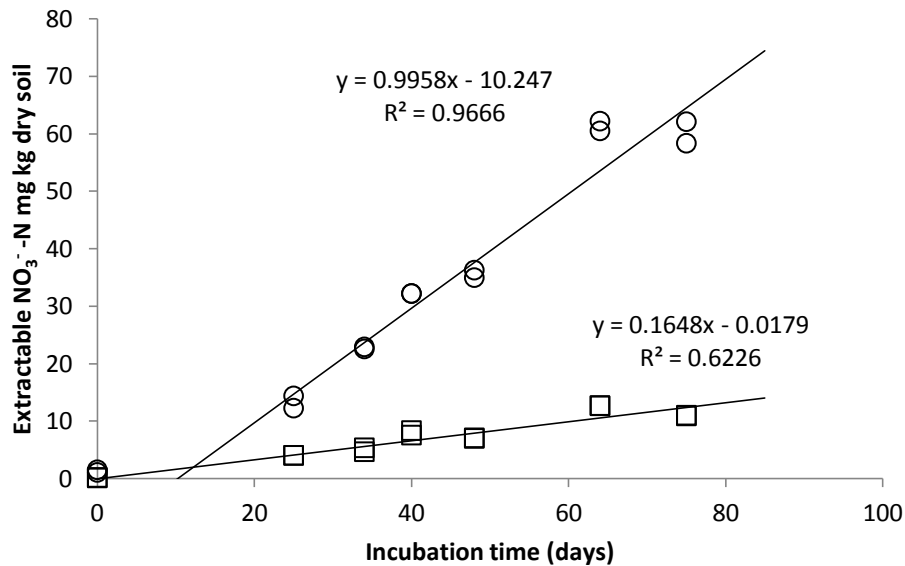


**Figure 5.3** Change in extractable  $\text{NO}_3^-$ -N in Manawatu ( $\circ$ ) and Dannevirke ( $\square$ ) soils incubated at  $20^\circ\text{C}$  and 75% FC following treatment DCD and urea solution ( $30 \text{ mg DCD kg}^{-1}$  soil and urea as  $27 \text{ mgN kg}^{-1}$  soil).

In Chapter 6 the effect of the DCD concentration on rate of nitrification is explored in more detail.

### 5.5.2 DCD absorption isotherms

For a range of initial DCD solution concentrations from 1 to  $200 \text{ mg l}^{-1}$  both soils showed weak sorption of DCD, the majority of DCD remaining in solution (Figure 5.4).

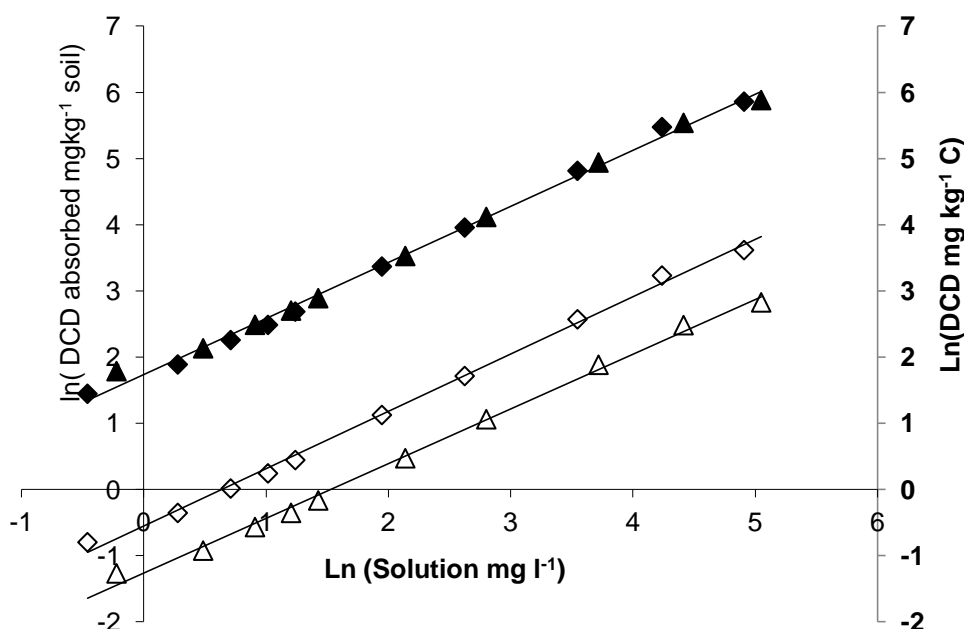


**Figure 5.4** Freundlich absorption isotherm plots for DCD in Manawatu ( $\Delta$ ), Dannevirke ( $\diamond$ ) top soil (3-10 cm) and the DCD soil carbon isotherm for both soils (solid fill) on the secondary axis.

**Table 5.4** Freundlich coefficients derived from the isotherm plot (Figure 5.4 for Manawatu and Dannevirke top soil 3-10 cm and soil carbon ( $C_{ad} = a C_1^b$ ))

	<i>a</i> mg kg <sup>-1</sup> dry soil	<i>b</i>
<b>Manawatu</b>	0.299	0.8325
<b>Dannevirke</b>	0.576	0.8929
	mg kg <sup>-1</sup> C	
<b>Soil carbon</b>	8.980	0.8669

The sorption capacity of DCD by the Manawatu ( $a = 0.30 \text{ mg kg}^{-1}$  dry soil) and Dannevirke soils ( $a = 0.58 \text{ mg kg}^{-1}$  dry soil) are significantly lower than those previously reported with  $a$  ranging from 4.28-5.35  $\text{mg kg}^{-1}$  dry soil and  $b$  (0.77-0.79) for a Mollisol and Alfisol soil in China (Zhang *et al.* 2004). Zhang *et al.* (2004) however had milled their soils to pass a 0.145 mm sieve, which is likely to have dramatically increased the surface area of both soils elevating their adsorption

capacities. This led Zhang *et al.* (2004) to conclude that DCD adsorption to soil organic matter may offer DCD protection from degradation. The lack of sorption by aggregated Manawatu and Dannevirke soils (sieved to pass 4 mm) shows that this may not be the case in these two New Zealand soils. The sorption of DCD in both soils can be fully explained by the soil organic matter content expressed by the soil carbon isotherm (Figure 5.4). A measure of soil carbon may allow prediction of a soil's DCD sorption characteristics.

### 5.5.3 Release rate of coated DCD

The release rates of DCD from the coated PDCD3 and PDCD4 granules into water at 20 °C (Figure 5.5) followed a similar profile to that of the coated urea (Section 2.6).

However the application of the hydraulic convection model was not possible as, the micro-granules were too small to assess the mean film thickness and distribution. The release rate of DCD was empirically modelled using a least square fit of an exponential function of cumulative % release over time (Figure 5.5, Table 5.5).

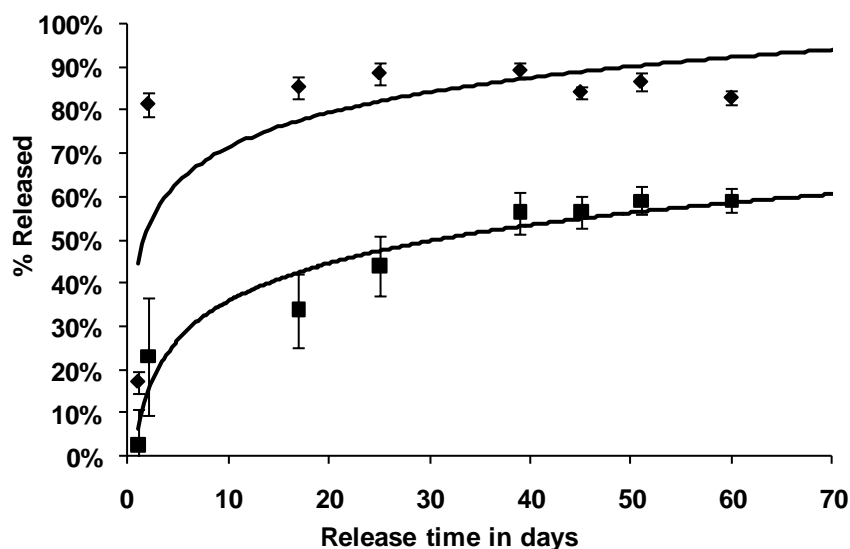


**Figure 5.5** DCD release rate from polymer coated products in water, ◆ PDCD3, ■ PDCD4.

**Table 5.5 Cumulative release rate function of polymer coated DCD in water and 20°C for coating levels of 3 and 4.**

<i>Product</i>	<i>Cumulative % DCD released function</i>
<b>PDCD3</b>	0.1162ln(day) + 0.446
<b>PDCD4</b>	0.1274ln(day) + 0.0639

These results showed the thinner coating level of only 3 layers ( PDCD3) provides little slowing of release while the 4 layer coating level (PDCD4) was most likely to give the required release rate to establish a rapid presence of DCD in the soil followed by some residual release. The rapid release from PDCD3 (80% at time zero) would leave most of the applied DCD exposed to microbial degradation in soil.

## **5.6 Diffusion Column study- observations and model development**

### **5.6.1 Total DCD in soil over time**

The total DCD present in the cores was determined by the summation of DCD measured in core sections (0.2, 0.6, 1.4, 2.5, 3.5 and 4.5 cm) is presented in Figure 5.6 and 5.7. The uncoated DCD (Figure 5.6) showed a rapid initial fall in DCD content associated with a first order degradation rate of  $-0.022 \text{ d}^{-1}$  to  $-0.023 \text{ d}^{-1}$  in Dannevirke and Manawatu soils, respectively. Following the addition of urine on day 28 there was an interruption in the degradation of DCD between days 34 and 41 followed by a reduction in degradation rate  $k$  to  $-0.012$  and  $-0.013$  for the Dannevirke and Manawatu soils, respectively.

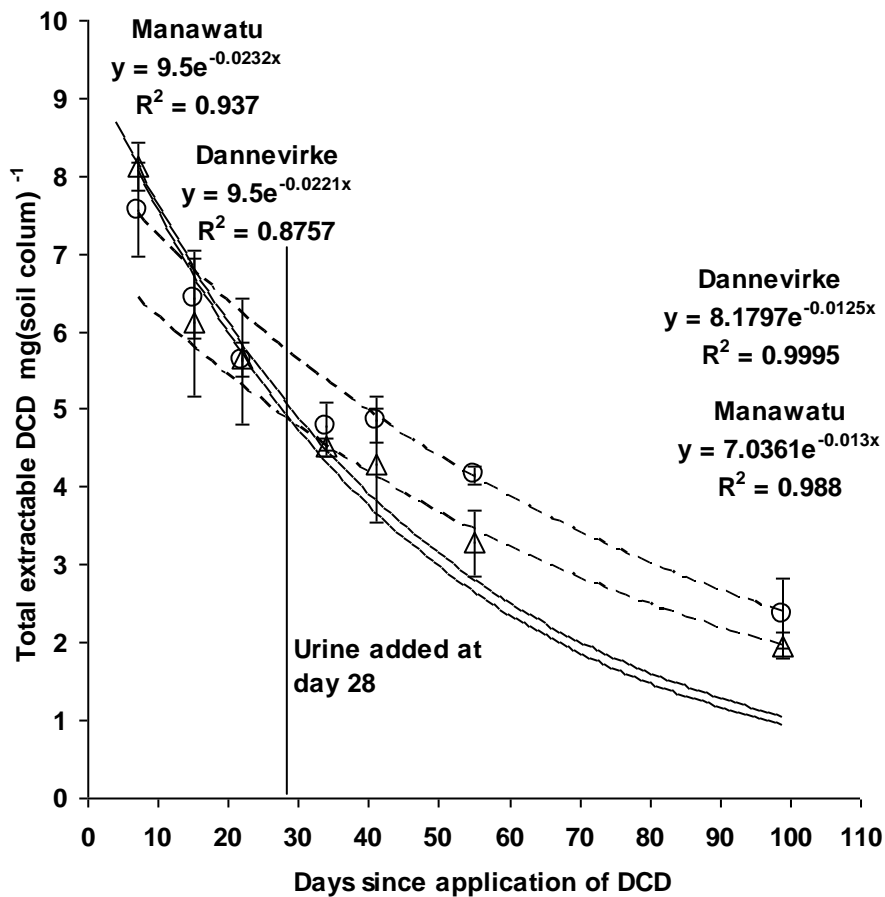


**Figure 5.6** Measured degradation of DCD ( $\text{mg (soil column)}^{-1}$ ) in cores of Manawatu ( $\Delta$ ) and Dannevirke ( $\circ$ ) soils following the application of uncoated DCD (9.5 mg) at day 1 and fresh cow urine (44ml) added at day 28, incubated at  $20^{\circ}\text{C}$  and 75% of field capacity for a total of 99 days. Initial decay function to day 21 (solid lines) and post urination decay function from day 41 (dashed lines)(Error bars  $\pm$  P<0.05).

For the PDCD treatments, the accumulation of DCD in the soil did not follow the release rates measured in water (Figure 5.7), reflecting a more complex release. To interpret the DCD accumulation profile associated with the PDCD treatment the model of DCD release and degradation (Appendix 2) was applied. These modelled results show clearly that the reduction in degradation rate of DCD alone cannot explain the

observed levels of DCD and an increase in DCD release is required (Table 5.7) following urination.

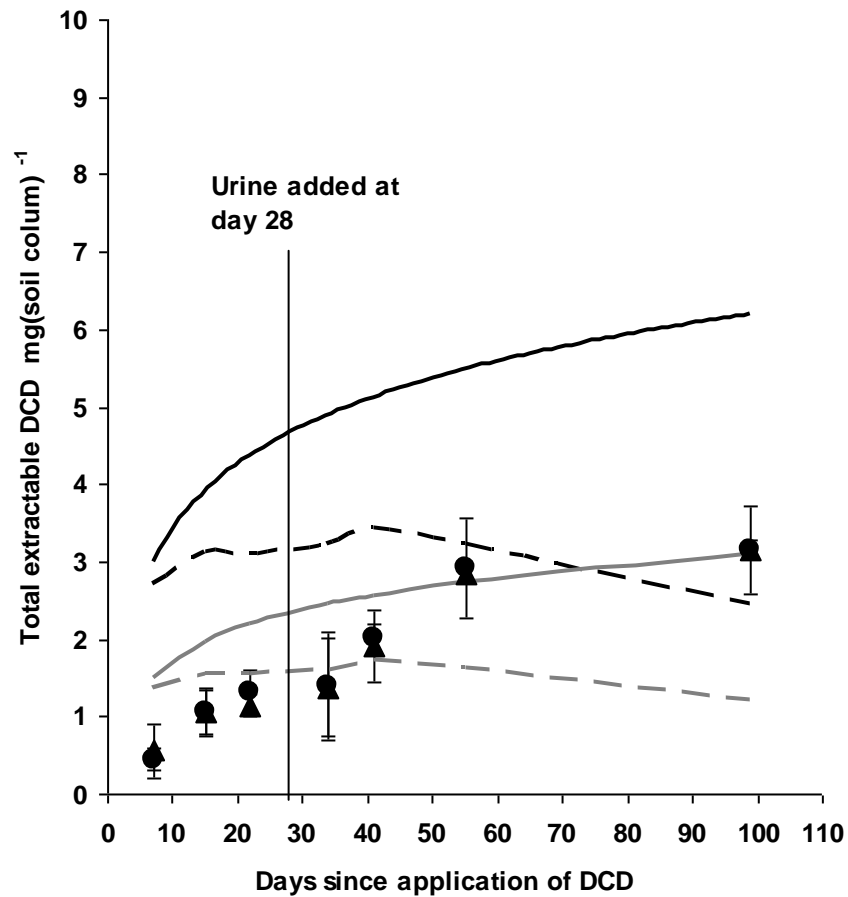


**Figure 5.7** Measured and modelled results for DCD (mg (soil column)<sup>-1</sup>) accumulation in Manawatu (▲) and Dannevirke (●) soil columns treated with 9.5 mg of DCD in the form of PDCD4. The black lines represents the release rate of DCD by water, gray lines the estimated rate in soil based on the  $\theta = 0.39$  and dashed lines simultaneous release and degradation of DCD using the two rate functions (Error bars LSD ( P<0.05)).

### ***5.6.2 DCD concentrations at each soil depth over time***

The effect of the polymer coating of DCD (PDCD) and its associated slowing of the DCD release rate is clearly shown in Figure 5.7 and Figure 5.8. The PDCD in both soils maintained a constant low level of DCD in the upper 0.6 cm of the soil column over the 99 day period, while below this depth a significant increase in DCD concentration with time is observed (Figure 5.8). This contrasts with the results for the uncoated DCD, which produced high concentrations of DCD in the soil cores from day 7 that were rapidly degraded by biological activity over the 99 days to yield low concentrations similar to the PDCD treatments at the final measurement.

The potential effectiveness of the treatments to inhibit nitrification require the soil DCD concentration to be greater than 5 kgDCDha<sup>-1</sup> to 10 cm depth (5µgDCD g<sup>-1</sup>dry soil)(Di and Cameron 2005). This concentration cannot be applied as a universal rule because the effectiveness of DCD is highly dependent on soil properties, with a significant inhibitor effect at >1µgDCD g<sup>-1</sup> dry soil being observed in low organic matter soils (McCarty and Bremner 1989). Based on the > 5µgDCD g<sup>-1</sup> dry soil limit it would be expected that the PDCD treatments in both soil types would result in inhibition of nitrification to 1.4 cm depth at day 7, to 2.5 cm at day 22, to 3.5 cm at day 41, and full core inhibition to 5.0 cm by day 55 ( Figure 5.8).

Additional analysis of the final surface soil sections (0 to 0.2 cm, day 99) showed half of the cores contained significant residues (2.4 mg±0.4), while the other half contained little residual DCD averaging 0.3 mg±0.2. This high variability is due to the small sample size of the remaining sample following the initial water extraction and distribution of PDCD particles in the soil. The presence of significant residual DCD level shows that PDCD in 50% of cases increases the longevity of DCD in the soil system over uncoated DCD.

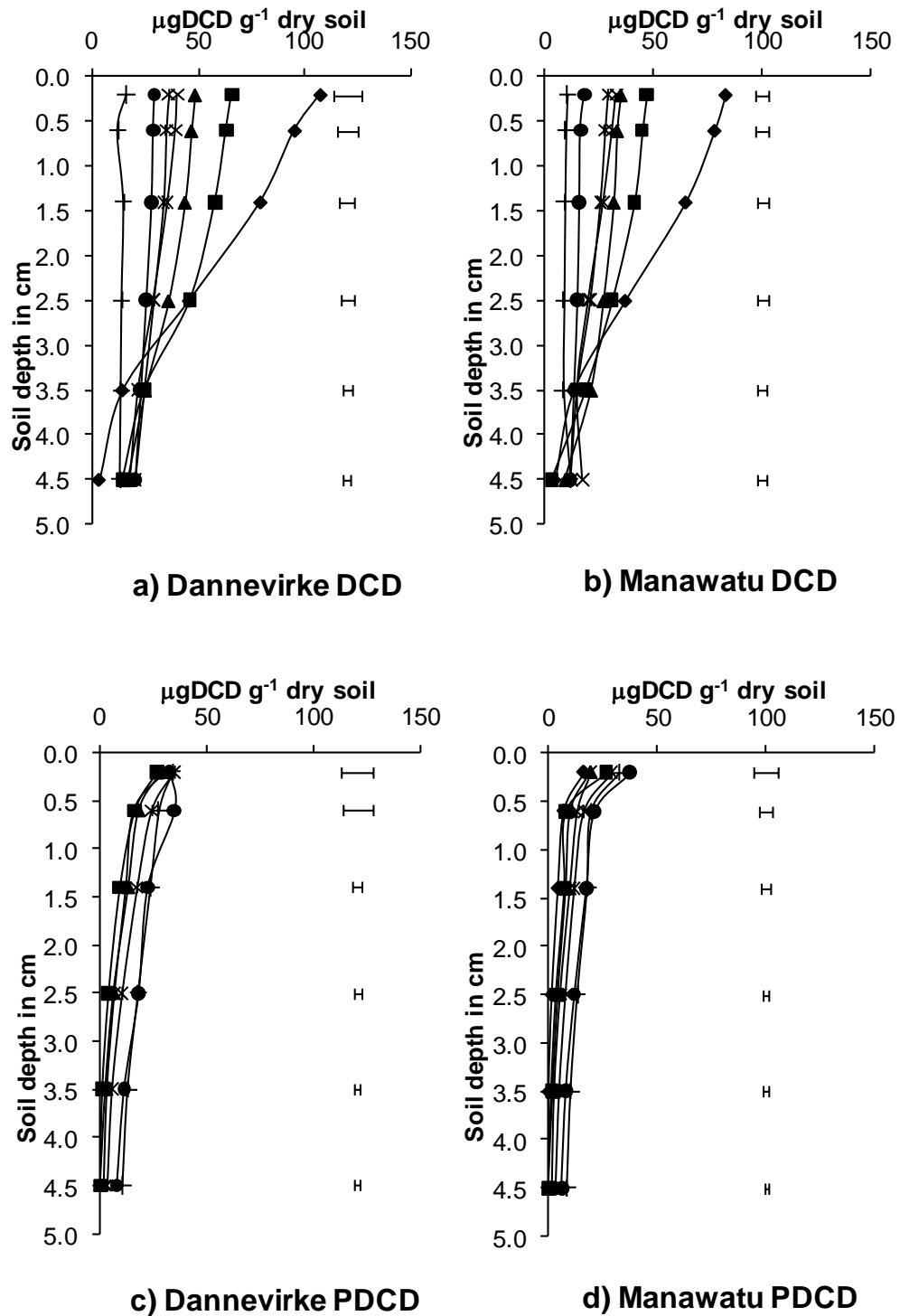


**Figure 5.8** Concentration of DCD at different soil depths in the Dannevirke and Manawatu soil at increasing time following the application of uncoated DCD (DCD) and RLP Coated DCD (PDCD) to the core surface (♦ day 7, ■ day 15, ▲ day 21, × day 34, \* day 41, ● day 55 and + day 99).

## 5.7 Model application to predict DCD profiles

### 5.7.1 Uncoated DCD

The DCD diffusion/degradation model was parameterised (Table 5.6) using values for each parameter derived either from the support experiments, or, from the physical conditions and concentration of materials used in the main experiment.

The model was constructed using Visual Basic in Microsoft Excel, with variable data being inputted in a spread sheet, with a button activated macro to run the program and output data to file, Appendix 2.

**Table 5.6 Model parameters for DCD diffusion and degradation in Manawatu and Dannevirke soils**

<i>Model parameters</i>	<i>Manawatu</i>	<i>Dannevirke</i>
Initial DCD added (moles)	0.000113	0.000113
Core surface area (cm <sup>2</sup> )	44	44
Soil core depth (cm)	5	5
Volumetric soil water content	0.271	0.521
Soil bulk density (g cm <sup>-3</sup> )	1.17	0.9
Tortuosity factor	0.26	0.35
Diffusion coefficient of DCD in water (cm <sup>2</sup> s <sup>-1</sup> )	1.00E-05	1.00E-05
Freundlich coefficient <i>a</i> (mol cm <sup>-3</sup> )	0.014	0.081
Freundlich coefficient <i>b</i>	0.832	0.892
Day of urine application	28	28
Degradation rate1 constant (d <sup>-1</sup> ) ( <i>Prior to urine application</i> )	0.023	0.023
Degradation rate2 constant (d <sup>-1</sup> ) ( <i>Post urine application</i> )	0.012	0.012

The application of the model to predict the pattern of DCD distribution in soil after the application of uncoated DCD treatment shows a good correlation between the predicted quantities of DCD in each soil section compared to that measured in both the Dannevirke (Figures 5.9 and 5.10) and Manawatu (Figures 5.11 and 5.12) soils.

In both soils initially greater DCD concentrations were predicted at days subsequent to the application of urine than was observed. This deviation of modelled and observed

amounts of DCD resulted from the suppression of DCD degradation after urine application. This is not surprising as urine has a biocidal effect through increases in, pH, free  $\text{NH}_3$ , and salinity (Alexander 1977; Harris 1981; Monaghan and Barraclough 1992) and chemical components such as hippuric acid (Kool et al. 2006; Bertram et al. 2009; Clough et al. 2009) which is metabolized in soil to benzoic acid a potent biocide. The addition of urine also releases dissolved organic carbon (DOC) from soils (Ghani et al. 2006) providing a more reduced carbon source than DCD, potentially acting as a competitive inhibitor to DCD degradation.

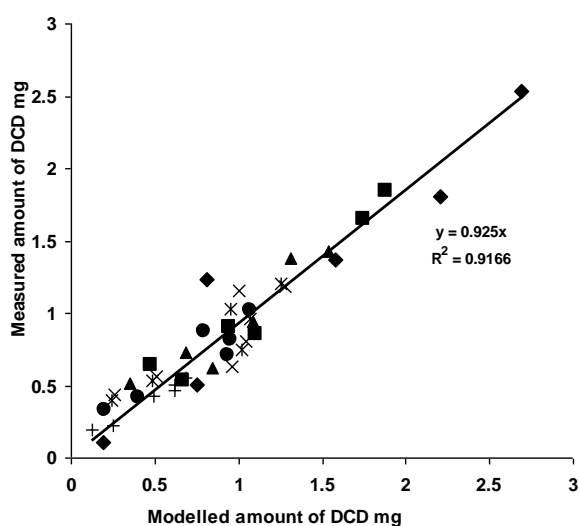


**Figure 5.9** Correlation of modelled and measured amounts of DCD at different depths in the Dannevirke soil (◆ day 7, ■ day 15, ▲ day 21, × day \* day 41, ● day 55 and + day 99; Model parameters are given Table 5.6).

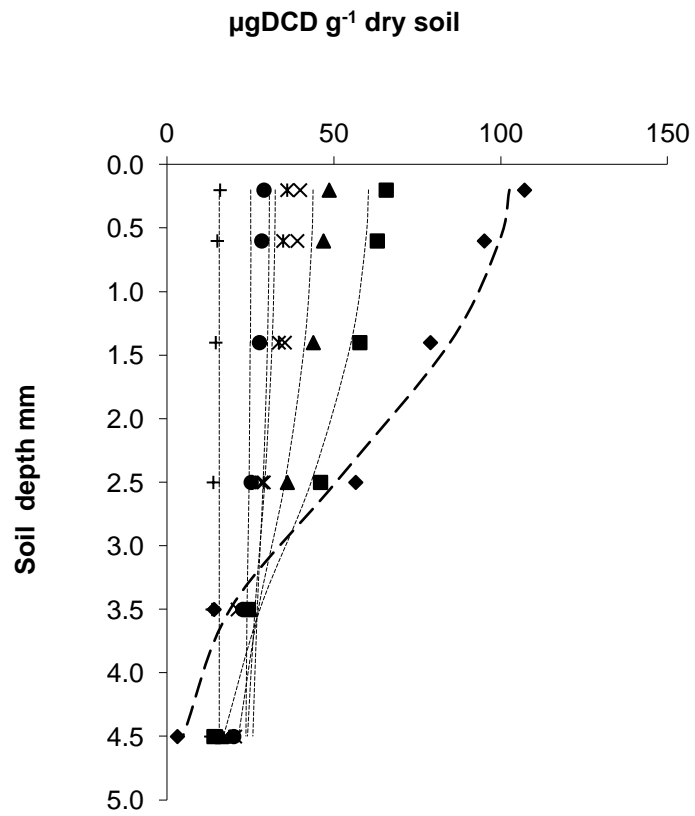


**Figure 5.10** Concentration of DCD in the Dannevirke soil core profile with modelled DCD profile( dashed lines) at each sampling period (♦ day 7, ■ day 15, ▲ day 21, × day 34, \* day 41, ●day 55 and + day 99; Model parameters are given Table 5.6).

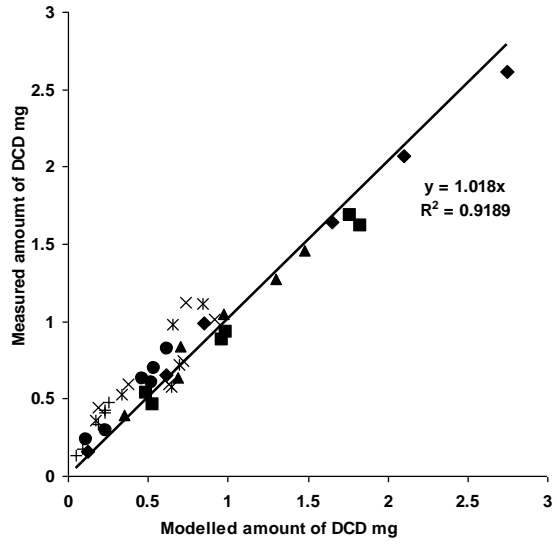


**Figure 5.11** Correlation of modelled and measured amounts of DCD at different depths in the Manawatu soil (♦ day 7, ■ day 15, ▲ day 21, × day 34, \* day 41, ● day 55 and + day 99; Model parameters are given Table 5.6).

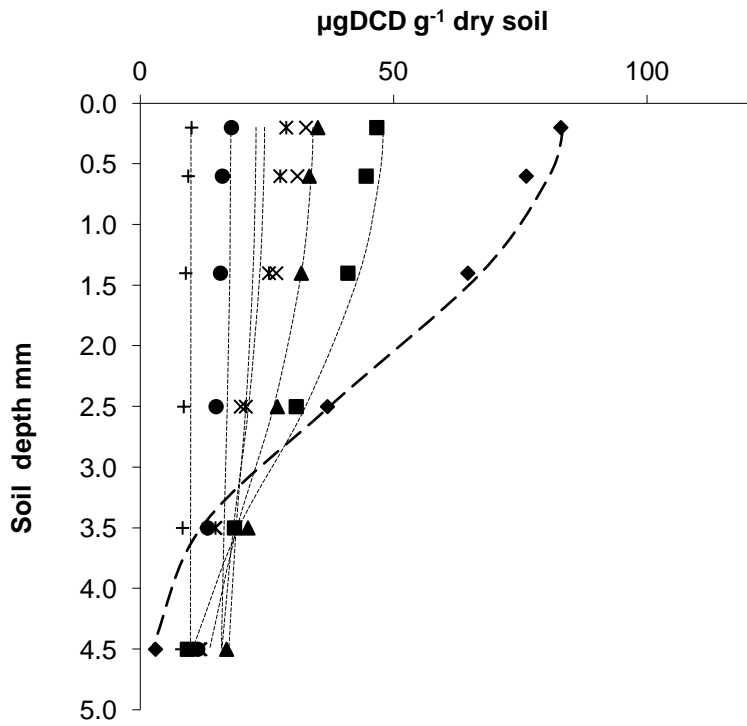


**Figure 5.12** Concentrations of DCD in Manawatu soil core profiles with modelled DCD profile( dashed lines) at each sampling period (♦ day 7, ■ day 15, ▲ day 21, × day 34, \* day 41, ● day 55 and + day 99; Model parameters Table 5.6).

### 5.7.2 Coated PDCDs

The model was altered to accommodate the slow release of DCD from the PDCD by defining the release rate of DCD across the surface to be that observed in the water release trial, which released 6.3% of the total DCD by day 1, followed by a falling rate (Equation 5.5) with all other parameters as in Table 5.6.

$$\text{Flux}(0) = ((\text{mol} * 0.139 * (\text{tstep} * \text{dt})^{-1.006}) * \text{dt}) \quad \text{Eq 5.5}$$

The model failed to predict the quantities of DCD in the soil section profiles to which the PDCD had been applied to the Dannevirke (Figure 5.13) and Manawatu (Figure 5.14) soils. The inability of the model to predict the DCD concentrations in the soils was caused by two factors. Firstly the model overestimated the initial release rate of DCD from the PDCD into the soil in the first 7 days. Secondly, the release of DCD following urine application is under estimated. This is illustrated in Figures 5.13 and 5.14, with the individual regression lines illustrating the “fan of failure”.

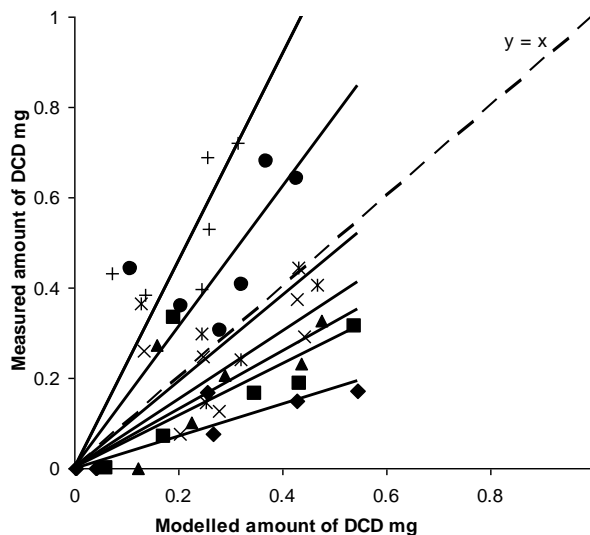


**Figure 5.13** Correlation of modelled and measured amounts of DCD at different depths in the Dannevirke soil treated with PDCD (♦ day 7, ■ day 15, ▲ day 21, × day 34, \* day 41, ● day 55 and + day 99; Model parameters are given in Table 5.5 & 5.6).

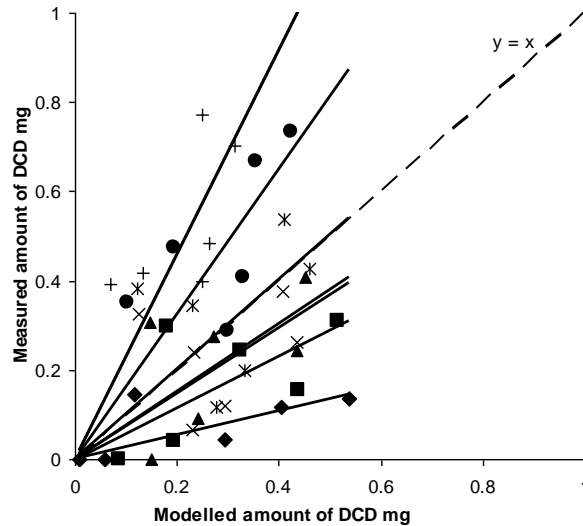


**Figure 5.14** Correlation of modelled and measured amounts of DCD at different depths in the Manawatu soil treated with PDCD (♦ day 7, ■ day 15, ▲ day 21, × day 34, \* day 41, ● day 55 and + day 99; Model parameters are given in Table 5.5 & 5.6)

The over estimation of the initial DCD release rates at the soil surface is most likely due to the initial poor contact between the soil and the coated granule which reduced the migration of water into and DCD out of the coated granule. Following the addition of urine to the cores, which pooled on the core surface, the contact between DCD and the soil was improved allowing the increased exchange of water and DCD between the granule and soil. In addition to this increase in physical contact the addition of urine increases both the pH and ionic strength (Section 6.3 p.155) which may influence the release of DCD. These factors affecting DCD release pre and post urine addition requires further research.

As the release rate of DCD from the PDCD could not be reliably modelled for a the surface application to soil from the water release rate data and the effect of urine on the release rate is uncertain, the release of DCD was empirically modelled based on the change in total core DCD levels (Figure 5.7) corrected for degradation. This analysis showed two significant release periods of DCD, the first following the application of PDCD and the second following the addition of urine. The first initial fast release 0-15 days (Table 5.7) was most likely associated with the release from imperfectly coated

granules and a moist soil surface. This was followed by a rapid fall in DCD release, possible due to slight surface drying. This slowing of DCD release continued until the addition of urine, after which the second rapid release of DCD occurs. This was also associated with a slowing in DCD degradation; however the rise in release rate was too great to be explained by this alone. The increased soil contact, surface moisture, pH and soil solution concentration are the most likely factors affecting the release of DCD post urine application.

**Table 5.7** Modelled release rate of DCD from polymer coated DCD in soil at 75% FC and 20°C

<i>Step Wise Release rate Time period Days</i>	<i>Release rate in %/day</i>	
	<b>Manawatu</b>	<b>Dannevirke</b>
<b>0-7</b>	0.92	0.80
<b>7-15</b>	0.87	0.92
<b>15-22</b>	0.27	0.51
<b>22-34</b>	0.43	0.40
<b>34-41</b>	0.91	0.99
<b>41-55</b>	1.00	1.00
<b>55-99</b>	0.44	0.42

The application of this stepwise release rate function produces good correlations between the model and both soils, (Figure 5.15 and 5.16).

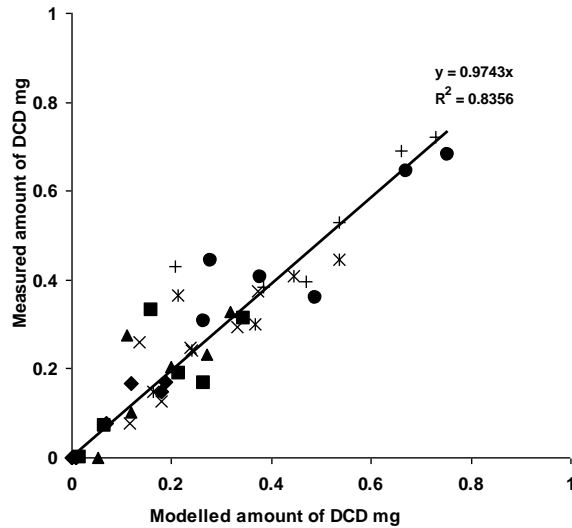


**Figure 5.15** Correlation of modelled and measured amounts of DCD at different depths in the Manawatu soil treated with PDCD. (◆ day 7, ■ day 15, ▲ day 21, × day 34, \* day 41, ● day 55 and + day 99; Model parameters are given in Table 5.6 & 5.7)

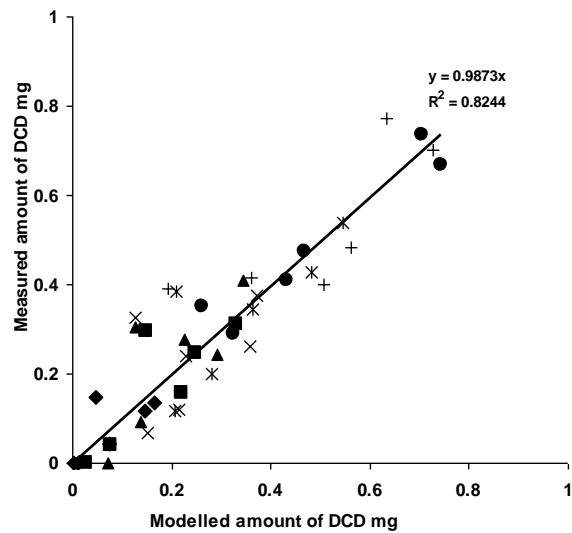


**Figure 5.16** Correlation of modelled and measured amounts of DCD at different depths in the Dannevirke soil treated with PDCD. (◆ day 7, ■ day 15, ▲ day 21, × day 34, \* day 41, ● day 55 and + day 99; Model parameters are given in Table 5.6 & 5.7)

## **5.8 Application of model to determine longevity of PDCD release over DCD**

The development and optimisation of the model allows the prediction of concentration and effectiveness of the PDCD compared to uncoated DCD at deeper soil profiles, higher application rates and longer time frames to compare the two products. In the Manawatu soil the effect of application rates of 21, 42 and 63 kgDCD ha<sup>-1</sup> in both forms (Figure 5.17) shows that PDCD provides good initial inhibition of nitrification (critical DCD concentration threshold > 5 µg DCD /g soil) to a depth of 4 cm in 30 days which persisted until day 300 at the application rate of 42 kgDCD ha<sup>-1</sup>, whereas at this rate the uncoated DCD produces rapid protection to a depth of 6 cm within 15 days, which persisted until day 180. The uncoated DCD at this single application rate resulted in an initially high and possibly toxic level of DCD (>100 µg DCD g<sup>-1</sup>) in the upper 2 cm of the soil column.

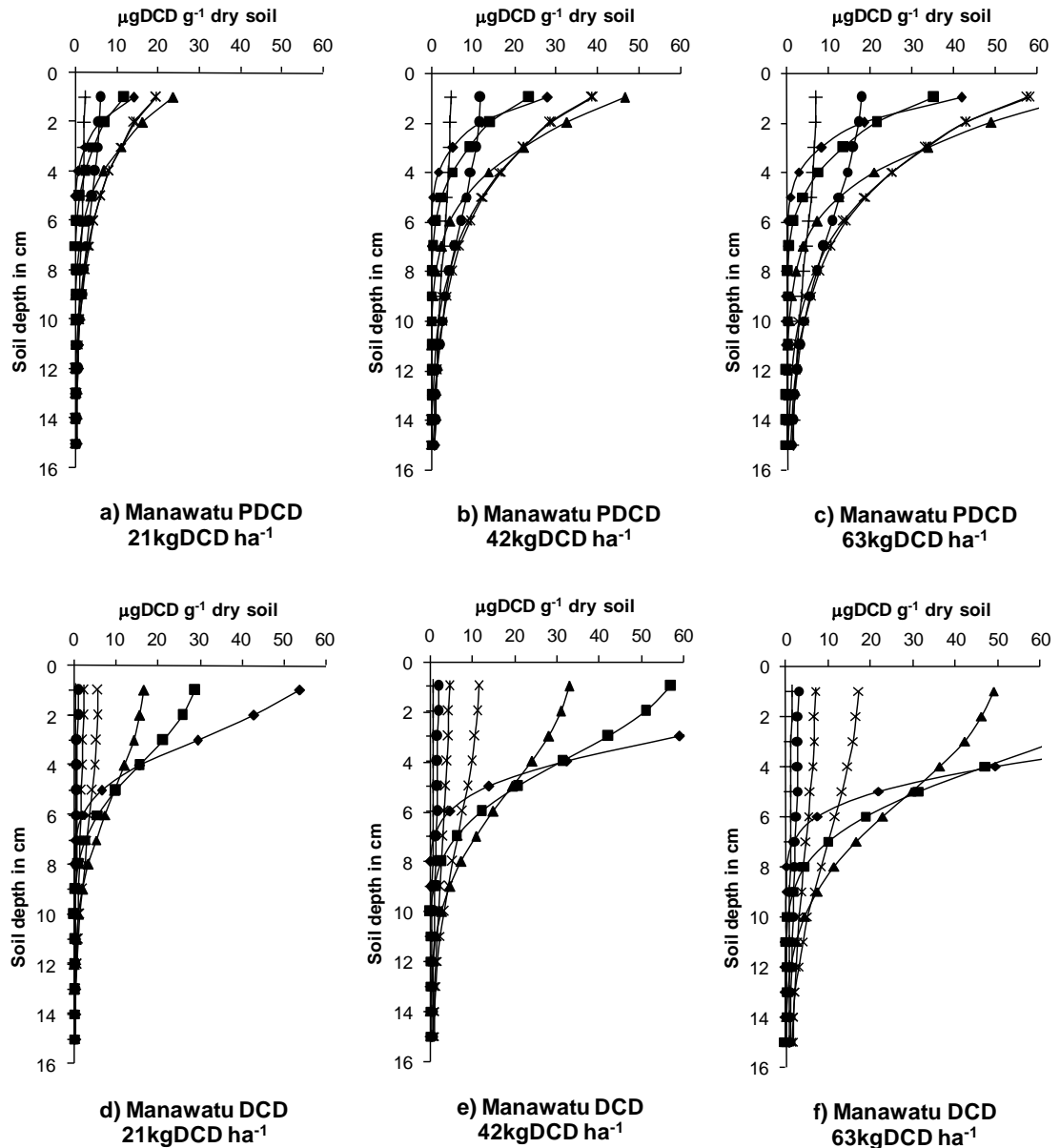


**Figure 5.17** Modelled soil DCD concentrations in soil columns 150mm deep for DCD and PDCD applied to Manawatu silt loam over 300 days (◆ day 15, ■ day 30, ▲ day 60, × day 120, \* day 180, ● day 240 and + day 300; Model parameters are given in Table 5.7 & 5.8)

The model shows that PDCD has the potential to nearly double the effective persistence of the equivalent application of DCD. However for initial effect the application rate

must be high in the order of 40 kgDCD ha<sup>-1</sup> to give effective inhibition within the first 30days following application.

This large increase in application rate to insure rapid penetration of the soil profile can also be achieved by adding 20% of uncoated DCD to the application as illustrated in Figure 5.18, which produces a rapid inhibitor effect to 5 cm in 15 days and is persistent in urine affected soil for up to 240 days at 20°C.

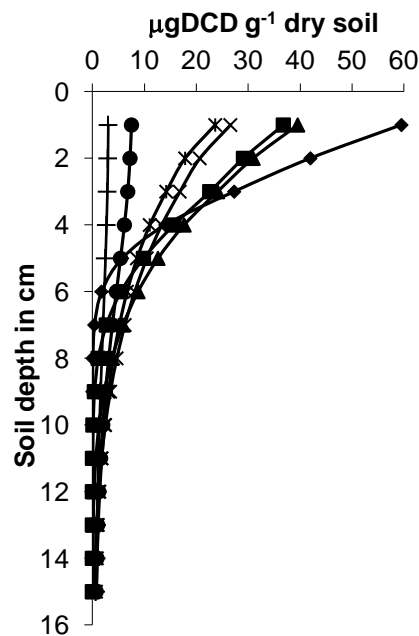


**Figure 5.18** Modelled soil DCD concentrations in soil columns 150mm deep for combination of PDCD:DCD (80:20) applied to Manawatu silt loam at 25 kgDCD ha<sup>-1</sup> over 300 day (◆ day 15, ■ day 30, ▲ day 60, × day 120, \* day 180, ●day 240 and + day 300; Model parameters are given in Table 5.7 & 5.8).

## 5.9 Conclusion:

The movement of DCD in soil is rapid in the case of uncoated DCD where the initial high surface concentration produces rapid diffusion of DCD throughout the soil column within, one week following application. In the case of the PDCD the diffusion is slow due to the low surface flux of DCD entering the column. This resulted in levels of DCD in some depths of the soil column being below the critical 5µgDCDg<sup>-1</sup> required for full

nitrification inhibition. Therefore only partial inhibition of nitrification is initially expected for applications of PDCD at levels below  $32 \text{ kg ha}^{-1}$  ( $21 \text{ kgDCD ha}^{-1}$ ) at depths greater than 3 cm and within 30 days. Modelling based on increased applications of 63 and  $90 \text{ kg PDCD ha}^{-1}$  ( $40$  and  $60 \text{ kg DCD ha}^{-1}$  equivalence) gave full inhibition of nitrification in the soil column to 4 and 5 cm depth in 30 days, respectively. The PDCD at these elevated application levels produced significant inhibition of nitrification for at least 300 days following application (under trial conditions) without producing toxic levels of DCD in the soil. Under the same modelling conditions uncoated DCD produced rapid inhibition of the soil column to a depth of 6 cm in 15 days at both  $42$  and  $63 \text{ kg DCD ha}^{-1}$ , however this was only persistent for 180 days. PDCD at all levels dramatically increased the persistence of DCD in the soil by 120 days.

The modelling of mixed PDCD and DCD in the proportions of 80:20 respectively has shown that at  $25 \text{ kgDCD ha}^{-1}$  rapid inhibition of nitrification can be obtained to 5 cm in depth in 15 days, while still maintaining the persistence of the slow release PDCD.

Further research is required to explain whether the increase in rate is the result of the dry-wet-moist cycles associated with the urine application or as a chemical result of urine application (pH, ionic strength, etc.).

## **Chapter 6 Nitrification inhibitory effect of polymer coated DCD in two contrasting New Zealand soils.**

---

### **6.1 Introduction**

The application of polymer coated DCD (PDCD) to pasture soils has the potential to extend the effectiveness of DCD as a nitrification inhibitor (Chapter 5) in urine affected soils. Extended inhibition of nitrification in urine patches will only occur if the DCD and urine derived  $\text{NH}_4^+$  remains in intimate association. The potential for PDCD to mitigate nitrate leaching and  $\text{N}_2\text{O}$  emission from urine patches is dependent on this.

These effects of urine-N and DCD are measured in the core profiles over 68 days following urine application. The measured results are compared with the combined DCD diffusion model (Chapter 5) and a urine-N model. Others (McCarty and Bremner 1989; Di and Cameron 2004; Kelliher et al. 2008; Menneer et al. 2008) have reported differences in the effect of DCD on inhibition of nitrification etc. without reporting the fate of DCD. Di and Cameron (2004a) reported the residual concentration of DCD but did not report the movement of DCD in the soil samples with respect to the source of  $\text{NH}_4^+$ . It is important to understand the co-location of DCD and  $\text{NH}_4^+$  in such experiments if inhibitor technology is to be improved, particularly by the use of slow releases DCD products such as those developed in Chapter 5.

The soil core experiment (Chapter 5) established to model DCD movement in soil, also provided the opportunity to study the fate of urine N that was applied 28 days after the cores were treated with DCD. In this Chapter (6) a model is developed to explain the measured redistribution of urine N, its hydrolysis, adsorption and nitrification in the soil cores.

The objective of this chapter is to measure the movement of both DCD and its association with urine  $\text{NH}_4^+$  and the inhibition of nitrification associated with DCD and soil depth. This information in conjunction with the DCD diffusion model (Chapter 5) is used to model the effectiveness of PDCD under field conditions to a depth of 50 cm.

The urine  $\text{NH}_4^+$  distribution is modelled as a non-saturated plug flow followed by diffusion/hydrolysis of urea, adsorption and nitrification of  $\text{NH}_4^+$ , with the partial inhibitory effects of soil depth and DCD being accounted for.

## **6.2 Methodology**

### **6.2.1 Measurement of soil mineral N**

The soil sampled from DCD treated and untreated core sections post urine addition (Chapter 5, Section 5.3.1) were extracted in 2M KCl at a ratio of 2g soil: 20ml extract. The extract was then analysed for  $\text{NH}_4^+$ -N and  $\text{NO}_3^-$ -N using an auto-analyser (Blakemore et al. 1987).

### **6.2.2 Estimation of nitrification rate with depth**

The effect of soil depth on the rate of nitrification has been alluded to in a number of reports (Macduff and White 1985; Hosen et al. 2002; Liu et al. 2006), however the development of a direct relationship between nitrification rate and soil depth has not been published for urine amended soils. In the urine patch with its high  $\text{NH}_4^+$ -N concentrations (600 to 1000 mgN  $\text{kg}^{-1}$ ) the rate of nitrification is assumed to be zero order (Flowers and Arnold 1983) as the soil microbiological system will be unable to grow sufficiently due to  $\text{NH}_3$  toxicity and growth limiting factors such as copper availability (Bollmann and Conrad 1997) and soil pH.

In this soil column study the rate of nitrification is estimated based on the change in extractable  $\text{NH}_4^+$ -N with time for the core section treated with urine only, as the diffusion of nitrate between sections was too rapid.

### **6.2.3 Measurement of soil DCD concentration**

The measurements of DCD in each section, at the sampling times has previously been reported in Chapter 5 section 5.3.1.

#### 6.2.4 Measurement of inhibitory effect of DCD on nitrification

The inhibitory effect of DCD on nitrification has been shown to be non-substrate-competitive but has a dependence on soil type and organic matter content (McCarty and Bremner 1989). Inhibition of an enzyme or biological growth can be described using a modified Michaelis–Menten equation 6.1 (Banerji and Bajpai 1994), which assumes the rate is not substrate ( $\text{NH}_4^+$ ) but enzyme or population limited.

$$\frac{1}{U} = \frac{1}{U_{max}} + \frac{[DCD]}{U_{max} K} \quad \text{Eq. 6.1}$$

where  $U$  ( $\mu\text{mol g}^{-1} \text{d}^{-1}$ ) is the observed nitrification rate,  $U_{max}$  ( $\mu\text{mol g}^{-1} \text{d}^{-1}$ ) is the maximum nitrification rate,  $[DCD]$  ( $\mu\text{mol g}^{-1}$ ) is the soil DCD concentration and  $K$  ( $\mu\text{mol g}^{-1}$ ) an inhibitor constant. This equation can be rearranged to express the proportional inhibitor effect  $U/U_{max}$  which is commonly reported as a percent inhibition.

$$\frac{U_{max}}{U} = 1 + \frac{[DCD]}{K} \quad \text{Eq. 6.2}$$

Based on equation 6.2,  $K$  was determined for the Dannevirke and Manawatu soils used in the core studies by a plot of  $\frac{U_{max}}{U}$  and  $[DCD]$

#### 6.2.5 Mass flow of solute

The addition of urine to a soil results in a significant mass flow that redistributes both urine and existing soil solution as a function of volumetric displacement of the vacant pore space to field capacity. For example the initial penetration of urine into the soil excluding channelling can be defined by the maximum volume of liquid in the soil at field capacity as defined by  $V = \theta A/d$ . Thus for an application of 10 mm of urine (2L per  $0.2 \text{ m}^2$  (Ball et al. 1979)) the distance of penetration is  $x = \text{mm}(\text{urine})/(\theta_{\text{max}} - \theta)$ . For a soil with a maximum field capacity of 0.4 at 50% field capacity the urine application of 10mm will initially penetrate 50 mm, and at 75% field capacity will penetrate 100mm, from this initial soil position diffusion may occur which can be numerically modelled.

### 6.2.6 Urine $\text{NH}_4^+$ -N isotherm

The adsorption isotherm for the urine derived  $\text{NH}_4^+$  ions was determined for both the Dannevirke and Manawatu topsoils (3-10cm) by incubating air dry soil (10g) in 35 ml centrifuge tubes with a series of dilute urine solutions from 6000 to 100 mg N/l containing 20mg/l DCD to prevent nitrification. The solutions were applied to duplicate soil samples at a 100% FC and the soils incubated for 5 days with their lids off in a 100% humidity chamber at 20°C. Following this the incubated soil was extracted with 20 ml of water on an end over end shaker for 1 hr, centrifuged (9000 rpm for 3 min.) with all liquid being removed and filtered. The tubes were then weighed to account for extraction carryover of soil solution and then extracted with 20ml of 2 M KCl to determine exchangeable ammonium. The isotherm was then graphed on a natural log – log plot of water soluble  $\text{NH}_4^+$ -N mg/l (water extract concentration) versus KCL extractable  $\text{NH}_4^+$ -N mg/kg. The slope of this line is  $b$  and y-intercept is  $a$  of the Freundlich equation  $C_s = a C_l^b$ .

### 6.2.7 Modelling

Using a modelling approach similar to the DCD diffusion, absorption and degradation model developed in Chapter 5, a model is developed here to explain the fate of urine N derived  $\text{NH}_4^+$ -N. The model uses the following simplified set of assumptions.

1. The urine is initially distributed via mass flow filling vacant soil pore space in the surface soil zone to field capacity. (This model does not take into account channelling and bypass flows to deep soil depths)
2. Volatilisation and immobilisation of  $\text{NH}_4^+$ -N are estimated from urine  $\text{NH}_4^+$ -N N recovery from the soil.
3. Urea is allowed to diffuse without adsorption or degradation for an initial period of 2 to 3 days. Following this all N is ammonium and adsorbs and nitrifies.
4. The nitrification/degradation of soil  $\text{NH}_4^+$ -N can be represented by a zero order rate process dependent on depth.

5. Assuming the inhibitory effect of DCD on nitrification follows the non-competitive inhibitor velocity function, Equation 6.2.

$$\frac{U_{max}}{U} = 1 + \frac{[DCD]}{K} \quad \text{Eq. 6.2}$$

This model required the additional measurement of  $\text{NH}_4^+$ -N soil adsorption isotherms and the nitrification rate profile, which was obtained from mineral N measurements on the non-DCD treated cores, described in Chapter 5.3.1.

The DCD and urine  $\text{NH}_4^+$ -N models are combined by using the predicted DCD concentration with depth and time to calculate the relative nitrification velocity  $\frac{U}{U_{max}}$  for each soil at different times and depths. The relative nitrification velocity was then summarised into the six soil depths and five day time intervals which was used by the urine/ $\text{NH}_4^+$ -N model to calculate nitrification throughout the soil profile over time.

The urine/ $\text{NH}_4^+$ -N model was written in visual basic within Excel 2007(Appendix 4).

## 6.3 Results

### 6.3.1 Urine $\text{NH}_4^+$ -N isotherm

The  $\text{NH}_4^+$ -N recovered in soil solution plus adsorbed on the soil surface accounted for 65% and 76% of the applied urine N at a concentration of  $6000 \text{ mgN l}^{-1}$  for the Manawatu and Dannevirke soil, respectively. The remaining N was assumed to either have been volatilised as  $\text{NH}_3$  gas or immobilised into soil organic matter. It is assumed the presence of DCD prevents the formation of  $\text{NO}_3^-$  indicating 35% and 24% loss of applied urine N via immobilisation and volatilisation.

The  $\text{NH}_4^+$ -N adsorption isotherm, Figure 6.1, produced a good fit with the Freundlich equation. Table 6.1 gives the Freundlich coefficients for both soils.

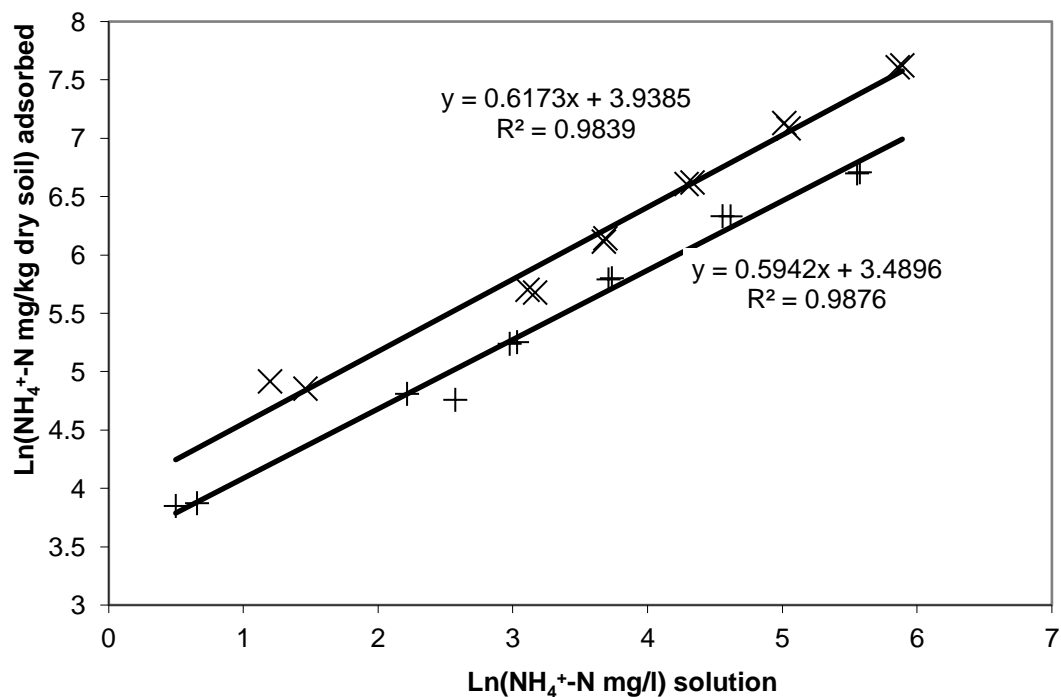


**Figure 6.1**  $\text{NH}_4^+$ -N Freundlich isotherm plots for urine treated Manawatu Silt loam (+) and Dannevirke loam (x).

**Table 6.1** Freundlich isotherm coefficients for  $\text{NH}_4^+$ -N adsorption in urine treated Manawatu and Dannevirke soils.

	<i>-a-</i> mg/kg	<i>-b-</i>
<b>Manawatu</b>	38.34	0.5942
<b>Dannevirke</b>	46.21	0.6173

These results (Figure 6.1, Table 6.1) show that  $\text{NH}_4^+$  ions are more strongly retained in both soils compared to DCD, as the coefficient *b* in both soils are lower than 0.83 and 0.86 for DCD in Manawatu and Dannevirke soil (Table 5.4). This expected to limit the movement of ammonium-N from the urine affected zones of the soil cores relative to the DCD.

### 6.3.2 Nitrification rate with depth

The nitrification rate of ammonium with soil depth was initially estimated based on the change in extractable  $\text{NH}_4^+$ -N concentration with time in the soil cores sectioned at 0-

0.2 cm, 0.2-0.6 cm, 0.6-1.4 cm, 1.4-2.5 cm, 2.5-3.5 cm and 3.5-4.5 cm for the two soil types treated with urine without DCD (Figures 6.2 & 6.3).

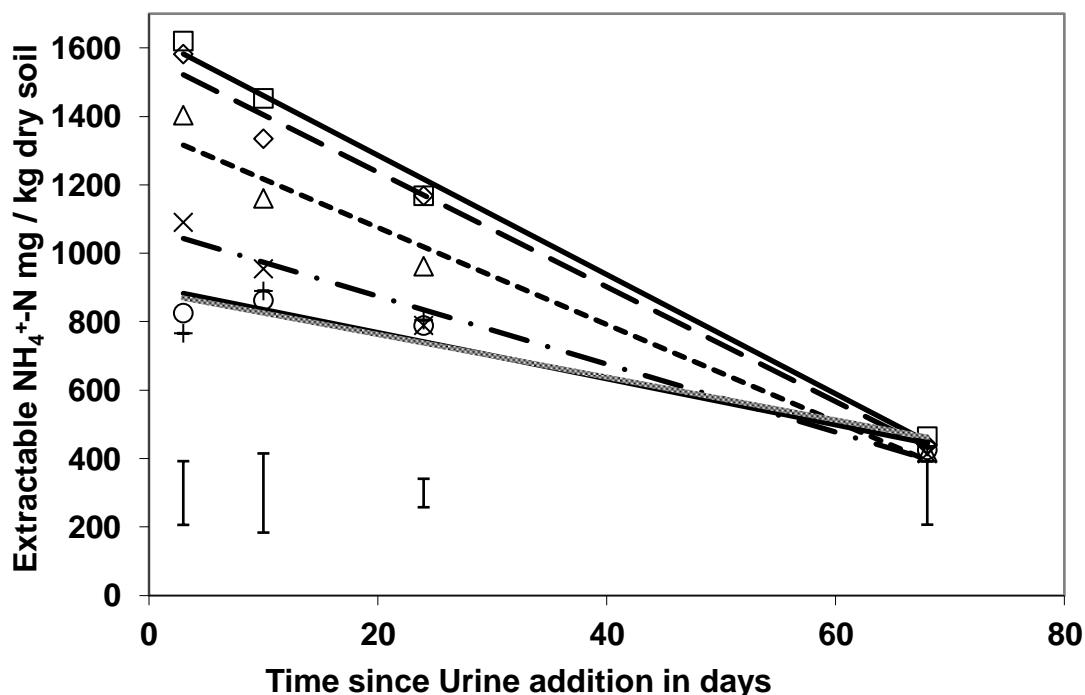


**Figure 6.2** The change in soil extractable  $\text{NH}_4^+$ -N concentrations in Dannevirke soil layers over time following dairy urine application ( $\square$  0-0.2 cm,  $\diamond$  0.2-0.6 cm,  $\triangle$  0.6-1.4 cm,  $\times$  1.4-2.5 cm,  $+$  2.5-3.5 cm and  $\circ$  3.5-4.5 cm depths; Lines of best (fit slope Table 6.2); vertical error bars LSD ( $P=0.05$ )).

Irrespective of soil depth the change in  $\text{NH}_4^+$ -N concentration with time were fitted best by linear relationships. This supports the assumption that nitrification is approximated by a zero order reaction. The rates of change, were greatest in the Manawatu soil (Figure 6.2). It was assumed that nitrification accounted for the decrease in  $\text{NH}_4^+$ -N concentration. This was supported by the decrease in the whole soil core  $\text{NH}_4^+$ -N concentration being equal to the increase in whole soil core  $\text{NO}_3^-$ -N concentrations (Figures 6.4 and 6.5). The higher rate of nitrification in the Manawatu soil can be explained by a number of possible factors including higher, or more active, nitrifier population and, or higher available  $\text{NH}_3$  due to higher pH (Section 6.4) and lower adsorption (Table 6.1)

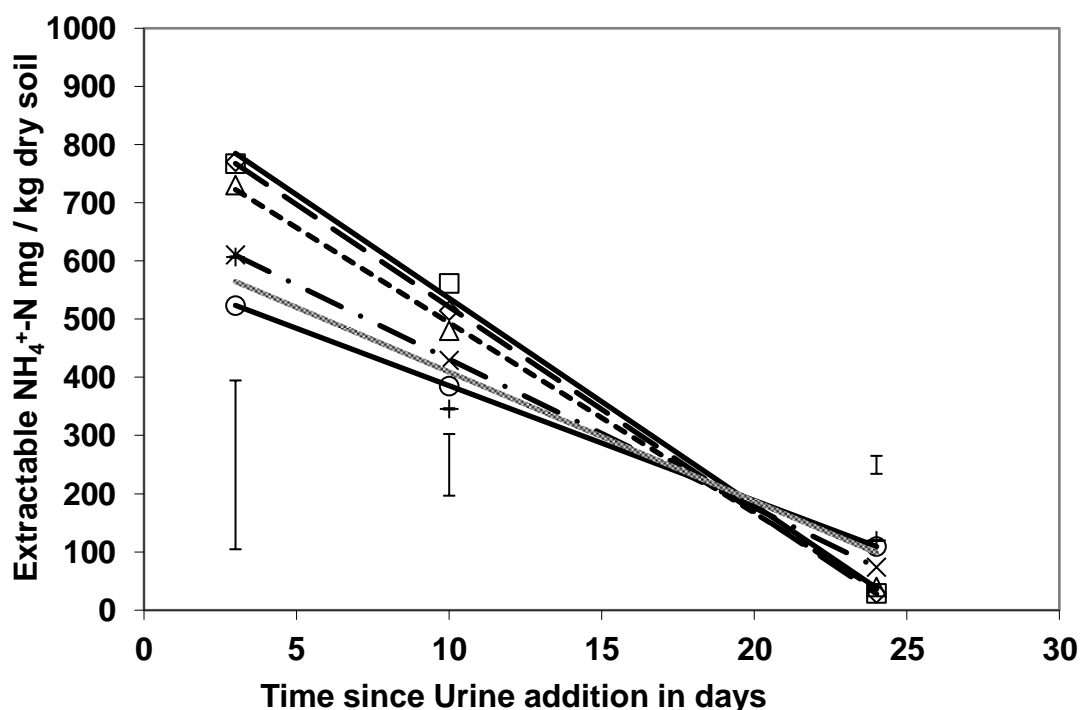


**Figure 6.3** The change in soil extractable  $\text{NH}_4^+$ -N concentrations in Manawatu soil layers over time following dairy urine application ( $\square$  0-0.2 cm,  $\diamond$  0.2-0.6 cm,  $\triangle$  0.6-1.4 cm,  $\times$  1.4-2.5 cm,  $+$  2.5-3.5 cm and  $\circ$  3.5-4.5 cm depths; lines of best fit (slopes Table 6.2); vertical error bars LSD ( $P=0.05$ )).

The same initial urine N application was made to both soils. Therefore the difference in  $\text{NH}_4^+$ -N concentrations between soils is the result of a number of factors. The initial urine distribution within the soil cores resulted in most of the applied urine N remaining in the upper 2.5 cm of the Dannevirke soil, whereas the urine moved more uniformly through the Manawatu soil. The cation exchange capacity, adsorption and pH buffering were also lower for the Manawatu soil resulting in higher losses of applied urine N. As the results are presented on a weight basis the difference in bulk density between the two soils also reduces the apparent  $\text{NH}_4^+$ -N concentration.

Nitrification rates in both soils had maxima ( $U_{max}$ ) in the top 0.2 cm and fell at a rate of 14.0 % and 17.8 % per cm to 62 % and 46% of  $U_{max}$  at 3.5 -4.5 cm the Manawatu and Dannevirke, respectively (Table 6.2). This inhibitory effect of soil depth has been reported by Macduff and White (1985) for a clay soil under grazed pasture. The  $U_{max}$  however was measured at the 2-10 cm depth in their study because the upper 0-2 cm of

soil was discarded. This probably resulted in a low estimate of  $U_{max}$ , which showed a fall in rate of only 3% per cm of soil depth.

**Table 6.2** Nitrification velocity  $U$  ( $\text{mol g}^{-1} \text{day}^{-1}$ ) in Manawatu and Dannevirke soil cores as a function of soil depth in cm.

Soil depth	Manawatu $\text{mol g}^{-1} \text{d}^{-1}$	Dannevirke $\text{mol g}^{-1} \text{d}^{-1}$	Manawatu % $U_{max}$	Dannevirke % $U_{max}$
0-0.2cm	2.2E-06	1.4E-06	100%	100%
0.2-0.6cm	2.2E-06	1.3E-06	99%	96%
0.6-1.4cm	2.0E-06	1.1E-06	92%	81%
1.4-2.5cm	1.6E-06	7.8E-07	72%	57%
2.5-3.5cm	1.2E-06	6.1E-07	55%	44%
3.5-4.5cm*	1.4E-06*	6.3E-07	62%*	46%*

\* Results are higher than expected due to feedback ammonium diffusion from lower boundary.

In undisturbed soil, nitrification rates may decrease with depth for a number of reasons (reduced  $\text{O}_2$  supply, reduced substrate ( $\text{NH}_4^+/\text{NH}_3$ ), change in nitrifier population, change in pH etc.), however in these repacked soil cores the contributing factors are limited to reduced  $\text{O}_2$  and reduction in initial substrate  $\text{NH}_4^+$  concentration (Figure 6.2 and 6.3).

The values in Table 6.2 are used as initial estimates of nitrification in the modelling of the fate of N from urine application to soil cores (Section 6.4).

### 6.3.3 Soil core incubation with urine application

Measured values of total soil extractable  $\text{NH}_4^+$ -N and  $\text{NO}_3^-$ -N varied with soil treatment and time in the soil cores (Figure 6.4). The overall effects of the treatments are presented in Figures 6.4 and 6.5.

The two soil types had dramatic differences in average nitrification rates. The Manawatu silt loam having double the nitrification rate ( $2.19 \times 10^{-6} \text{ mol g}^{-1} \text{ d}^{-1}$ ) of the Dannevirke silt loam ( $1.13 \times 10^{-6} \text{ mol g}^{-1} \text{ d}^{-1}$ ). This indicated a significantly lower nitrification potential in the Dannevirke soil. This difference in nitrification potential is

clearly seen in Figure 6.4 and 6.5 in terms of the rate of decreases in soil  $\text{NH}_4^+$ -N and increase in soil  $\text{NO}_3^-$ -N concentrations.

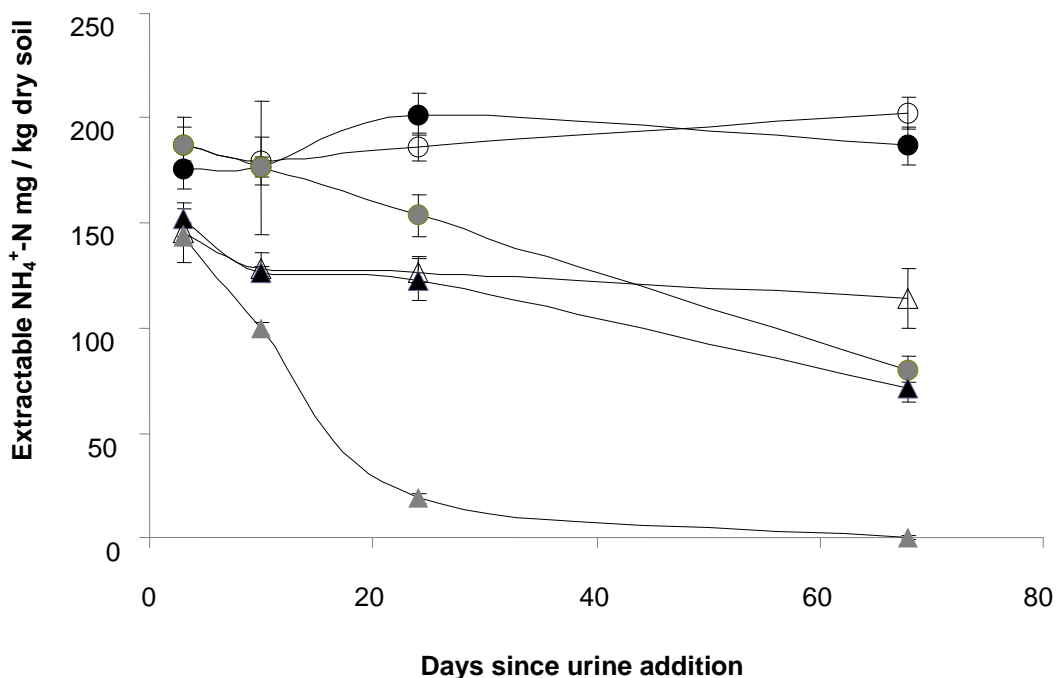


**Figure 6.4** Change in extractable  $\text{NH}_4^+$ -N (mean core concentrations) over time (relative to control) following urine application. Error bars 95% confidence interval ( $\circ$  Dannevirke,  $\Delta$  Manawatu, no fill is DCD, Black is PDCD and grey is no DCD).

The effectiveness of the DCD treatments are expressed in terms of % inhibition ( $100 - (U/U_{max}) * 100$ ) for the whole cores and at individual depths based on the data presented in Table 6.2.

In terms of overall inhibitory effect over the 68 days both DCD and PDCD produced total inhibition of ammonium oxidation in the Dannevirke soil. Whereas in the Manawatu soil the effectiveness of both forms of DCD was less, Table 6.3.

The difference between the forms became more pronounced in the Manawatu soil following 28 days of incubation with urine. This is unexpected, as the soil DCD levels in the Manawatu soil did not reach a maximum until day 68 for the PDCD.

**Table 6.3** % Inhibition of nitrification in total soil cores over 68 days of incubation

<i>Treatments</i>	<i>Dannevirke</i>	<i>Manawatu</i>
DCD	100	93.3
PDCD	100	80.8

The decreases in  $\text{NH}_4^+$ -N concentrations were mirrored in the increases in  $\text{NO}_3^-$ -N concentrations. The PDCD and DCD treatments produced no significant concentrations of  $\text{NO}_3^-$ -N above the control in the Dannevirke loam, however, significant  $\text{NO}_3^-$ -N concentrations were present for both treatments in the Manawatu soil cores (Figure 6.5).

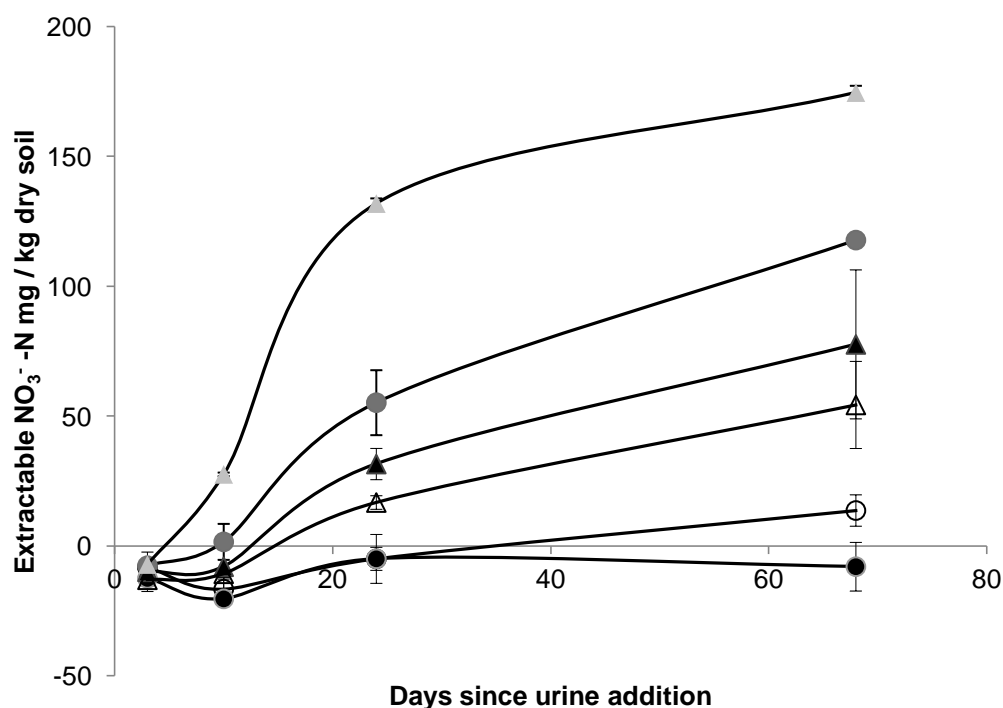


**Figure 6.5** Change in extractable  $\text{NO}_3^-$ -N (mean core concentration) over time (relative to control) following urine application. Error bars 95% confidence interval (○ Dannevirke △ Manawatu, no fill is DCD, Black is PDCD and grey is no DCD).

### 6.3.4 Nitrification with depth

In the Dannevirke soil cores the urine application resulted in an uneven vertical distribution of  $\text{NH}_4^+$ -N in the soil with the highest concentrations ( $> 1100 \text{ mg NH}_4^+$ -N  $\text{kg}^{-1}$  dry soil) found in the upper 1.4 cm. The soil  $\text{NH}_4^+$ -N was then redistributed and oxidised in the soil columns over the following 68 days by the combined effects of diffusion and nitrification (Figure 6.6 and 6.7). The diffusion processes are most clearly seen in the DCD treated Dannevirke soil cores (Figure 6.6), with  $\text{NH}_4^+$ -N concentrations in soil depths greater than 14mm increasing over time and the reduction in  $\text{NH}_4^+$ -N concentrations from soil in the upper layers.

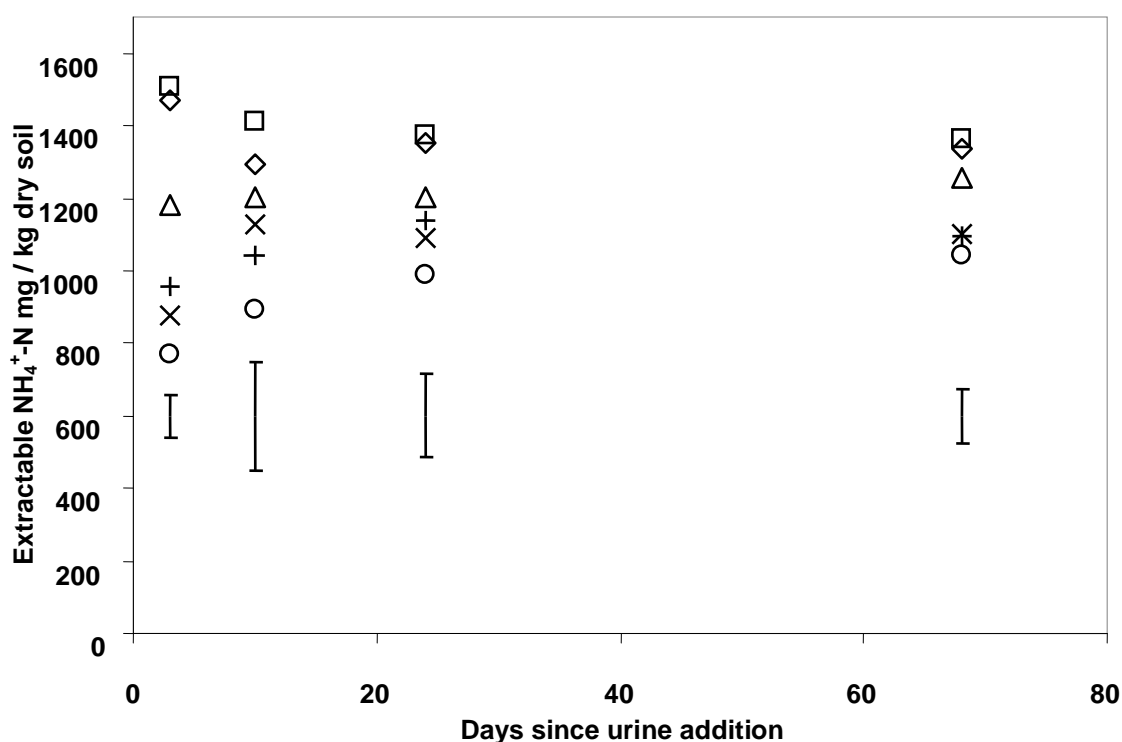


**Figure 6.6** The change with time of extractable  $\text{NH}_4^+$ -N concentrations in Dannevirke soil treated with DCD and dairy urine (□ 0-0.2 cm, ◇ 0.2-0.6 cm, △ 0.6-1.4 cm, × 1.4-2.5 cm, + 2.5-3.5 cm and ○ 3.5-4.5 cm depths; vertical error bars LSD (P=0.05)).

In the Dannevirke cores treated with PDCD the patterns of  $\text{NH}_4^+$ -N change with time are similar to those discussed for DCD treated soil. The difference is that evidence of

the movement of  $\text{NH}_4^+$ -N is less clear at depths below 1.4 cm. The soil depths <1.4 cm had initial DCD concentration that were  $> 10\text{mg DCD kg}^{-1}$  dry soil, providing full nitrification inhibition. Whereas with increasing depth full inhibition of nitrification (Figure 5.8) would not be complete until DCD movement from the granule had raised DCD concentrations. Initial lack of inhibition probably accounts for the initial drop in soil  $\text{NH}_4^+$ -N in the soil depths  $>1.4$  cm between day 3 and 10. Then either  $\text{NH}_4^+$  ions diffuse to this layer or DCD blocks nitrification causing  $\text{NH}_4^+$  ions to accumulate in these layers over the following 58 day period.

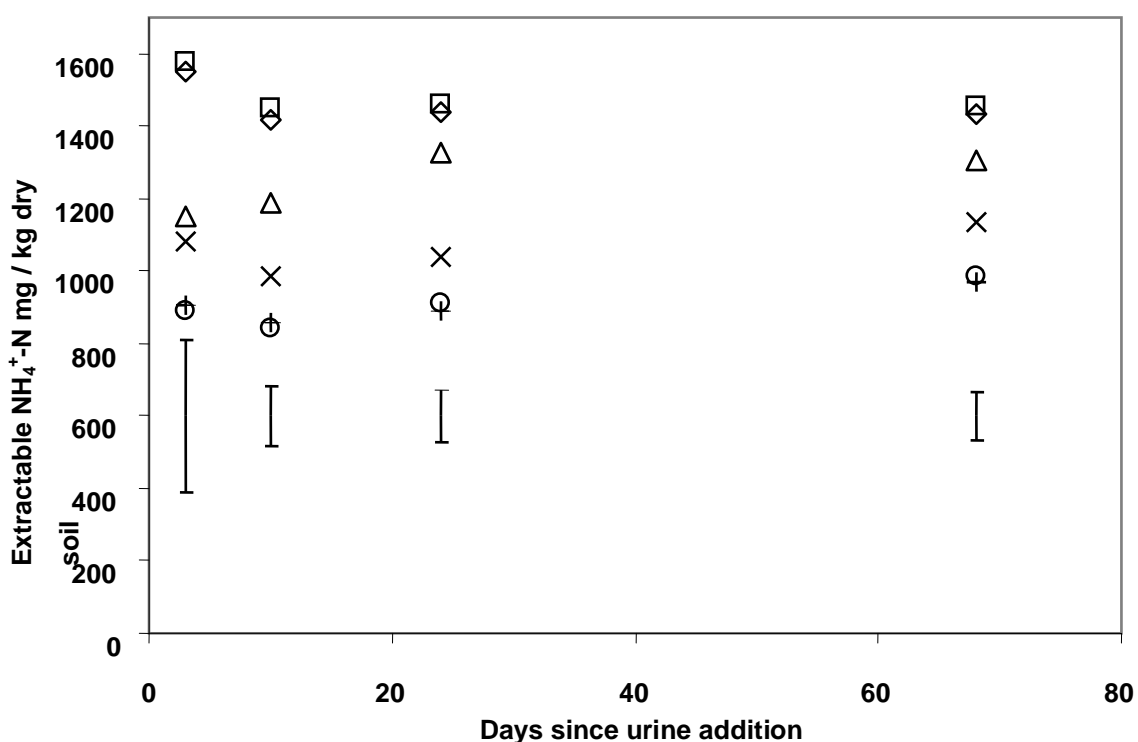


**Figure 6.7** The change with time of extractable  $\text{NH}_4^+$ -N concentrations in Dannevirke soil treated with PDCD and dairy urine (◇ 0-0.2 cm, □ 0.2-0.6 cm, △ 0.6-1.4 cm, × 1.4-2.5 cm, + 2.5-3.5 cm and ○ 3.5-4.5 cm depths; Vertical error bars LSD (P=0.05)).

In the Manawatu soil cores the initial distribution of  $\text{NH}_4^+$ -N was more uniform (Figures 6.8 compared to Figure 6.6) than in the Dannevirke soil due to the lower water

holding capacity. This resulted in urine application moving through most of the Manawatu soil core.

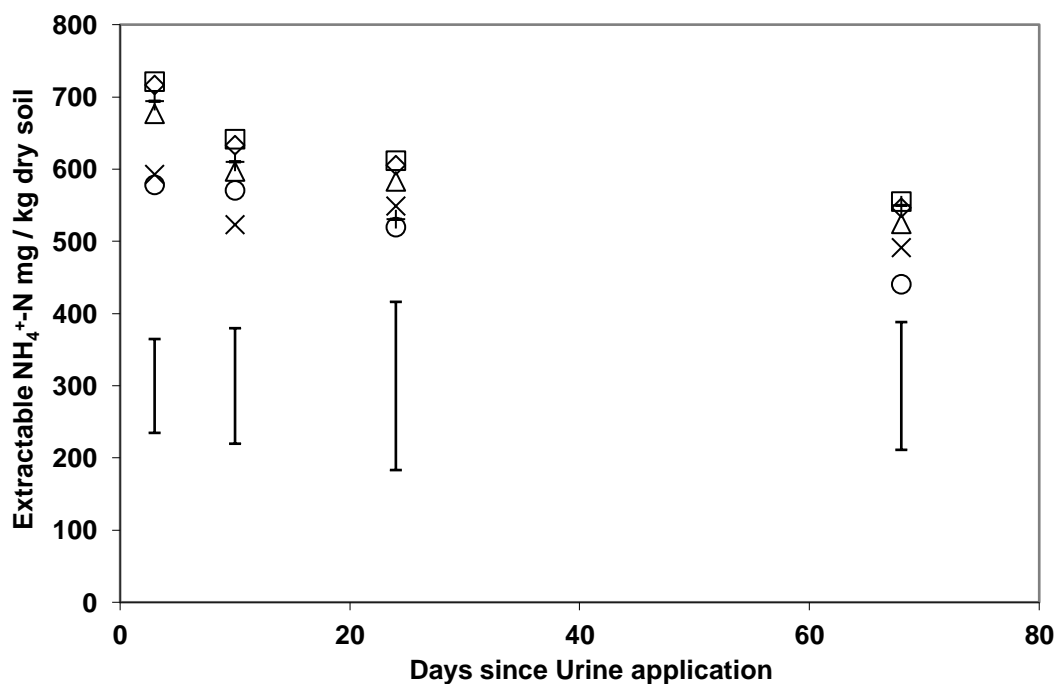


**Figure 6.8** The change with time in extractable  $\text{NH}_4^+$ -N concentrations in Manawatu soil treated with DCD (□ 0-0.2 cm, ◇ 0.2-0.6 cm, △ 0.6-1.4 cm, × 1.4-2.5 cm, + 2.5-3.5 cm and ○ 3.5-4.5 cm depths; vertical error bars LSD (P=0.05)).

There appears to be (Figures 6.8 and 6.9) no significant movement of  $\text{NH}_4^+$ -N by diffusion as the concentration gradient over the core depth is limited compared to the Dannevirke concentration profile (Figures 6.5 and 6.6). The higher nitrification activity of the Manawatu soil (Figure 6.4 and 6.5) allowed rapid conversion of the  $\text{NH}_4^+$ -N to  $\text{NO}_3^-$ -N, which resulted in only partial inhibition of nitrification over the 68 day period, 93.3% and 80.8% for the DCD and PDCD treatments, respectively. There is also no significant difference observed throughout the soil core depth in terms of nitrification due to the closeness of results and the large error term involved in the measurements.

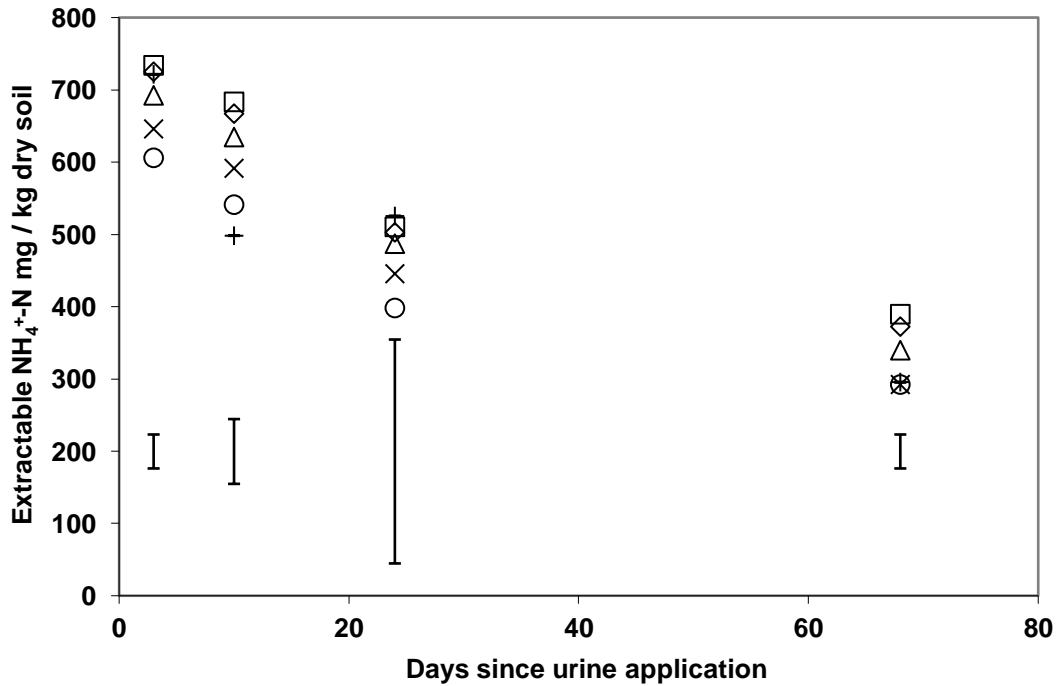


**Figure 6.9** The change with time of extractable  $\text{NH}_4^+\text{-N}$  concentrations in Manawatu soil treated with PDCD and dairy urine ( $\square$  0-0.2 cm,  $\diamond$  0.2-0.6 cm,  $\triangle$  0.6-1.4 cm,  $\times$  1.4-2.5 cm,  $+$  2.5-3.5 cm and  $\circ$  3.5-4.5 cm depths; vertical error bars LSD ( $P=0.05$ )).

### 6.3.5 Inhibitor constant for Manawatu and Dannevirke soils

The inhibitor constant for both soils was determined by plotting  $\frac{U_{max}}{U}$  against the mean inhibitor concentration  $[\text{DCD}]$  ( $\mu\text{mol g}^{-1}$ ) using data drawn from the initial incubation trial data and data kindly provided by J. Asing (per. Com.). The resulting plot (Figure 6.10) shows a linear relationship between  $\frac{U_{max}}{U}$  and  $[\text{DCD}]$  until  $\frac{U_{max}}{U}$  is greater than 5, at which point 80% inhibition of nitrification has occurred. Beyond this point the data becomes less ideal possibly due to the difficulties in measuring very low rates of nitrification. This is particularly evident in the initial DCD degradation trial data, when  $\frac{U_{max}}{U}$  vs  $[\text{DCD}]$  deviates significantly from a linear relationship above  $\frac{U_{max}}{U} > 3$ .

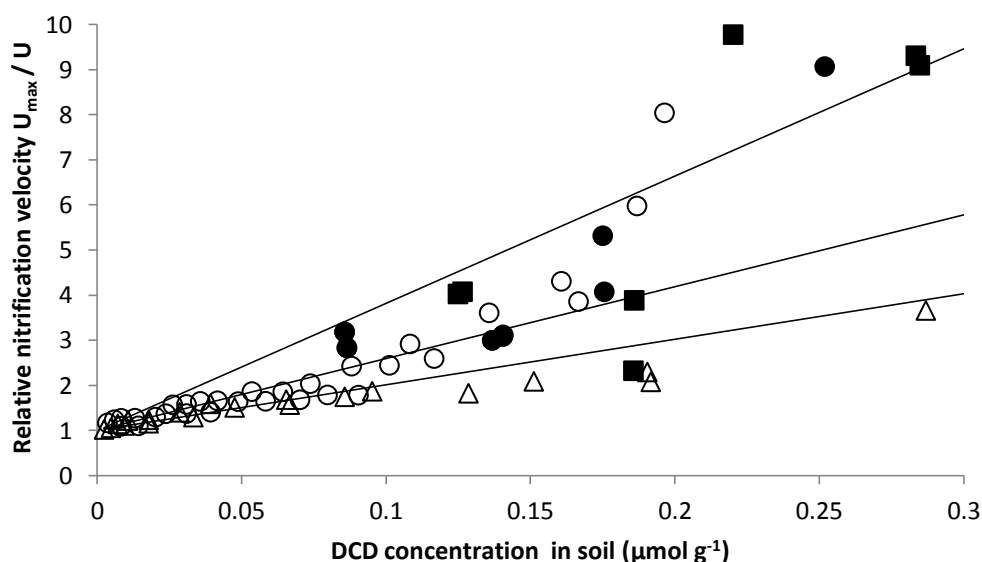


**Figure 6.10** Inhibitor effect plot of DCD concentration in soil vs. relative nitrification velocity in Manawatu soils ( $\Delta$  silt loam and  $\circ$  fine sandy loam data J. Asing ) and initial DCD degradation incubation trials ( $\bullet$  Manawatu and  $\blacksquare$  Dannevirke soils)

The inhibitor constant  $K$  was obtained for each soil from linear regression of the data, using relative velocity values of  $< 5$  and an intercept of 1 (Table 6.4).

**Table 6.4** Inhibitor response constant ( $K$ ) for Manawatu and Dannevirke soils and Iowa soils, Harps, Webster and Storden (McCarty and Bremner 1989)

Soil Description	$K \mu\text{mol g}^{-1} \text{dry soil}$	$R^2$
Manawatu		
Fine sandy loam*	0.0627	0.89
Silt loam*	0.0990	0.87
Trial soil (Fine sandy loam)	0.0350	0.70
Dannevirke Coarse granular soil	Undefined due to variable low nitrification rate	
Iowa soils**		
Harps**	0.0962	
Webster**	0.0478	
Storden**	0.0230	

(\* ) from data provided by J. Asing, Massey University (\*\* ) from published data McCarty and Bremner (1989).

The inhibitor constants ( $K$ ) are used in the modelling simulation (Section 6.4) and fall into a similar range as calculated from published data (e.g. McCarty and Bremner, 1989).

The results show that for a particular soil-microbiological system a distinct level of DCD will be required to effect nitrification inhibition greater than 90%. For example the Manawatu fine sandy loam with  $K = 0.062$  will require a minimum level of  $0.558 \mu\text{mol DCD g}^{-1}$  ( $4.6 \mu\text{gDCD g}^{-1}$ ), whereas a more sensitive soil may require very little DCD. For  $K = 0.026$ , the level is  $0.234 \mu\text{mol DCD g}^{-1}$  ( $2.0 \mu\text{gDCD g}^{-1}$ ). To complicate this issue the base nitrification rate for soils also varies as seen in Table 6.2, thus to achieve an overall reduction in nitrate accumulation in soil with both high  $K$  and  $U_{max}$  values is difficult as observed with the Manawatu soils (Table 6.3 and Figure 6.5)

### **6.3.6 Soil pH profiles and electrical conductivity**

The addition of urine to the two soils resulted in an initial increase in soil pH (measured by water extraction at 1:2 ratio w/v) from the control values  $5.13 \pm 0.06$  and  $5.68 \pm 0.03$  to an average over the profile at day 7 of  $7.0 \pm 0.4$  and  $7.6 \pm 0.3$  for the Dannevirke and Manawatu soils, respectively. The distribution of pH throughout the cores (Figures 6.11 and 6.12) reveals the Manawatu soil to be more uniformly affected while the Dannevirke was predominantly affected in the upper 2.5 cm. In all cases the pH rise did not exceed pH 9 which may result in inhibition of bacteria.

The soil electrical conductivity measured on water extracts (extraction ratio 1:2 w/v) showed a rise in conductivity from 0.5 mS (1bar) to between 1.1 to 1.8 mS (2.4 to 3.9 bar) for the inhibitor treatments and up to 2.5 mS (5.4 bar) for the urine only. This increase in ionic strength (electrical conductivity) of the soil and increase in soil water potential ( $\Psi = 0.367 \times (\text{mS} \times 6)$ ) is expected to have limited effects on soil micro-biological activity reducing soil respiration and N mineralisation by 6 to 12% (Sommers et al. 1981).

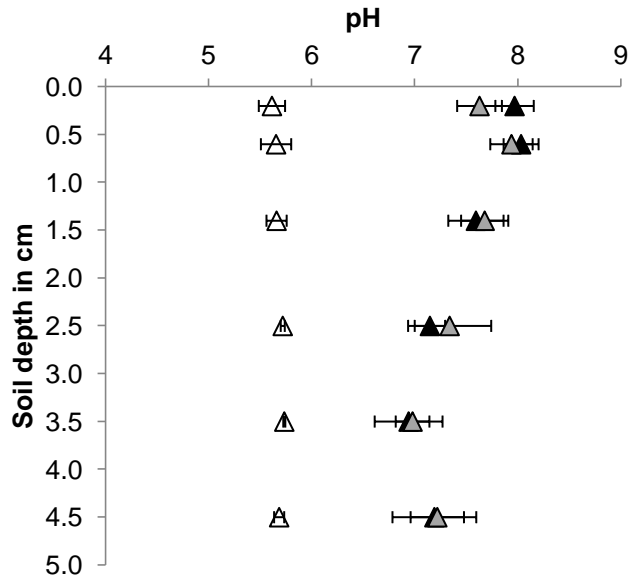


**Figure 6.11** Soil core pH profile Manawatu soil 7 days following urine addition, ▲ PDCD, ▲ DCD and Δ control with no urine.

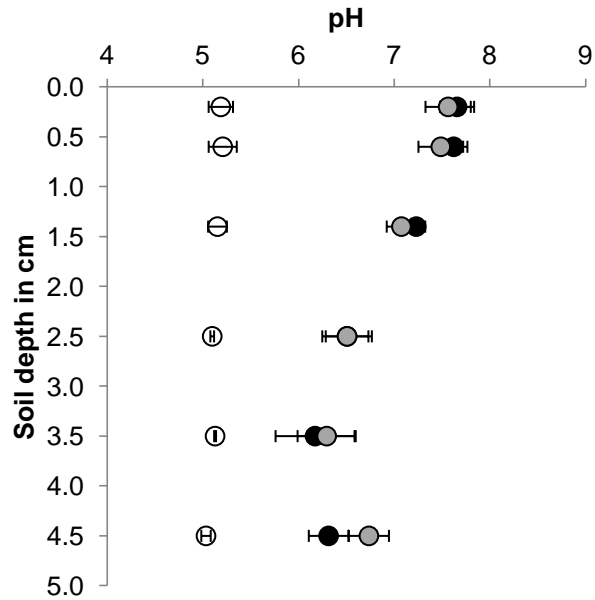


**Figure 6.12** Soil core pH profile of Dannevirke soil 7 days following urine addition, ● PDCD, ● DCD and ○ is the control with no urine.

The range of these results suggest that the inhibition of DCD degradation following urine addition is not due to either increased pH or salinity but due to another factor not as yet revealed.

#### **6.4 Modelling urine movement and conversion**

The model (Appendix 3) was applied to the DCD treated cores using the initial urine affected depth of 3 and 4.5 cm for the Dannevirke and Manawatu soils respectively, for an application of 600 kg N ha<sup>-1</sup> as urine. The urine is then allowed to diffuse and adsorb as urea into the lower depths of the core while the total quantity of potential NH<sub>4</sub><sup>+</sup>-N is reduced by the loss via volatilisation of 25 and 35% for the Dannevirke and Manawatu soils, respectively. Following the 3 day period of urea diffusion and sorption, the remaining urine N is treated as NH<sub>4</sub><sup>+</sup>-N, which diffuses but is strongly adsorbed (Table 6.1) and is nitrified at a rate determined by depth (Table 6.2) and the inhibitor constant of the soil (Table 6.4).

The modelled distribution of urine derived NH<sub>4</sub><sup>+</sup>-N in both soil types produced good correlations between the measured quantities of NH<sub>4</sub><sup>+</sup>-N in individual soil sections, (Figure 6.13 and 6.14) with R<sup>2</sup> values of 0.8 and 0.7 for the Manawatu and Dannevirke soils, respectively. The data points for the DCD treated Manawatu silt loam cores from the sampling on day 26 have been excluded from the correlation due to high variability in the samples which cannot be explained. The main limitation in the model is the assumed uniform initial distribution of urine N within the soil profile, which is reflected in the difference in R<sup>2</sup> values between the two soils. The uniform distribution of urine N in the Manawatu soil (Figures 6.8 and 6.9) showed a higher correlation between the model and measured results than the no-uniform urine N distribution of the Dannevirke soil (Figures 6.6 and 6.7).

For the model to be future developed for field application several additional modules are required; a urine distribution module which takes into account by pass flow and pooling of urine, a daily water balance and drainage module, and a daily or hourly temperature module to correctly calculate DCD degradation and nitrification rates.

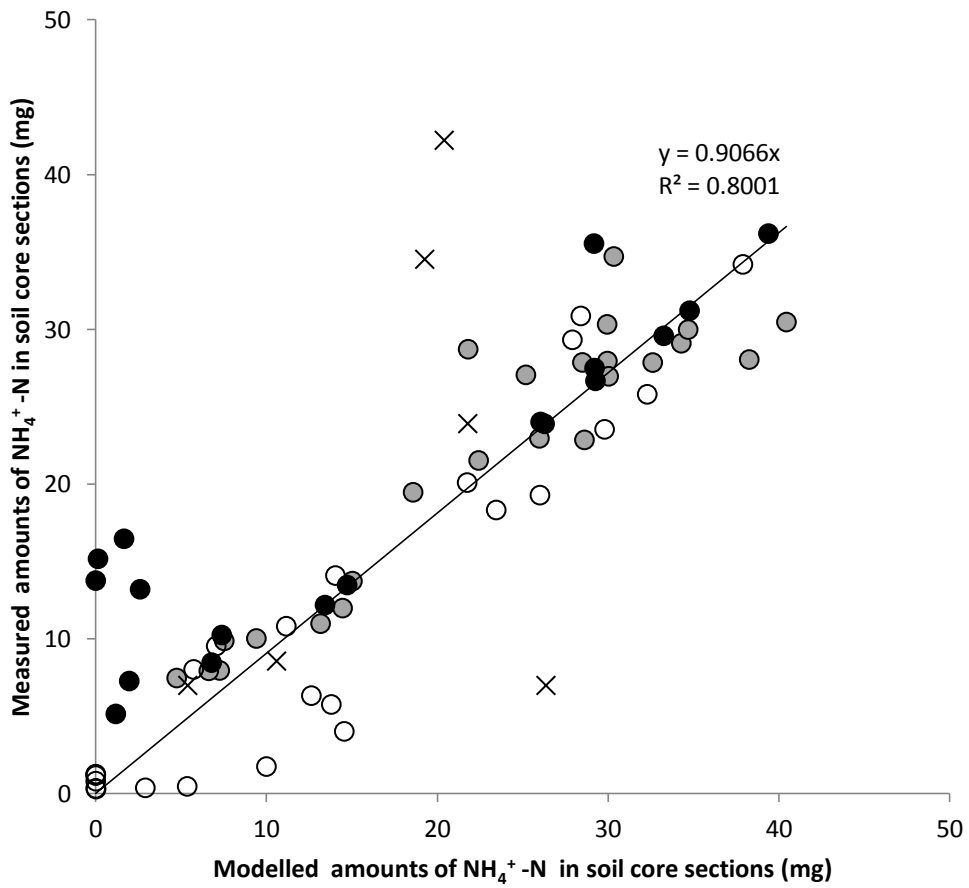


**Figure 6.13** Correlation plots of modelled and measured amounts of soil NH<sub>4</sub><sup>+</sup>-N in soil sections for Manawatu soil cores treated with dairy urine over 68 day (● soil + DCD, ● soil + PDCD, ○ soil alone, × excluded data; Modelling parameters Tables 6.1, 6.2 and 6.4 and  $K = 0.035$ ).

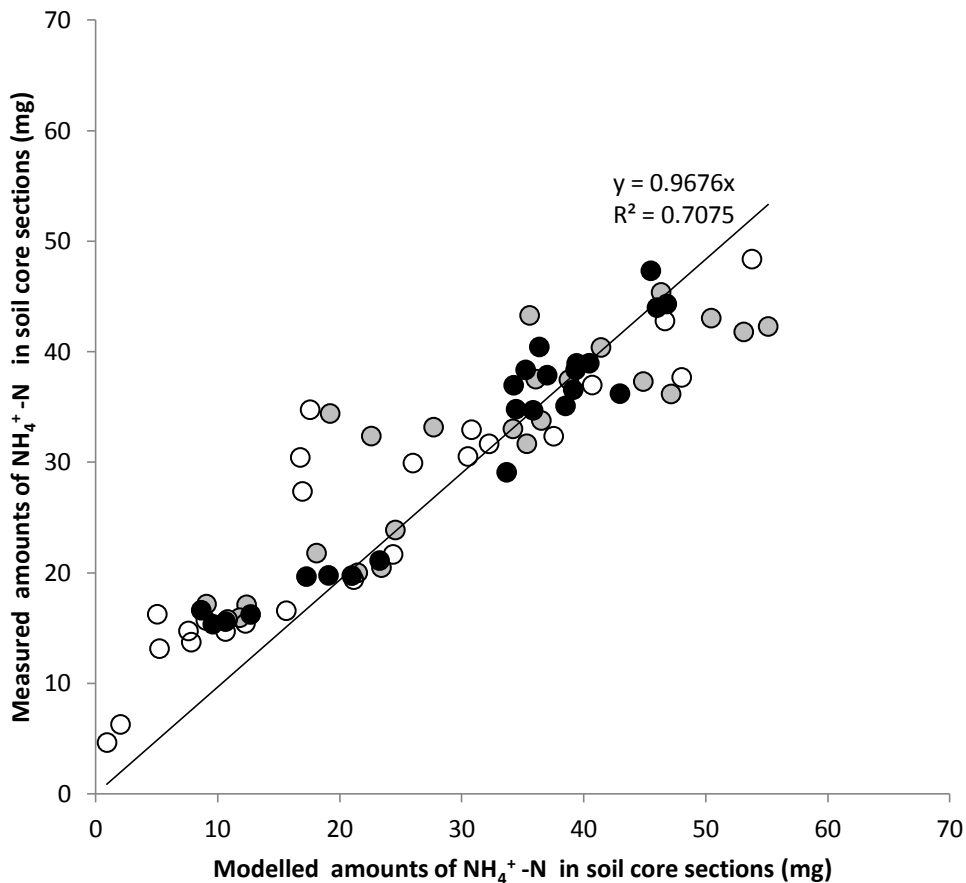


**Figure 6.14** Correlation plots of modelled and measured amounts of soil  $\text{NH}_4^+$  -N in soil sections for Dannevirke soil cores treated with dairy urine over 65 days (● soil + DCD, ● soil + PDCD and ○ soil alone; Modelling parameters Tables 6.1, 6.2 and 6.4 and  $K = 0$ ).

## 6.5 Conclusion

The application of DCD in the coated (PDCD) and uncoated (DCD) forms produced significant reductions in nitrification in both soil types. The PDCD effectiveness was however limited in soils with high nitrifying activity and higher  $K$  values  $> 0.06$  such as the Manawatu soil. The low water holding capacity of the Manawatu soil also increased the urine N penetration depth resulting in poor initial association of DCD released from the PDCD and the urine N. The PDCD was effective in the Dannevirke soil due to a

very low  $K$  value making any level of DCD effective in inhibiting nitrification. The high water holding capacity of the Dannevirke soil also limited the penetration of urine N to the upper soil profile, allowing good proximity of DCD and urine N.

The addition of the inhibitor constant  $K$  to the modelling system allowed accurate modelling of the fate of urine applied N to be carried out for both DCD and PDCD treatment soils. The value of  $K$ , is only estimated by best fit of data to modelled results and a more accurate measurement of this factor is required in the future to complete the development of the model.

## Chapter 7

### Conclusions and recommendations for future work

---

#### 7.1 Conclusions

The review of literature revealed the potential to produce low cost reactive layer polyurethane coated urea and nitrification inhibitor DCD to assist in the mitigation of nitrate leaching and nitrous oxide emissions in pastoral farming. This requires furthering of current scientific understanding in terms of:

1. The release mechanism of the reactive layer polyurethane coated urea (UCU) and nitrification inhibitor (PDCD) to assist in the explanation of observed release of urea and DCD in field and repacked core studies, respectively.
2. In the development of the reactive layer polyurethane coated nitrification inhibitor, PDCD, for the treatment of potential urine affected soils. The understanding of the movement of both the inhibitor DCD from the surface application of PDCD and urine was required. In addition to the interactions of the inhibitor, soil and urine N, which were measured and characterised in the modelling of the fate of urine N within the soil profile.

##### *7.1.1 Mechanism of release from UCU*

A new mechanism of urea release from urethane coated granules was modelled from an assumption that the coating was water repellent and micro-porous. Under these conditions only water vapour diffusion through gas filled pores may enter the coated granule and dissolve the internal core. The increase in volume within the coated granule then allows solution to be expelled from the granule into the surrounding soil. The rate of urea and DCD release, was found to be significantly affected by the coating thickness ( $l_o$ ) implying the dependence of water vapour permeability ( $W'$ ) on coating thickness. The relationship between  $W'$  and  $l_o$  was experimentally estimated and modelled as an exponential decay to a minimum value (Equation 2.37). The distribution of coating thicknesses within the population of granules was determined gravimetrically and the model applied. This showed that these two factors played a

significant role in the release characteristics of the coated urea, as a granule with coatings less than 0.0026 cm released rapidly while above this value granules released slowly. The addition of palmitic acid to the coating was found to increase the initial release rate, interpreted as an increase in minimum water vapour permeability ( $W'_{min}$ ) indicating an increase in porosity of the coating. In addition to the  $W'(l_o)$  relationship, it was expected that the change in volume of the coated granule, due to morphological changes would have resulted in an increased delay in urea release, this was not observed in the release data, possibly due to the high tensile strength and low elasticity of the coating. In water extraction trials it was found the model, without a release lag time, fitted the observed release of urea with an  $R^2$  0.93. The main deviations of observations from the modelled data occurred within the first few days, when the model had underestimated the urea release.

### ***7.1.2 Field trials of modified RLP coated urea 5UCU and 7UCU***

It was concluded from the field trials of 5UCU and 7UCU in winter applications to pasture that a single application of 150 kgN could be safely applied without risk of nitrate leaching and decreased N use efficiency. Pasture herbage N content and DM production for the 5UCU and 7UCU treatments were used to model urine N returns, that were 5 to 10 kgN ha<sup>-1</sup> less, over the 150 day trial, than those predicted for un-coated urea fertilised treatment.

At the end of the trial significant quantities of urea (39 and 52% of applied N for 5UCU and 7UCU, respectively) remained unreleased or unaccounted for. The fate of this urea was shown to be related to the soil moisture with no observed release of urea at 7% moisture content, while at 18.3% release of urea was observed in both 5UCU and 7UCU. These results indicate that the unreleased urea is likely to become available in the subsequent autumn, when the soil moisture increases. A longer term trial is required to investigate this hypothesis.

### ***7.1.3 Evaluation of PDCD in repacked soil core studies***

The movement of DCD from both uncoated and the coated DCD (PDCD) by diffusion showed that DCD is capable of rapidly diffused from the soil surface to effect inhibition

of nitrification. The results of the absorption isotherm showed that DCD was weakly bound by soil organic matter and degraded rapidly in non-urine affected soil. The application of urine ( $600 \text{ kgN ha}^{-1}$ ) appeared to have stalled or reduced the degradation rate of DCD. The effectiveness of DCD inhibition of nitrification was found to be related to DCD soil concentration by an inhibitor response constant (K), which varies between soils making the assessment of K important in the determination of effective DCD application levels.

The modelling of DCD movement from the surface applied PDCD showed that to achieve rapid inhibition of nitrification a mixture of uncoated DCD and PDCD was required at a ratio 2:8. This combination applied at a rate of  $26 \text{ kg DCD ha}^{-1}$  showed the potential to inhibit nitrification for up to 270 days at soil temperatures of  $20^\circ\text{C}$ , increasing the longevity of uncoated DCD at the same rate by 120 days.

The results of the repacked core studies and modelling have indicated that the combined DCD: PDCD mixture should go to field trials to confirm the modelled effects.

## **7.2 Further work**

Further work is required to extend the release rate modelling of coated products to allow accurate predictions of release based on polymer coating and granule properties. The initial 20 day period of release requires further investigation with focus on the volume change and re-equilibrium processes of release, which may result in the higher than predicted release rates. These processes may require the measurement of granule volume, internal pressure and release rate on individual coated granules using micro-sensors; possibly attached via a capillary tube allowing pressure measurements.

Under field conditions without irrigation the 5UCU and 7UCU product produced significant reductions in both direct losses of nitrate-N via leaching and estimated urine N return to pasture. This work requires to be validated under irrigation with grazing and the addition of herd urine and milk urea testing to confirm the reduction in urine return.

The initial modelling study of PDCD as a nitrification inhibitor for urine affected soils suggests that the combination of DCD and PDCD may increase the inhibition of nitrification in high temperature areas. This would require a combination of lysimeter and drainage plots to determine the infield effect of the product. The modelling also showed the significance of both the inhibitor response constant  $K$  and maximum nitrification rate on the potential of DCD to reduce nitrate accumulation in soil. This work requires further development to determine spatial variability within farm and regional areas to identify optimal areas and regions for DCD and PDCD application.

## Appendix 1 Model of release of urea from reactive layer polyurethane coated urea

The release rate model/macro for the hydraulic convection of urea from a reactive layer polyurethane extracted in water used the data from the input parameters from “Sheet1” to calculate the cumulative amount of solute released for individual coated granules in a population of 500 granules with randomised volume change, granule radii and film thickness based on the measured means and standard deviations of these factors. The resulting array is then accumulated into daily totals which are divided by the total granule weight to give a daily proportion released printed to the output field “Proportion released”, Figure A1.

	Units	Mean	S.D	Days	Proportion released
Volume Change	V/V	0.16	0.21	1	0.0254808
Granule Radii	cm	0.26	0.036	2	0.0509615
Film thickness	cm	0.0026	0.00035	3	0.0764423
Granule density	g/cc	1.26		4	0.1018748
Temperature °C	°C	20		5	0.127277
Days	d	200		6	0.1527522
				7	0.1783303
				8	0.2038513
				9	0.2285616
				10	0.2537142
				11	0.2787453
Minimum Water vapour Permeability		2.68E-08		12	0.3037059
				13	0.3276152
				14	0.3518922
				15	0.3760902
				16	0.3993048
				17	0.4221006
				18	0.4439898
				19	0.4654591
				20	0.4855935
				21	0.505234
				22	0.5239622
				23	0.5419779
				24	0.5593481

	5% MDI	7% MDI	10% MDI	20% Palmic Acid
Mean film thickness $l_0$ cm	0.0026	0.0036	0.0052	0.0027
	0.00035	0.0007	0.001	0.0005

Figure A1 Layout of input parameters and output fields for the Hydraulic convection model in Excel 2007

Sub hydrolic\_convection()

'Variables

DeltaV = Worksheets("Sheet1").Cells(4, 4)	'Input $\gamma$
sddeltaV = Worksheets("Sheet1").Cells(4, 5)	'Input $\sigma_\gamma$
gradii = Worksheets("Sheet1").Cells(5, 4)	'Input R
sdradii = Worksheets("Sheet1").Cells(5, 5)	'Input $\sigma_R$
film = Worksheets("Sheet1").Cells(6, 4)	'Input $l_o$
sdfilm = Worksheets("Sheet1").Cells(6, 5)	'Input $\sigma_{l_o}$
Temp = Worksheets("Sheet1").Cells(8, 4)	'Input Temp
densityS = Worksheets("Sheet1").Cells(7, 4)	'Input $\rho_s$
numberdays = Worksheets("Sheet1").Cells(9, 4)	'Input number of days
Wmin = Worksheets("Sheet1").Cells(14, 4)	'Input $W'_{\min}$

'Calculated saturated concentration of urea solution g/cc

$$\text{Conc} = 0.00696 * \text{Temp} + 0.45$$

' Calculation of saturated solution water activity

$$\text{molConc} = \text{Conc} * 1000 / 60$$

$$\text{be} = 1$$

$$\text{b} = -0.0608$$

$$\text{n} = 0.283$$

$$\text{a0} = 1 / (1 + 0.018 * (\text{be} - \text{b} * (\text{molConc} ^ \text{n})) * \text{molConc})$$

' Calculation Delta P in Pa

$$\text{Pwvo} = 133.32 * \text{Exp}(20.386 - (5132 / (273 + \text{Temp})))$$

$$\text{DeltaP} = (1 - \text{a0}) * \text{Pwvo}$$

Dim mass(501)

Dim Sum(500)

ReDim Cs(1 + numberdays)

ReDim Release(1 + numberdays)

ReDim amount(500 + 1, 1 + numberdays)

ReDim Cumlative(1 + numberdays)

For j = 1 To 500

10 radii = Application.WorksheetFunction.NormInv(Rnd, gradii, sdradii)

If radii < 0.1 Then GoTo 10

20 v = Application.WorksheetFunction.NormInv(Rnd, DeltaV, sddeltaV)

If v < 0.02 Then GoTo 20

```

30  fi = Application.WorksheetFunction.NormInv(Rnd, film, sdfilm)
    If fi < 0.0001 Then GoTo 30
    mass(j) = 4 / 3 * Pi * (radii ^ 3) * densityS

' Modelled water vapour permeability as a function of mean coating thickness
  W = Wmin + 0.00000405 * Exp(-2800 * fi)

' proportion released per day of original mass equation 2.15
  Constantrate = ((3 * W * DeltaP * Conc) / (radii * fi * densityS))

'Calculation of lag time T1 and the end of the constant rate period T2

  T1 = 0
  T1 = Int((v * radii * fi) / (3 * W * DeltaP))

  T2 = Int((1 - (v + 1) * Conc / densityS) / Constantrate) + T1

For t = 1 To numberdays

  Time delay
  Release(t) = 0

'Constant rate period

  If t > T1 Then Release(t) = Constantrate * Int(t - T1)

'Falling rate period

  If t > T2 Then
    Cs(T2) = Conc
    'd = t - 1
    mol = Cs(t - 1) * 1000 / 60
    If mol < 0 Then mol = 0
    be = 1
    b = -0.0608
    n = 0.283

    a = 1 / (1 + 0.018 * (be - b * (mol ^ n)) * mol)
    dC = 3 * W * Pwvo * (1 - a) * Cs(t - 1) / (radii * fi)
    Cs(t) = Cs(t - 1) - dC

    Release(t) = 1 - ((v + 1) * Cs(t - 1) / densityS)
  End If

```

```

    amount(j, t) = (Release(t) * mass(j))
Next
Next

'Output summation of daily amounts released and conversion to proportion of total
mass
  r = 200
  c = 500

  For i = 1 To r
    For K = 1 To c
      amount(K + 1, i) = amount(K + 1, i) + amount(K, i)

    Next K

  Next i
  For m = 1 To 500
    mass(m + 1) = mass(m + 1) + mass(m)
  Next

  For s = 1 To 200

  Worksheets("Sheet1").Cells(s + 2, 9) = amount(501, s) / mass(501)

  Next

End Sub

```

### A1.1 Field conditions

Under field conditions, climatic and soil data was required in addition to the granule properties; these are the volumetric water content and daily mean temperature. This data is entered into the fields in the spread sheet and used by the macro to adjust the daily release rates for climactic variations.

As T1 and T2 can no longer be simply calculated the macro/model uses an accumulative release criteria to determine when the granule soil core has dissolved. This was based on temperature and solubility of urea  $(\text{mass}(j) * (1 - ((v + 1) * \text{Conc} / \text{densityS}))$ .

	A	B	C	D	E	F	G	H	I	J	K	L	M
1													
2						Volumetric	Daily Temp	Days	Proportion				
3			Units	Mean	S.D	Moisture			released				
4		Volume Change	V/V	0.16	0.21	0.5	5.3	1	0.0051483				
5		Granule Radii	cm	0.26	0.036	0.5	5.2	2	0.0102489				
6		Film thickness	cm	0.0027	0.0005	0.5	11.9	3	0.019598				
7		Granule density	g/cc	1.26		0.5	10	4	0.0275008				
8		Temperature °C		20		0.5	9.7	5	0.0351946				
9		Days	d	200		0.5	10	6	0.0430974				
10						0.5	7.9	7	0.0496633				
11						0.438	3.6	8	0.0535029				
12						0.474	2.9	9	0.0573816				
13						0.5	3.5	10	0.0617047				
14		Minimum Water vapour Permeability		4.00E-08		0.5	8.4	11	0.0684984				
15						0.5	12.3	12	0.0780882				
16						0.5	12.5	13	0.0878429				
17						0.497333333	11.8	14	0.0969456				
18						0.492	10.8	15	0.1052257				
19						0.487333333	10.6	16	0.113253				
20						0.492666667	10.5	17	0.1212758				
21						0.487333333	7.4	18	0.1273003				
22						0.482	5.4	19	0.1322334				
23						0.477333333	6.3	20	0.1375067				
24		5% MDI	7% MDI	10% MDI	20% Palmic	0.472	6.5	21	0.1427897				
						0.466666667	8.8	22	0.1491866				

**Figure A1.1 Layout of input parameters and output fields for Hydraulic convection model with daily field data in Excel 2007**

Sub hydraulic \_convection()

'Variables

DeltaV = Worksheets("Sheet1").Cells(4, 4)	'Input $\gamma$
sddeltaV = Worksheets("Sheet1").Cells(4, 5)	'Input $\sigma_\gamma$
gradii = Worksheets("Sheet1").Cells(5, 4)	'Input R
sdradii = Worksheets("Sheet1").Cells(5, 5)	'Input $\sigma_R$
film = Worksheets("Sheet1").Cells(6, 4)	'Input $l_o$
sdfilm = Worksheets("Sheet1").Cells(6, 5)	'Input $\sigma_{l_o}$
Temp = Worksheets("Sheet1").Cells(8, 4)	'Input Temp
densityS = Worksheets("Sheet1").Cells(7, 4)	'Input $\rho_s$
numberdays = Worksheets("Sheet1").Cells(9, 4)	'Input number of days
Wmin = Worksheets("Sheet1").Cells(14, 4)	'Input $W'_{min}$

' Define arrays

Dim mass(501)

Dim Sum(500)

ReDim Cs(1 + numberdays)

ReDim Release(1 + numberdays)

ReDim Amount(500 + 1, 1 + numberdays)

ReDim RateM(500 + 1, 1 + numberdays)

ReDim Cumlative(1 + numberdays)

ReDim DailyTemp(1 + numberdays)

ReDim SW(1 + numberdays)

' Import daily temperature and soil water data from sheet

For H = 1 To numberdays

DailyTemp(H) = Worksheets("Sheet1").Cells(H + 2, 7)

SW(H) = Worksheets("Sheet1").Cells(H + 2, 6)

Next

' Define random granule

For j = 1 To 500

10 radii = Application.WorksheetFunction.NormInv(Rnd, gradii, sdradii)

If radii < 0.1 Then GoTo 10

20 v = Application.WorksheetFunction.NormInv(Rnd, DeltaV, sddeltaV)

If v < 0.02 Then GoTo 20

30 fi = Application.WorksheetFunction.NormInv(Rnd, film, sdfilm)

```

If fi < 0.0001 Then GoTo 30
mass(j) = 4 / 3 * Pi * (radii ^ 3) * densityS
' Modelled water vapour permeability as a function of mean coating thickness

```

```

'Begin time step

```

```

For t = 1 To numberdays
  lll = Amount(j, t - 1)
  w = (Wmin + 0.00000405 * Exp(-2800 * fi))
  If t = 1 Then g = 0

```

```

'Constant rate period
  If lll < (mass(j) * (1 - ((v + 1) * Conc / densityS))) Then

```

```

'Calculated saturated concentration of urea solution g/cc
  Conc = 0.00696 * DailyTemp(t) + 0.45

```

```

' Calculation of saturated solution water activity
  molConc = Conc * 1000 / 60
  be = 1
  b = -0.0608
  n = 0.283
  a0 = 1 / (1 + 0.018 * (be - b * (molConc ^ n)) * molConc)

```

```

'Calculation Delta P in Pa
  Pwvo = 133.32 * Exp(20.386 - (5132 / (273 + DailyTemp(t))))
  DeltaP = (1 - a0) * Pwvo

```

```

  RateM(j, t) = ((3 * w * SW(t) * DeltaP * Conc) / (radii * fi * densityS)) '
  proportion released per day of original mass equation 2.15

```

```

End If

```

```

'Falling rate period

```

```

  If lll > (mass(j) * (1 - ((v + 1) * Conc / densityS))) Then

```

```

    g = g + 1
    T2 = t - g

```

```

'Calculation Delta P in Pa
  Pwvo = 133.32 * Exp(20.386 - (5132 / (273 + DailyTemp(t))))
  Cs(T2) = Conc

```

```

mol = Cs(t - 1) * 1000 / 60
If mol < 0 Then mol = 0
be = 1
b = -0.0608
n = 0.283

a = 1 / (1 + 0.018 * (be - b * (mol ^ n)) * mol)
DeltaP = (1 - a) * Pwvo
dC = 3 * w * SW(t) * Pwvo * (1 - a) * Cs(t - 1) / (radii * fi)
Cs(t) = Cs(t - 1) - dC
RateM(j, t) = ((3 * w * SW(t) * (v + 1) * DeltaP * Cs(t - 1)) / (radii * fi *
densityS))

Release(t) = RateM(j, t) + Release(t - 1)
End If
Release(t) = RateM(j, t) + Release(t - 1)
Amount(j, t) = (Release(t) * mass(j))

Next

Next
r = 200
c = 500

For i = 1 To r
For K = 1 To c

Amount(K + 1, i) = Amount(K + 1, i) + Amount(K, i)

Next K

Next i
For m = 1 To 500
mass(m + 1) = mass(m + 1) + mass(m)
Next

For s = 1 To 200

Worksheets("Sheet1").Cells(s + 2, 9) = Amount(501, s) / mass(501)

Next

End Sub

```

## Appendix 2 Model of diffusion, sorption and degradation of DCD in soil

The model as discussed in Chapter 5 is written as a button operated macro “Diffusion” positioned below the “Input Parameters” column D. Following the model calculations the estimated DCD concentration ( $\mu\text{g g}^{-1}$  dry soil) in each soil layer is printed back to the worksheet column H onwards. In this model both fast release and slow release DCD can be calculated simultaneously by the proportioning the of “Application rate” in  $\text{kgDCD ha}^{-1}$  as fast and slow release forms.

	A	B	C	D	E	F	G	H	I	J	K
1				Input Parameters			Soil depth cm				
2			Portion fast release DCD	0.2			0.2	64.46379122	38.23749407	38.61681439	25.59034381
3							0.3	63.34101283	37.68565047	38.04803357	25.02842954
4							0.4	62.17201495	37.12480237	37.45149829	24.47985144
5			Soil water holding capacity v/v	0.271			0.5	60.95620077	36.55494924	36.84889985	23.94421294
6			Distance between model layers dx cm	0.1			0.6	59.89354821	35.9761092	36.23324929	23.42112924
7			Diffusivity of DCD in water $\text{cm}^2 \text{d}^{-1}$	1.00E-05			0.7	58.38459457	35.38832185	35.60501478	22.91022702
8			Time step dt	s	100		0.8	57.03041828	34.79165178	34.96487502	22.41114432
9			Run time d	300	259200	in seconds	0.9	55.63280427	34.18619251	34.31369922	21.92353025
10			Application rate	kgDCD/ha	25		1	54.19323496	33.57207074	33.65252415	21.44704474
11			Moisture deficit	v/v	0		1.1	52.71483761	32.94945066	32.98252906	20.98135831
12			Depth	cm	15		1.2	51.20035803	32.318538	32.30500901	20.52615201
13							1.3	49.65311943	31.67958373	31.62134749	20.08111699
14							1.4	48.07678061	31.0328872	30.93298896	19.64595405
15			Freundlich coefficient a	mol/cc	0.01407		1.5	46.47529219	30.37879861	30.24141198	19.22037413
16			Freundlich coefficient b		0.8325		1.6	44.85285127	29.71772057	29.54810361	18.80409742
17			SOIL BULK DENSITY	$\text{g cm}^{-3}$	1.16		1.7	43.21385501	29.05010898	28.85453556	18.39685344
18							1.8	41.56285381	28.3764729	28.1621426	17.99838083
19			Degradation rate constant	$\text{d}^{-1}$	0.023		1.9	39.90450441	27.69737363	27.47230355	17.60842699
20			Urine application day		28		2	38.24352357	27.01342294	26.78632507	17.22674788
21			Second degradation rate	$\text{d}^{-1}$	0.012		2.1	36.5846427	26.32528063	26.10542846	16.85310808
22							2.2	34.93256398	25.63365132	25.43073947	16.48728022
23							2.3	33.29191835	24.93928069	24.76328107	16.12904501
24							2.4	31.66722576	24.24295126	24.10398898	15.77819085
25							2.5	30.0628581	23.54547774	23.45368987	15.43451392
26							2.6	28.48300498	22.84770203	22.81290194	15.09781753
27							2.7	26.93164283	22.150488	22.18243744	14.76791233
28			Step wise release	rate %/day	portion released	Cumulative	2.8	25.41250729	21.45471621	21.56270701	14.44461588
29			0-7	0.92%	6%	6%	2.9	23.92906924	20.76127836	20.95410535	14.12775256
30			7-15	0.87%	7%	13%	3	22.48451454	20.07107192	20.35693801	13.81715334
31			15-22	0.27%	2%	15%	3.1	21.08127242	19.38499463	19.77142886	13.51265556
32			22-34	0.43%	5%	20%	3.2	19.72327777	18.70393927	19.19772806	13.21410272
33			34-41	0.91%	6%	27%	3.3	18.41141205	18.02878842	18.63592019	12.9213443
34			41-55	1.00%	14%	41%	3.4	17.1480479	17.36040948	18.0803239	12.63423566
35			55-99	0.44%	19%	60%	3.5	15.92472290	16.69064900	17.54504222	12.35282571

Figure A2. Worksheet layout for DCD release, diffusion, adsorption and degradation in soil at 20°C.

Sub CommandButton1\_Click()  
'Input vareable data from sheetsheet

Fast = Worksheets("calculation sheet").Range("D2")

MaxSW = Worksheets("calculation sheet").Range("D5")

DXL = Worksheets("calculation sheet").Range("D6")

De = Worksheets("calculation sheet").Range("d7")

dt = Worksheets("calculation sheet").Range("d8")

RateDCD = Worksheets("calculation sheet").Range("D10")

SWD = Worksheets("calculation sheet").Range("D11") ' Soil water deficit in V/V

SDepth = Worksheets("calculation sheet").Range("D12") ' Soil depth of total column

f = Worksheets("calculation sheet").Range("d13")

a = Worksheets("calculation sheet").Range("d15")

b = Worksheets("calculation sheet").Range("d16")

DENSITY = Worksheets("calculation sheet").Range("d17")

degrate = Worksheets("calculation sheet").Range("D19")

UrinationD = Worksheets("calculation sheet").Range("D21")

degrate2 = Worksheets("calculation sheet").Range("D22")

ReleaseR = Worksheets("calculation sheet").Range("D28")

ReleaseR2 = Worksheets("calculation sheet").Range("D29")

ReleaseR3 = Worksheets("calculation sheet").Range("D30")

ReleaseR4 = Worksheets("calculation sheet").Range("D31")

ReleaseR5 = Worksheets("calculation sheet").Range("D32")

ReleaseR6 = Worksheets("calculation sheet").Range("D33")

ReleaseR7 = Worksheets("calculation sheet").Range("D34")

rps = (Int(SDepth / DXL))

' Number of layers

' Array Definitions

Dim Newt(10)

ReDim C(1 + rps)

ReDim Cs(1 + rps)

ReDim rg(1 + rps)

ReDim Flux(1 + rps)

ReDim SW(1 + rps)

ReDim output(1, 1 + RSP)

ReDim adsorp(1 + rps)

' Global constants

molDCD = RateDCD \* 10 ^ (-5) / 84

SW(1) = MaxSW - SWD

$$Cs(1) = \text{molDCD} * \text{Fast} / (\text{SW}(1) * \text{DXL})$$

'DCD Diffusion

Time step

For Tstep = 1 To z

' Granule flux defined by a series of constant rate steps

If Tstep < (7 \* 86400 / dt) Then releaserate = ReleaseR

If Tstep > (7 \* 86400 / dt) Then releaserate = ReleaseR2

If Tstep > (15 \* 86400 / dt) Then releaserate = ReleaseR3

If Tstep > (22 \* 86400 / dt) Then releaserate = ReleaseR4

If Tstep > (34 \* 86400 / dt) Then releaserate = ReleaseR5

If Tstep > (41 \* 86400 / dt) Then releaserate = ReleaseR6

If Tstep > (55 \* 86400 / dt) And Tflux < molDCD \* (1 - Fast) Then releaserate = ReleaseR7

If Tstep > (55 \* 86400 / dt) And Tflux > molDCD \* (1 - Fast) Then releaserate = 0

$$\text{Flux}(0) = ((\text{releaserate} / 86400) * \text{dt} * \text{molDCD} * (1 - \text{Fast}))$$

$$\text{Tflux} = \text{Tflux} + \text{Flux}(0)$$

'Layer step

For LL = 1 To rps

' Flux between layers

$$\text{Flux}(\text{LL}) = \text{De} * f * \text{SW}(1) * \text{dt} * (\text{C}(\text{LL}) - \text{C}(\text{LL} + 1)) / \text{DXL}$$

'Zero flux at base

$$\text{If } \text{LL} = (\text{rps} - 1) \text{ Then } \text{Flux}(\text{LL}) = 0$$

'Concentration of DCD mol/cc(LIQUID)

$$\text{Cs}(\text{LL}) = \text{Cs}(\text{LL}) + ((\text{Flux}(\text{LL} - 1) - \text{Flux}(\text{LL})) / (\text{DXL}))$$

'Newton Raphson calculation of

$$\text{Newt}(1) = \text{Cs}(\text{LL}) / 10000000$$

If Cs(LL) < 1E-50 Then GoTo 100

For x = 1 To 5

$$\text{Newt}(x + 1) = \text{Newt}(x) - ((a * \text{Newt}(x) ^ b + \text{SW}(1) * \text{Newt}(x) - \text{Cs}(\text{LL})) / (a * b * \text{Newt}(x) ^ (b - 1) + \text{SW}(1)))$$

$$\text{C}(\text{LL}) = \text{Newt}(5)$$

Next

Degradation of DCD in soil

```
100 If Tstep < (UrinationD * 86400 / dt) Then degrate = degrade 'Initial rate
    If Tstep > (UrinationD * 86400 / dt) Then degrate = 0 'Stall following urination
    If Tstep > (41 * 86400 / dt) Then degrate = degrate2 ' Post urination rate
```

```
Cs(LL) = Cs(LL) * Exp(-degrate * dt / 86400)
```

'Output of soil profile data at 15,30,60,120,240 and 300 days

Next

```
If Tstep = Int(15 * 86400 / dt) Then
    For J = 0 To (1 + rps)
```

```
Worksheets("calculation sheet").Cells(J + 1, 8) = Cs(J) * 84 * 10 ^ 6
```

```
Worksheets("calculation sheet").Cells(1, 8) = Tflux * 84 * 10 ^ 6
```

Next

End If

```
If Tstep = Int(30 * 86400 / dt) Then
    For J = 0 To (1 + rps)
```

```
Worksheets("calculation sheet").Cells(J + 1, 9) = Cs(J) * 84 * 10 ^ 6
```

```
Worksheets("calculation sheet").Cells(1, 9) = Tflux * 84 * 10 ^ 6
```

Next

End If

```
If Tstep = Int(60 * 86400 / dt) Then
    For J = 0 To (1 + rps)
```

```
Worksheets("calculation sheet").Cells(J + 1, 10) = Cs(J) * 84 * 10 ^ 6
```

```
Worksheets("calculation sheet").Cells(1, 10) = Tflux * 84 * 10 ^ 6
```

Next

End If

```
If Tstep = Int(120 * 86400 / dt) Then
    For J = 0 To (1 + rps)
```

```
Worksheets("calculation sheet").Cells(J + 1, 11) = Cs(J) * 84 * 10 ^ 6
```

```
Worksheets("calculation sheet").Cells(1, 11) = Tflux * 84 * 10 ^ 6
```

Next

End If

```
If Tstep = Int(180 * 86400 / dt) Then
    For J = 0 To (1 + rps)
```

```
Worksheets("calculation sheet").Cells(J + 1, 12) = Cs(J) * 84 * 10 ^ 6
```

```
Worksheets("calculation sheet").Cells(1, 12) = Tflux * 84 * 10 ^ 6
```

Next

End If

```

If Tstep = Int(240 * 86400 / dt) Then
  For J = 0 To (1 + rps)

Worksheets("calculation sheet").Cells(J + 1, 13) = Cs(J) * 84 * 10 ^ 6
Worksheets("calculation sheet").Cells(1, 13) = Tflux * 84 * 10 ^ 6

Next
  End If
If Tstep = Int(299 * 86400 / dt) Then
  For J = 0 To (1 + rps)

Worksheets("calculation sheet").Cells(J + 1, 14) = Cs(J) * 84 * 10 ^ 6
Worksheets("calculation sheet").Cells(1, 14) = Tflux * 84 * 10 ^ 6
Next
  End If
Next

End Sub

```

## Appendix 3 Model of diffusion, sorption and Nitrification of dairy urine in soil

The model determines the fate of urine N in the soil profile uses a similar layout as the DCD model which supplies this model with the predicted DCD concentrations for soil depth and time, in the form of an input array. The initial depth of urine penetration to in the soil “Urine effective depth” and the urine N concentration are used as the initial condition, from which the urea and ammonia is allowed to diffuse and nitrify. The model is operated by the click command button function.

	A	B	C	D	E	F	G	H	I	J	K	L	M	N	O
1						Depth cm	Output								
2						0.1	6.06829E-05	5.76289E-05	5.07127E-05	2.90305E-05				5.40765E-05	3.54979E-05
3						0.2	6.06786E-05	5.76129E-05	5.06898E-05	2.90047E-05				5.40882E-05	3.55453E-05
4						0.3	6.06698E-05	5.75806E-05	5.06439E-05	2.89531E-05				5.41116E-05	3.56408E-05
5						0.4	6.06574E-05	5.75357E-05	5.05792E-05	2.88814E-05				5.41422E-05	3.57635E-05
6						0.5	6.0641E-05	5.74778E-05	5.04954E-05	2.87895E-05				5.41810E-05	3.59151E-05
7						0.6	6.06201E-05	5.74062E-05	5.040E-05	2.8677E-05				5.42253E-05	3.60974E-05
8						0.7	6.05955E-05	5.7326E-05	5.02761E-05	2.85524E-05				5.42685E-05	3.62966E-05
9						0.8	6.05664E-05	5.72364E-05	5.01463E-05	2.84158E-05				5.43099E-05	3.64345E-05
10						0.9	6.0532E-05	5.71364E-05	5.00029E-05	2.82663E-05				5.4349E-05	3.65948E-05
11						1	6.04912E-05	5.70252E-05	4.98456E-05	2.81044E-05				5.43852E-05	3.67534E-05
12						1.1	6.04426E-05	5.69017E-05	4.96741E-05	2.79296E-05				5.4418E-05	3.69133E-05
13						1.2	6.03849E-05	5.67648E-05	4.94884E-05	2.77419E-05				5.44466E-05	3.70775E-05
14						1.3	6.03164E-05	5.66134E-05	4.9288E-05	2.75409E-05				5.44701E-05	3.72494E-05
15						1.4	6.02354E-05	5.64462E-05	4.90728E-05	2.73264E-05				5.44878E-05	3.74328E-05
16						1.5	6.01403E-05	5.62643E-05	4.8845E-05	2.71017E-05				5.44865E-05	3.75733E-05
17						1.6	6.00291E-05	5.60664E-05	4.86043E-05	2.68664E-05				5.4465E-05	3.76753E-05
18						1.7	5.98994E-05	5.58514E-05	4.83505E-05	2.66204E-05				5.4422E-05	3.77427E-05
19						1.8	5.97487E-05	5.56181E-05	4.80836E-05	2.63634E-05				5.4356E-05	3.77791E-05
20						1.9	5.95745E-05	5.53655E-05	4.78032E-05	2.60952E-05				5.42654E-05	3.77884E-05
21						2	5.93742E-05	5.50925E-05	4.75093E-05	2.58155E-05				5.41485E-05	3.77743E-05
22						2.1	5.91451E-05	5.47982E-05	4.72019E-05	2.55239E-05				5.40037E-05	3.77409E-05
23						2.2	5.88846E-05	5.44818E-05	4.68807E-05	2.52202E-05				5.38295E-05	3.76923E-05
24						2.3	5.85904E-05	5.41426E-05	4.65459E-05	2.49039E-05				5.36245E-05	3.76328E-05
25						2.4	5.82602E-05	5.37801E-05	4.61974E-05	2.45747E-05				5.33874E-05	3.75671E-05
26						2.5	5.78919E-05	5.33937E-05	4.58353E-05	2.4232E-05				5.31174E-05	3.75003E-05
27						2.6	5.74842E-05	5.29835E-05	4.54596E-05	2.38753E-05				5.28143E-05	3.7438E-05
28	5.88E-06					2.7	5.70365E-05	5.25522E-05	4.50738E-05	2.3509E-05				5.24669E-05	3.73322E-05
29						2.8	5.65486E-05	5.21003E-05	4.46781E-05	2.31325E-05				5.20761E-05	3.71919E-05
30	2.00E-01	2.92E-06	0-2mm			2.9	5.60205E-05	5.1628E-05	4.42727E-05	2.27452E-05				5.16423E-05	3.70201E-05
31	6.00E-01	2.52E-06	2-6mm			3	5.54532E-05	5.11361E-05	4.3858E-05	2.23464E-05				5.11701E-05	3.6824E-05
32	1.40E+00	2.34E-06	6-14mm			3.1	5.46484E-05	5.06256E-05	4.34343E-05	2.19355E-05				5.06596E-05	3.661E-05
33	2.50E+00	1.82E-06	14-25mm			3.2	5.4209E-05	5.00976E-05	4.30021E-05	2.15115E-05				5.01155E-05	3.63849E-05
34	3.50E+00	1.41E-06	25-35mm			3.3	5.35385E-05	4.95534E-05	4.25617E-05	2.10734E-05				4.95423E-05	3.61556E-05
35	4.50E+00	1.59E-06	35-45mm			3.4	5.28414E-05	4.89948E-05	4.21135E-05	2.062E-05				4.89456E-05	3.59297E-05
36						3.5	5.21233E-05	4.84235E-05	4.16581E-05	2.01501E-05				4.83319E-05	3.57148E-05
37						3.6	5.13905E-05	4.78416E-05	4.11957E-05	1.96618E-05				4.77088E-05	3.55192E-05
38						3.7	5.06574E-05	4.72815E-05	4.076E-05	1.92058E-05				4.70732E-05	3.52964E-05

Figure A3 Worksheet layout for modelled urine N nitrification and movement in soil cores at 20°C.

Sub CommandButton1\_Click()

'Input variables data from sheetsheet

```
Product$ = Worksheets("calculation").Range("D2")
MaxSW = Worksheets("calculation").Range("D5")
area = Worksheets("calculation").Range("d4")
DENSITY = Worksheets("calculation").Range("d17")
Z = Worksheets("calculation").Range("d9")
sa = Worksheets("calculation").Range("D4") *
Worksheets("calculation").Range("D5")

dt = Worksheets("calculation").Range("d8")
Dim Cap(1)
Dim soildep(1)
aa = Worksheets("calculation").Range("d15")
ab = Worksheets("calculation").Range("d16")
aD = Worksheets("calculation").Range("d7")
f = Worksheets("calculation").Range("d13")
Pg = 1900
dxl = Worksheets("calculation").Range("D6")
Sdepth = Worksheets("calculation").Range("D12")
rps = (Int(Sdepth / dxl))
iter = Int(86400 / dt)
SWD = Worksheets("calculation").Range("D11")
ua = Worksheets("calculation").Range("d21")
ub = Worksheets("calculation").Range("d22")
UD = Worksheets("calculation").Range("d26")
du = Worksheets("calculation").Range("d27")
Dim Newt(10)
Urinationdepth = Worksheets("calculation").Range("D25")
Urineconc = Worksheets("calculation").Range("D24")
degrate = Worksheets("calculation").Range("D19")
'Zero order Nitrification soil zones
degrateZ1 = Worksheets("calculation").Range("D30")
degrateZ2 = Worksheets("calculation").Range("D31")
degrateZ3 = Worksheets("calculation").Range("D32")
degrateZ4 = Worksheets("calculation").Range("D33")
degrateZ5 = Worksheets("calculation").Range("D34")
degrateZ6 = Worksheets("calculation").Range("D35")
Volat = Worksheets("calculation").Range("D20")
Dim inhib(7, 16) As Variant

dt = Worksheets("calculation").Range("d8")
ReDim C(1 + rps)
```

```

ReDim Cs(1 + rps)
ReDim rg(1 + rps)
ReDim Flux(1 + rps)
ReDim SW(1 + rps)
ReDim output(1, 1 + RSP)
ReDim ads(1 + rps)
For ihd = 1 To 6
  For iht = 1 To 15
inhib(ihd, iht) = Worksheets("calculation").Cells(57 + ihd, 5 + iht)
  Next
Next

```

Urineconc = Urineconc \* (1 - Volat)

SW(1) = MaxSW - SWD

'DCD Diffusion

'Initial Conditions

Urinedepth = Urinationdepth

If Urinationdepth > Sdepth Then Urinedepth = Sdepth

For IntCon = 1 To (Urinedepth / dxl)

Cs(IntCon) = Urineconc / Urinationdepth

Next

'time step

For tstep = 1 To Z

'layer step

For ll = 1 To rps

'Urea diffusion

If tstep < Int(86400 \* du / dt) Then D = UD

If tstep > Int(86400 \* du / dt) Then D = aD

'FLUX IN MOLES

Flux(ll) = D \* f \* SW(1) \* dt \* (C(ll) - C(ll + 1)) / dxl

'Zero flux at base

If ll = (rps - 1) Then Flux(ll) = 0

'CONCENTRATION IN MOLES/CC(LIQUID)

Cs(ll) = Cs(ll) + ((Flux(ll - 1) - Flux(ll)) / (dxl))

'Newton Raphson

'Urea diffusion for 48 hr then change to ammonia

If tstep < Int(86400 \* du / dt) Then a = ua

If tstep > Int(86400 \* du / dt) Then a = aa

If tstep < Int(86400 \* du / dt) Then b = ub

If tstep > Int(86400 \* du / dt) Then b = ab

Newt(1) = Cs(ll) / 100000000000#

```

    If Cs(l1) < 1E-20 Then GoTo 100
    For x = 1 To 8
        Newt(x + 1) = Newt(x) - ((a * Newt(x) ^ b + SW(1) * Newt(x) - Cs(l1)) / (a * b *
Newt(x) ^ (b - 1) + SW(1)))

        C(l1) = Newt(8)
    Next

'degradation
If l1 > 0 Then degrate = degrateZ1 * (inhib(1, Int(tstep / (5 * 86400)) + 1))
If l1 > Int(0.2 / dx1) Then degrate = degrateZ2 * (inhib(2, Int(tstep / (5 * 86400)) +
1))
If l1 > Int(0.6 / dx1) Then degrate = degrateZ3 * (inhib(3, Int(tstep / (5 * 86400)) +
1))
If l1 > Int(1.4 / dx1) Then degrate = degrateZ4 * (inhib(4, Int(tstep / (5 * 86400)) +
1))
If l1 > Int(2.5 / dx1) Then degrate = degrateZ5 * (inhib(5, Int(tstep / (5 * 86400)) +
1))
If l1 > Int(3.5 / dx1) Then degrate = degrateZ6 * (inhib(6, Int(tstep / (5 * 86400)) +
1))

100 'If l1 < Int(2.5 / dx1) Then degraTN = degrate
    'If l1 > Int(2.5 / dx1) Then degraTN = degrate / 1.2
    'If l1 > Int(3.5 / dx1) Then degraTN = degrate / 1.4

    Cs(l1) = Cs(l1) - (degrate * (dt / 86400))

    If Cs(l1) < 0 Then Cs(l1) = 0

Next
If tstep = Int(3 * 86400 / dt) Then
    For J = 0 To (1 + rps)

Worksheets("calculation").Cells(J + 1, 8) = Cs(J)
Next
End If
If tstep = Int(10 * 86400 / dt) Then
    For J = 0 To (1 + rps)

Worksheets("calculation").Cells(J + 1, 9) = Cs(J)

Next
End If
If tstep = Int(24 * 86400 / dt) Then
    For J = 0 To (1 + rps)

```

```
Worksheets("calculation").Cells(J + 1, 10) = Cs(J)
```

```
Next
```

```
End If
```

```
If tstep = Int(68 * 86400 / dt) Then
```

```
    For J = 0 To (1 + rps)
```

```
Worksheets("calculation").Cells(J + 1, 11) = Cs(J)
```

```
Next
```

```
End If
```

```
Next
```

```
End Sub
```

## References

---

Agrium (2007a). Potato use recommendations.  
[www.agrium.com/esn/docs/potato\\_info\\_sheet.pdf](http://www.agrium.com/esn/docs/potato_info_sheet.pdf).

Agrium (2007b). Winter wheat on the canadian prairies.  
[www.agrium.com/ESN/doc/winter\\_wheat\\_info\\_sheet\[1\].pdf](http://www.agrium.com/ESN/doc/winter_wheat_info_sheet[1].pdf).

Alexander, M. (1977). Introduction to soil microbiology. New York, John Wiley and Sons. 467 pp.

Allen, S. E., C. M. Hunt and G. L. Terman (1971a). Nitrogen release from sulfur-coated urea, as affected by coating weight, placement and temperature." *Agronomy Journal*. **63**(4): 529- 533.

Allen, S. E. and D. A. Mays (1971b). Sulfur-coated fertilizers for controlled release: Agronomic evaluation. *Journal of Agriculture and Food Chemistry* **19**(5): 809-812.

Azam, F., G. Benckiser, C. Muller and J. C. G. Ottow (2001). Release, movement and recovery of 3,4-dimethylpyrazole phosphate (DMPP), ammonium, and nitrate from stabilized nitrogen fertilizer granules in a silty clay soil under laboratory conditions. *Biology and Fertility of Soils* **34**(2): 118-125.

Ball, R., D. R. Keeney, P. W. Theobald and P. Nes (1979). Nitrogen balance in urine-affected areas of New Zealand pasture. *Agronomy Journal*. **71**: 309-314.

Banerji, S. K. and R. K. Bajpai (1994). Cometabolism of pentachlorophenol by microbial species. *Journal of Hazardous Materials* **39**(1): 19-31.

Barraclough, P. B. and P. B. Tinker (1981). The determination of ionic diffusion coefficients in field soils. 1. Diffusion coefficients in sieved soil in relation to water content and bulk density. *Journal of Soil Science* **32**: 225-236.

Bergstrom, L. and N. Brink (1986). Effects of differentiated applications of fertilizer n on leaching losses and distribution of inorganic N in the soil. *Plant and Soil* **93**(3): 333-345.

Bertram, J. E., T. J. Clough, R. R. Sherlock, L. M. Condron, M. O'Callaghan, N. Wells and J. L. Ray (2009). Hippuric acid and benzoic acid inhibition of urine derived N<sub>2</sub>O emissions from soil. *Global Change Biology* **15**: 2067-2077.

Bishop, P. A., H. Y. Liu, M. J. Hedley and P. Loganathan (2008). New Zealand made controlled release coated urea increases winter growth rates of italian ryegrass with lower N leaching than uncoated urea. In: Proceedings of the New Zealand Grasslands Association **70**: 141-145.

Blakemore, L. C., P. L. Searle and B. K. Daly (1987). Methods for chemical analysis of soils. New Zealand Soil Bureau Scientific Report. **No. 80**:103 pp.

Blaylock, A.D., J. Kaufmann, and R.D. Dowbenko (2005). Nitrogen fertilizer technologies. In: Western Nutrient Management Conference proceedings Vol. 6. Salt Lake City, UT.  
[http://isnap.oregonstate.edu/WERA\\_103/2005\\_Proccedings/Blaylock%20Nitrogen%20Fertilizer%20pg8.pdf](http://isnap.oregonstate.edu/WERA_103/2005_Proccedings/Blaylock%20Nitrogen%20Fertilizer%20pg8.pdf)

Bollmann, A. and R. Conrad (1997). Recovery of nitrification and production of no and N<sub>2</sub>O after exposure of soil to acetylene. *Biology and Fertility of Soils* **25**(1): 41-46.

Castillo, A. R., E. Kebreab, D. E. Beever and J. France (2000). A review of efficiency of nitrogen utilisation in lactating dairy cows and its relationship with environmental pollution. *Journal of Animal and Feed Sciences* **9**: 1-32.

Castillo, A. R., E. Kebreab, D. E. Beever, J. H. Barbi, J. D. Sutton, H. C. Kirby and J. France (2001). The effect of protein supplementation on nitrogen utilization in lactating dairy cows fed grass silage diets. *Journal of Animal Science* **79**(1): 247-253.

Chen, C. S. (1989). Water activity - concentration models for solutions of sugars, salts and acids. *Journal of Food Science* **54**(5): 1318-1321.

Chen, D. L., Y. Li, P. Grace and A. R. Mosier (2008). N<sub>2</sub>O emissions from agricultural lands: A synthesis of simulation approaches. *Plant and Soil* **309**(1-2): 169-189.

Clough, T. J., J. L. Ray, L. E. Buckthought, J. Calder, D. Baird, M. O'Callaghan, R. R. Sherlock and L. M. Condron (2009). The mitigation potential of hippuric acid on N<sub>2</sub>O emissions from urine patches: An in situ determination of its effect. *Soil Biology and Biochemistry* **41**: 2222-2229.

Corre, W. J. and K. B. Zwart (1995). Effects of DCD addition to slurry on nitrate leaching in sandy soils. *Netherlands Journal of Agricultural Science* **43**(2): 195-204.

De Klein, C. A. M. and R. S. P. Van Logtestijn (1994). Denitrification and N<sub>2</sub>O emission from urine-affected grassland soil. *Plant and Soil* **163**(2): 235-241.

Detrick, J. H. and F. T. J. Carney (1994). Machine system and process for producing attrition resistant slow release fertilizer, Pursell Industries. US Patent No. 5,374,292.

Di, H. J. and K. C. Cameron (2002a). Nitrate leaching and pasture production from nitrogen sources on shallow stoney soil under flood-irrigated dairy pasture. *Australian Journal of Soil Research* **40**(2): 317-334.

Di, H. J. and K. C. Cameron (2002b). The use of a nitrification inhibitor, dicyandiamide (DCD), to decrease nitrate leaching and nitrous oxide emissions in a simulated grazed and irrigated grassland. *Soil Use and Management* **18**(4): 395-403.

Di, H. J. and K. C. Cameron (2004a). Effects of temperature and application rate of a nitrification inhibitor, dicyandiamide (DCD), on nitrification rate and microbial biomass in a grazed pasture soil. *Australian Journal of Soil Research* **42**: 927-932.

Di, H. J. and K. C. Cameron (2004b). Treating grazed pasture soil with a nitrification inhibitor, ECO-N<sup>tm</sup>, to decrease nitrate leaching in deep sandy soil under spray irrigation-a lysimeter study. *New Zealand Journal of Agricultural Research* **47**: 351-361.

Di, H. J. and K. C. Cameron (2005). Reducing environmental impacts of agriculture by using a fine particle suspension nitrification inhibitor to decrease nitrate leaching from grazed pastures. *Agriculture, Ecosystems and Environmental* **109**: 202-212.

Di, H. J. and K. C. Cameron (2008). Sources of nitrous oxide from N<sup>15</sup>-labelled animal urine and urea fertiliser with and without a nitrification inhibitor, dicyandiamide (DCD). *Australian Journal of Soil Research* **46**: 76-82.

Di, H. J., K. C. Cameron, J. P. Shen, C. S. Winefield, M. O'Callaghan, S. Bowatte and J. Z. He (2009). Nitrification driven by bacteria and not archaea in nitrogen-rich grassland soils. *Nature Geoscience* **2**(9): 621-624.

Dillon, P. (2006). Achieving high dry-matter intake from pasture with grazing dairy cows. In: A. Elgersma, J. Dijkstra and S. Tamminga (Eds.): Fresh herbage for dairy cattle. Springer. 194 pp.

Diping, L., W. Haobin, X. Xiucheng and H. Cuihong (1998). Controlled release fertilizer and preparation thereof. USA, Zhengzhou Centre of Popularization & Research. US Patent No.5,849,060.

Du, C. W., J. M. Zhou and A. Shaviv (2006). Release characteristics of nutrients from polymer-coated compound controlled release fertilizers. *Journal of Polymers and the Environment*. **14**(3): 223-230.

Erickson, A. J., R. S. Ramsewak, A. J. Smucker and M. G. Nair (2000). Nitrification inhibitors from the roots of leucaena leucocephala. *Journal of Agriculture and Food Chemistry*. **48**(12): 6174-6177.

Flowers, T. H. and P. W. Arnold (1983). Immobilization and mineralization of nitrogen in soils incubated with pig slurry or ammonium-sulfate. *Soil Biology and Biochemistry*. **15**(3): 329-335.

Fox, R. C. (1968). Slow-release coating composition consisting of wax and ethylene vinyl-acetate. USA, Chevron Research Co. Delaware. US Patent No.4,369,055.

Francis, G. S., K. M. Bartley and F. J. Tabley (1998). The effect of winter cover crop management on nitrate leaching losses and crop growth. *Journal of Agricultural Science* **131**: 299-308.

Fujita, T., C. Takahashi, M. Ohshima, T. Ushioda and H. Shimizu (1977). Method of producing coated fertilizers. USA. US Patent No.4,019,890.

Fujita, T., C. Takahashi, S. Yoshida and S. H (1983). Coated granular fertilizer capable of controlling the effect of temperature upon dissolution-out rate. USA, Chissoasahi Fertilizer Co., Ltd (Tokyo, JP). US Patent No.4,369,055.

Furuta, T., R. H. Sciaroni and J. R. Breece (1967). Sulfur-coated urea fertilizer for controlled-release nutrition of container-grown ornamentals. *California Agriculture* **21**(9): 4-5.

Ghani, A., M. Dexter, M. Kear, S. Lindsey and S. Ledgard (2006). Influence of plant litter and animal excreta on leaching of dissolved organic nitrogen and carbon in pastoral soil. In: 18th World Congress of Soil Science. Philadelphia, Pennsylvania, USA. <http://a-c-s.confex.com/crops/wc2006/techprogram/P12275.HTM>

Goertz, H. M. (1993). Technology development in coated fertilisers. In: Proceedings of the Dahlia Greidinger Memorial International Workshop on Controlled/Slow Release Fertilisers, Haifa, Technion. [http://gwri-ic.technion.ac.il/main.php?location=news&action=show\\_proceed&year=93](http://gwri-ic.technion.ac.il/main.php?location=news&action=show_proceed&year=93)

Goertz, H. M., R. J. Timmons and G. R. McVey (1993). Sulphur coated fertilizer and process for the preparation thereof. US Patent No.5,21,465

Gosting, L. J. and D. F. Akeley (1952). A study of the diffusion of urea in water at 25-degrees with the gouy interference method. *Journal of the American Chemical Society* **74**(8): 2058-2060.

Guillard, K. and K. L. Kopp (2004). Nitrogen fertilizer form and associated nitrate leaching from cool-season lawn turf. *Journal of Environmental Quality* **33**: 1822-1827.

Hansen, L. I. (1965). Granular fertilizer having a plurality of coatings and the process of making. USA, Archer-Daniels-Midland. US Patent No.3,223,518.

Hansen, L. I. (1966). Slow release fertilizer granule having a plurality of urethane resin coating. USA, Archer-Daniels-Midland. US Patent No.3,264,089.

Harris, R. F. (1981). Water potential relations in soil microbiology, Soil Science Society of America, Madison, Wisconsin, US. 151 pp.

Hauck, R.D. (1980) Mode of action of nitrification inhibitors. In: J.J. Meisinger, G.W. Randall, M.L. Vitosh, M. Stelly, D.M. Kroll, M.K. Cousin, (Eds.), Nitrification Inhibitors Potentials and Limitations. American Society of Agronomy, Madison, Wisconsin, USA. 129 pp.

- Haynes, R. J. and P. H. Williams (1993). Nutrient cycling and soil fertility in grazed pasture ecosystem. *Advances in Agronomy* **49**: 119-199.
- Hendrickson, L. L. and D. R. Keeney (1979). Bioassay to determine the effect of organic-matter and pH on the effectiveness of nitrapyrin (n-serve) as a nitrification inhibitor. *Soil Biology and Biochemistry*. **11**(1): 51-55.
- Herlihy, M. and W. Quirke (1975). Persistence of 2-chloro-6-(trichloromethyl)-pyridine in soil. *Communications in Soil Science and Plant Analysis*. **6**(5): 513-520.
- Hewitt, A. E. (1993). New Zealand soil classification. *Landcare Research Science Series*(1): 133 pp.
- Hoogendoorn, C. J., C. M. de-Klein, A. J. Rutherford, C. Letica and B. P. Devantier (2008). The effect of increasing rates of nitrogen fertiliser and a nitrification inhibitor on nitrous oxide emissions from urine patches on sheep grazed hill country pasture. *Australian Journal of Experimental Agriculture* **48**: 147-151.
- Hosen, Y., K. Paisancharoen and H. Tsuruta (2002). Effects of deep application of urea on  $\text{NO}$  and  $\text{N}_2\text{O}$  emissions from an andisol. *Nutrient Cycling in Agroecosystems* **63**(2-3): 197-206.
- Hudson, A. P. and F. E. Woodward (1993). Abrasion resistant coating for fertilizers. US, O M Scott & Sons Co. US Patent No. 5,300,135
- Huett, D. O. (1997). Fertiliser use efficiency by containerised nursery plants 1. Plant growth and nutrient uptake. *Australian Journal of Agricultural Research* **48**: 251-258.
- Hutchinson, C., S. E, S. P, M. J and L.-W. P (2003). Testing of controlled release fertilizer programs for seep irrigated irish potato production. *Journal of Plant Nutrition* **26**(9): 1709-1723.
- Hyman, M. R., I. B. Murton and D. J. Arp (1988). Interaction of ammonia monooxygenase from nitrosomonas-europaea with alkanes, alkenes, and alkynes. *Applied and Environmental Microbiology* **54**(12): 3187-3190.

- Irigoyena, I., J. Muro, M. Azpilikueta, P. Aparicio-Tejo and C. Lamsfus (2003). Ammonium oxidation kinetics in the presence of nitrification inhibitors DCD and DMPP at various temperatures. *Australian Journal of Soil Research* **41**(6): 1177-1183.
- Jarrell, W. M. and L. Boersma (1979). Model for the release of urea by granules of sulfur-coated urea applied to soil. *Soil Science Society of America Journal*. **43**(5): 1044-1050.
- Jarrell, W. M. and L. Boersma (1980). Release of urea by granules of sulfur-coated urea. *Soil Science Society of America Journal*. **44**(2): 418-422.
- Joshi, B. S. and R. Prasad (1977). The effects of rates of application and sources of nitrogen on nitrate concentration in oat forage. *Journal of the British Grassland Society* **32**: 213-216.
- Juliette, L. Y., M. R. Hyman and D. J. Arp (1993a). Inhibition of ammonia oxidation in nitrosomonas-europaea by sulfur-compounds - thioethers are oxidized to sulfoxides by ammonia monooxygenase. *Applied and Environmental Microbiology* **59**(11): 3718-3727.
- Juliette, L. Y., M. R. Hyman and D. J. Arp (1993b). Mechanism-based inactivation of ammonia monooxygenase in nitrosomonas-europaea by allylsulfide. *Applied and Environmental Microbiology* **59**(11): 3728-3735.
- Kanerva, S., V. Kitunen, O. Kiikkila, J. Lojonen and A. Smolander (2006). Response of soil C and N transformations to tannin fractions originating from scots pine and norway spruce needles. *Soil Biology Biochemistry*. **38**(6): 1364-1374.
- Kanerva, S., V. Kitunen, J. Lojonen and A. Smolander (2008). Phenolic compounds and terpenes in soil organic horizon layers under silver birch, norway spruce and scots pine. *Biology and Fertility of Soils* **44**(4): 547-556.
- Kawahara, K. and C. Tanford (1966). Viscosity and density of aqueous solutions of urea and guanidine hydrochloride. *Journal of Biological Chemistry* **241**(13): 3228-3232.
- Kelliher, F. M., T. J. Clough, H. Clark, G. Rys and J. R. Sedcole (2008). The temperature dependence of dicyandiamide (DCD) degradation soil: A data synthesis. *Soil Biology and Biochemistry*. **40**: 1878-1882.

Kirk, G. J. and P. H. Nye (1985). The dissolution and dispersion of dicalcium phosphate dihydrate in soil. I A predictive model for a planar source. *Journal of Soil Science* **36**: 445-459.

Ko, B.-S., Y.-S. Cho and H.-K. Rhee (1996). Controlled release of urea from rosin-coated fertilizer particles. *Industrial Engineering Chemical and Research* **35**: 250-257.

Kool, D. M., E. Hoffland, W. J. Eduard, Hummelink and J. W. van Groenigen (2006). Increased hippuric acid content of urine can reduce soil N<sub>2</sub>O fluxes. *Soil Biology and Biochemistry*. **38**: 1021-1027.

Kosuge, N., T. Fujita, Y. Yamashita, S. Yoshida, K. Yamahira and S. Miyoshi (1992). Coated granular fertilizer, Chisso Corporation, Osaka, Japan. US Patent No.5,147,442.

Ledgard, S. F., J. W. Penno and M. S. Sprosen (1999). Nitrogen inputs and losses from clover/grass pastures grazed by dairy cows, as affected by nitrogen fertilizer application. *Journal of Agricultural Science* **132**(2): 215-225.

Liu, X. J., A. R. Mosier, A. D. Halvorson and F. S. Zhang (2006). The impact of nitrogen placement and tillage on NO, N<sub>2</sub>O, CH<sub>4</sub> and CO<sub>2</sub> fluxes from a clay loam soil. *Plant and Soil* **280**(1-2): 177-188.

Lorenz, O. A., B. L. Weir and J. C. Bishop (1972). Effect of controlled-release nitrogen fertilizers on yield and nitrogen absorption by potatoes, cantaloupes, and tomatoes. *Journal of American Society of Horticultural Science* **97**(3): 334-337.

Ma, B. L., J. Ying and D. Balchin (2005). Impact of sample preservation methods on the extraction of inorganic nitrogen by potassium chloride. *Journal of Plant Nutrition* **28**: 785-796.

Macduff, J. H. and R. E. White (1985). Net mineralization and nitrification rates in a clay soil measured and predicted in permanent grassland from soil-temperature and moisture-content. *Plant and Soil* **86**(2): 151-172.

MacLeod, C. J. and H. Moller (2006). Intensification and diversification of New Zealand agriculture since 1960: An evaluation of current indicators of land use change. *Agriculture, Ecosystems and Environmental* **115**: 201-218.

MAF (2007). Fertiliser-application. from [www.maf.govt.nz/statistics/fertiliser/](http://www.maf.govt.nz/statistics/fertiliser/).

Magesan, G. H., R. E. White and D. R. Scotter (1996). Nitrate leaching from drained, sheep-grazed pasture. I. Experimental results and environmental implications. *Australian Journal of Soil Research* **34**: 55-67.

Mao, J. A., L. Z. Yang, Y. M. Shi, J. A. Hu, Z. Piao, L. J. Mei and S. X. Yin (2006). Crude extract of astragalus mongholicus root inhibits crop seed germination and soil nitrifying activity. *Soil Biology and Biochemistry*. **38**(2): 201-208.

Maschmedt, D. J. and P. S. Cocks (1976). "Sulphur-coated urea compared with urea and ammonium nitrate as a source of nitrogen for swards of annual ryegrass( *lolium rigidum* gaud.)." *Agricultural Record* **3**: 4-7.

McCarty, G. W. (1999). Modes of action of nitrification inhibitors. *Biology and Fertility of Soils* **29**(1): 1-9.

McCarty, G. W. and J. M. Bremner (1989). Laboratory evaluation of dicyandiamide as a soil nitrification inhibitor. *Communications in Soil Science and Plant Analysis*. **20**(19-20): 2049-2065.

McClellan, G. H. and R. M. Scheib (1975). Texture of sulfur coatings on urea. *Advances in Chemistry Series* **141**: 18-32.

Menneer, J. C., M. S. Sprosen and S. F. Ledgard (2008). Effect of timing and formulation of dicyandiamide (DCD) application on nitrate leaching and pasture production in a bay of plenty pastoral soil. *New Zealand Journal of Agricultural Research* **51**(3): 377-385.

Monaghan, R. M. and D. Barraclough (1992). Some chemical and physical factors affecting the rate and dynamics of nitrification in urine-affected soil. *Plant and Soil* **143**: 11-18.

Monaghan, R. M., L. C. Smith and S. F. Ledgard (2009). The effectiveness of a granular formulation of dicyandiamide (DCD) in limiting nitrate leaching from a grazed dairy pasture. *New Zealand Journal of Agricultural Research* **52**(2): 145-159.

Moore, W. P. (1987). Attrition resistant controlled release fertilizers, Melamine Chemicals Inc.US Patent No.4,711,659.

Moore, W. P. (1989). Attrition resistant, controlled release fertilizers, Melamine Chemicals Inc.US Patent No.4,804,403.

Moore, W. P. (1990). One step method of coating nutrient particles, Melamine Chemicals, Inc.US Patent No.4,969,947.

Pasda, G., R. Hahndel and W. Zerulla (2001). Effect of fertilizers with the new nitrification inhibitor dmpp (3,4-dimethylpyrazole phosphate) on yield and quality of agricultural and horticultural crops. *Biology and Fertility of Soils* **34**(2): 85-97.

Patra, D. D., U. Kiran and P. Pande (2006). Urease and nitrification retardation properties in natural essential oils and their by-products. *Communications in Soil Science and Plant Analysis*. **37**(11-12): 1663-1673.

Pauly, D. G., M. Nyborg and S. S. Malhi (2002). Controlled-release P fertilizer concept evaluation using growth and P uptake from barley from three soils in a greenhouse. *Canadian Journal of Soil Science* **82**: 201-210.

Pollock, K. M. (1989). Grass establishment and performance on a high country soil fertilized with nitrogen. *New Zealand Journal of Agricultural Research* **32**(1): 7-15.

Pollock, K. M., D. Scott and J. S. Robertson (1994). Development of a high country winter-feed option using irrigated nitrogen-fertilised tall fescue. In: Proceedings of the New Zealand Grassland Association **56**: 193-196.

Popay, A. J. and J. R. Crush (2010). Influence of different forage grasses on nitrate capture and leaching loss from a pumice soil. *Grass Forage Science*. **65**(1): 28-37.

Raban, S. (1994). Release mechanisms of membrane coated fertilisers. *Agricultural Engineering*. Haifa, Technion-IIT. **M.Sc.** 103 pp.

Rachhpal-Singh and P. H. Nye (1984). Diffusion of urea, ammonium and soil alkalinity from surface applied urea. *Journal of Soil Science* **35**: 529-538.

Rindt, D. W., G. M. Blouin and J. G. Getsinger (1968). Sulfur coating on nitrogen fertilizer to reduce dissolution rate. *Journal of Agriculture and Food Chemistry* **16**(5): 773-778.

Saggar, S., N. S. Bolan, R. Bhandral, C. B. Hedley and J. Luo (2004). A review of emissions of methane, ammonia, and nitrous oxide from animal excreta deposition and farm effluent application in grazed pastures. *New Zealand Journal of Agricultural Research* **47**: 513-544.

Sahrawat, K. L., D. R. Keeney and S. S. Adams (1987). Ability of nitrapyrin, dicyandiamide and acetylene to retard nitrification in a mineral and an organic soil. *Plant and Soil* **101**(2): 179-182.

Salman, O. A. (1989). Polyethylene-coated urea. 1. Improved storage and handling properties. *Industrial Engineering Chemical and Research* **28**: 630-632.

Sartain, J. B. and D. L. Ingram (1984). Influence of container medium, lime, and nitrogen source on growth of woody ornamentals. *Journal of American Society of Horticultural Science* **109**(6): 882-886.

Schwarzer, C. and K. Haselwandter (1996). Rapid quantification of the nitrification inhibitor dicyandiamide in soil samples, nutrient media and bacterial cell-free extracts. *Journal of Chromatography A* **732**: 390-393.

Sharma, G. C., L. Gashaw and L. M. Mugwira (1982). Japanese holly growth and release pattern of ammonium and nitrate from controlled-release fertilizer. *Scientia Horticulturae* **16**: 291-297.

Shaviv, A. (2001). Advances in controlled-release fertilizers. *Advances in Agronomy* **71**: 1-52.

Shaviv, A., S. Raban and E. Zaidel (2003a). Modeling controlled nutrient release from a population of polymer coated fertilizer: Statistically based model for diffusion release. *Environmental Science and Technology* **37**(10): 2257-2262.

Shaviv, A., S. Raban and E. Zaidel (2003b). Modeling controlled nutrient release from polymer coated fertilizers: Diffusion release from single granules. *Environmental Science and Technology*. **37**(10): 2251-2256.

Sherlock, R. R. and K. M. Goh (1983). Initial emission of nitrous-oxide from sheep urine applied to pasture soil. *Soil Biology and Biochemistry* **15**(5): 615-617.

Shoji, S., J. Delgado, A. Mosier and Y. Miura (2001). Use of controlled release fertilizers and nitrification inhibitors to increase nitrogen use efficiency and to conserve air and water quality. *Communications in Soil Science Plant Analysis*. **32**(7-8): 1051-1070.

Shoji, S. and H. Kanno (1994). Use of polyolefin-coated fertilizer for increasing fertilizer efficiency and reducing nitrate leaching and nitrous oxide emissions. *Fertilizer Research* **39**: 147-152.

Silva, R. G., K. C. Cameron, H. J. Di and E. E. Jorgensen (2005). A lysimeter study to investigate the effect of dairy effluent and urea on cattle urine N losses, plant uptake and soil retention. *Water Air and Soil Pollution* **164**(1-4): 57-78.

Smith, L. C., C. A. M. de Klein, R. M. Monaghan and W. D. Catto (2008). The effectiveness of dicyandiamide in reducing nitrous oxide emissions from a cattle-grazed, winter forage crop in southland, New Zealand. *Australian Journal of Experimental Agriculture* **48**: 160-164.

Smith, L. C., R. M. Monaghan, S. F. Ledgard and W. D. Catto (2005). The effectiveness of different nitrification inhibitor formulations in limiting nitrate accumulation in a southland pastoral soil. *New Zealand Journal of Agricultural Research* **48**(4): 517-529.

Sommers, L. E., C. M. Gilmour, R. E. Wildung and S. M. Beck (1981). The effect of water potential on decomposition processes in soils. In: J. F. Parr (Ed.), Water potential relations in soil microbiology. Wisconsin, Soil Science Society of America: 151 pp.

Spence, J. (1994). Background analysis and introduction to shell theory. In: J. Spence and A. S. Tooth (Eds.), Pressure vessel design: Concepts and principles. London, Chapman & Hall: 491pp.

Sprosen, M. S., S. F. Ledgard and S. B. Lindsey (2009). Effect of rate and form of dicyandiamide application on nitrate leaching and pasture production from a volcanic ash soil in the waikato. *New Zealand Journal of Agricultural Research* **52**(1): 47-55.

Stein, L. Y., L. A. Sayavedra-Soto, N. G. Hommes and D. J. Arp (2000). Differential regulation of AMOa and AMOb gene copies in nitrosomonas europaea. FEMS Microbiology Letters **192**(2): 163-168.

Subbarao, G. V., M. Kishii, K. Nakahara, T. Ishikawa, T. Ban, H. Tsujimoto, T. S. George, W. L. Berry, C. T. Hash and O. Ito (2009). Biological nitrification inhibition (BNI)-is there potential for genetic interventions in the triticeae? Breeding Science **59**(5): 529-545.

Subbarao, G. V., K. Nakahara, T. Ishikawa, T. Yoshihashi, O. Ito, H. Ono, M. Ohnishi-Kameyama, M. Yoshida, N. Kawano and W. L. Berry (2008). Free fatty acids from the pasture grass brachiaria humidicola and one of their methyl esters as inhibitors of nitrification. Plant and Soil **313**(1-2): 89-99.

Subbarao, G. V., H. Y. Wang, O. Ito, K. Nakahara and W. L. Berry (2007). NH<sub>4</sub><sup>+</sup> triggers the synthesis and release of biological nitrification inhibition compounds in *brachiaria humidicola* roots. Plant and Soil **290**: 245-257.

Theeuwes, F. (1975). Elementary osmotic pump. Journal of Pharmaceutical Sciences **64**(12): 1987-1991.

Trenkel, M. E. (1997). Controlled-release and stabilized fertilizers in agriculture. International Fertilizer Industry Association, Paris. 156 pp.  
<http://www.fertilizer.org/ifa/HomePage/LIBRARY/Our-selection2/Fertilizer-use.html>

Turner, M. A. and A. N. Macgregor (1978). Evaluation of terrazole as a nitrifidant for improving efficiency of use of nitrogenous fertilizers on pasture. New Zealand Journal of Agricultural Research **21**(1): 39-45.

van Erp, P. J., V. J. G. Houba and M. L. van Beusichem (2001). Effect of drying temperature on amount of nutrient elements extracted with 0.01 M CaCl<sub>2</sub> soil extraction procedure. Communications in Soil and Plant Analysis **32**: 33-48.

Wachendorf, C., F. Taube and M. Wachendorf (2005). Nitrogen leaching from <sup>15</sup>N labelled cow and dung applied to grassland on a sandy soil. Nutrient Cycling in Agroecosystems **73**: 89-100.

Wang, F., J. Bear and A. Shaviv (1998). Modelling simultaneous release, diffusion and nitrification of ammonium in the soil surrounding a granule or nest containing ammonium fertilizer. European Journal of Soil Science **49**: 351-364.

Weiske, A., G. Benckiser, T. Herbert and J. C. G. Ottow (2001). Influence of the nitrification inhibitor 3,4-dimethylpyrazole phosphate (DMPP) in comparison to dicyandiamide (DCD) on nitrous oxide emissions, carbon dioxide fluxes and methane oxidation during 3 years of repeated application in field experiments. *Biology and Fertility of Soils* **34**(2): 109-117.

Williams, P. A. M., E. G. Ferrer, N. Baeza, O. E. Piro, E. E. Castellano and E. J. Baran (2005). Transition metal promoted addition of methanol to cyanoguanidine. Molecular structure and properties of the generated copper(ii) and nickel(ii) complexes. *Zeitschrift für anorganische und allgemeine Chemie* **631**(8): 1502-1506.

Wynnyk, N. P. et al. (2004). Controlled release fertilizer and method for production thereof. Canada, Agrium Inc. Canadian Patent No. A 2436007.

Zakir, H., G. V. Subbarao, S. J. Pearse, S. Gopalakrishnan, O. Ito, T. Ishikawa, N. Kawano, K. Nakahara, T. Yoshihashi, H. Ono and M. Yoshida (2008). Detection, isolation and characterization of a root-exuded compound, methyl 3-(4-hydroxyphenyl) propionate, responsible for biological nitrification inhibition by sorghum (*sorghum bicolor*). *New Phytologist* **180**(2): 442-451.

Zaman, M., S. Saggar, J. D. Blennerhassett and J. Singh (2009). Effect of urease and nitrification inhibitors on n transformation, gaseous emissions of ammonia and nitrous oxide, pasture yield and n uptake in grazed pasture system. *Soil Biology and Biochemistry*. **41**(6): 1270-1280.

Zhang, H. J., Z. J. Wu and Q. X. Zhou (2004). Dicyandiamide sorption-desorption behavior on soil and peat humus. *Pedosphere* **14**(3): 395-399.

Zvomuya, F., C. J. Rosen, M. P. Russelle and S. C. Gupta (2003). Ground water quality nitrate leaching and nitrogen recovery following application of polyolefin-coated urea to potato." *Journal of Environmental Quality* **32**: 480-489.